University of Huddersfield Repository

Aburas, Omaro A Emhmed

Investigation of aldehyde oxidase and xanthine oxidoreductase in rainbow trout (Oncorhynchus mykiss)

Original Citation

Aburas, Omaro A Emhmed (2014) Investigation of aldehyde oxidase and xanthine oxidoreductase in rainbow trout (Oncorhynchus mykiss). Doctoral thesis, University of Huddersfield.

This version is available at http://eprints.hud.ac.uk/id/eprint/23543/

http://eprints.hud.ac.uk/

Investigation of aldehyde oxidase and xanthine oxidoreductase in rainbow trout (*Oncorhynchus mykiss*)

Omaro Aburas B.Sc., M.Sc.
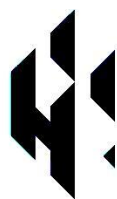
University of HUDDERSFIELD

Department of Chemical and Biological Science

University of Huddersfield

United Kingdom

Thesis submitted in partial fulfilment of the requirements for the Degree of Doctor of Philosophy

July 2014

Abstract

Molybdo-flavoenzymes (MFEs), aldehyde oxidase (AOX) and xanthine oxidoreductase (XOR) are involved in the oxidation of N-heterocyclic compounds and aldehydes, many of which are environmental pollutants, drugs and vitamins. This biotransformation generally generates more polar compounds that are more easily excreted, thus MFEs have been classed as detoxication enzymes.

To date there has been scant study of the properties, substrate and inhibitor specificities of MFEs in non-mammalian vertebrate organisms. This investigation focuses on MFEs in rainbow trout (*Oncorhynchus mykiss*) as it belongs to a class of fish that host a single AOX (AOXβ) and one XOR.

In this study the substrate specificity of rainbow trout liver AOX and XOR was investigated using HPLC and spectrophotometric assays. AOX in hepatic cytosol was found to be able to catalyse the oxidation of azanaphthalenes belonging to a group of compounds that are environmental pollutants such as phenanthridine, phthalazine and cinchonine. In addition, xenobiotic aromatic aldehydes (vanillin and dimethylaminocinnamaldehyde) and drugs such as allopurinol and pyrazinamide were substrates. Several endogenous vitamins including pyridoxal (vitamin B6), all-trans retinal (vitamin A) and N^1-methylnicotinamide were also biotransformed by the rainbow trout AOX. In contrast to liver no AOX activity was detectable in kidney and gill tissue. XOR activity in rainbow trout liver was measurable with the endogenous purine xanthine, purine drug metabolites (1-methylxanthine and 6-thioxanthine) and N-heterocyclic drugs (allopurinol and pyrazinamide). Unlike mammalian XOR that can utilise both NAD^+ and O_2 as

electron acceptors, trout XOR was exclusively NAD^+-dependent with no activity being detected with O_2.

Eadie-Hofstee plots were using to determine the Km and Vmax of rainbow trout AOX and XOR with different substrates and it was found the Vmax of the rainbow trout enzymes were generally lower and Km generally higher than mammalian AOX and XOR.

Inhibitors of mammalian AOX were tested to determine if they could interact with the piscine AOX. Environmental pollutants (17α-ethinyl estradiol and phenanthridine), an endogenous steroid (estradiol) and drugs (chlorpromazine and menadione) were found to be effective inhibitors and were classed as competitive, non-competitive and uncompetitive respectively using Lineweaver-Burk plots. The drug metabolite, oxipurinol, was a non-competitive inhibitor of rainbow trout XOR.

In order to further characterise trout AOX protein purification was carried out. In contrast to mammalian AOX, the piscine enzyme was not thermotolerant at 55°C nor was it inhibited by benzamidine, thus heat treatment and affinity chromatography could not be used as a purification steps. Trout AOX was purified 210-fold using ammonium sulphate fractionation, together with ion exchange and gel filtration chromatography. The native molecular mass of the piscine AOX was 295 kDa, which is similar to mammalian AOXs.

In conclusion this study yields new insight into groups of anthropogenic environmental pollutants, drugs and vitamins that are substrates and inhibitors of an ancestral vertebrate AOX. The toxicological relevance of these findings is discussed.

ACKNOWLEDGEMENTS

No project such as can be carried out by only one individual. I would like to express my thanks to God who is the source and origin of all knowledge.

I fell highly privileged to express my heartiest gratitude to the worthy and kind supervisor, Dr Dougie Clarke for his dynamic supervision, constructive criticism and affectionate behaviour throughout this study. His wide knowledge and logical way of thinking has been of great value for me. And his intensive and creative comments have helped me step by step throughout this project.

My sincere deepest gratitude to all my family for their support and encouragement through this work, I would like to thank my colleagues at the school of Applied Sciences who shared great research ideas during my time in Huddersfield University.

Table of Contents

List of Tables:

List of Figures:

List of Abbreviations:

Abbreviation:	Definition:
2-PY:	N^1-methyl-2-pyridone-5-carboxamide
4-PY:	N^1-methyl-4-pyridone-3-carboxamide
6-MP:	6-mercaptopurine
ADP:	Adenosine diphosphate
AhR:	Aryl hydrocarbon receptors
ALDH:	Aldehyde dehydrogenase
AMP:	Adenosine monophosphate
AOX:	Aldehyde oxidase
AOH1:	Aldehyde oxidase homologue 1
ATP:	Adenosine triphosphate
ATR:	All-trans retinal (vitamin A)
BSA:	Bovine serum albumin
CV:	Coefficient of variation
CYP:	Cytochrome P450
DAD:	Diode array detector
DMAC:	Dimethylaminocinnamaldehyde
DCPIP:	2, 6-dichlorophenol-indophenol
EBT:	Erochrome black T
FAD:	Flavin adenine dinucleotide
GMP:	Guanosine monophosphate
IMP:	Inosine monophosphate
HPLC:	High performance liquid chromatography
H_2O_2:	Hydrogen peroxide
kDa:	kilo Dalton
K_m:	Michaelis constant
LOD:	Limit of detection

Abbreviation:	Definition:
LOQ:	Lower limit of Quantification
MFEs:	Molybdo-flavoenzymes
MoCo:	Molybdenum cofactor
MTT:	Dimethylthiazol-diphenyl tetrazolium bromide
MB:	Methylene blue
mM:	Millimolar
NMN:	N^1-methylnicotinamide
NAD$^+$:	Nicotinamide adenine dinucleotide
INT:	Iodonitro-tetrazolium
NPAHs:	Nitrogen containing polycyclic aromatic hydrocarbons
NBT:	Nitro blue tetrazolium
NADH:	Nicotinamide adenine dinucleotide (reduced form)
PMS:	Phenazine methosulphate
PAOX:	Pseudogene aldehyde oxidase
PBS:	Phosphate buffer saline
PCR:	Polymerase chain reaction
RSD:	Relative standard deviation
TTC:	Tetrazolium chloride
TAN:	Total ammonia nitrogen
XDH:	Xanthine dehydrogenase
XO:	Xanthine oxidase.
XOR:	Xanthine oxidoreductase

1. Introduction.

The term used to describe the chemical substances which are foreign to animal life is xenobiotics. These chemical substances include drugs,cosmetics,food additives, environmental pollutants, pesticides, flavouring fragrances and industrial chemicals(Idle and Gonzalez. 2007).Many of these chemical substances access our bodies by the diet, atmosphere, drinking water and drug administration. These substances go through a broad varieties of processes of detoxication of which generally generate compounds that are much less toxic, much more polar, and also quickly excretable (Timbrell. 2009). Of these processes oxidation has an important purpose in the metabolism of such xenobiotics. The microsomal cytochrome P-450 mono-oxygenase plays an important role in this biotransformation process; however the cytosolic enzymes are also involved in this biotransformation process. This thesis is concerned with two cytosolic molybdo-flavoenzymes (MFEs), namely aldehyde oxidase (AOX; EC 1. 2. 3. 1) and xanthine oxidoreductase (XOR; EC 1. 2. 3. 2). In mammals the second of these enzymes, XOR, exists as two forms xanthine dehydrogenase (XDH; EC 1. 17. 1. 4) and xanthine oxidase (XO; EC 1. 17. 3. 2) that are derived from a single gene and both have identical primary amino acid sequence. The native dehydrogenase form that uses NAD^+ as an electron acceptor can be converted to the XO form that uses O_2 as an electron acceptor by cysteine oxidation or limited proteolysis (Nishino and Nishino. 1997, Nishino *et al.*, 2008). The change from the XDH to the XO form is associated with a conformational change in protein structure that prevents the bulky NAD^+ from entering the electron acceptor binding site while the smaller oxygen can enter this site (Nishino and Nishino. 1997, Nishino *et al.*, 2008). The conversion of XDH to XO has only been demonstrated in mammalian species that have specific cysteines

(e.g in rats XDH has cysteine 535 and cysteine 992) and lysines (e.g in rats XDH has lysine 754 and lysine 771) that are the site of proteolytic cleavage. The conversion of XDH to XO *in vivo* that result in the enzyme using molecular oxygen as electron acceptor results in oxygen free radicals being generated which have been shown to be responsible for protein damage, DNA mutation and cell membrane disintegration linked with many diseases such as cancer, liver damage and cardiovascular disease (Nishinaka *et al.*, 2001). These enzymes are present in almost all organisms from bacteria to human (Beedham. 2001, Garattini *et al.*, 2008, Garattini *et al.*, 2009, Pryde *et al.*, 2010, Garattini and Terao. 2011, Garattini and Terao. 2012, Hartmann *et al.*, 2012, Kurzawski *et al.*, 2012, Garattini and Terao. 2013).

1.1. Molybdo-flavoenzyme structure

Both MFEs enzymes, AOX and XOR, are composed of molybdenum cofactor (MoCo), one flavin adenine dinucleotide (FAD) and a pair of non-identical metal sulfur centers [2Fe-2S] (Palmer *et al.*, 1969, Nishino. 1994, Borges *et al.*, 2002, Nishino *et al.*, 2002, Garattini *et al.*, 2008, Pryde *et al.*, 2010, Garattini and Terao. 2011, Garattini and Terao. 2012, Garattini and Terao. 2013). Molybdo-flavoenzymes are homodimers as active forms and are composed from a pair of identical subunits of approximately 150 kDa (Figure 1). Their structure is split into three distinct domains as follows: an 85 kDa C-terminal domain that include Moco along with the substrate binding site, and an N-terminus that includes a 20 kDa domains with a couple of [2Fe-2S] clusters, and a 45 kDa flavin adenine dinucleotide (FAD) joining domain (Kisker. 1997, Hille. 2005, Mendel and Bittner. 2006a, Wollers. 2008, Garattini and Terao. 2012, Garattini and Terao. 2013, Mendel. 2013).

2
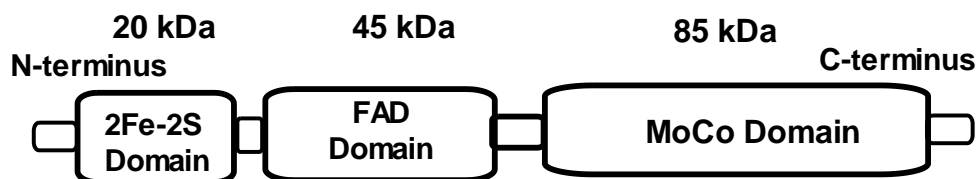
Figure 1: The domain structure of the AOX and XDH enzyme family.

The N-terminus domain binds the two Fe_2S_2 clusters, the center domain include the FAD binding site and the C-terminus domain is the location of this Mo-pterin cofactor (Mendel and Bittner. 2006a, Mendel. 2013).

The crystallization of mammalian molybdo-flavoenzymes has provided much information about the domain structure of molybdo-flavoenzymes (Romao *et al.*, 1995, Enroth *et al.*, 2000, Truglio *et al.*, 2002, Pryde *et al.*, 2010, Mahro *et al.*, 2011, Coelho *et al.*, 2012, Garattini and Terao. 2012, Kikuchi *et al.*, 2012, Garattini and Terao. 2013, Mendel. 2013). Both bovine XO and XDH have been determined by X-ray crystallography to be separated into three sub-domains. The first sub-domain (residues 1-165) at the N-terminus has a pair of iron-sulphur cofactors. It is linked to the FAD binding domain (residues 226-531) by a long portion connected with amino acids (residues 166-225) to another linker portion (residues 532-861) this then links to a specific sub-domain containing on the molybdenum cofactor (residues 590-1,332), which is located close to the interfaces of the FAD binding domain and the iron sulphur(Enroth *et al.*, 2000, Kikuchi *et al.*, 2012).

1.2. Molybdenum cofactor and the catalytic mechanism of molybdo-flavoenzymes

Molybdenum itself is biologically inactive unless bound to a tricyclic pterin compound where it then forms molybdenum cofactor (Moco) (Figure 2). Moco is situated at the active site of AOX and XOR(Mendel and Bittner. 2006b). The pterin structure coordinates to the molybdenum metal by an enedithiolate side chain (Hille. 2005). The molybdo-flavo enzymes, AOX and XOR, contain an active site that is believed to be in a five-coordinate complex with two enedithiolate ligands of the molybdopterin cofactor, one oxo group, one sulfide group, and one hydroxyl or water molecule. This coordination results in a square pyramidal geometric structure and is the site for substrate binding and enzyme inhibition (Brondino *et al.*, 2005).
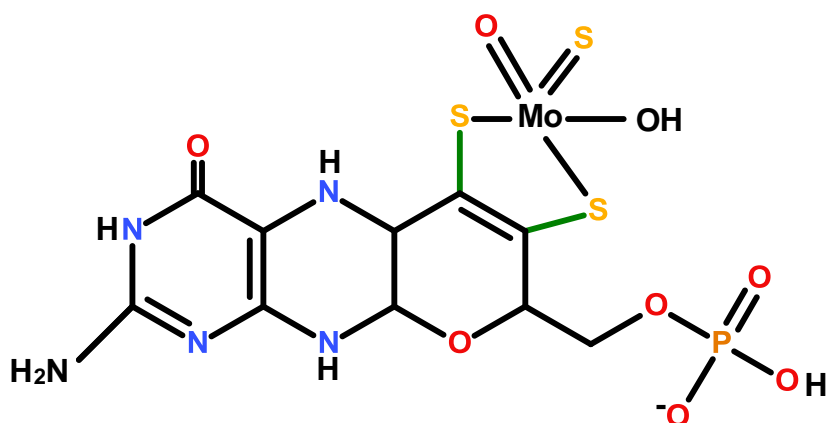
Figure 2: Molybdenum Cofactor structure in molybdenum enzymes.

The active site structure is attached with the pyranopterin compound through two enedithiolate side chains (green colour) to produce the molybdenum cofactor. Based on Mendel, 2013.

The molybdenum cofactor's purpose is to transfer electrons out of the molybdenum center following the oxidation reaction has taken place. This results in the reduction of molybdenum from Mo (VI) to Mo (IV) (Hille. 2005, Okamoto *et al.*, 2013). The movement of electron flow in MFEs is shown in (Figure 3), in which the Fe/S I and Fe/S II are a pair of iron-sulfur center.

Mo-pterin ⟶ Fe/SI ⟶ Fe/SII ⟶ FAD
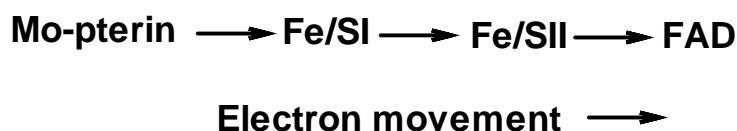
Electron movement ⟶

Figure 3: The movement of electron flow out from the molybdenum center of molybdo-flavoenzymes. According to Okamoto *et al*., 2013.

The molybdo-flavoenzymes AOX and XOR exhibit two types of reactions at the same time involving the molybdenum cofactor, oxidative and reductive half reactions. The oxidative half reaction at the molybdenum site, and the reduction half reaction at the FAD site are shown in (Figure 4) (Calzei *et al.*, 1995, Hille and Nishino. 1995, Nishino and Okamoto. 2000, Okamoto *et al.*, 2004, Hille. 2005, Brondino *et al.*, 2006, Kitamura *et al.*, 2006, Pryde *et al.*, 2010, Okamoto *et al.*, 2013). Electron donors such as vanillin act at molybdenum site, reducing it from Mo (VI) to the Mo (IV) state. The reducing equivalents transfer directly to the FAD site or via the iron-sulfur center as shown in (Figure 5)(Calzei *et al.*, 1995, Hille and Nishino. 1995, Beedham. 1998, Kitamura *et al.*, 2006, Beedham. 2010).

The reduction half reaction takes place at the FAD site, and the enzyme is reoxidized by interaction with oxygen in case of AOX and XO or with NAD^+ in case of XDH, and $FADH_2$ is reduced into FAD. The reduction of oxygen leads to formation of superoxide anion and hydrogen peroxide, and these two products

damage the cell, but the cell itself has an enzyme to protect from this attack; for superoxide anion the enzyme superoxide dismutase and for hydrogen peroxide the enzyme hydrogen peroxidase (Kelley *et al.*, 2010). XDH displays partial oxidase activity under conditions in which NAD^+ levels are diminished, such as the ischemic/hypoxic microenvironment encountered in vascular inflammation (Harris and Massey. 1997). This same inflammatory milieu leads to enhanced XO levels and thus increased XO-derived ROS formation, resulting in activation of redoxdependent cell signaling reactions and alterations in vascular function, and reduction of NAD^+ leads to formation of NADH and H^+. In the presence of an alternative electron donor, MFEs can mediate the reduction of various compounds such as in my example, it reduced the fenthion sulfoxide to its reduced form fenthion as shown in (Figure 4) (Kitamura *et al.*, 2003, Okamoto *et al.*, 2004, Hille. 2005, Kitamura *et al.*, 2006, Beedham. 2010, Pryde *et al.*, 2010). These enzymes can be alternately reduced by the substrate after which re-oxidised by their individual electron acceptors at the FAD site. *In vitro*, potassium ferricyanide and 2, 6-dichloroindophenol (DCIP) have proven to be effective unnatural electron acceptors for these enzymes that it can be reduced at FAD site (Figure 4) (Krenitsky *et al.*, 1972, Beedham. 1985, Slef and Stadtman. 2000, Kitamura *et al.*, 2006).
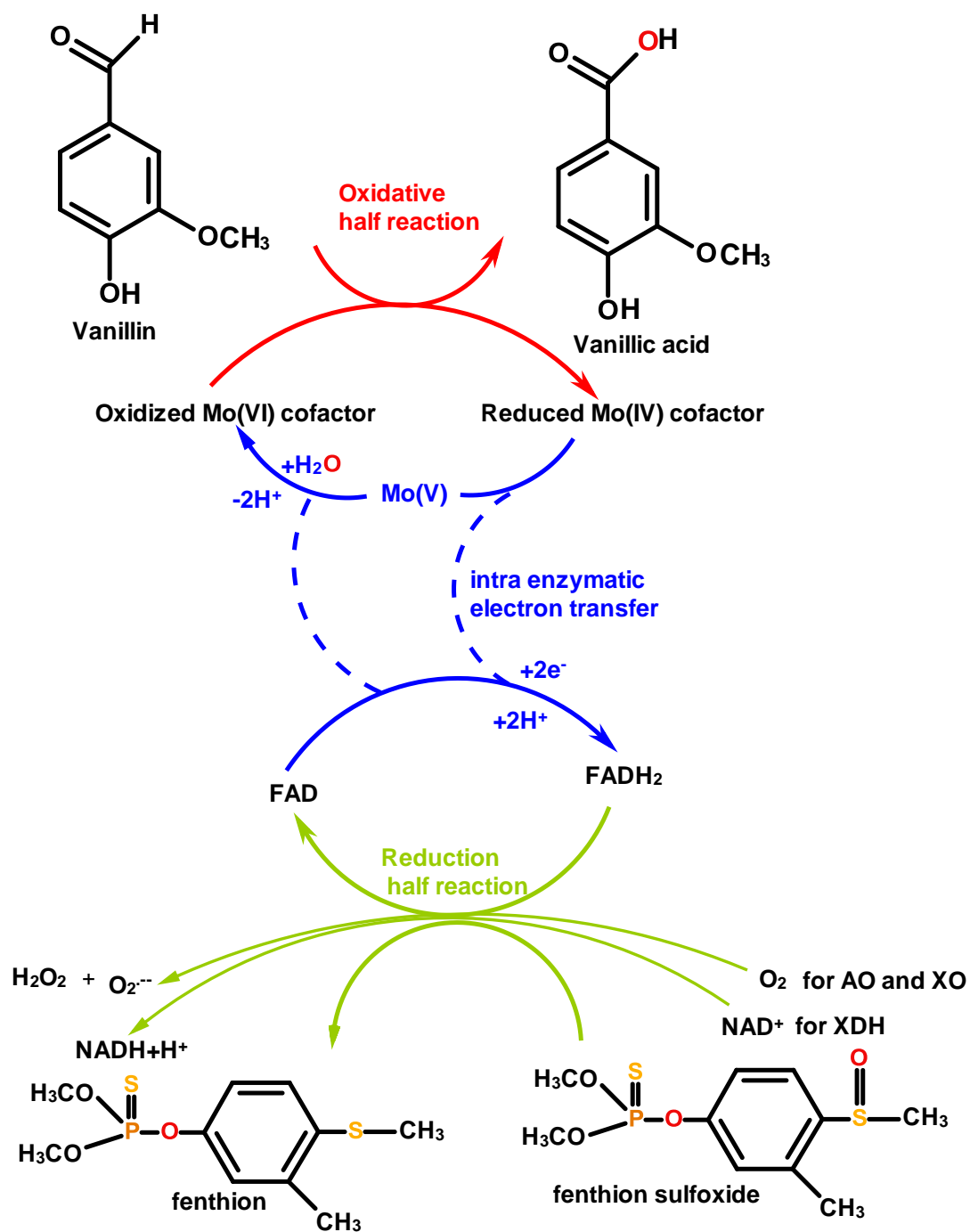
Figure 4: Oxidative and reduction half reaction and electron flow out from the molybdenum center of molybdo-flavoenzymes.

According to (Hille and Nishino. 1995, Nishino and Okamoto. 2000, Okamoto *et al.*, 2004, Beedham. 2010, Okamoto *et al.*, 2013).

The mechanism of AOX and XOR inhibitors was proposed by Fridovich and Handler. (1962), Rajagopalan and Handler (1962, 1964 and 1968) and Beedham C (1987) that suggest 4 electrons carriers in molybdenum center of rabbit hepatic AOX and XOR are responsible for the mechanism and reaction with artificial electron acceptors. These studies demonstrated that ferricyanide, methylene blue, phenazine methosulphate react at the iron sulphur cluster and 2, 6 dichlorophenol-indophenol (DCPIP) at near to the molybdenum cofactor and that dyes nitroblue tetrazolium (NBT), trinitrobenzensulfonic acid and dimethylthiazol-diphenyltetrazolium bromide (MTT) react at the FAD site. Cytochrome c and with oxygen in addition to NAD^+ also react at the FAD center as in seen (Figure 5) (Fridovich and Handler. 1962, Rajagopalan *et al.*, 1962, Rajagopalan and Handler. 1964a, Rajagopalan *et al.*, 1968, Beedham. 1987).
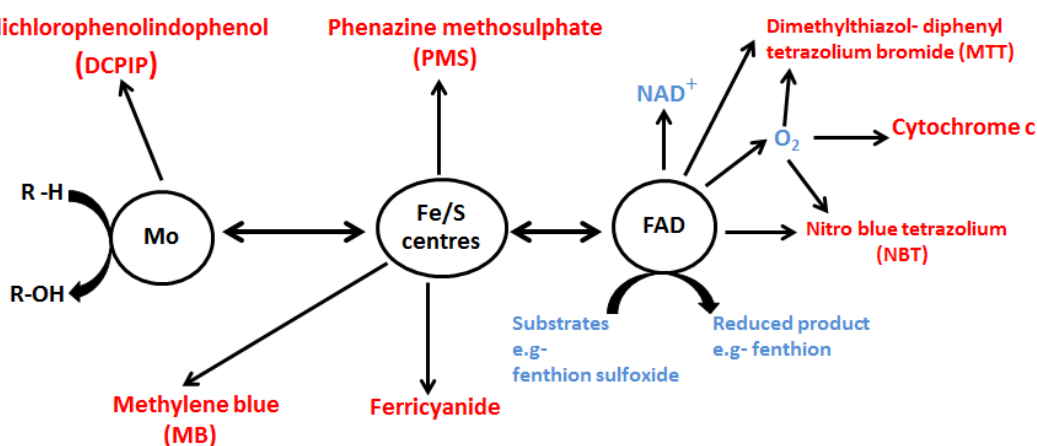
Figure 5: Postulated linear electron transfer sequence and site of electron egress to acceptors. Red colour indicates artificial electron acceptor and blue colour indicates natural acceptors.

In molybdo-flavoenzymes reactions the oxygen atom used in the hydroxylation reaction of the carbon center of substrates containing N-heterocycle or aldehyde functional groups is derived from water molecule rather than that from oxygen (O_2) itself as shown in (Figure 6) (Hille. 2005).

$$\text{R-H} + \text{H}_2\text{O} \xrightarrow[\text{XOR}]{\text{AOX}} \text{R-OH} + 2\text{H}^+ + 2\text{e}^-$$

Substrate   Water Molecule   Oxidized Substrate   Protons   Reducing Equivalents
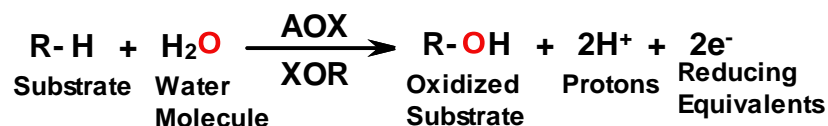
Figure 6: Oxidation reaction by molybdo-flavoenzymes AOX and XOR.

Oxidation reaction catalyzed by molybdo-flavoenzymes AOX and XOR generating an oxidized substrate and also two reducing equivalents (Hille and Sprecher. 1987, Xia *et al.*, 1999, Beedham. 2001, Hille. 2005, Brondino *et al.*, 2006, Okamoto *et al.*, 2013).

An example of an aldehyde substrate (vanillin) and its corresponding metabolite a carboxylic acid (vanillic acid) is shown in Figure 7, while another example for an N-heterocycle (1-methylxanthine) and its corresponding metabolite a uric acid (1-methyluric acid) is shown in Figure 8.
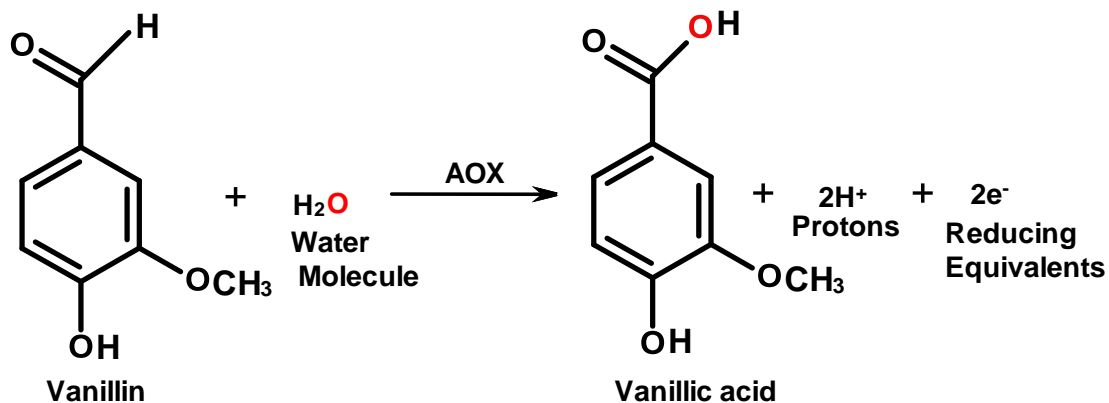
Figure 7: Oxygen atom transfer reaction molybdo-flavoenzyme involving an aldehyde.

The oxygen incorporated into the vanillic acid is from a water molecule. According to (Obach. 2004, Arnaud. 2011).
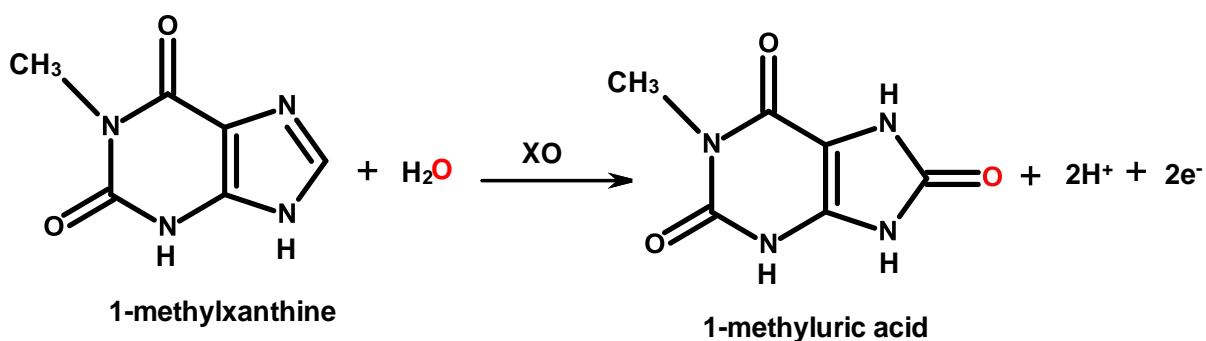
Figure 8: Oxygen atom transfer reaction molybdo-flavoenzyme involving an N-heterocycle

The oxygen incorporated into the 1-methyluric acid is from a water molecule. According to (Obach. 2004, Arnaud. 2011).

1.3. Substrate specificity of aldehyde oxidase and xanthine oxidoreductase

Many different aliphatic compounds such as aromatic aldehydes and also N-heterocyclic compounds are substrates for AOX and XOR that are biotransformed to their carboxylic acid or hydroxylated N-heterocyclic metabolites (Beedham. 2001, Garattini *et al.*, 2003, Garattini *et al.*, 2008, Garattini and Terao. 2011, Garattini and Terao. 2012, Garattini and Terao. 2013). Although the class of substrates of MFEs are similar in their structure, AOX and XOR differ in inhibitor response as well as substrate specificity (Krenitsky *et al.*, 1986, Beedham. 2001, Kitamura *et al.*, 2006, Mendel and Bittner. 2006a, Kundu *et al.*, 2007, Beedham. 2010, Pryde *et al.*, 2010, Garattini and Terao. 2012, Garattini and Terao. 2013). A list of AOX and XOR substrates that illustrate the substrate specificity of the two enzymes are given in Table 1, many of which were utilised in the study detailed in this thesis.

Table 1: Examples of mammalian molybdo-flavoenzyme substrates

Substrates	AOX	XOR	References
Allopurinol **(hyperuricemia drug)**	++	+++++	(Krenitsky *et al.*, 1972, Krenitsky *et al.*, 1986, Reiter *et al.*, 1990, Yamamoto *et al.*, 1991, Beedham. 2001, Garattini and Terao. 2011, Garattini and Terao. 2012, Garattini and Terao. 2013)
Azaarenes (phenanthridine, phthalazine[**], acridine, quinoline, isoquinoline, 1-hydroxyisoquinoline, 3-hydroxyisoquinoline, quinoxaline, quinazoline and cinnoline) **Environmental pollutants**	+++++	- ++[**]	(Sorouraddin *et al.*, 2009, Garattini and Terao. 2011, Garattini and Terao. 2012, Rashidi *et al.*, 2013), (Beedham *et al.*, 1990, Obach. 2004, Panoutsopoulos and Beedham. 2004, Kitamura *et al.*, 2006, Barr and Jones. 2011, Garattini and Terao. 2011, Garattini and Terao. 2012, Garattini and Terao. 2013)
Cinchona alkaloid (cinchonine, cinchonidine, quinine and quinidine) **Drugs and environmental pollutants**	+++++	-	(Palmer *et al.*, 1969, Beedham *et al.*, 1992, Itoh *et al.*, 2006, Al-Tayib. 2009, Liu *et al.*, 2009)
Hypoxanthine **(endogenous purine)**	-	+++++	(Krenitsky *et al.*, 1972, Kitamura *et al.*, 2006, Chen *et al.*, 2012, Pasalic *et al.*, 2012, Okamoto *et al.*, 2013)
6-Mercaptopurine **(anti-cancer drug)**	++	+++++	(Kitamura *et al.*, 2006, Rashidi *et al.*, 2007, Garattini and Terao. 2011, Sorouraddin *et al.*, 2011, Garattini and Terao. 2012)
Methotrexate **(anti-cancer drug)**	+++++	-	(Johns. 1967, Beedham. 1985, Chladek *et al.*, 1997, Jordan *et al.*, 1999, Kitamura *et al.*, 1999, Beedham. 2001, Kitamura *et al.*, 2006, Liu *et al.*, 2009)
1-Methylxanthine **(caffeine metabolite)**	-	+++++	(Krenitsky *et al.*, 1972, Reinke *et al.*, 1987, Arnaud. 2011)
N[1]-Methylnicotinamide **(endogenous vitamin metabolite)**	+++++	+	(Murashige *et al.*, 1966, Krenitsky *et al.*, 1972, Ohkubo and Fujimura. 1978, Kitamura *et al.*, 2006, Tayama *et al.*, 2007, Kitamura *et al.*, 2008, Peretz *et al.*, 2012)
Pyrazinamide **(tuberculosis drug)**	++	+++++	(Yamamoto *et al.*, 1987, Yamamoto *et al.*, 1991, Shibutani *et al.*, 1999, Kitamura *et al.*, 2006)
Pyridoxal **(vitamin B6)**	+++++	-	(Stanulovic and Chaykin. 1971, Krenitsky *et al.*, 1972, Kitamura *et al.*, 2006, Garattini and Terao. 2011, Garattini and Terao. 2012, Peretz *et al.*, 2012, Garattini and Terao. 2013)
All-trans retinal **(vitamin A aldehyde)**	+++++	-	(Kitamura *et al.*, 2006, Garattini *et al.*, 2008, Terao *et al.*, 2009, Garattini and Terao. 2011, Garattini and Terao. 2012, Chen and Reese. 2013, Garattini and Terao. 2013)
Vanillin **(present in food stuffs)**	+++++	-	(Beedham. 2001, Obach. 2004, Panoutsopoulos *et al.*, 2005, Garattini and Terao. 2011, Garattini and Terao. 2012, Garattini and Terao. 2013)
Xanthine **(endogenous purine)**	-	+++++	(Krenitsky *et al.*, 1972, Yamamoto *et al.*, 2007, Chen *et al.*, 2012, Pasalic *et al.*, 2012, Okamoto *et al.*, 2013)

(+++++ = high activity ++   = intermediate activity + = low activity - = no activity). ** Of the azaarenes listed only phthalazine is a substrate for XOR.

With regards endogenous roles of MFEs the best known role of XOR is in endogenous purine degradation in which it is involved in the biotransformation of hypoxanthine into xanthine and into the more polar metabolite uric acid (Figure 9) (Krenitsky *et al.*, 1972, Nishino and Okamoto. 2000, Kitamura *et al.*, 2006, Garattini *et al.*, 2008, Okamoto *et al.*, 2013).
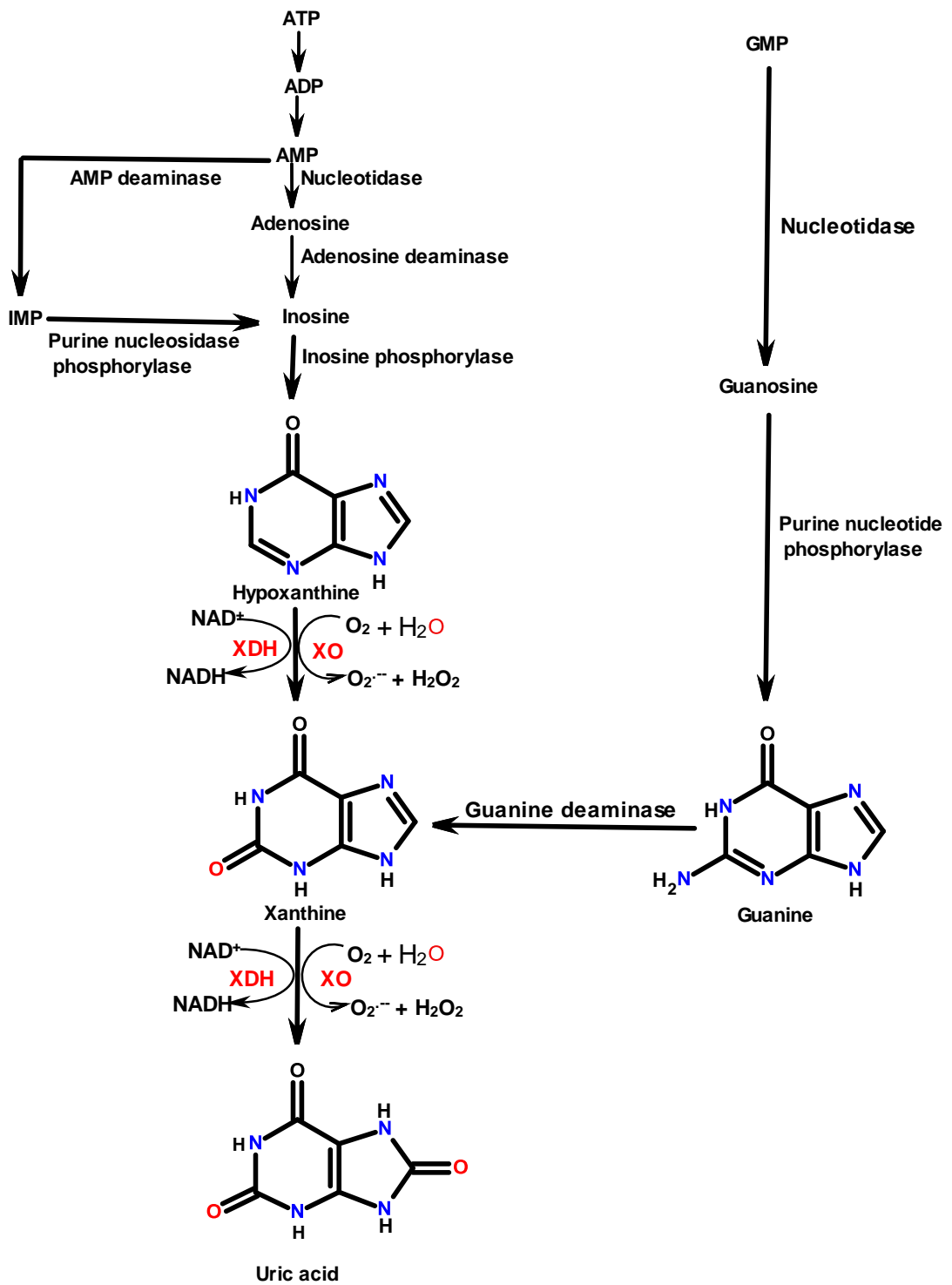
Figure 9: Role of xanthine oxidoreductase in endogenous purine catabolism in mammals.

ADP: adenosine diphosphate, AMP: adenosine monophosphate, ATP: adenosine triphosphate, GMP: guanosine monophosphate, IMP: inosine monophosphate, XDH: xanthine dehydrogenase, XO: xanthine oxidase(Pacher *et al.*, 2006, Chen *et al.*, 2012, Pasalic *et al.*, 2012, Okamoto *et al.*, 2013).

Due to structural similarity to the endogenous substrates, many exogenous methylated xanthines are also substrates for XOR. XOR is involved in the oxidative metabolism of the exogenous food constituent and pharmacological agent caffeine (1, 3, 7 trimethylxanthine). This is shown in Figure 10, where cytochrome P450 1A2 is involved in the initial demethylation steps and XOR is involved in the final oxidation to generate the polar 1-methyluric acid that is excreted(Krenitsky *et al.*, 1972, Hamelin *et al.*, 1994, Streetman *et al.*, 2000, Arnaud. 2011).
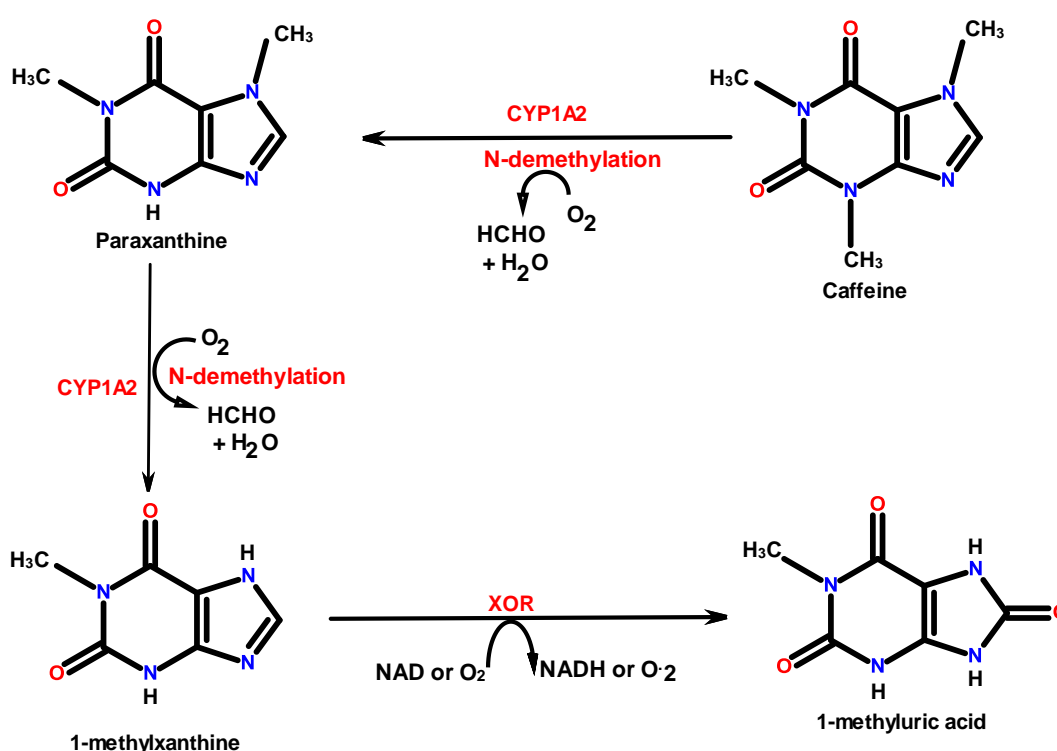
Figure 10: The role of xanthine oxidoreductase in caffeine metabolism.

CYP: cytochrome P-450. XOR: xanthine oxidoreductase (Relling *et al.*, 1992, Hamelin *et al.*, 1994, Baselt and Cravey. 1996, Arnaud. 2011).

With regards AOX there are three well documented endogenous substrates. All-trans retinaldehyde is an endogenous substrate for AOX (Figure 11), that plays an important role in the visual process. It has been suggested that AOX may play an important role in this visual process by biotransformation of all-trans retinaldehyde

to its corresponding carboxylic acid metabolite which is retinoic acid, which known as the active form of vitamin A(Beedham. 2001, Kitamura *et al.*, 2006, Garattini *et al.*, 2008, Garattini and Terao. 2011, Garattini and Terao. 2012, Garattini and Terao. 2013). The biotransformations of all-trans retinaldehyde by AOX to its corresponding carboxylic acid metabolite all-trans retinoic acid (RA) was first observed in rabbit liver cytosol, who discovered that the biotransformation activity did not need addition of NAD^+ for its biotransformation process (Tomita *et al.*, 1993, Tsujita *et al.*, 1994, Garattini *et al.*, 2008, Chen and Reese. 2013, Garattini and Terao. 2013).
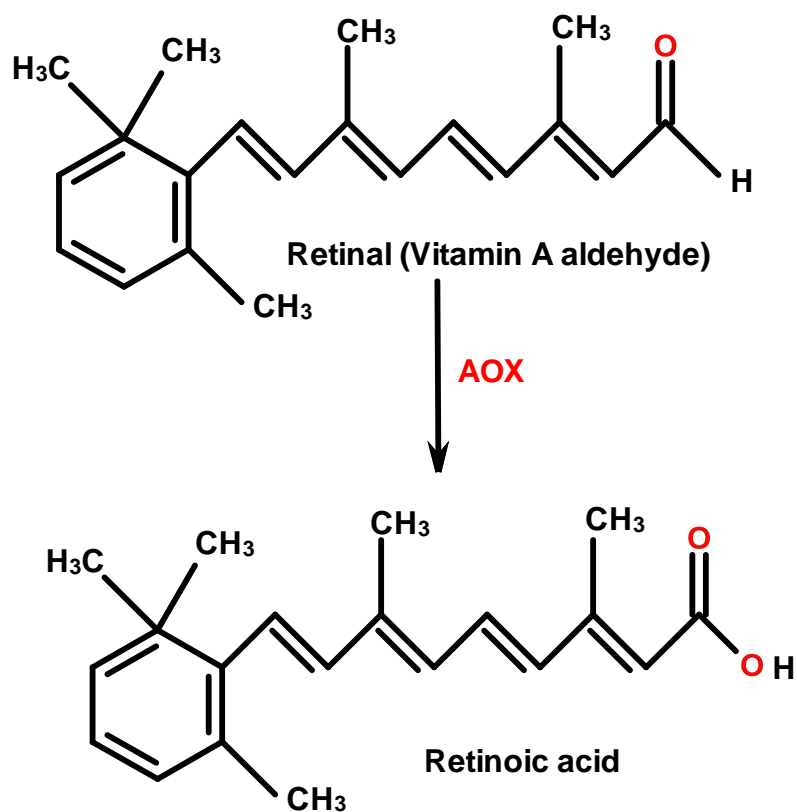
Figure 11: Biotransformation of all-trans retinal to retinoic acid by aldehyde oxidase. Based on. Chen and Reese, 2013.

Another endogenous aldehyde that is an AOX substrate is pyridoxal (vitamin B6). Pyridoxal its biotransformed to its corresponding carboxylic acid metabolite (4-pyridoxic acid) by AOX (Figure 12) (Beedham. 2001, Garattini *et al.*, 2003, Kitamura *et al.*, 2006, Garattini *et al.*, 2008, Garattini and Terao. 2011, Garattini and Terao. 2012, Peretz *et al.*, 2012, Garattini and Terao. 2013). Interestingly in mice pyridoxal can be biotransformed by purified mouse aldehyde oxidase AOX1 as well as AOH1 but it is not a substrate for AOH2 (Garattini *et al.*, 2008).
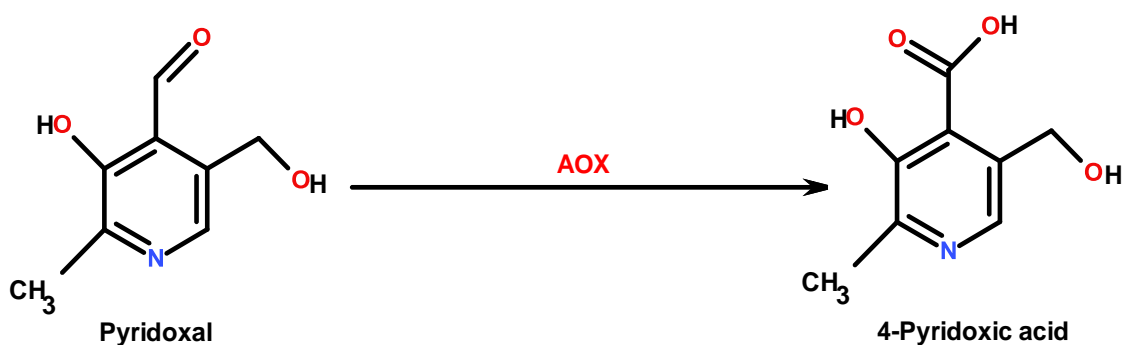
Figure 12: Oxidation of pyridoxal to 4-pyridoxic acid by aldehyde oxidase. According to. Peretz *et al*., 2012.

As well as the oxidation of non-charged N-heterocyclic AOX is also involved in the oxidation of charged N-heterocyclic which have a CH=N$^+$ group. An example for such a compounds as corresponding metabolite of vitamin B3 (N^1-methylnicotinamide) that metabolised by AOX and XO (Figure 13) (Murashige *et al.*, 1966, Ohkubo and Fujimura. 1978, Beedham. 1987, Shibata *et al.*, 1988, Beedham. 2001, Sugihara *et al.*, 2006, Kundu *et al.*, 2007, Pryde *et al.*, 2010).
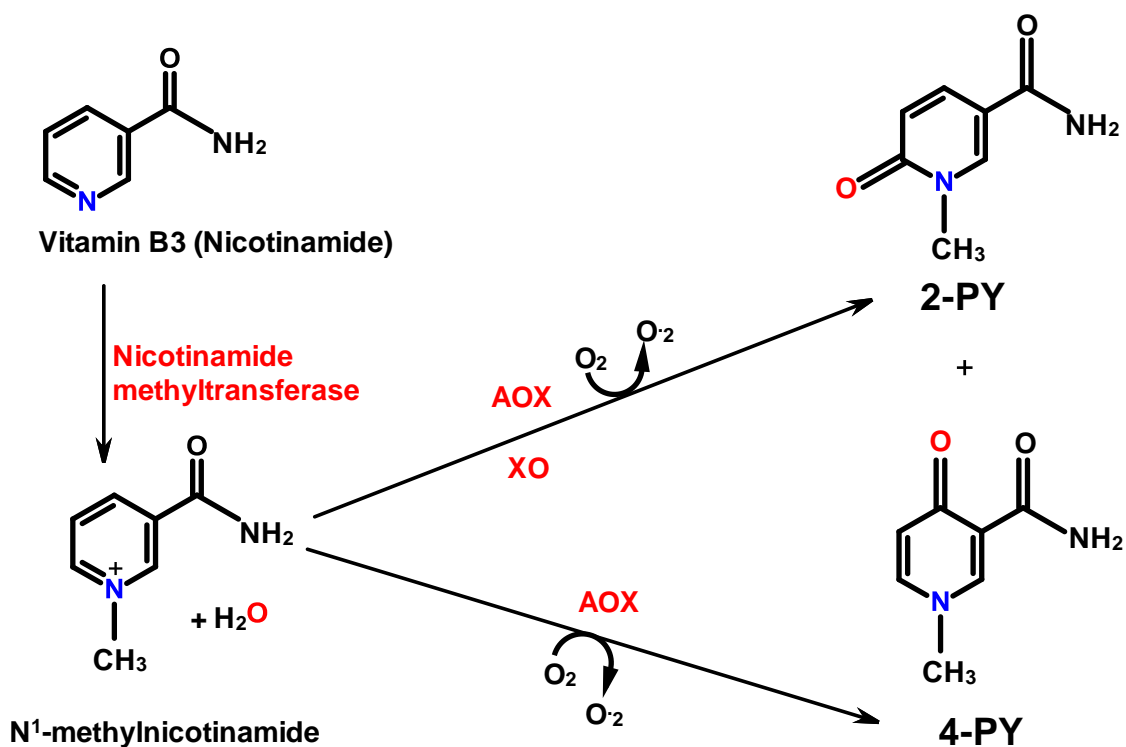
Figure 13: Biotransformation of vitamin B3 in mammals.

The oxidation of N^1-methylnicotinamide by AO to N^1-methyl-2-pyridone-5-carboxamide (2-PY) and N^1-methyl-4-pyridone-5-carboxamide (4-PY).Started with methylation of nicotinamide by nicotinamide methyltransferase according to Pryde *et al*., 2010.

As well as aldehydes, AOX can also catalyse the oxidation of nitrogen containing polycyclic aromatic hydrocarbons (NPAHs) which have a CH=N- group (Table 1) that are environmental pollutant, an example for these compounds is phthalazine (Figure 14), which its biotransformed to its corresponding metabolite 1-phthalazinone by mammalian AOX(Stubley *et al.*, 1979, Beedham *et al.*, 1990, Obach. 2004, Panoutsopoulos and Beedham. 2004, Barr and Jones. 2011).
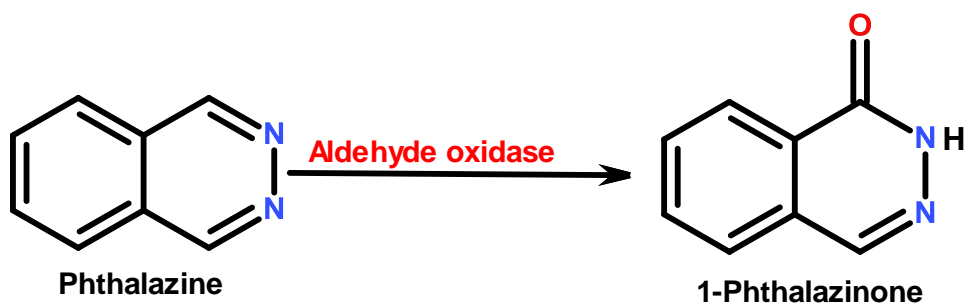
Figure 14: Oxidation of phthalazine by aldehyde oxidase to 1-phthalazinone (Obach. 2004, Barr and Jones. 2011).

Another example for an nitrogen containing polycyclic aromatic hydrocarbons (NPAHs) AOX substrate is phenanthridine that is biotransformed to more polar metabolite phenanthridinone by AOX (Figure 15) aiding its excretion (Blumer *et al.*, 1977, Beedham. 2001, Kitamura *et al.*, 2006, Sorouraddin *et al.*, 2009). Phenanthridine is an azaarene pollutant found in terrestrial and aquatic environments from industrial activities associated with fossil fuels (Blumer *et al.*, 1977, Balch *et al.*, 1995, Osborne *et al.*, 1997, de Voogt and Laane. 2009).
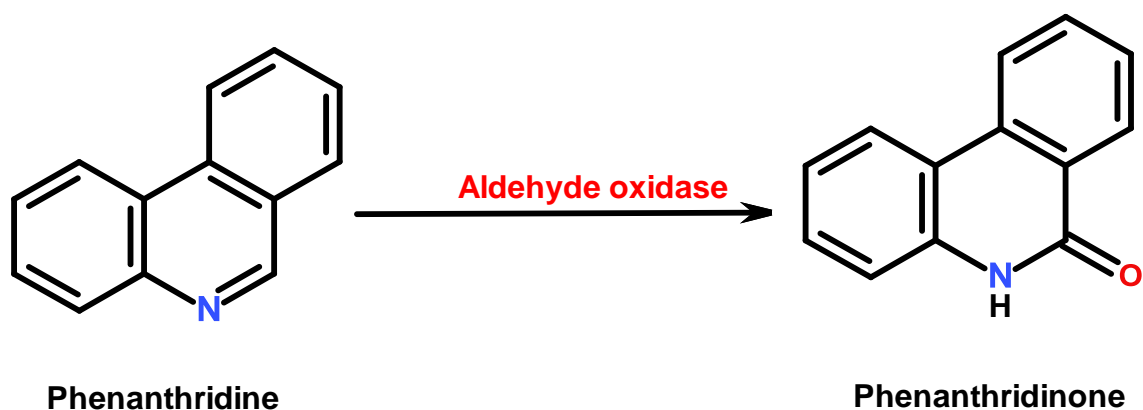
Figure 15: Biotransformation of phenanthridine to its metabolite phenanthridinone by AOX. Based on .Sorouraddin *et al.*, 2009.

One important drug substrate for AOX is the pteridine compound methotrexate (4-amino-N[10]-methylpteroyl-L-glutamic acid). This anti-leukemia drug is biotransformed by AOX to 7-hydroxymethotrexate (Figure 16) (Kitamura *et al.*, 2006, Garattini *et al.*, 2008, Liu *et al.*, 2009, Pryde *et al.*, 2010, Garattini and Terao. 2011, Garattini and Terao. 2012, Garattini and Terao. 2013).
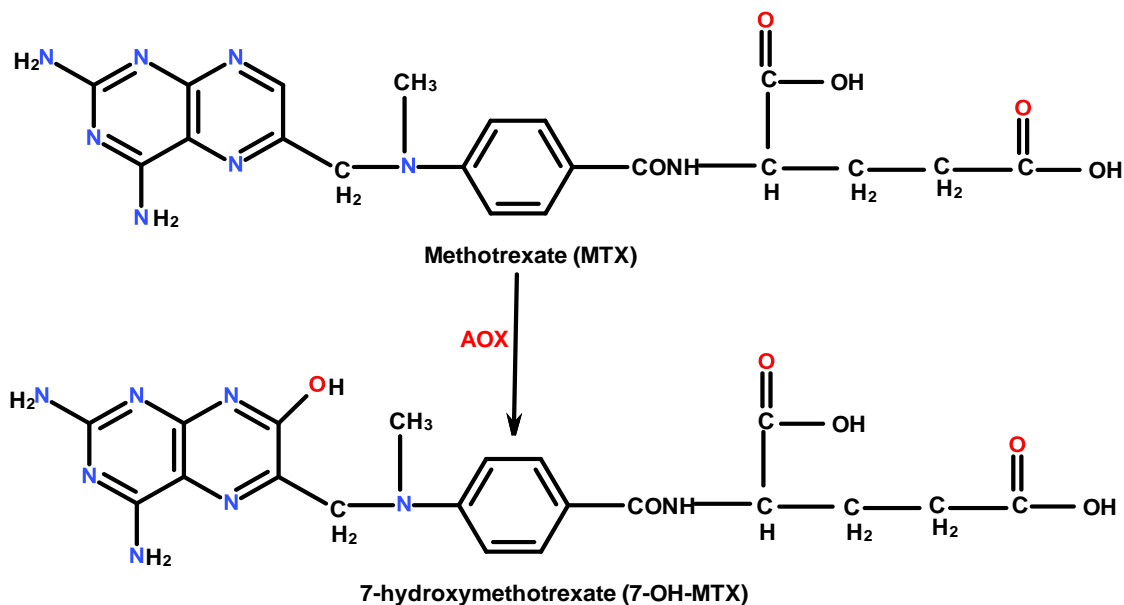
Figure 16: Metabolism of methotrexate to its corresponding metabolite 7-hydroxymethotrexate by AOX. According to (Liu *et al.*, 2009, Pryde *et al.*, 2010, Garattini and Terao. 2013).

Another example of a substrate for AOX as well as XOR is 6-mercaptopurine. This purine drug is biotransformed by XO to 6-mercaptopurine-2-one (6-thioxanthine) and 8-hydroxy-6-mercaptopurine and further biotransformation to its final metabolite 6-thiouric acid by both AOX and XOR. 6-methylmercaptopurine which is another metabolite of 6-mercaptopurine is produced by methyltransferase which is also further biotransformation to final metabolite 8-oxo-6-methylmercaptopurine by both XO and AOX (Figure 17) (Beedham. 2001, Kitamura *et al.*, 2006, Rashidi *et al.*, 2007, Sorouraddin *et al.*, 2011, Garattini and Terao. 2013).
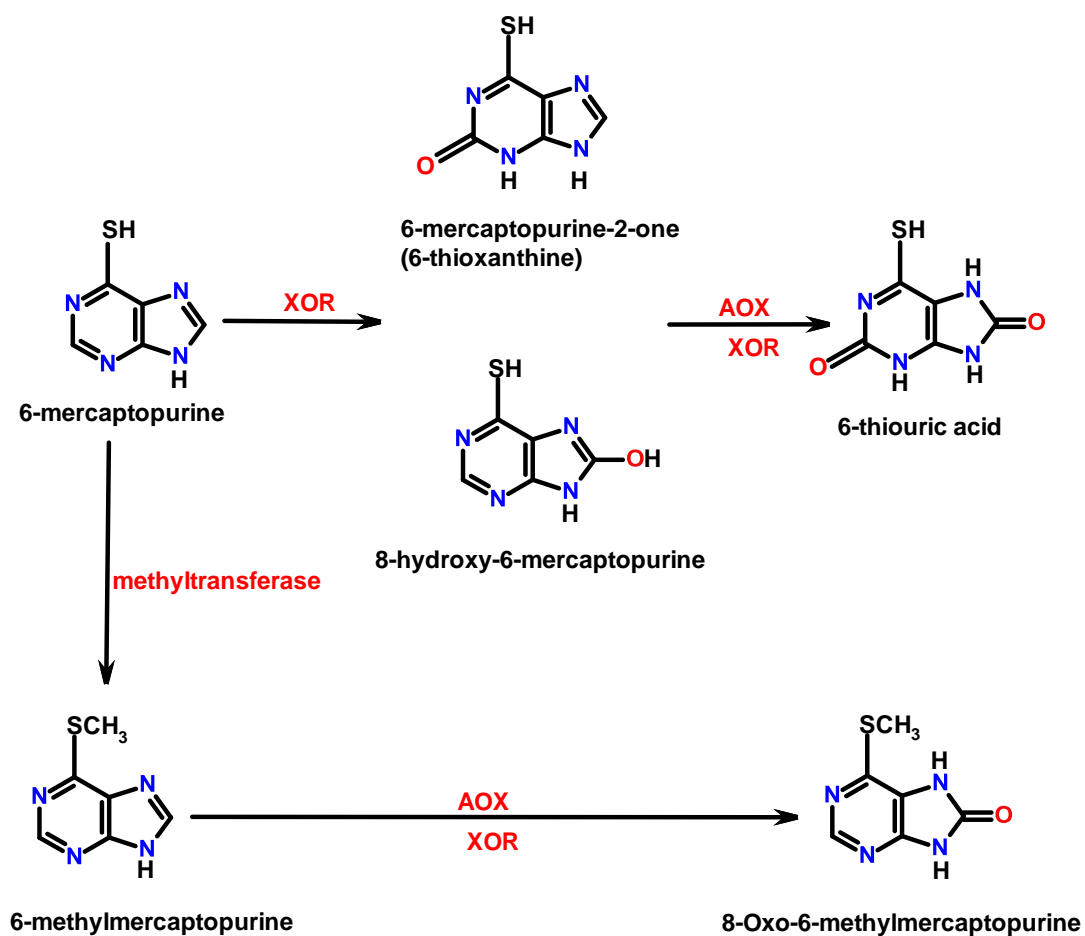
Figure 17: Biotransformation of 6-mercaptopurineby AOX and XOR.

According to (Beedham. 2001, Rashidi *et al.*, 2007, Sorouraddin *et al.*, 2011, Garattini and Terao. 2013)

Both AOX and XOR are also involved in reductive activity with many substrates in the presence of an electron donor in anaerobic condition. (Beedham. 2001, Obach. 2004, Kitamura *et al.*, 2006, Beedham. 2010). The reductive activity of AOX is generally found to be greater than that of XOR with many substrates according to (Beedham. 2001). Tables 2 and 3 summarise the reductive activities of AOX and XOR with different compounds.

Table 2: Aldehyde oxidase catalyzed reduction of different compounds in mammals.

AOX substrates	AOX generated metabolites	References
Acetophenone oxime, salicylaldoxime and benzamidoxime	Corresponding oxo compounds and a ketimine	(Tatsumi and Ishigai. 1987)
Aromatic and heterocyclic hydroxamic acids (e.g salicylhydroxamic acid, nicotinohydroxamic acid and anthranilhydroxamic acid	Amides (salicylamide, nicotinamide and anthranilamide)	(Sugihara and Tatsumi. 1986, Katsura *et al.*, 1993)
Fenthion sulfoxide	Fenthion	(Leoni *et al.*, 2008)
Methyl red and orange	Cleavage of the azo linkage, Dimethyl-p-phenylenediamine and O-amino benzoic acid	(Kitamura and Tatsumi. 1983, Stoddart and Levine. 1992, Miyajima *et al.*, 2000)
Nicotinamide-N-oxide, imipramine-N-oxide, cyclobenzaprine-N-oxide and s-(-)-nicotine-1-N-oxide	Their parent amines (nicotinamide, imipramine, cyclobenzaprine and nicotine)	(Kitamura and Tatsumi. 1984, Sugihara *et al.*, 1996, Kitamura *et al.*, 2001)
Nitrated polycyclic hydrocarbons	Hydroxylamines	(Tatsumi *et al.*, 1986)
Nitrosoamines (N-nitrosodiphenylamine)	Hydrazines (1,1-diphenylhydrazine)	(Tatsumi *et al.*, 1983)
Sulindac sulfoxide	Sulindac sulfide	(Pay *et al.*, 1980, Duggan. 1981, Kitamura *et al.*, 2001)
Zonisamide	2-sulfamoylacetylphenol	(Kitamura *et al.*, 2001)

Table 3: Xanthine oxidoreductase catalyzed reduction of different compounds in mammals.

XOR substrates	XOR generated metabolites	References
6-bromomethyl-(9H)-purine	6-methylpurine	(Porter. 1990)
Doxorubicin	Its semiquinone metabolites	(Yee and Pritsos. 1997, Barnabe *et al.*, 2002)
Mitomycin C	2,7-diaminomitosene	(Pan *et al.*, 1984, Gustafson and Pritsos. 1992)
Nitrated polycyclichydrocarbons	Hydroxylamines	(Tatsumi *et al.*, 1986)
S-(-)-nicotine-1-N-oxide	Nicotine	(Sugihara *et al.*, 1996)

1.4. Molybdo-flavoenzymes inhibitors.

For many years, inhibitors of AOX and XOR have been described with varying degrees of detail(Rajagopalan *et al.*, 1962). The inhibitors have been used in many *in vitro* systems such as partially purified enzyme, recombinant expressed enzyme, liver cytosol and liver slices and across several species most notably rabbit, guinea pig and human. Inhibitors are proposed to affect different domains and prosthetic groups in AOX and XOR (Johns. 1967, Yoshihara and Tatsumi. 1985, Yoshihara and Tatsumi. 1997, Sugihara *et al.*, 1999, Beedham. 2001, Kitamura *et al.*, 2003, Vila *et al.*, 2004, Pacher *et al.*, 2006, Diamond *et al.*, 2010, Pryde *et al.*, 2010, Barr and Jones. 2011).

1.4.1. Aldehyde oxidase inhibitors

Examples of AOX inhibitors are menadione, estradiol, chlorpromazine and phenanthridine which are of widely differing chemical structure (Figure 18). Menadione (vitamin K_3) is a quinone that was discovered as a specific non-competitive AOX inhibitor by Rajagopalan et *al*., (1962) in rabbit liver with N^1-methylnicotinamide as a substrate. Since then many other researchers have confirmed this in a multitude of species summarised in Table 4 and 5 with a variety of AOX

substrates. Estradiol was found to be a non-competitive AOX inhibitor by Johns (1967) in human liver with variety of AOX substrates as summarised in Table 4.

Menadione

Phenanthridine

Estradiol

17α-ethinyl estradiol

Raloxifene

Chlorpromazine
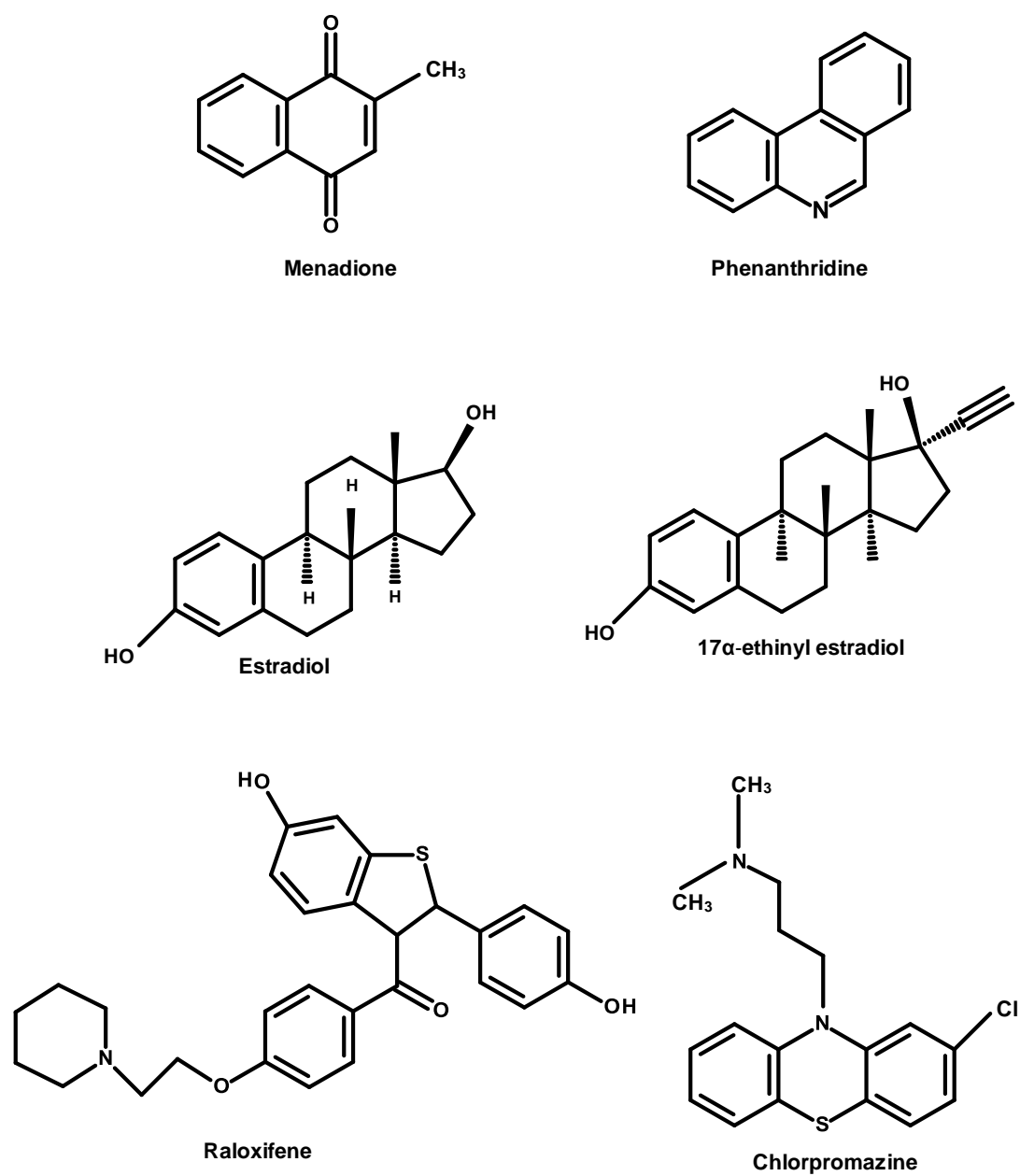
Figure 18: Structures of the aldehyde oxidase inhibitors. According to Merck Index (2014)

Species/tissue	Substrate	Inhibitor	Substrate Concentration	Inhibitor Concentration	Ki or inhibition %	Mode of inhibition	References
Human/liver	Phthalazine and DMAC	Raloxifene	5-100μM	1-10μM	0.8nM	Uncompetitive	(Choughule *et al.*, 2013)
Human/ liver	Phthalazine and vanillin	Menadione, estradiol and 17α-ethinyl estradiol	2μM	50μM	0.29μM and 0.57μM respectively	Mixed mode of inhibition, almost uncompetitive	(Obach. 2004)
Human /liver	Phthalazine	Menadione	2μM	50μM	0.20μM	Non-competitive	(Obach *et al.*, 2004)
Human /liver	Phthalazine	Chlorpromazine	2μM	50μM	0.57μM	competitive	(Obach *et al.*, 2004)
Human /liver	Phthalazine	estradiol, 17α-ethinyl estradiol	2μM	50μM	0.29μM and 0.57μM	Uncompetitive	(Obach *et al.*, 2004)
Human /liver	Phthalazine	Raloxifene	2μM	50μM	0.0029μM	Uncompetitive	(Obach *et al.*, 2004)
Human /liver	Benzaldehyde, phenazine methosulfate (PMS)	Menadione	56 μM	15 μM, 0.08 μM and 5 μM	55%	Non-competitive	(Johns. 1967)
Human /liver	Benzaldehyde, phenazine methosulfate (PMS)	β-estradiol	56 μM	15 μM, 0.08 μM and 5 μM	50%	Non-competitive	(Johns. 1967)
Human /liver	Benzaldehyde, phenazine methosulfate (PMS)	Chlorpromazine	56 μM	15 μM, 0.08 μM and 5 μM	51%	Competitive	(Johns. 1967)
Human /liver	2-Hydroxypyrimidine, benzaldehyde	Chlorpromazine	0.5μM	1 mM and 0.4 mM	45%	Competitive	(Johns. 1967)
Human/ liver	2-hydroxy-5-fluropyrimidine	Menadione	0.54μM	25 μM	46%	Non-competitive	(Johns. 1967)
Human/ liver	Phthalazine and DMAC	Raloxifene, estradiol, ethinyl estradiol, menadione and chlorpromazine	5-100μM	0.1μm to 5μM	0.29μM, 0.57μM, 0.2μM and 0.57μM	Uncompetitive, non-competitive	(Barr and Jones. 2011, Barr and Jones. 2013)
Human/liver	Phthalazine	Chlorpromazine and estradiol	0.03-25μM (3μM)	50μM	0.27 μM and 0.62 μM respectively	Non-competitive and uncompetitive	(Nirogi *et al.*, 2013)

Table 4: Summary of the effects of prototypical inhibitors on human aldehyde oxidase.

Species/tissue	Substrate	Inhibitor	Substrate Concentration	Inhibitor Concentration	Ki or inhibition %	Mode of inhibition	References
Bovine/ liver	N^1-methylnicotinamide	Phenanthridine	12 mM	0.2 mM	-	Competitive	(Yielding and Tomkins. 1961)
Guinea pig/liver	DMAC	Raloxifene	5-100μM	1-10μM	3.2μM	Uncompetitive	(Choughule *et al.*, 2013)
Guinea pig /liver	Phthalazine	Raloxifene	5-100μM	1-10μM	42nM	Uncompetitive	(Choughule *et al.*, 2013)
Rhesus monkey /liver	All-trans retinal (vitamin A)	Menadione	0.01mM, 0.1mM and 1mM	0.02mM, 0.2mM and 2mM	60%, 28% and 15%	Non-competitive	(Lakshmanan *et al.*, 1964)
Rhesus monkey/liver	DMAC	Raloxifene	5-100μM	1-10μM	22μM	competitive	(Choughule *et al.*, 2013)
Rhesus monkey/liver	Phthalazine	Raloxifene	5-100μM	1-10μM	230 nM	competitive	(Choughule *et al.*, 2013)
Rabbit /liver	Phthalazine	Benzamidine	2μM	5mM	-	-	(Stell *et al.*, 1989)
Rabbit / liver	Benzaldehyde, phenazine methosulfate (PMS)	Chlorpromazine	56 μM and 0.5μM	5 μM	50% and 48%	Competitive	(Johns. 1967)
Rabbit/ liver	Benzaldehyde, 2-hydroxpyrimidine and N^1-methylnicotinamide	Menadione, chlorpromazine and KCN	2mM	200μM and 500μM, 500μM and 1000μM respectively	78%, 48%, 48% and 18%	Non-competitive	(Dick *et al.*, 2005, Dick *et al.*, 2007)
Rabbit /liver	N^1-methylnicotinamide	Menadione	1.5 mM	0.1 μM	85%	Non-competitive	(Rajagopalan *et al.*, 1962)
Rabbit /liver	N^1-methylnicotinamide	Estradiol	5 mM	0.2 μM	62%	Non-competitive	(Rajagopalan *et al.*, 1962)
Rabbit /liver	Phenazine methosulphate, nitro blue tetrazolium (NBT)	Menadione	5 mM	1.6 μM	-	Non-competitive	(Rajagopalan and Handler. 1964a)
Rabbit /liver	Phenazine methosulphate, nitro blue tetrazolium (NBT)	Estradiol	5 mM	16 μM	-	Non-competitive	(Rajagopalan and Handler. 1964a)
Sea bream /liver	2-hydroxypyrimidine, N^1-methylnicotinamide or butyraldehyde	Menadione and β-estradiol	12 mM	0.1 mM	75% and 60%	Non-competitive	(Kitamura *et al.*, 2003)
Sea bream /liver	2-hydroxypyrimidine, N^1-methylnicotinamide or butyraldehyde	Chlorpromazine	12 mM	0.1 mM	78%	Non-competitive	(Kitamura *et al.*, 2003)

Table 5: Summary of the effect of aldehyde oxidase inhibitors with non-human species.

Since then many other researchers have confirmed this in human, rabbit and sea bream liver as summarised in Table 4 and 5 with a variety of AOX substrates. The discovery of the related xenoestrogen oral contraceptive drug 17α-ethinyl estradiol as an uncompetitive AOX inhibitor was made by in Obach 2004 in human liver with phthalazine and vanillin as a substrates. Another non-competitive inhibitor of AOX is the drug chlorpromazine Johns (1967) in a different species with benzaldehyde and phenazine methosulphate as a substrate as summarised in Table 5. Since then many other researchers have confirmed this in a human, rabbit and sea bream liver as summarised in Table 4 and 5 with a variety of AOX substrates. Interestingly the osteoporosis drug raloxifene has been found to have competitive and non-competitive properties as an AOX inhibitor by many researchers such as Barr and Jones 2011, 2013 and Choughule *et al*. (2013) in human, guinea pig and rhesus monkey liver with phthalazine and DMAC as a substrate (Table 4). The environmental NPAHs, phenanthridine is a competitive inhibitor in bovine liver with N^1-methylnicotinamide as a substrate (Yielding and Tomkins. 1961). Finally the first researchers to find benzamidine as a specific AOX inhibitor was Stell *et al*. (1989) in rabbit liver with phthalazine as a substrate as summarised in Table 5.

1.4.2. Oxipurinol as a specific xanthine oxidoreductase inhibitor

With regards XOR inhibitor oxipurinol is the best documented. The inhibitor oxipurinol is generated when the anti-gout substrate drug allopurinol is biotransformed by XOR (Figure 19).
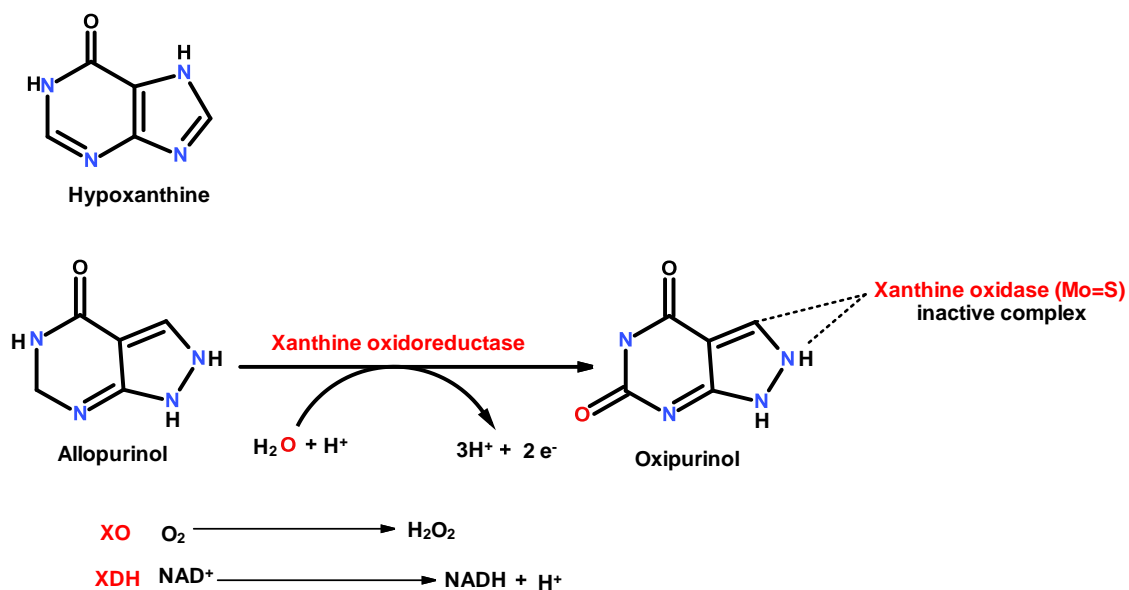
Figure 19: Generation of the xanthine oxidoreductase inhibitor oxipurinol from allopurinol. According to Barr and Jones, 2011, Barr and Jones, 2013.

The first researcher to find allopurinol and oxipurinol as a specific XOR inhibitor was by Elion. (1966) in bovine milk, mouse and human liver with xanthine as a substrate. Since then many other researchers have confirmed this in a multitude of species summarised in (Table 6) with xanthine and pterin as XOR substrates. The mode of inhibition with allopurinol and oxipurinol is competitive (Okamoto *et al*., 2008) and Nishino *et al*., 2008) (Table 6).

Species/tissue	Substrate	Inhibitor	Substrate Concentration	Inhibitor Concentration	Ki or inhibition %	References
Bovine /milk	Xanthine	Oxipurinol	0.15mM	100μM	1 μM	(Okamoto *et al.*, 2008)
Bovine/ milk	Hypoxanthine and xanthine	Oxipurinol	0.15mM	100μM	0.1 μM	(Nishino *et al.*, 2008, Okamoto *et al.*, 2008)
Bovine/ milk	Xanthine	Allopurinol	0.15mM	3.3 μM	0.9 nM	(Okamoto *et al.*, 2003)
Bovine/ milk	Xanthine	Allopurinol	40 μM	14-28 μM	6.3μM	(Elion. 1966)
Mouse/liver	Xanthine	Allopurinol	40 μM	14-28 μM	1.2 μM	(Elion. 1966)
Human/liver	Xanthine	Allopurinol	40 μM	14-28 μM	1.1 μM	(Elion. 1966)
Human/ liver	Pterin	Allopurinol	0.6-10μM	100μM	86%	(Obach. 2004)
Human/ liver	Xanthine	Allopurinol	0.15mM	0.1-2mM	4 μM	(Krenitsky *et al.*, 1986)
Wistar rat/liver	Pterin	Allopurinol	-	100μM	-	(Derbre *et al.*, 2012)

Table 6: Summary of the effects of xanthine oxidoreductase inhibitors allopurinol and oxipurinol with different mammalian species.

1.5. Species variation in molybdo-flavoenzyme activity.

Molluscs, crustaceans, insects, bacteria, fungi and all vertebrate classes have been found to contain the two molybdo-flavoenzymes (AOX and XOR)(Krenitsky *et al.*, 1972, Wurzinger and Hartenstein. 1974, Moura *et al.*, 1976, Woolfolk and Downard. 1977, Pometto and Crawford. 1983, Turner *et al.*, 1987, Glatigny and Scazzocchio. 1995, Romao *et al.*, 1995, Xu and Johnson. 1995, Schrader *et al.*, 1999, Beedham. 2001, Yasuhara *et al.*, 2002, Garattini *et al.*, 2008, Beedham. 2010).Many species differences show marked quantitative effects when using cinchonidine as substrate the AOX activity was lower in monkey than that in rabbits (Fukiya *et al.*, 2010). When is used zebularine as substrate with mouse, monkey and human and it was found that the activity of AOX was highest with mouse than that with monkey and human(Klecker *et al.*, 2006).Sugihara et al.(1997) found when using benzaldehyde and N^1-methylnicotinamide as substrates with human and monkey that the AOX activity with human was lower than that with monkey(Sugihara *et al.*, 1997). In comparison, rabbit AOX has lower reductase activity toward zonisamide as a substrate as compared to monkey(Kitamura *et al.*, 2001). When Kitamura and Tatsumi.(1984) used nicotinamide N-oxide as substrate with rabbits, hogs, guinea pig, hamster, rat and mice and it was found that all had similar AOX reductase activity(Kitamura and Tatsumi. 1984). On the other hand,Hirao et al.(1994) found lower AOX reductase activity with rat AOX than that with rabbit AOX when naphthalene 1,2-oxide and also benzo [a] pyrene-4,5-oxide were used as substrates(Hirao *et al.*, 1994).

1.5.1. Vertebrate molybdo-flavoenzymes

The number of MFE genes varies between mammals. It was found that the numbers of active AOX genes in vertebrates are ranged from 1 to 4 (Dickinson. 1971, Lindsley and Zimm. 1992 , Terao *et al.*, 2006, Garattini *et al.*, 2008, Garattini *et al.*, 2009, Terao *et al.*, 2009, Garattini and Terao. 2011, Garattini and Terao. 2012, Garattini and Terao. 2013, Kurosaki *et al.*, 2013).Some vertebrates such as Glires have four of AOX genes and one XOR gene (rat, mice, pika as well as rabbit)(Garattini *et al.*, 2008, Terao *et al.*, 2009, Garattini and Terao. 2011, Garattini and Terao. 2013, Kurosaki *et al.*, 2013). Mouse AOXs are the best characterised AOX genes and proteins for all vertebrates; Table 7 summarizes the tissue distribution and substrate specificity of mouse AOX. It is interesting that other mammalian species possess a reduced complement of functional MFE genes. Dogs (*Canis lupus familiaris*) possess two AOX genes (AOX4 and AOX3L1) and one XOR, while bovine (*Bos taurus*) has three AOX genes (AOX1, AOX4 and AOX3L1) and one XOR(Terao *et al.*, 2006, Kurosaki *et al.*, 2013).Humans have just one functional AOX gene (AOX1) and one XOR gene (Garattini *et al.*, 2008, Garattini and Terao. 2012, Garattini and Terao. 2013, Kurosaki *et al.*, 2013).The chicken (*Gallus gallus*) possesses two AOX genes (AOX1 and AOX2)and one XOR(Terao *et al.*, 2006, Kurosaki *et al.*, 2013).Cat (*Felix catus*) has just one functional AOX gene (AOX3L1) and one XOR gene(Garattini and Terao. 2013, Kurosaki *et al.*, 2013), while Cynomolgus monkey*(Macaca fascicularis)*and Rhesus monkey (*Macaca mulatta*) have two AOX genes (AOX1 and AOX3L1) and three AOX genes (AOX1,AOX4 and AOX3L1) respectively and one XOR(Garattini and Terao. 2013, Kurosaki *et al.*, 2013).Horse (*Equus caballus*) has three AOX genes (AOX1, AOX4 and AOX3L1) and one XOR gene ((Kurosaki *et al.*, 2013). Baboon (*Papio Hamadryas*)has three AOX genes (AOX1, AOX4 and AOX3L1) and only one

XOR gene (Kurosaki *et al.*, 2013). Interestingly dogs and cats do not express an AOX enzyme in hepatic tissue unlike other mammalian species studied (Terao *et al.*, 2006, Garattini and Terao. 2013, Kurosaki *et al.*, 2013).A listing of the current knowledge of MFEs AOX and XOR in several non-glire species is given on (Table 8 and 9).

Table 7: Summary of molybdo-flavoenzymes in mice

The substrate specificity along with tissue distribution of molybdo-flavoenzymes in mice. Based on (Kurosaki *et al.*, 2013).

Old enzyme nomenclature of AOX/XOR	New enzyme nomenclature of AOX/XOR	Tissue distribution	Known substrates	References
AOX1	Aox1	Liver, lung, heart, kidney, testis, brain, eye, spinal cord and spleen	Butyraldehyde, nicotinamide, octanal, phthalazine, all-trans retinaldehyde, pyridoxal, vanillin, 2-hydroxpyrimidine	(Moriwaki *et al.*, 1996, Kurosaki *et al.*, 1999, Wright *et al.*, 1999, Kurosaki *et al.*, 2004, Vila *et al.*, 2004, Garattini *et al.*, 2008, Garattini *et al.*, 2009, Garattini and Terao. 2011, Garattini and Terao. 2012, Garattini and Terao. 2013, Kurosaki *et al.*, 2013)
AOH1	Aox3	Liver, lung and testis	Benzaldehyde,butyraldehyde, octanal,phthalazine, phenanthridine, all-trans retinaldehyde, 2-hydroxpyrimidine	(Tomita *et al.*, 1993, Moriwaki *et al.*, 1996, Kurosaki *et al.*, 1999, Wright *et al.*, 1999, Terao *et al.*, 2001, Kurosaki *et al.*, 2004, Vila *et al.*, 2004, Garattini *et al.*, 2008, Garattini *et al.*, 2009, Garattini and Terao. 2011, Garattini and Terao. 2012, Garattini and Terao. 2013, Kurosaki *et al.*, 2013)
AOH2	Aox4	Skin, stomach, Haderian gland, sebaceous gland, epidermis,eye, pancreas, brain and esophagus	Phenanthridine, all-trans retinaldehyde	(Holmes. 1979, Sasai and De Robertis. 1997, Terao *et al.*, 2001, Kurosaki *et al.*, 2004, Vila *et al.*, 2004, Garattini *et al.*, 2008, Garattini *et al.*, 2009, Garattini and Terao. 2011, Garattini and Terao. 2012, Garattini and Terao. 2013, Kurosaki *et al.*, 2013)
AOH3	Aox3L1	Skin, Bowmans gland and olfactory mucosa	Benzaldehyde, octanal, phthalazine, all-trans retinaldehyde, 2-hydroxpyrimidine	(Kurosaki *et al.*, 2004, Vila *et al.*, 2004, Garattini *et al.*, 2008, Garattini *et al.*, 2009, Garattini and Terao. 2011, Garattini and Terao. 2012, Garattini and Terao. 2013, Kurosaki *et al.*, 2013)
XOR	Xdh	Liver, muscle, mammary glands, oesophagus, stomach, duodenum, jejunum, lleum, colon, rectum, lung, kidney, heart, small intestine and spleen	Hypoxanthine, xanthine	(Yoshimura and Oka. 1989, Terao *et al.*, 1992, Falciani *et al.*, 1994, Kurosaki *et al.*, 1995, Kuroisaki *et al.*, 1996, McManaman *et al.*, 1999, McManaman *et al.*, 2002 , Terao *et al.*, 2006, Garattini *et al.*, 2008, Kurosaki *et al.*, 2013)

Table 8: Summary of aldehyde oxidase genes and tissue distribution in different species

Species	AOX	Tissue distribution	References
Baboon (*Papio Hamadryas)*	AOX1,AOX4 and AOX3L1	Intestine extract. heart, kidney and liver	(Holmes and Vandeberg. 1986, Garattini *et al.*, 2008, Kurosaki *et al.*, 2013)
Bovine (*Bos taurus*)	AOX1,AOX4 and AOX3L1	Lung, eye, kidney, testis, liver, spleen and ciliary body	(Shimada *et al.*, 1989, Calzei *et al.*, 1995, Beedham. 2001, Terao *et al.*, 2006, Garattini *et al.*, 2008, Kurosaki *et al.*, 2013)
Cat (*Felix catus*)	AOX3L1	Small intestine and kidney	(Krenitsky *et al.*, 1974, Beedham. 2001, Terao *et al.*, 2006, Garattini *et al.*, 2008, Garattini and Terao. 2013, Kurosaki *et al.*, 2013)
Chicken (*Gallus gallus*)	AOX1 and AOX2	Liver, Kidney brain, skin, muscle, thymus, trachea, lung, spleen, pancreas, stomach, adrenal gland and testis	(Krenitsky *et al.*, 1974, Nishino and Nishino. 1989, Nishino *et al.*, 1989, Terao *et al.*, 2006, Garattini *et al.*, 2008, Kurosaki *et al.*, 2013)
Cynomolgus monkey (*Macaca fascicularis*)	AOX1 and AOX3L1	Liver and nasal mucosa	(Kawashima *et al.*, 1999, Sugihara *et al.*, 2000, Diamond *et al.*, 2010, Van Rompay. 2012, Kurosaki *et al.*, 2013)
Dog (*Canis lupus familiaris*)	AOX4 and AOX3L1	Testis, Nasal mucosa, lacrimal glands, skin and oesophagus	(Krenitsky *et al.*, 1974, Vila *et al.*, 2004, Terao *et al.*, 2006, Garattini *et al.*, 2008, Kurosaki *et al.*, 2013)
Horse (*Equus caballus*)	AOX1,AOX4 and AOX3L1	Liver	(Seeley *et al.*, 1984, Prichard *et al.*, 1991, Räsänen *et al.*, 1993, Garattini *et al.*, 2008, Kurosaki *et al.*, 2013)
Human (*Homo sapiens*)	AOX1	Lung, liver and brain	(Krenitsky *et al.*, 1974, Minoshima *et al.*, 1995, Terao *et al.*, 1998, Beedham. 2001, Moriwaki *et al.*, 2001, Peretz *et al.*, 2007, Garattini *et al.*, 2008, Garattini and Terao. 2011, Garattini and Terao. 2012, Garattini and Terao. 2013, Kurosaki *et al.*, 2013)
Rhesus monkey (*Macaca mulatta*)	AOX1,AOX4 and AOX3L1	Liver and nasal mucosa	(Krenitsky *et al.*, 1974, Sugihara *et al.*, 1997, Garattini *et al.*, 2008, Fukiya *et al.*, 2010, Garattini and Terao. 2011, Tawa *et al.*, 2011, Garattini and Terao. 2012, Garattini and Terao. 2013, Kurosaki *et al.*, 2013)

Table 9: Summary of xanthine oxidoreductase tissue distribution in different species

Species	Tissue distribution	References
Baboon (*Papio Hamadryas*)	Intestine and liver	((Holmes and Vandeberg. 1986, Garattini *et al.*, 2008, Kurosaki *et al.*, 2013)
Bovine (*Bos taurus*)	Heart, liver, mammary gland and milk	(Shimada *et al.*, 1989, Calzei *et al.*, 1995, Beedham. 2001, Terao *et al.*, 2006, Garattini *et al.*, 2008, Kurosaki *et al.*, 2013)
Cat (*Felix catus*)	Liver, small intestine and kidney	(Krenitsky *et al.*, 1974, Beedham. 2001, Terao *et al.*, 2006, Garattini *et al.*, 2008, Kurosaki *et al.*, 2013)
Chicken (*Gallus gallus*)	Skin, lung, brain, liver, muscle, spinal cord, thymus, trachea, spleen, pancreas, stomach, adrenal gland and testis	(Nishino and Nishino. 1989, Nishino *et al.*, 1989, Terao *et al.*, 2006, Garattini *et al.*, 2008, Kurosaki *et al.*, 2013)
Cynomolgus monkey (*Macaca fascicularis*)	Testis, small intestine, brain and liver	(Kawashima *et al.*, 1999, Sugihara *et al.*, 2000, Diamond *et al.*, 2010, Van Rompay. 2012, Kurosaki *et al.*, 2013)
Dog (*Canis lupus familiaris*)	Nasal mucosa, skin, spleen, lacrimal glands and oesophagus	(Krenitsky *et al.*, 1974, Vila *et al.*, 2004, Terao *et al.*, 2006, Garattini *et al.*, 2008, Kurosaki *et al.*, 2013)
Horse (*Equus caballus*)	Lung, skeletal muscle, liver and small intestine	(Seeley *et al.*, 1984, Prichard *et al.*, 1991, Räsänen *et al.*, 1993, Garattini *et al.*, 2008, Kurosaki *et al.*, 2013)
Human (*Homo sapiens*)	Spleen, lung, mammary gland, kidney, liver, stomach, skeletal muscle and milk	(Krenitsky *et al.*, 1974, Minoshima *et al.*, 1995, Terao *et al.*, 1998, Beedham. 2001, Moriwaki *et al.*, 2001, Peretz *et al.*, 2007, Garattini *et al.*, 2008, Garattini and Terao. 2011, Garattini and Terao. 2012, Garattini and Terao. 2013, Kurosaki *et al.*, 2013)
Rhesus monkey (*Macaca mulatta*)	Testis, small intestine, brain and liver	(Krenitsky *et al.*, 1974, Sugihara *et al.*, 1997, Garattini *et al.*, 2008, Fukiya *et al.*, 2010, Garattini and Terao. 2011, Tawa *et al.*, 2011, Garattini and Terao. 2012, Garattini and Terao. 2013, Kurosaki *et al.*, 2013)

1.5.2. Molybdo-flavoenzymes in fish

AOX and XOR in fish are responsible for metabolism of various compounds such as aromatic aldehydes and N-heterocyclic compounds (Lakshmanan *et al.*, 1964, Krenitsky *et al.*, 1974, Wurzinger and Hartenstein. 1974, Cleare *et al.*, 1976, Kamiński and Jeżewska. 1985, Tatsumi *et al.*, 1992, Johnson *et al.*, 1993, Schlenk. 1998, Bleeker *et al.*, 2001, Ueda *et al.*, 2001, Ueda *et al.*, 2002, Basha and Rani. 2003, Kitamura *et al.*, 2003, Pandey *et al.*, 2003, Ziegler. 2003, Isamah and Asagba. 2004, Resende *et al.*, 2005, Asagba *et al.*, 2010, Hegazi *et al.*, 2010, Kurosaki *et al.*, 2013). These studies either measured the activity directly by monitoring substrate or product concentrations or used artificial electron acceptors as shown in (Table 10 and Figure 3).

1.5.2.1. Aldehyde oxidase activity in fish liver

As described in previous sections AOX activity is principally found in hepatic tissue of mammals(Garattini and Terao. 2013, Kurosaki *et al.*, 2013) and several workers have also demonstrated activity in this tissue in bony fish, among the most primitive vertebrates to have this activity. The first report of AOX in fish was by Lakshamanan *et al*. (1964) who examined the oxidation of the aldehydes of both vitamin A1 (all-trans retinal) and vitamin A2 (3,4-dehydro-all-trans retinal) to the corresponding acids by aldehyde oxidase enzyme in the liver of several freshwater-fish (*Ophiocephalus muralius*, *Labeo calbasu*) and (*Cyprinus carpio communis*) as shown in (Table 10). The study also found that the enzyme from freshwater-fish livers was inhibited by the AOX inhibitor menadione (Lakshmanan *et al.*, 1964).

Table 10.Summary of *in vitro* studies of hepatic aldehyde oxidase activity in fish species.

Common name, (Latin name)	Substrate	Electron acceptor	AOX activity	References
African catfish *(Clarias gariepinus)*	Benzaldehyde	2,6-DCPIP	143.8	(Isamah and Asagba. 2004)
Electric catfish *(Malapterurus electricus)*	Benzaldehyde	2,6-DCPIP	130	(Isamah and Asagba. 2004)
African catfish *(Clarias gariepinus)*	Benzaldehyde	2,6-DCPIP	1316.8[7d] , 629.35[21d]	(Asagba *et al.*, 2010)
Lesser spangled emperor *(Lthrinus choerorynchus)*	Benzaldehyde	MTT	+	(Johnson *et al.*, 1993)
Rankin cod *(Epinephelus multinotatus)*	Benzaldehyde	MTT	+	(Johnson *et al.*, 1993)
Red emperor *(Lutjanus sebae)*	Benzaldehyde	MTT	+	(Johnson *et al.*, 1993)
Sea bream*(Pagrus major)*	Benzaldehyde	O$_2$	4.35	(Kitamura *et al.*, 2003)
Spangled emperor *(Lethrinus nebulosus)*	Benzaldehyde	MTT	+	(Johnson *et al.*, 1993)
Sea bream*(Pagrus major)*	DMAC	O$_2$	7.3	(Kitamura *et al.*, 2003)
Goldfish*(Carassius auratus)*	2-hydroxypyrimidine	Fenthion sulphoxide	0.18	(Kitamura *et al.*, 2003)
Goldfish*(Carassius auratus)*	2-hydroxypyrimidine	2-nitrofluorene	+	(Ueda *et al.*, 2001)
Goldfish*(Carassius auratus)*	2-hydroxypyrimidine	Sodium nifurstyrenate	++	(Tatsumi *et al.*, 1992)
Sea bream*(Pagrus major)*	2-hydroxypyrimidine	2-nitrofluorene	0.25	(Ueda *et al.*, 2002)
Sea bream*(Pagrus major)*	2-hydroxypyrimidine	Sodium nifurstyrenate	6.5	(Tatsumi *et al.*, 1992)
Smooth dogfish*(Mustelus canis)*	6-methylpurine	Ferricyanide	73	(Krenitsky *et al.*, 1974)
Largemouth bass *(Micropterus salmoides)*	6-methylpurine	Ferricyanide	10	(Krenitsky *et al.*, 1974)
Florida pompano *(Trachinotus carolinus)*	6-methylpurine	Ferricyanide	10	(Krenitsky *et al.*, 1974)
Sea mullet *(Menticirrhus saxatilis)*	6-methylpurine	Ferricyanide	10	(Krenitsky *et al.*, 1974)
Blue fish*(Pomatomus saltatrix)*	6-methylpurine	Ferricyanide	17	(Krenitsky *et al.*, 1974)
Spanish mackerel *(Scomberonorus maculatus)*	6-methylpurine	Ferricyanide	<26	(Krenitsky *et al.*, 1974)
Bluegill*(Lepomis macrochirus)*	6-methylpurine	Ferricyanide	35	(Krenitsky *et al.*, 1974)
Channel catfish *(Icatalurus punctatus)*	6-methylpurine	Ferricyanide	23	(Krenitsky *et al.*, 1974)
Summer flounder *(Paralichthyes dentatus)*	6-methylpurine	Ferricyanide	47	(Krenitsky *et al.*, 1974)
Goldfish*(Carassius auratus)*	6-methylpurine	Ferricyanide	27	(Krenitsky *et al.*, 1974)
Norfolk spot *(Leiostomus xanthurus)*	6-methylpurine	Ferricyanide	30	(Krenitsky *et al.*, 1974)
Pumpkinseed sunfish *(Lepomis gibbosus)*	6-methylpurine	Ferricyanide	57	(Krenitsky *et al.*, 1974)
Nile tilapia juveniles *(Oreochromis niloticus)*	Phthalazine	Ferricyanide	275	(Hegazi *et al.*, 2010)
Northern hog sucker *(Hypentelium nigricans)*	Vanillin	O$_2$	+	(Wurzinger and Hartenstein. 1974)
White sucker *(Catostamus commersoni)*	Vanillin	O$_2$	+	(Wurzinger and Hartenstein. 1974)
Northern pike*(Esox lucius)*	Vanillin	O$_2$	+	(Wurzinger and Hartenstein. 1974)
Pumpkinseed sunfish *(Lepomis gibbosus)*	Vanillin	O$_2$	++	(Wurzinger and Hartenstein. 1974)
Walleye*(Stizostedion vitreum)*	Vanillin	O$_2$	++	(Wurzinger and Hartenstein. 1974)
Orange-fin labeo *(Labeo calbasu)*	Vitamin A$_1$ and A$_2$	O$_2$	67[A1], 70.2[A2]	(Lakshmanan *et al.*, 1964)
Great snakehead *(Ophiocephalus muralius)*	Vitamin A$_1$ and A$_2$	O$_2$	100.1[A1], 112.3[A2]	(Lakshmanan *et al.*, 1964)
Common carp *(Cyprinus carpio communis)*	Vitamin A$_1$ and A$_2$	O$_2$	41.9[A1], 42.55[A2]	(Lakshmanan *et al.*, 1964)

Abbreviations: AOX activity nmol/min/mg liver, DMAC - p-dimethylaminocinnamaldehyde, 2, 6 DCPIP -2, 6-dichlorophenol-indophenol. MTT - Dimethylthiazol-diphenyltetrazolium bromide, A1, A2- vitamin A1 and A2, 7d and 21d (Acclimatised for 14 days in large aquaria then kept in bowls of 20 litres for 7 days and 21 days).

Ten years later Krenitsky *et al*., (1974) examined the activity of AOX with 6-methylpurine as a substrate and potassium ferricyanide as electron acceptor in the liver of several fish. The study found that highest activity of AOX with pumpkinseed sunfish (*Lepomis gibbosus*) and lowest activity with blue fish (*Pomatomus saltatrix*) as shown in (Table 10) (Krenitsky *et al.*, 1974). In the same years, Wurzinger and Hartenstein, (1974) used vanillin as an AOX substrate with O_2 as an electron acceptor to measure AOX activity in livers of several fish species such as Northern hog sucker (*Hypentelium nigricans*), Northern pike (*Esox lucius*), pumpkinseed sunfish (*Lepomis gibbosus*) and walleye (*Stizostedion vitreum*) (Table 10)(Wurzinger and Hartenstein. 1974). Following these earlier studies it was not till two decades later that there was further research published on fish AOX. Tatsumi *et al*, (1992) examined the activity of aldehyde oxidase in goldfish (*Carassius auratus*) and sea bream (*Pagrus major*) livers using 2-hydroxypyrimidine as aldehyde oxidase substrate and sodium nifurstyrenate as electron acceptor as shown in (Table 10) (Tatsumi *et al.*, 1992). Johanson *et al*. (1993) examined allozymes of aldehyde oxidase (allelic variants of this enzyme) in the livers of four different species of fish which are commercially farmed in Australia, red emperor (*Lutjanus sebae*), spangled emperor (*Lethrinus nebulosus*), lesser spangled emperor (*Lethrinus choerorynchus*) and Rankin cod (*Epinephelus multinotatus*). This study used electrophoresis and stained the allozymes in the gels, using benzaldehyde as AOX substrate and hypoxanthine as XOR substrate (Table 10) (Johnson *et al.*, 1993). The electron acceptor dimethyl-diphenyltetrazolium bromide (MTT) was used to visualize electrophoretic variants of AOX and investigate the genetic similarities of these species of fish. The study demonstrated that whilst there was statistically significant variation in allelic frequencies in three of the species, there were no clear geographical groupings of populations. Supporting previous

evidence that populations of these fish are extensively connected, even over large geographical distance. Consecutive studies by Ueda *et al*, (2001 and 2002) examined the activity of aldehyde oxidase in goldfish (*Carassius auratus*) and sea bream (*Pagrus major*) livers, using benzaldehyde oxidation as direct assay and 2-hydroxypyrimidineas substrate with 2-nitrofluorene as electron acceptor in an anaerobic and indirect assay as shown in (Table 10)(Ueda *et al.*, 2001, Ueda *et al.*, 2002). Kitamura *et al*, (2003) also examined the activity of aldehyde oxidase with sea bream (*Pagrus major*) and goldfish (*Carassius auratus*), while using different aldehyde oxidase substrates such as benzaldehyde, dimethylaminocinnamaldehyde (DMAC) as direct assays. They also used 2-hydroxypyrimidine, N^1-methylnicotinamide or butyraldehyde as electron donor and the organothiophosphate insecticide fenthion as an electron acceptor as shown in (Table 10) (Kitamura *et al.*, 2003). Isamah and Asagba, (2004) and Asagba *et al*, (2010) tested the AOX activity with benzaldehyde as a substrate with African catfish (*Clarias gariepinus*) and electric catfish (*Malapterurus electricus*) in liver using 2, 6-dichlorpheno-indophenol (2, 6-DCPIP) as an artificial electron acceptor as shown in (Table 10)(Isamah and Asagba. 2004, Asagba *et al.*, 2010). While Hegazi et al, (2010). examined the activity of aldehyde oxidase in juvenile Nile tilapia (*Oreochromis niloticus*) liver using phthalazine as substrate and potassium ferricyanide as an electron acceptor, which reduced into ferricyanide as shown in (Table 10)(Hegazi *et al.*, 2010).

Several fish have been reported to have no AOX activity as shown in (Table 11). As well as *in vitro* studies, *in vivo* studies have suggested AOX activity towards NPAHs environmental pollutants exist in fish. Bean *et al* (1985) demonstrated that quinoline was metabolised to hydroxyquinoline in rainbow trout (*Oncorhynchus mykiss*) (Bean *et al.*, 1985). Bleeker *et al*, (2001) examined the metabolism of the environmental

pollutant phenanthridine in carp (*Cyprium carpio*) liver and bile into its metabolite 6(5H)-phenanthridinone (phenanthridone) suggesting that fish AOX catalysed this biotransformation (Bleeker *et al.*, 2001).

Table 11: Summary of fish species that have no detectable hepatic AOX activity. Based on Wurzinger and Hartenstein, (1974)

Common name	Latin name	Substrate	Electron acceptor
Stoneroller Minnow	*Campostoma anomalous*	Vanillin	O_2
Carp	*Cyprium carpio*	Vanillin	O_2
Cutlips Minnow	*Exoglossum maxilingua*	Vanillin	O_2
Fathead Minnow	*Pimephales promelas*	Vanillin	O_2
Margined Madtom	*Noturus insignis*	Vanillin	O_2
Yellow Perch	*Perca flavescens*	Vanillin	O_2

1.5.2.2. Extrahepatic aldehyde oxidase activity in fish

Krenitsky *et al.*, (1974) examined the activity of aldehyde oxidase with 6-methylpurine and potassium ferricyanide as electron acceptor. Two Cypriniformes and one Perciformes were tested for extrahepatic tissue distribution in intestine and kidney. All species studied had measurable extrahepatic activity that was found to be two and one fold lower respectively compared with liver, the activity in extrahepatic tissue less than that in hepatic tissue (Table 12) (Krenitsky *et al.*, 1974). Asagba *et al*, (2010) tested the AOX activity using benzaldehyde as a substrate with a Siluriformes (African catfish) in kidney, gills, muscle and brain using 2,6-dichlorpheno-indophenol (2,6-DCPIP) as an artificial electron acceptor as shown in (Table 12). Interestingly Asagba *et al* (2010) found that AOX activity decreased in African catfish acclimatised for 14 days in large aquaria then kept in bowls of 20 litres for 7 days and 21 days. Although the reason for this was not given this could be due to stress as two fish of approximately 30 cm were kept in small 20 litre bowl.

Table 12: Summary of extrahepatic and hepatic AOX activity in fish species. Based on Krenitsky et al, (1974)*, and Asagba et al, (2010) **.

Order	Family	Common name	Latin name	Habitat	Organ	AOX
Cypriniformes*	Cyprinidae	**Goldfish**	*Carassius auratus*	**F/P**	**liver**	**27**
Cypriniformes*	Cyprinidae	**Goldfish**	*Carassius auratus*	**F/P**	**intestine**	**<14**
Cypriniformes*	Cyprinidae	**Goldfish**	*Carassius auratus*	**F/P**	**kidney**	**19**
Perciformes*	Sciaenidae	**Norfolk spot**	*Leiostomus xanthurus*	**S/P**	**liver**	**< 30**
Perciformes*	Sciaenidae	**Norfolk spot**	*Leiostomus xanthurus*	**S/P**	**intestine**	**19**
Siluriformes **	Clariidae	**African catfish**	*Clarias gariepinus*	**F/P**	**liver 7d**	**1316.8**
Siluriformes **	Clariidae	**African catfish**	*Clarias gariepinus*	**F/P**	**liver 21d**	**629.35**
Siluriformes **	Clariidae	**African catfish**	*Clarias gariepinus*	**F/P**	**kidney 7d**	**640.38**
Siluriformes **	Clariidae	**African catfish**	*Clarias gariepinus*	**F/P**	**kidney 21d**	**460.48**
Siluriformes **	Clariidae	**African catfish**	*Clarias gariepinus*	**F/P**	**gill 7d**	**248.3**
Siluriformes **	Clariidae	**African catfish**	*Clarias gariepinus*	**F/P**	**gill 21d**	**349.7**
Siluriformes **	Clariidae	**African catfish**	*Clarias gariepinus*	**F/P**	**muscle 7d**	**148.45**
Siluriformes **	Clariidae	**African catfish**	*Clarias gariepinus*	**F/P**	**muscle 21d**	**107.5**
Siluriformes **	Clariidae	**African catfish**	*Clarias gariepinus*	**F/P**	**brain 7d**	**275.8**
Siluriformes **	Clariidae	**African catfish**	*Clarias gariepinus*	**F/P**	**brain 21d**	**125.6**

Activity measured: AOX activity µmol/min/g of tissue. Abbreviations: (S) salt water (marine), and (F) fresh water, (D) Demersal (benthic), (P) Pelagic, 7d and 21d (Acclimatised for 14 days in large aquaria then kept in bowls of 20 litres for 7 days and 21 days)

1.5.2.3. Aldehyde oxidase as reductase activity in fish

The reductase activity of AOX has long been established since Krenitsky found it in 1974(Krenitsky *et al.*, 1974). The first report of AOX as a reductase in fish was by Tatsumi *et al*, (1992). Tatsumi's group examined the activity of aldehyde oxidase as reductase with antibacterial sodium nifurstyrenate as electron acceptor which was reduced into cyano-pentenone, as an anaerobic and indirect reaction in goldfish (*Carassius auratus*) and sea bream (*Pagrus major*) livers, using 2-hydoxypyrimidine as an electron donor as shown in (Table 7)(Tatsumi *et al.*, 1992). A decade later Ueda *et al*, (2001 and 2002) examined the reductase activity of aldehyde oxidase using 2-nitrofluorene which is a nitropolycyclic aromatic hydrocarbon (environmental pollutants found in automobile exhaust) as an electron acceptor. They demonstrated that this was reduced into 2-aminofluorene in goldfish (*Carassius auratus*) liver, using 2hydroxypyrimidine as electron donor (Table 10) and inhibited by menadione as shown in (Table 10) (Ueda *et al.*, 2001, Ueda *et al.*, 2002). Kitamura *et al*, (2003)

examined the activity of aldehyde oxidase as reductase using fenthion sulphoxide (an insecticide) as electron acceptor which it reduced into fenthion in goldfish (*Carassius auratus*), using 2-hydroxypyrimidine as an electron donor as shown in (Table 10) (Kitamura *et al.*, 2003). Collectively these studies on AOX as a reductase in fish liver demonstrated that the enzyme has the capacity to reductively metabolise compounds that are environmental pollutants demonstrating the importance of the study of this important detoxication enzyme in these organisms. *In vivo* the physiological relevance of reductase activity is not known as these xenobiotic electron acceptors will be competing with a natural endogenous electron acceptor.

1.5.2.4. Xanthine oxidoreductase activity in fish

It was not until 10 years after AOX activity was reported in fish that the first report of XOR activity in fish appeared Krenitsky *et al*, (1974). Using xanthine as XOR substrate with NAD^+ or ferricyanide as an electron acceptor as shown in (Table 13)Krenitsky *et al* (1974) found activity in 11 fish species (Krenitsky *et al.*, 1974). Wurzinger and Hartenstein, (1974) also examined the activity of XOR using hypoxanthine as a XOR substrate, using NAD^+ as an electron acceptor in the liver of several fish species as shown in (Table 13) (Wurzinger and Hartenstein. 1974). Cleare *et al*, (1976) demonstrated XOR activity with several fish liver species such as brill (*Scophthalmus rhombus*), cod (*Gadus morhua*), dab (*Limanda limanda*), lemon sole (*Microstomus kitt*), mackerel (*Scomber scombrus*), plaice (*Pleuronectes platessa*), perch (*Perca fluviatilis*) and whiting (*Merlangius merlangus*) using xanthine as a XOR substrate, O_2 or 2,6-dichlorophenol-indophenol (2,6-DCPIP) and NAD^+ as an electron acceptor as shown in (Table 13)(Cleare *et al.*, 1976).

Table 13: *In vitro* studies of hepatic xanthine oxidoreductase activity in fish species measured using spectrophotometry.

Common name, Latin name	Substrate	Electron acceptor	XO	XOR	% XDH	References
Carp (*Cyprinus carpio***)**	Hypoxanthine	NAD$^+$	**0**	**0**	++	(Wurzinger and Hartenstein. 1974)
Cutlips minnow (*Exoglossum maxilingua***)**	Hypoxanthine	NAD$^+$	**0**	**0**	++	(Wurzinger and Hartenstein. 1974)
Margined madtom (*Noturus insignis***)**	Hypoxanthine	NAD$^+$	**0**	**-**	+	(Wurzinger and Hartenstein. 1974)
Northern hog sucker *(Hypentelium nigricans)*	Hypoxanthine	NAD$^+$	**0**	**-**	+	(Wurzinger and Hartenstein. 1974)
Stoneroller minnow *(Campostoma anomalous)*	Hypoxanthine	NAD$^+$ and INT	**0**	**0**	++	(Wurzinger and Hartenstein. 1974)
White sucker(*Catostamus commersoni***)**	Hypoxanthine	NAD$^+$	**0**	**-**	+	(Wurzinger and Hartenstein. 1974)
Yellow perch (*Perca flavescens***)**	Hypoxanthine	NAD$^+$	**0**	**-**	++	(Wurzinger and Hartenstein. 1974)
Brown trout (*Salmo trutta***)**	Purine	NAD$^+$	**+**	**3-9**	+	(Resende *et al.*, 2005)
Zebra fish (*Danio rerio***)**	Pteridine	O$_2$ or NAD$^+$	**+**	**+**	+	(Ziegler. 2003)
African catfish (*Clarias gariepinus***)**	Xanthine	O$_2$	**+**	**76^{7d}, 60^{21d}**	+	(Asagba *et al.*, 2010)
African catfish (*Clarias gariepinus***)**	Xanthine	O$_2$	**+**	**197**	+	(Isamah and Asagba. 2004)
Electric catfish (*Malapterurus electricus***)**	Xanthine	O$_2$	**+**	**255.8**	+	(Isamah and Asagba. 2004)
Channel catfish (*Icatalurus punctatus***)**	Xanthine	Ferricyanide and NAD$^+$	**<3**	**100**	97	(Krenitsky *et al.*, 1974)
Spanish mackerel *(Scomberonorus maculatus)*	Xanthine	NAD$^+$ and Ferricyanide	**14**	**120**	88.4	(Krenitsky *et al.*, 1974)
Pumpkinseed sunfish (*Lepomis gibbosus***)**	Xanthine	NAD$^+$ and Ferricyanide	**<2**	**95**	97.9	(Krenitsky *et al.*, 1974)
Sea mullet (*Menticirrhus saxatilis***)**	Xanthine	NAD$^+$ and Ferricyanide	**-**	**150**	100	(Krenitsky *et al.*, 1974)
Norfolk Spot (*Leiostomus xanthurus***)**	Xanthine	NAD$^+$ and Ferricyanide	**<6**	**180**	96.7	(Krenitsky *et al.*, 1974)
Gold fish (*Carassius auratus***)**	Xanthine	NAD$^+$ and Ferricyanide	**8**	**120**	93.4	(Krenitsky *et al.*, 1974)
Largemouth bass (*Micropterus salmoides***)**	Xanthine	NAD$^+$ and Ferricyanide	**<3**	**410**	99.3	(Krenitsky *et al.*, 1974)
Florida pompano (*Trachinotus carolinus***)**	Xanthine	NAD$^+$	**-**	**180**	100	(Krenitsky *et al.*, 1974)
Summer flounder (*Paralichthyes dentatus***)**	Xanthine	NAD$^+$ and Ferricyanide	**5**	**210**	97.6	(Krenitsky *et al.*, 1974)
Blue fish (*Pomatomus saltatrix***)**	Xanthine	Ferricyanide and NAD$^+$	**2**	**38**	94.7	(Krenitsky *et al.*, 1974)
Bluegill (*Lepomis macrochirus***)**	Xanthine	NAD$^+$ and Ferricyanide	**<3**	**180**	98.4	(Krenitsky *et al.*, 1974)
Megrim (*Lepidorhombus whiffagonis***)**	Xanthine	O$_2$ or 2,6-DCPIP	**5**	**0**	**0**	(Cleare *et al.*, 1976)
Pike (*Esox lucius***)**	Xanthine	O$_2$ or 2,6-DCPIP and NAD$^+$	**0**	**123**	**100**	(Cleare *et al.*, 1976)
Whiting (*Merlangius merlangus***)**	Xanthine	O$_2$ or 2,6-DCPIP and NAD$^+$	**0**	**98**	**100**	(Cleare *et al.*, 1976)
Cod (*Gadus morhua***)**	Xanthine	O$_2$ or 2,6-DCPIP and NAD$^+$	**0**	**98**	**100**	(Cleare *et al.*, 1976)
Dab (*Limanda limanda***)**	Xanthine	O$_2$ or 2,6-DCPIP and NAD$^+$	**0**	**221**	**100**	(Cleare *et al.*, 1976)
Brill (*Scophthalmus rhombus***)**	Xanthine	O$_2$ or 2,6-DCPIP	**0**	**197**	**100**	(Cleare *et al.*, 1976)
Lesser spotted dogfish *(Scyliorhinus canicula)*	Xanthine	O$_2$ or 2,6-DCPIP	**0**	**24**	**100**	(Cleare *et al.*, 1976)
Ray (*Dipturus canutus***)**	Xanthine	O$_2$ or 2,6-DCPIP	**0**	**148**	**100**	(Cleare *et al.*, 1976)
Herring (*Clupea harengus***)**	Xanthine	O$_2$ or 2,6-DCPIP	**0**	**221**	**100**	(Cleare *et al.*, 1976)
White pollack (*Pollachius virene***)**	Xanthine	O$_2$ or 2,6-DCPIP	**0**	**0**	**100**	(Cleare *et al.*, 1976)
Haddock (*Melanogrammus aeglefinus***)**	Xanthine	O$_2$ or 2,6-DCPIP	**0**	**-**	**100**	(Cleare *et al.*, 1976)
Summer flounder (*Paralichthyes dentatus***)**	Xanthine	O$_2$ or 2,6-DCPIP	**0**	**-**	**100**	(Cleare *et al.*, 1976)
Black sole (*Solea solea***)**	Xanthine	O$_2$ or 2,6-DCPIP	**0**	**-**	**100**	(Cleare *et al.*, 1976)
White sole (*Solea solea***)**	Xanthine	O$_2$ or 2,6-DCPIP	**0**	**73**	**100**	(Cleare *et al.*, 1976)
White trout (*Salmo trutta***)**	Xanthine	O$_2$ or 2,6-DCPIP	**0**	**116**	**100**	(Cleare *et al.*, 1976)
Gurnard (*Chelidonichthys cuculus***)**	Xanthine	O$_2$ or 2,6-DCPIP	**0**	**14**	**100**	(Cleare *et al.*, 1976)
John dory (*Zeus faber***)**	Xanthine	O$_2$ or 2,6-DCPIP	**0**	**-**	**100**	(Cleare *et al.*, 1976)
Lemon sole (*Microstomus kitt***)**	Xanthine	O$_2$ or 2,6-DCPIP	**0**	**52**	**100**	(Cleare *et al.*, 1976)
Mackerel (*Scomber scombrus***)**	Xanthine	O$_2$ or 2,6-DCPIP	**0**	**44**	**100**	(Cleare *et al.*, 1976)
Plaice (*Pleuronectes platessa***)**	Xanthine	O$_2$ or 2,6-DCPIP	**0**	**79**	**100**	(Cleare *et al.*, 1976)
Perch (*Perca fluviatilis***)**	Xanthine	2,6-DCPIP	**0**	**248**	**100**	(Cleare *et al.*, 1976)
Carp (*Cyprinus carpio***)**	Xanthine or Hypoxanthine	NAD$^+$ or O$_2$	**+**	**-**	**99.4**	(Kamiński and Jeżewska. 1985)
Giant catfish (*Wallago attu***)**	Xanthine	NAD$^+$ or O$_2$	**+**	**528**	+	(Pandey *et al.*, 2003)
Nile tilapia juveniles *(Oreochromis niloticus)*	Xanthine	NAD$^+$	**+**	**120**	**-**	(Hegazi *et al.*, 2010)
Mozambique tilapia *(Oreochromis mossambicus)*	Xanthine	NAD$^+$	**+**	**167**	+	(Basha and Rani. 2003)

Abbreviations: 2, 6-DCPIP – 2, 6-dichlorophenol-indophenol. MTT - Dimethylthiazol-diphenyltetrazolium bromide, PMS-phenazine methosulphate. INT – iodonitro-tetrazolium, 7d and 21d (Acclimatised for 14 days in large aquaria then kept in bowls of 20 litres for 7 days and 21 days), XOR = sum of activity with O$_2$ and NAD$^+$ as electron acceptor, XO = activity with O$_2$ as electron acceptor.

In addition, Kaminski and Jezewska, (1985) examined the activity of XOR in carp (*Cyprinus carpio*) liver using xanthine or hypoxanthine as substrate and NAD^+ or O_2 as an electron acceptor as shown in (Table 13) (Kamiński and Jeżewska. 1985). While, Johnson *et al*, (1993) examined the activity of XO with several fish liver species such as lesser spangled emperor (*Lthrinus choerorynchus*), rankin cod (*Epinephelus multinotatus*), red emperor (*Lutjanus sebae*) and spangled emperor (*Lethrinus nebulosus*) with hypoxanthine as substrate and dimethylthiazol-diphenyltetrazolium (MTT)as an electron acceptor as shown in (Table 15) (Johnson *et al.*, 1993). Pandey *et al*, (2003) used xanthine as XO substrate and(PMS) phenazine methosulphate as an electron acceptor to examine the activity of XO in giant catfish (*Wallago attu*) liver as shown in (Table 13)(Pandey *et al.*, 2003). Basha and Rani, (2003) examined the activity of XDH with Mozambique tilapia (*Oreochromis mossambicus*) liver, using xanthine as substrate and NAD^+ as an electron acceptor as shown in (Table 13)(Basha and Rani. 2003). In addition, Ziegler, (2003) examined the activity of XOR using pteridine as substrate and O_2 or NAD^+ as an electron acceptor with zebra fish (*Danio rerio*) liver as shown in (Table 13) (Ziegler. 2003). Isamah and Asagba, (2004) using xanthine as substrate and O_2 as an electron acceptor to examine the activity of XO in several Western Niger-Delta fish liver species such as African catfish (*Clarias gariepinus*) and electric catfish (*Malapterurus electricus*) as shown in (Table 13)(Isamah and Asagba. 2004). Resende et al, (2005) examined the activity of XDH in brown trout (*Salmo trutta*) liver, using purine as substrate and NAD^+ as an electron acceptor, as shown in (Table 13) (Resende *et al.*, 2005). Xanthine as substrate and O_2 as an electron acceptor in African catfish (*Clarias gariepinus*) liver from Delta State, Nigeria as shown in (Table 13) (Asagba *et al.*, 2010). In addition, Hegazi et al, (2010) examined the activity of XDH in Nile tilapia juveniles (*Oreochromis niloticus*)

liver. Using xanthine as substrate and NAD^+ as an electron acceptor, as shown in (Table 13)(Hegazi *et al.*, 2010). Several fish have been reported to have no XOR activity as shown in (Table 14).

Table 14: Summary of fish species that had no detectable XOR activity.

Common name	Latin name	substrate	Electron acceptor	Reference
Smooth dogfish	*Mustelus canis*	Xanthine	NAD^+ and Ferricyanide	(Krenitsky *et al.*, 1974)
Northern pike	*Esox lucius*	Hypoxanthine	NAD^+	(Wurzinger and Hartenstein. 1974)
Pumpkinseed sunfish	*Lepomis gibbosus*	Hypoxanthine	NAD^+	(Wurzinger and Hartenstein. 1974)
Walleye	*Stizostedion vitreum*	Hypoxanthine	NAD^+	(Wurzinger and Hartenstein. 1974)

As well as the spectrophotometric studies above many different researchers also used electrophoresis and histochemical dye methods to investigate the hepatic xanthine oxidoreductase activity in different fish as seen in (Table 15).

Table 15: Summary of *in vitro* studies of hepatic xanthine oxidoreductase activity in fish species using electrophoresis and histochemical dye methods

Common name, Latin name	Substrate	Electron acceptor	XOR	XDH	References
lesser spangled emperor (*Lthrinus choerorynchus*)	Hypoxanthine	MTT	+	+	(Johnson *et al.*, 1993)
Rankin cod (*Epinephelus multinotatus*)	Hypoxanthine	MTT	+	+	(Johnson *et al.*, 1993)
Red emperor (*Lutjanus sebae*)	Hypoxanthine	MTT	+	+	(Johnson *et al.*, 1993)
Spangled emperor (*Lethrinus nebulosus*)	Hypoxanthine	MTT	+	+	(Johnson *et al.*, 1993)
Spotted murrel (*Channa punctatus*)	Xanthine	MTT	-	-	(Sastry and Rao. 1984)
Spotted murrel (*Channa punctatus*)	Xanthine	MTT	-	-	(Sastry and Rao. 1982)
Barbell (*Barbus bocagei*)	Xanthine	PMS	-	-	(Peixoto *et al.*, 2013)
Orangefin labeo (*Labeo calbasu*)	Hypoxanthine	MTT	+	+	(Singh *et al.*, 2010)
White sea bream (*Diplodus sargus*)	Hypoxanthine	MTT	+	-	(Lenfant. 2003)
Juvenile Chinese sturgeon (*Acipenser sinensis*)	Hypoxanthine	MTT	+	-	(Feng *et al.*, 2012)
White crappie (*Pomoxis annularis*) **adult**	Hypoxanthine	EBT	+	+	(Epifanio and Philipp. 1993)
White crappie (*Pomoxis annularis*) **embryos or larva**	Hypoxanthine	EBT	+	-	(Epifanio and Philipp. 1994)
Black crappie (*Pomoxis nigromaculatus*) **adult**	Hypoxanthine	EBT	+	+	(Epifanio and Philipp. 1993)
Black crappie (*Pomoxis nigromaculatus*) **embryos or larva**	Hypoxanthine	EBT	+	-	(Epifanio and Philipp. 1994)
Atlantic mackerel (Scomber scombrus)	Xanthine	TTC	+	+	(Smith and Jamieson. 1978)
Japanese medaka (*Oryzias latipes*)	Xanthine	PMS + NBT	+	+	(Nakano and Whiteley. 1965)

Abbreviations: TTC – Tetrazolium chloride, EBT – Erochrome black T, MTT - Dimethylthiazol-diphenyltetrazolium bromide, PMS- phenazine methosulphate, NBT- nitro blue tetrazolium.

1.5.2.5. Extrahepatic xanthine oxidoreductase activity in fish

Krenitsky *et al*, (1974) used a spectrophotometric assay, xanthine as XOR substrate and NAD^+ or ferricyanide as electron acceptor to measure extrahepatic XOR activity in several fish species. Two Cypriniformes and one Perciformes were tested for extrahepatic tissue distribution in intestine and kidney XOR activity. All species studied had measurable extrahepatic activity that was found to be 4-fold lower in intestine and 1.5-fold more in kidney compared with liver , the highest activity was found in the kidney of the goldfish (*Carassius auratus*) (Table 16) (Krenitsky *et al.*, 1974). The activity of extrahepatic XOR tested by Resende *et al*, (2005)was tested in one Salmoniformes in which the activity found in kidney of brown trout (*Salmo trutta*) was found to be 2-fold more compared with liver (Table 16)(Resende *et al.*, 2005). Hegazi *et al*, (2010) also examined the extrahepatic activity of XOR in one Perciformes and found the activity in white muscle of juvenile Nile tilapia (*Oreochromis niloticus*) 1.3-fold lower compared with liver (Table 16) (Hegazi *et al.*, 2010). Temple *et al*., (1979) examined the extrahepatic XOR activity in intestine of goldfish (*Carassius auratus*) with 100% XDH (Temple *et al.*, 1979). Sastry and Rao. (1982 and 1984) found the activity of XOR in different tissue of spotted murrel (*Channa punctatus)* in kidney, gills, brain, intestine and muscle (Sastry and Rao. 1982, Sastry and Rao. 1984). . Hari and Neeraja (2012) examined the extrahepatic activity of XOR in one Cypriniformes and found the activity in the kidney of Common carp (*Cyprinus carpio*) as XO(Hari and Neeraja. 2012). Nakano and Whiteley (1965) examined the extrahepatic activity of XOR in one Beloniformes and found the activity in intestines of Japanese medaka (*Oryzias latipes)* (Nakano and Whiteley. 1965).

Table 16: Extrahepatic XOR activity in fish

Order	Family	Common name	Latin name	Habitat	Organ	XO	XOR	% XDH
Cypriniformes *	Cyprinidae	Goldfish	*Carassius auratus*	F/P	liver	8	120	93.4
Cypriniformes *	Cyprinidae	Goldfish	*Carassius auratus*	F/P	Intestine	3	33	91
Cypriniformes ****	Cyprinidae	Goldfish	*Carassius auratus*	F/P	Intestine	-	-	100
Cypriniformes *	Cyprinidae	Goldfish	*Carassius auratus*	F/P	Kidney	11	190	94.2
Cypriniformes †††	Cyprinidae	Common carp	*Cyprinus carpio*	S/P	Kidney	42.6	-	-
Perciformes *	Sciaenidae	Norfolk spot	*Leiostomus xanthurus*	S/P	liver	<6	180	96.7
Perciformes *	Sciaenidae	Norfolk spot	*Leiostomus xanthurus*	S/P	Intestine	<4	90	<95.6
Perciformes ***	Cichlidae	Nile tilapia juveniles	*Oreochromis niloticus*	F/P	liver	+	160	99.4
Perciformes ***	Cichlidae	Nile tilapia juveniles	*Oreochromis niloticus*	F/P	White muscle	-	120	-
Perciformes †	Sciaenidae	Spotted murrel	*Channa punctatus*	S/P	liver	6.2	-	-
Perciformes†	Sciaenidae	Spotted murrel	*Channa punctatus*	S/P	kidney	8.6	-	-
Perciformes †	Sciaenidae	Spotted murrel	*Channa punctatus*	S/P	gills	2.9	-	-
Perciformes†	Sciaenidae	Spotted murrel	*Channa punctatus*	S/P	intestine	2.7	-	-
Perciformes†	Sciaenidae	Spotted murrel	*Channa punctatus*	S/P	brain	8.2	-	-
Perciformes †	Sciaenidae	Spotted murrel	*Channa punctatus*	S/P	muscles	5.5	-	-
Perciformes ††	Sciaenidae	Spotted murrel	*Channa punctatus*	S/P	liver	3.7	-	-
Perciformes ††	Sciaenidae	Spotted murrel	*Channa punctatus*	S/P	kidney	5.7	-	-
Perciformes ††	Sciaenidae	Spotted murrel	*Channa punctatus*	S/P	gills	4.2	-	-
Perciformes ††	Sciaenidae	Spotted murrel	*Channa punctatus*	S/P	intestine	8.0	-	-
Perciformes ††	Sciaenidae	Spotted murrel	*Channa punctatus*	S/P	brain	5.0	-	-
Perciformes ††	Sciaenidae	Spotted murrel	*Channa punctatus*	S/P	muscles	3.8	-	-
Salmoniformes **	Salmonidae	Brown trout	*Salmo trutta*	F/P	liver	+	3-9	+
Salmoniformes **	Salmonidae	Brown trout	*Salmo trutta*	F/P	Kidney	+	1.5-5	+
Beloniformes ††††	adrianichthyidae	Japanese medaka	*Oryzias latipes*	S/P	Liver	-	-	+
Beloniformes ††††	adrianichthyidae	Japanese medaka	*Oryzias latipes*	S/P	Gut	-	-	+

Abbreviations: F-freshwater fish, S- saltwater fish, P- pelagic. Activity measured: XDH and XO activity nmol/min/mg of tissue, XO urate formed with O_2, XOR urate formed with O_2 and NAD^+. Based on Krenitsky *et al*, (1974)*, Resende *et al*, (2005) **, Hegazi *et al*,(2010) ***, Temple *et al*, (1979) ****, (Sastry and Rao 1984) †,(Sastry and Rao 1982)††, (Hari and Neeraja 2012)†††and (Nakano and Whiteley 1965)††††.

1.5.3. Molybdo-flavoenzymes as pollution monitoring in fish

As AOX and XOR biotransform substrates to more polar compounds, several research groups have measured the activity of these enzymes in animals exposed to pollutant to determine if they are increased or decreased and could be used as pollution biomarkers. Basha and Rani, (2003) examined induction of enzymes in fish in response to oxidative stress caused by heavy metals (such as cadmium, zinc, mercury and copper) which are released into ponds, lakes and rivers in industrial effluents in India. They discovered significant elevations of detoxification enzymes including XO in the liver and kidney of the freshwater teleost, tilapia (*Oreochromis mossabicus*), using xanthine as substrate and NAD^+, iodophenyl-tetrazolium chloride (INT) as electron acceptor. As a result of cadmium toxicity and it was found that the XOR increased ~1.8 fold in liver and in kidney(Table 17) (Basha and Rani. 2003). Pandey *et al*. (2003) examined biomarker responses including XO in several tissues of the freshwater giant catfish (*Wallago attu*), obtained from two different sites, which varied in levels of pollution, along the river Yamuna in India (see Table 17 and 18),Water from the site, was more heavily polluted as a result of increased industrial activity and chemical use, was found to have higher pH and lower level of dissolved oxygen compared to the less polluted site. Using xanthine as substrate and phenazine methosulphate (PMS) as electron acceptor, the researchers found that XO activity was significantly higher in fish taken from the heavily polluted area and used this evidence to propose that such XO be used future monitoring of aquatic ecosystem pollution. They found that activity was increased 2.47-fold in liver, 4.49-fold in gill and 2.11-fold in kidney(Pandey *et al.*, 2003).Interestingly Sastry and Rao (1982 and 1984) examined the pollution effect of mercuric chloride with spotted murrel (*Channa punctatus)* liver and found no change on XOR activity by using xanthine as substrate

(Table 19). In addition the activity of hepatic XOR tested with heavy metal pollution with barbell (*Barbus bocagei*)found no change on its activity (Peixoto *et al.*, 2013) (Table 17).

Table 17: Hepatic OR activity as a biomarkers for pollution in fish.

Common name	Latin name	Pollutant	Fold increase/ decrease	References
African catfish	*Clarias gariepinus*	Heavy metal	2.51 increase	(Isamah and Asagba. 2004)
African catfish	*Clarias gariepinus*	Cadmium (5 mg/L 7 days)	No change	(Asagba *et al.*, 2010)
African catfish	*Clarias gariepinus*	Cadmium (5 mg/L 21 days)	No change	(Asagba *et al.*, 2010)
Electric catfish	*Malapterurus electricus*	Heavy metal	2.37 increase	(Isamah and Asagba. 2004)
Giant catfish	*Wallago attu*	Heavy metal	2.47 increased	(Pandey *et al.*, 2003)
Mozambique tilapia	*Oreochromis mossabicus*	Cadmium (5 mg/L 15 days)	1.86 increase	(Basha and Rani. 2003)
Nile tilapia juveniles	*Oreochromis niloticus*	TAN (5 mg/L 70 days)	2.9 increase	(Hegazi *et al.*, 2010)
Nile tilapia juveniles	*Oreochromis niloticus*	TAN (10 mg/L 70 days)	3.5 increase	(Hegazi *et al.*, 2010)
Spotted murrel	*Channa punctatus*	Mercuric chloride (3 µg/liter)	No change	(Sastry and Rao. 1984)
Spotted murrel	*Channa punctatus*	Mercuric chloride (3 µg/liter)	No change	(Sastry and Rao. 1982)
Barbell	*Barbus bocagei*	Heavy metal	No change	(Peixoto *et al.*, 2013)

Abbreviations: 7d for 7 days exposure, 21d for 21 day exposure, 7d and 21d (acclimatised for 14 days in large aquaria then kept in bowls of 20 litres for 7 days and 21 days), TAN – Total ammonia nitrogen. Using xanthine as substrate.

Table 18: Extrahepatic XOR activity as biomarkers for pollution in fish.

Common name	Latin name	Pollutant	Fold increase/ decrease	Organ	References
African catfish	*Clarias gariepinus*	Cadmium (5 mg/L 7 days)	1.42 decreased	Kidney	(Asagba *et al.*, 2010)
African catfish	*Clarias gariepinus*	Cadmium (5 mg/L 21 days)	1.99 decreased	Kidney	(Asagba *et al.*, 2010)
African catfish	*Clarias gariepinus*	Cadmium (5 mg/L 7 days)	2.33 decreased	Gill	(Asagba *et al.*, 2010)
African catfish	*Clarias gariepinus*	Cadmium (5 mg/L 21 days)	2.28 decreased	Gill	(Asagba *et al.*, 2010)
African catfish	*Clarias gariepinus*	Cadmium (5 mg/L 7 days)	No change	Muscle	(Asagba *et al.*, 2010)
African catfish	*Clarias gariepinus*	Cadmium (5 mg/L 21 days)	No change	Muscle	(Asagba *et al.*, 2010)
African catfish	*Clarias gariepinus*	Cadmium (5 mg/L 7 days)	No change	Brain	(Asagba *et al.*, 2010)
African catfish	*Clarias gariepinus*	Cadmium (5 mg/L 21 days)	No change	Brain	(Asagba *et al.*, 2010)
Giant catfish	*Wallago attu*	Heavy metal	2.11 increased	Kidney	(Pandey *et al.*, 2003)
Giant catfish	*Wallago attu*	Heavy metal	4.49 increased	Gill	(Pandey *et al.*, 2003)
Mozambique tilapia	*Oreochromis mossabicus*	Cadmium (5 mg/L 15 days)	1.84 increase	Kidney	(Basha and Rani. 2003)
Nile tilapia juveniles	*Oreochromis niloticus*	TAN (5 mg/L 70 days)	2.25 increase	White muscle	(Hegazi *et al.*, 2010)
Nile tilapia juveniles	*Oreochromis niloticus*	TAN (10 mg/L 70 days)	2.6 increase	White muscle	(Hegazi *et al.*, 2010)
Spotted murrel	*Channa punctatus*	Mercuric chloride (3 µg/litre)	No change	Kidney	(Sastry and Rao. 1984)
Spotted murrel	*Channa punctatus*	Mercuric chloride (3 µg/litre)	2 increase	Gills	(Sastry and Rao. 1984)
Spotted murrel	*Channa punctatus*	Mercuric chloride (3 µg/litre)	No change	Intestine	Sastry and Rao.1984)
Spotted murrel	*Channa punctatus*	Mercuric chloride (3 µg/litre)	No change	Brain	(Sastry and Rao. 1984)
Spotted murrel	*Channa punctatus*	Mercuric chloride (3 µg/litre)	No change	Muscle	Sastry and Rao.1984)
Spotted murrel	*Channa punctatus*	Mercuric chloride (3 µg/litre)	No change	Kidney	(Sastry and Rao. 1982)
Spotted murrel	*Channa punctatus*	Mercuric chloride (3 µg/litre)	No change	Kidney	(Sastry and Rao. 1982)
Spotted murrel	*Channa punctatus*	Mercuric chloride (3 µg/litre)	No change	Kidney	(Sastry and Rao. 1982)
Spotted murrel	*Channa punctatus*	Mercuric chloride (3 µg/litre)	No change	Kidney	(Sastry and Rao. 1982)
Spotted murrel	*Channa punctatus*	Mercuric chloride (3 µg/litre)	No change	Kidney	(Sastry and Rao. 1982)
Common carp	*Cyprinus carpio*	Ammonia (5 mg/L 7 days)	2 decrease	Liver	(Hari and Neeraja. 2012)

Abbreviations: 7d for 7 days exposure, 21d for 21 day exposure, 7d and 21d (acclimatised for 14 days in large aquaria then kept in bowls of 20 litres for 7 days and 21 days), TAN – Total ammonia nitrogen. All activity was measured using xanthine as substrate.

Isamah and Asagba, (2004) examined XO and AOX activity in the liver of electric catfish (*Malapterurus electricus*) and African catfish (*Clarias gariepinus*), using xanthine and benzaldehyde as substrate respectively, taken from two different sites along the Warri river in the Western Niger-Delta (see Table 19). Different levels of pollution as result of various effluent entries into the river were present at the two sample sites. It was found that XO may act as a marker of stress due to pollution by potentially increasing with elevated levels of contaminants and it found the activity of XO increased 2.37-fold and AOX activity increased 1.46-fold in electric catfish (*Malapterurus electricus*) and in African catfish (*Clarias gariepinus*) AOX activity increased 2.35-fold and XO activity increased 2.51-fold (Table 17 and 19) (Isamah and Asagba. 2004). Asagba *et al*. (2010) examined induction of antioxidant defences in fish in response to oxidative stress caused by heavy metals such as cadmium, which are released into ponds, lakes and rivers in industrial effluents. They examined the effect of the exposure to cadmium over time on the activities of AOX in the liver, kidney and gills and xanthine oxidase in the liver of the catfish (*Clarias gariepinus*), using benzaldehyde and xanthine as substrate respectively(see Table 19). Asagba *et al*. (2010) was found the cadmium inhibited the activity of AOX and xanthine XOR in the liver, gill and kidney of catfish. They found the activity of AOX in liver decreased 35.7-fold, kidney with 7 day exposure decreased 2.23-fold and 21 day exposure decreased 1.62-foldand gills with 7 day exposure decreased 3.28-fold and 21 day exposure decreased 1.88-fold, while XO in kidney with 7 day exposure decreased 1.42-fold and 21 day exposure decreased 1.99-fold decreased and gills with 7 day exposure decreased 2.33-fold and 21 day exposure decreased 2.28-fold (Asagba *et al*., 2010). Hegazi *et al*. (2010) examined the induction of AOX and XO in liver with phthalazine and xanthine as substrates respectively in liver and white muscle of

Table 19: Hepatic and extrahepatic AOX activity as a biomarkers for pollution in fish.

Common name	Latin name	Pollutant	Substrates	Fold increase/ decrease	Organ	References
African catfish	*Clarias gariepinus*	Heavy metal	Benzaldehyde	2.35 increase	liver	(Isamah and Asagba. 2004)
African catfish	*Clarias gariepinus*	Cadmium (5 mg/L 7 days)	Benzaldehyde	35.7 decrease	liver	(Asagba *et al.*, 2010)
African catfish	*Clarias gariepinus*	Cadmium (5 mg/L 21 days)	Benzaldehyde	1.81decrease	liver	(Asagba *et al.*, 2010)
Electric catfish	*Malapterurus electricus*	Heavy metal	Benzaldehyde	1.46 increase	liver	(Isamah and Asagba. 2004)
Nile tilapia juveniles	*Oreochromis niloticus*	TAN (5 mg/L 70 days)	Phthalazine	2.1 increase	liver	(Hegazi *et al.*, 2010)
Nile tilapia juveniles	*Oreochromis niloticus*	TAN (10 mg/L 70 days)	Phthalazine	2.5 increase	liver	(Hegazi *et al.*, 2010)
African catfish	*Clarias gariepinus*	Cadmium (5 mg/L 7 days)	Benzaldehyde	2.23 decrease	kidney	(Asagba *et al.*, 2010)
African catfish	*Clarias gariepinus*	Cadmium (5 mg/L 21 days)	Benzaldehyde	1.62 decrease	kidney	(Asagba *et al.*, 2010)
African catfish	*Clarias gariepinus*	Cadmium (5 mg/L 7 days)	Benzaldehyde	3.25 decrease	gill	(Asagba *et al.*, 2010)
African catfish	*Clarias gariepinus*	Cadmium (5 mg/L 21 days)	Benzaldehyde	1.88 decrease	gill	(Asagba *et al.*, 2010)
African catfish	*Clarias gariepinus*	Cadmium (5 mg/L 7 days)	Benzaldehyde	1.15 decrease	muscle	(Asagba *et al.*, 2010)
African catfish	*Clarias gariepinus*	Cadmium (5 mg/L 21 days)	Benzaldehyde	0.91 decrease	muscle	(Asagba *et al.*, 2010)
African catfish	*Clarias gariepinus*	Cadmium (5 mg/L 7 days)	Benzaldehyde	1.69 increased	brain	(Asagba *et al.*, 2010)
African catfish	*Clarias gariepinus*	Cadmium (5 mg/L 21 days)	Benzaldehyde	1.27 decrease	brain	(Asagba *et al.*, 2010)

Abbreviations: 7d for 7 days exposure, 21d for 21 day exposure, 7d and 21d (acclimatised for 14 days in large aquaria then kept in bowls of 20 litres for 7 days and 21 days). TAN – Total ammonia nitrogen.

Nile tilapia juveniles (*Oreochromis niloticus)* in response to oxidative stress caused by chronic ammonia exposure (Table 18 and 19), which reduces growth rate performance causes gill hyperplasia, and induces hyperexcitability, coma, convulsions and finally death. The activity of hepatic XO was increased 2.9-fold and 3.5-fold following exposure to 5mg/L and 10mg/L of ammonia respectively. The activity of XO in white muscle increased 2.25-fold and 2.6-fold following exposure to 5mg/L and 10mg/L of ammonia respectively. While the activity of hepatic AOX increased 2.1-fold and 2.5-fold following exposure to 5mg/L and 10mg/L of ammonia respectively which causes oxidative damage to the biological systems(Hegazi *et al.*, 2010). Sastry and Rao (1982 and 1984) it examined the extrahepatic activity of XO with mercuric chloride using xanthine as substrate with spotted murrel (*Channa punctatus)* in kidney, gill, brain and

muscle and found no change in to its activity. While Hari and Neeraja (2012) examined the activity of XO with ammonia in Common carp (*Cyprinus carpio)* kidney and found 2-fold decrease of its activity.

1.5.4. Genetic and structural properties of molybdo-flavoenzymes in fish.

It was initially believed that the developmental model organism, zebra fish (*Danio rerio*) did not have MFE genes as computer searches of whole genomes failed to find them initially, while the genome in the fishes *Fugu rubripes* and also *Poecilia reticulata* had at the least the XOR gene (Garattini *et al.*, 2003).Later it was found the MFEs genes were present in all fish genomes examined including zebra fish as seen in table 20 with (Kurosaki *et al.*, 2013).Using genome sequencing data, Kurosaki *et al*., (2013) reconstructed the evolution of MFEs by predicting the structures of MFEs genes and pseudogenes. Their work demonstrated that bony fish are most primitive vertebrate with an AOX gene (AOXα), coming from the duplication of an ancestral XDH. They also showed that during fish evolution duplication of AOXα into AOXβ and pseudogenization of the ancestral AOXα occurred (Figure 20, 21)(Kurosaki *et al.*, 2013). An orthologs of the piscine AOXβ was observed to be preserved in amphibians and it is likely that this is the precursors of reptilian, avian and mammalianAOX1 found in the liver of most higher organisms including human where AOX1 it is the sole AOX enzyme, as in Table 7, 8, 9 and Figure 22. On the other hand amphibian AOXγ is a duplication of AOXβ and the likely ancestor of avian and reptilian AOX2 that, in turn, gave rise to mammalian AOX3L1 (Figure 22). Subsequent gene duplications generated the two mammalian genes, AOX3 and AOX4 (Figure 22). The evolution of vertebrate AOX genes is thus dominated by duplication ,pseudogenization and deletion events (Kurosaki *et al.*, 2013).Figure 22 shows how

AOX and XDH genes evolved in different species of vertebrates. Table 20 summarises our current knowledge of AOX and XDH genes and pseudogenes in fish, amphibians, reptiles, birds and mammals (Kurosaki *et al.*, 2013).
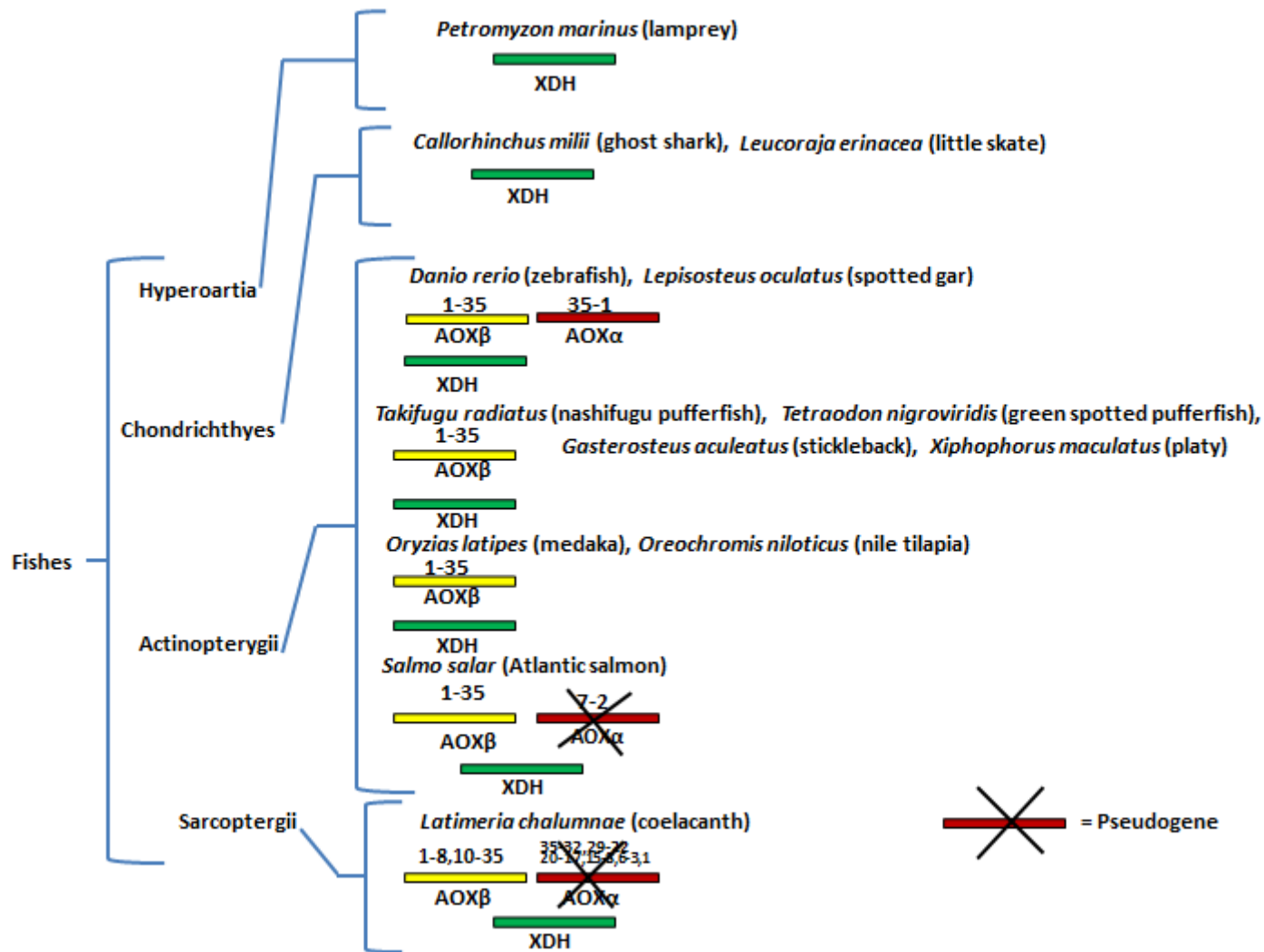
Figure 20: Summary of AOX and XDH genes in fish. Based on Kurosaki *et al.*, 2013. The green colour indicates XDH genes, the yellow colour indicates AOXβ genes and red colour indicates AOXαgenes. The numbers above the genes indicate the exons present and the crosses (X) indicate inactive pseudogenes that have exons missing.

	Fish		Comments
Jawless fish Cartilaginous fish	Lamprey (*Petromyzon marinus*) Little skate(*Leucoraja erinacea*) Australian ghost shark (*Callorhinchus milii*)		No AOX
			It is proposed AOXα evolved first, based on similarity of AOXα gene to XDH
Bony fish Cypriniformes Semionotiformes	Zebrafish (*Danio rerio*) Spotted gar (*Lepisosteus oculatus*)		AOXβ evolved from AOXα
Bony fish Salmoniformes Coelacanthiformes	Atlantic salmon (*Salmo salar*) Coelacanth (*Latimeria chalumnae*)		AOXα pseudogene : inactive gene
Tetraodontiformes Gasterosteiformes Cyprinodontiformes Beloniformes Perciformes	Fugu (*Takifugu rubripes*) Pufferfish (*Tetraodon nigroviridis*) Stickleback (*Gasterosteus aculeatus*) Platy (*Xiphophorus maculatus*) Medaka (*Oryzias latipes*) Nile tilapia (*Oreochromis niloticus*)		AOXα deleted from genome

Figure 21: Proposed evolution of AOX and XDH genes in fish. Based on Kurosaki *et al*., 2013. The green colour indicates XDH genes, the yellow colour indicates AOXβ genes and red colour indicates AOXα genes. The curved arrows indicate duplication events and the crosses (X) indicate inactive pseudogenes that have exons missing. [→] indicates direction of transcription.
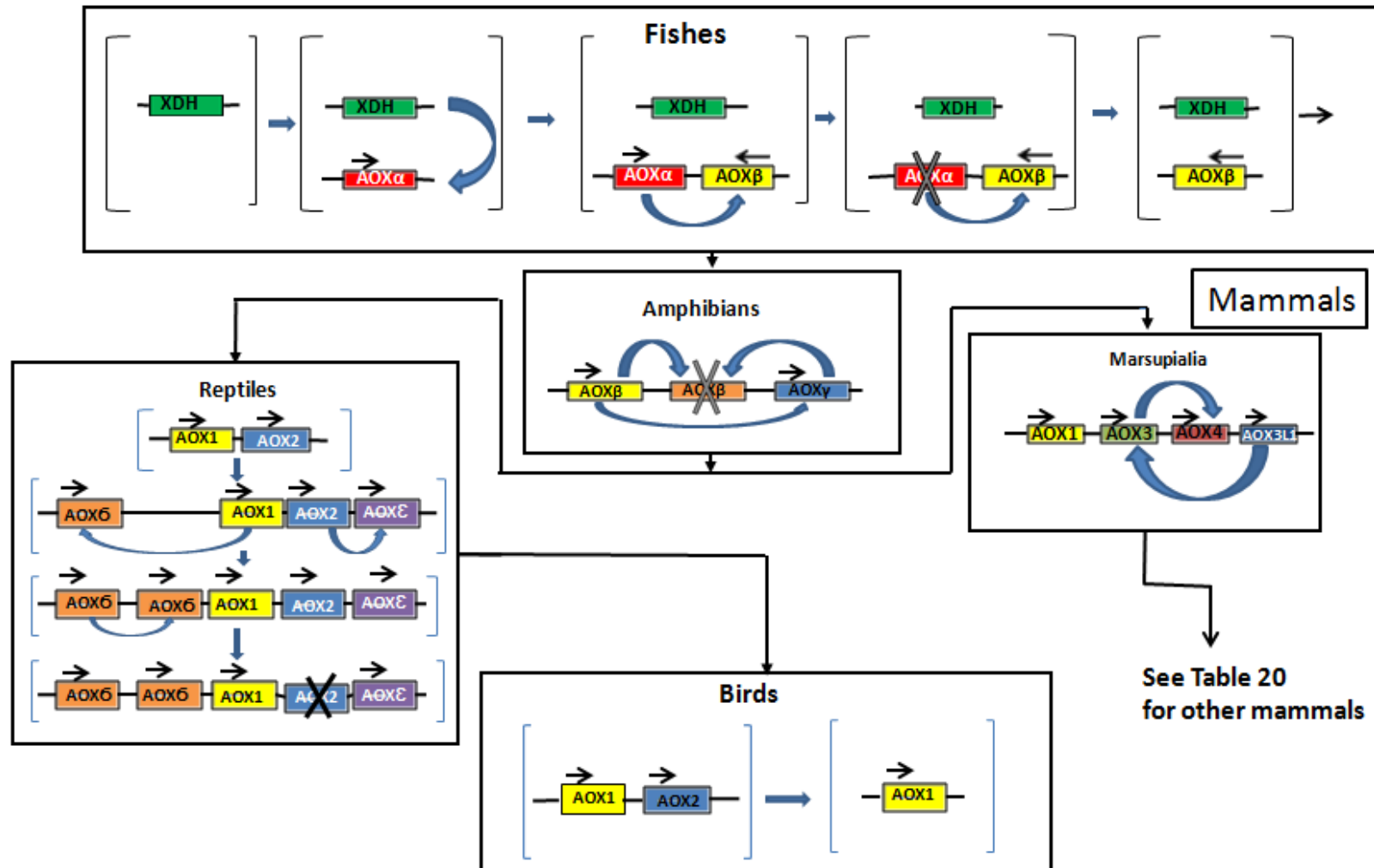
Figure 22: Summary of evolution of AOX and XDH genes in fishes, amphibians, reptiles, birds and mammals. Based on Kurosaki *et al.*, 2013.The green colour indicates XDH genes, the yellow colour indicates AOXβ and AOX1 genes, red colour indicates AOXα genes, blue colour indicates (AOX2) and the purple colour indicates (AOXℰ gene).The curved arrows indicate duplication events and the crosses (X) indicate inactive pseudogenes that have exons missing.[➔] Indicates direction of transcription.

Table 20: AOX and XOR genes in fish, amphibians, reptiles, birds and mammals

Organism	Class	Order	Family	Common name (*Species name*)	MFE genes present
Jawless fish (*Agnatha*)	Hyperoartia	Petromyzontiformes	Petromyzontidae	Lamprey (*Petromyzon marinus*)	XDH
Cartilaginous fish (*Chondrichthyes*)	Chondrichthyes	Rajiformes	Rajidae	Little skate (*Leucoraja erinacea*)	XDH
		Chimaeriformes	Callorhinchidae	Australian ghost shark (*Callorhinchus milii*)	XDH
Bony Fish (*Osteichthyes*)	Actinopterygii	Cypriniformes	Cyprinoidea	Zebrafish (*Danio rerio*)	AOXα, AOXβ,XDH
		Semionotiformes	Lepisosteidae	Spotted gar (*Lepisosteus oculatus*)	AOXα, AOXβ,XDH
		Tetraodontiformes	Tetraodontidae	Fugu (*Takifugu rubripes*)	AOXβ,XDH
				Pufferfish(*Tetraodon nigroviridis*)	AOXβ,XDH
		Gasterosteiformes	Gasterosteidae	Stickleback(*Gasterosteus aculeatus*)	AOXβ,XDH
		Cyprinodontiformes	Poeciliidae	Platy (*Xiphophorus maculatus*)	AOXβ,XDH
		Beloniformes	Adrianichthyidae	Medaka (*Oryzias latipes*)	AOXβ,XDH
		Perciformes	Cichlidae	Nile tilapia (*Oreochromis niloticus*)	AOXβ,XDH
		Salmoniformes	Salmonidae	Atlantic salmon (*Salmo salar*)	PAOXα, AOXβ,XDH
	Sarcopterygii	Coelacanthiformes	Coelacanthidae	Coelacanth (*Latimeria chalumnae*)	PAOXα, AOXβ,XDH
Amphibians	Amphibia	Anura	Pipidae	African frog (*Xenopus tropicalis*)	AOXβ,AOXγ,PAOXμ,XDH
Reptiles	Sauropsida	Testudines	Emydidae	Western painted turtle (*Chrysemys picta bellii*)	AOX1,AOX2,XDH
	Sauropsida	Testudines	Trionychidae	Chinese softshell turtle(*Pelodiscus sinensis*)	AOX1,AOX2,XDH
	Sauropsida	Squamata	Iguanidae	Anole lizard (*Anolis carolinensis*)	AOXδ,AOXε,AOX1,AOX2,XDH
	Sauropsida	Archosauria	Crocodylidae	American alligator (*Alligator mississippiensis*)	AOXδ,AOXε,AOXξ,AOX1,AOX2
	Sauropsida	Archosauria	Crocodylidae	Saltwater crocodile(*Crocodylus porosus*)	AOXδ,AOXε,AOXξAOX1,PAOX2
Birds	Aves	Galliformes	Phasianidae	Chicken(*Gallus gallus*) Turkey(*Meleagris gallopavo*)	AOX1,AOX2,XDH
	Aves	Psittaciformes	Psittacidae	Budgerigar(*Melopsittacus undulatus*)	AOX1,AOX2,XDH
	Aves	Passeriformes	Estrildidae	Zebra finch (*Taeniopygia guttata*)	AOX1,XDH
	Aves	Anseriformes	Anatidae	Mallard duck (*Anas platyrhynchos*)	AOX1,XDH
Mammals	Mammalia	Monotremata	Ornithorhynchidae	Platypus(*Ornithorhynchus anatinus*)	AOX1,AOX3,AOX3L1,AOX4,XDH1, PXDH2, PXDH 3, PXDH 4
	Mammalia	Didelphimorphia	Didelphinae	Opossum (*Monodelphis domestica*)	AOX1,AOX3,AOX3L1,AOX4,XDH
	Mammalia	Dasyuromorphia	Dasyuridae	Tasmanian devil(*Sarcophilus harrisii*)	AOX1,AOX3,AOX3L1,AOX4,XDH
	Mammalia	Diprotodontia	Macropodidae	Wallaby (*Macropus eugenii*)	AOX1,AOX3,AOX3L1,AOX4,XDH
	Mammalia	Afrosorcida	Tenrecidae	Lesser hedgehog tenrec(*Echinops telfairi*)	AOX1,AOX3,AOX3L1,XDH
	Mammalia	Proboscidea	Elephantidae	African elephant (*Loxodonta Africana*)	AOX1,AOX3,AOX3L1,AOX4,XDH
	Mammalia	Hyracoidea	Procaviidae	Rock hyrax (*Procavia capensis*)	AOX1,AOX3,AOX3L1,AOX4,XDH
	Mammalia	Cingulata	Dasypodidae	Armadillo (*Dasypus novemcinctus*)	PAOX1,AOX3,AOX3L1,AOX4,XDH
	Mammalia	Pilosa	Megalonychidae	Two toed sloth (*Choloepus hoffmanni*)	PAOX1, AOX3,AOX3L1,AOX4,XDH
	Mammalia	Chiroptera (Megachiroptera)	Pteropodidae	Flying fox (*Pteropus vampyrus*)	PAOX1, PAOX 3, PAOX 4,AOX3L1,XDH
	Mammalia	Chiroptera (Microchiroptera)	Vespertilionidae	Little brown bat (*Myotis lucifugus*)	PAOX3,AOX1,AOX3L1,AOX4,XDH
	Mammalia	Perissodactyla	Equidae	Horse(*Equus caballus*)	PAOX3,AOX1,AOX3L1,AOX4,XDH
	Mammalia	primates	Hominidae	Human (*Homo sapiens*)	PAOX3, PAOX3l1, AOX1, XDH

Based on (Kurosaki *et al.*, 2013).Abbreviation.P=pseudogene.

1.6. Purification of aldehyde oxidase and xanthine oxidoreductase enzymes.

MFEs have been purified from many different species with different methodologies as summarised in the (Tables 21, 22 and 23). Tables 21 and 22 summarise purification protocols for AOX from diverse number of organisms. Reviewing the literature on the subject reveals that the initial step of purification of AOX is generally subcellular fractionation to generate cytosol where the enzyme resides. A popular subsequent purification method used for AOX is heat precipitation. This method can be a useful step in the early stages of a purification scheme involving more heat stable proteins. It is generally achieved by incubating the protein mixture at known temperature for 10 minute, then cool in ice for 15 minute, then centrifugation at high centrifuge for 15 minute. These results in the denaturation of the unwanted less stable proteins in the mixture that are removed by precipitation. By this principle there can often by a 2-fold purification of a heat stable protein in the supernatant fraction (Bonner. 2007).The thermal stability of mammalian and Drosophila AOX has allowed this to be used successfully in 15 out of 18 purification protocols. Temperatures used for these purification protocols range from 50-68 °C with 50-55°C being the most common temperature used (Table 21 and 22). Interestingly heat treatment (50 – 70 °C) is also used in the purification of related MFEs, XOR (Table 23).

The next step commonly used in many AOX purification protocols is ammonium sulphate fractionation (Table 21 and 22). In this method the solubility of proteins is increased at low salt concentrations and is decreased at high salt concentrations. When a salt such as ammonium sulphate is added to a protein solution, the ions in the ammonium sulphate have a greater charge density than the proteins, they attract the

Species	Tissue	Enzyme	Purification steps	Molecular mass	Substrates	Fold purification a, b	Yield %	References
Guinea pig (*Cavia porcellus*)	Liver	AOX	Cytosol, 30-50% $(N_{H4})_2SO_4$, DEAE- cellulose, FMN – sepharose 4B, Sephacryl S-300	Native PAGE 300 kDa SDS PAGE 148 kDa	2-hydroxypyrimidine, N^1-methylnicotinamide,	120[a]	26	(Yoshihara and Tatsumi. 1985)
Hamster (*Hamster*)	Liver	AOX	Cytosol, heat at 50 °C, 30-50% $(NH_4)_2SO_4$, DEAE-cellulose, phenyl-Toyopearl, TSK-gel G3000SW$_{XL}$	Native PAGE 288 kDa SDS PAGE 145 kDa	Benzaldehyde	89[a]	12	(Sugihara *et al.*, 1999)
Mouse (*Mus musculus*)	Liver	AOH1	Cytosol, heat at 55 °C, 50% $(NH_4)_2SO_4$, Benzamidine sepharose 6B, MonoQ	SDSPAGE 147 kDa Zymogram MALDI-TOF MS	Phthalazine	173[a]	1.7	(Terao *et al.*, 2001)
Mouse (*Mus musculus*)	Liver	AOH2	Cytosol, heat at 55 °C, 50% $(NH_4)_2SO_4$, Benzamidine sepharose 6B, MonoQ	SDS PAGE 150 kDa MALDI-TOF MS Zymogram	All-trans retinaldehyde	346[a]	5	(Terao *et al.*, 2009)
Mouse (*Mus musculus*)	Nasal epithelial mucosa	AOH3	Cytosol, heat at 55 °C, 50% $(NH_4)_2SO_4$, MonoQ	SDS PAGE 150 kDa MALDI-TOF MS Zymogram western blot	Phthalazine, All-trans retinaldehyde, Benzaldehyde, 2-hydroxypyrimidine, Octanal	18[a]	26	(Kurosaki *et al.*, 2004)
Mouse (*Mus musculus*)	Liver	AOX	Cytosol, 30-50% $(NH_4)_2SO_4$, Benzamidine sepharose 6B, DEAE-cellulose	Native PAGE 265 kDa SDS PAGE 138 kDa	Benzaldehyde, DMAC, 2-hydroxypyrimidine	140[a]	-	(Yoshihara and Tatsumi. 1997)
Mouse (*Mus musculus*)	Liver	AOX1	Cytosol, heat at 55 °C, 50% $(NH_4)_2SO4$, Benzamidine sepharose 6B, MonoQ	SDS PAGE 150 kDa MALDI-TOF MS Zymogram, western blot	Phthalazine	627[a]	3	(Vila *et al.*, 2004)
Rat (*Rattus norvegicus*)	Liver	AOX	Crude extract, heat at 55 °C, 60% $(NH_4)_2SO_4$, HTP column, Benzamidine sepharose 6B, Sephadex G-25 column	Native PAGE 285 kDa SDS PAGE 150 kDa	DMAC	945[b]	13	(Maia and Mira. 2002)

Abbreviation: p-dimethylaminocinnamaldehyde - DMAC   a = from cytosol, b= from crud extract (homogenate)

Table 21: Summary of purification protocols for aldehyde oxidase from rodent species.

Species	Tissue	Enzyme	Purification steps	Molecular mass	Substrates	Fold purification a, b	Yield %	References
Bovine *(Bos taurus)*	Liver	AOX	Cytosol, heat at 60 °C, 40% $(NH_4)_2SO_4$, Fast-Q,Sephacryl, Benzamidine sepharose 6B	SDS PAGE 150 kDa	Phenanthridine	307[a]	3	(Calzei *et al.*, 1995)
Chicken *(Gallus gallus)*	Kidney	AOX1	Cytosol, heat at 55 °C, 40% $(NH_4)_2SO_4$, Benzamidine Sepharose 6B, MonoQ	SDS PAGE 150 kDa MALDI MS	All-trans retinaldehyde	-	-	(Terao *et al.*, 2006)
Drosophila *(Drosophila melanogaster)*	Flies	AOX	Cytosol, heat at 68 °C, 55-75% $(NH_4)_2SO_4$, Sephadex G200, DEAE -Cellulose	Native PAGE 280 kDa	Benzaldehyde	481[a]	18	(Andres. 1976)
Drosophila *(Drosophila melanogaster)*	Flies	AOX	Crude extract, CM-cellulose, 55-75% $(NH_4)_2SO_4$, DEAE –Cellulose, hydroxylapatite	-------------------	Benzaldehyde	361[b]	16	(Dickinson. 1970)
Sea bream *(Pagrus major)*	Liver	AOX	Cytosol, heat at 50 °C, 30-50% $((NH_4)_2SO_4$, DEAE-cellulose	-------------------	Benzaldehyde	33[a]	5.6	(Kitamura *et al.*, 2003)
Sea bream *(Pagrus major)*	Liver	AOX	Cytosol, heat at 45 °C, 30-45% $(NH_4)_2SO_4$, DEAE-cellulose column chromatography	-------------------	Benzaldehyde, 2-nitrofluorene 2-hydroxypyrimidine	-	-	(Ueda *et al.*, 2002)
Pig (Sus scrofa)	Liver	AOX	Crude extract, heat at 55 °C, 60% $(NH_4)_2SO_4$, Acetone precipitation, Alumina Cỳ, DEAE-cellulose, preparative electrophoresis	Disc gel electrophoresis 270 kDa	N^1-methylnicotinamide	115[b]	6.8	(Felsted *et al.*, 1973)
Rabbit *(Oryctolagus cuniculus)*	Liver	AOX	Crude extract, heat at 55 °C, 60% $(NH_4)_2SO_4$, Acetone precipitation, Calcium phosphate gel, DEAE-cellulose, preparative electrophoresis	Disc gel electrophoresis 260 kDa	N^1-methylnicotinamide	118[b]	14.4	(Felsted *et al.*, 1973)
Rabbit *(Oryctolagus cuniculus)*	Liver	AOX	Crude extract, heat at 58 °C, 50% $(NH_4)_2SO_4$, 50% Acetone precipitation, DEAE-Sephacel,HA-Ultrogel, Sephacryl S-300, MonoQ	Native PAGE 290 kDa SDS PAGE 144 kDa EPR spectroscopy	1-methylnicotinamide	-	-	(Turner *et al.*, 1995)
Rabbit *(Oryctolagus cuniculus)*	Liver	AOX	Crude extract, heat at 55 °C, 50% $(NH_4)_2SO_4$, Benzamidine sepharose 6B, MonoQ	SDS PAGE 150 kDa MALDI-TOF MS, Zymogram, western blot	Phthalazine	400[b]	64	(Stell *et al.*, 1989)

Abbreviation: a = from cytosol, b= from crude extract (homogenate)

Table 22: Summary of purification protocols for aldehyde oxidase from non-rodent species.

Species	Tissue	Enzyme	Purification steps	Molecular mass	Substrates	Fold purification a, b	Yield %	References
Chicken *(Gallus gallus)*	Liver	XDH	Crude extract, heat at 70°C, 30% $(NH_4)_2SO_4$, Sephadex G25, DEAE -Sephadex	Native PAGE 300 kDa	Xanthine + NAD^+	-	-	(Rajagopalan and Handler. 1967)
Drosophila *(Drosophila melanogaster)*	Flies	XDH	Crude extract, heat at 68°C, 30-50% $(NH_4)_2SO_4$, Sephadex G200, DEAE -Cellulose	Native PAGE 300 kDa	Isoxanthopterin + NAD^+	481[b]	18	(Andres. 1976)
Drosophila *(Drosophila melanogaster)*	Flies	XDH	Crude extract, 30-55% $(NH_4)_2SO_4$, Acetone 25-50%, DEAE –Cellulose, Sephacryl-HR200, Superose 12, MonoQ	SDS PAGE 150 kDa	Pterin+NAD^+	2840[b]	21	(Hughes *et al.*, 1994)
Carp *(Cyprinus carpio)*	Liver	XOR	Cytosol, 30-60% $(NH_4)_2SO_4$, Sephadex G-25, DEAE-Sephacel	---------------	Xanthine, Hypoxanthine + NAD^+	-	-	(Kamiński and Jeżewska. 1985)
Pig (Sus scrofa)	Liver	XO	Crude extract, heat at 55 °C, 60% $(NH_4)_2SO_4$, Acetone precipitation, Alumina Cỳ, DEAE-cellulose	---------------	Xanthine	83[b]	3	(Felsted *et al.*, 1973)
Rabbit *(Oryctolagus cuniculus)*	Liver	XO	Crude extract, heat at 55C°, 60% $(NH_4)_2SO_4$, Acetone precipitation.	---------------	Xanthine	98[b]	19	(Felsted *et al.*, 1973)
Rat *(Rattus norvegicus)*	Liver	XO	Crude extract, heat at 55°C, 60% $(NH_4)_2SO_4$, HTP, Q-Sepharose F.F.	Native PAGE 300 kDa SDS PAGE 150 kDa	Xanthine	1167[b]	19	(Maia and Mira. 2002)
Rat *(Rattus norvegicus)*	Liver	XOR	Crude extract, heat at 65 °C, 50% $(NH_4)_2SO_4$, Benzamidine Sepharose 6B, Sephadex G-50	SDS PAGE 150 kDa	Xanthine + NAD^+	199[b]	5.7	(McManaman *et al.*, 1996)
Rat *(Rattus norvegicus)*	Liver	XO	Crude extract, DEAE bath, 43% acetone precipitation, DEAE Sephacel pool, HA Ultrogel	SDS PAGE 137 kDa	Xanthine	781[b]	19	(Engerson *et al.*, 1987)
Rat *(Rattus norvegicus)*	Liver	XDH	Crude extract, DEAE bath, 43% acetone precipitation, DEAE Sephacel pool, HA Ultrogel	SDS PAGE 137 kDa	Xanthine+NAD^+	1060[b]	47	(Engerson *et al.*, 1987)

Abbreviations: a = from cytosol, b= from crude extract (homogenate)

Table 23: Summary of xanthine oxidoreductase purification from different species

water molecules away from the surfaces of the proteins. This exposes hydrophobic patches on the proteins causing them to interact with each other forming inter-protein complexes. When a protein complex becomes too large it comes out of solution as a precipitate (Bonner. 2007). In all 18 protocols for AOX purification, ammonium sulphate fractionation has been used as an enrichment step prior to chromatography (Table 21 and 22). Sometimes a single ammonium sulphate fractionation is used but some protocols use two steps of ammonium sulphate fractionation to generate a narrower precipitation range (Table 21 and 22). Ammonium sulphate fractionation used for the purification protocols of AOX range from 30-75 % saturation with 30-50 % saturation being the most common ammonium sulphate fractionation used.

With regards chromatography steps, four types of chromatography media have been used in the purification of AOXs namely ion exchange, gel filtration, hydrophobic interaction and affinity chromatography.

For AOX purification anion exchange media is the preferred ion exchange chromatography reagent used to separate negatively charged proteins. The molecular basis of this chromatography is that the resin in anion exchange columns contains cationic (positively charged) sites to bind proteins with a net negative charge. The bound proteins are then eluted by gradually increasing the salt concentration of the eluting buffer. A typical elution used is a gradient of $0 - 1M$ NaCL(Bonner. 2007). Anion exchange has been used in 10 out of 18 AOX purification protocols with DEAE-cellulose, 7 out of 18 AOX purification protocols with Mono-Q and 1 out of 18 AOX purification protocols with FAST-Q media being used. Anion exchange has been used in the purification of the related enzyme XOR (Table 23).

Gel filtration that separates molecules on the basis of their differences in size and shape have been used in 4 out of 18 AOX purification protocols (Table 21 and 22). Affinity chromatography that separates proteins on the basis of a reversible interaction between a protein or group of proteins and a specific ligand have been used in 9 out of 18 AOX purification protocols (Table 21 and 22). 8 out of 18 AOX purification protocols were with benzamidine sepharose 6B media being used on the basis of benzamidine being a competitive inhibitor of AOX (Table 21 and 22) (Stell *et al.*, 1989).

A literature survey (Table 21 and 22) reveals that to obtain a homogeneous preparation of AOX as assessed by SDS-PAGE or mass spectrometry generally the enrichment factor from liver is 89 – 2840 folds (Table 21 and 22). In order to achieve this yields range from 1.7 – 64 % (Table 21 and 22) liver AOX.

With regards substrates used to monitor the purification of AOX the most popular are 2-hydroxypyrimidine, N^1-methylnicotinamide, benzaldehyde, phthalazine, all-trans retinaldehyde, octanal, p-dimethylaminocinnamaldehyde (DMAC), phenanthridine and 2-nitrofluorene (Table 21 and 22). In these assays which are generally spectrophotometric some investigations do not directly measure substrate or product. These indirect assays use artificial electron acceptors such as dichloroindophenol (DCIP) and ferricyanide (Table 21 and 22).

With regards determining the native molecular mass of AOX, gel filtration has been used in 23 out of 28 protocols to determine this native molecular mass of purified enzyme preparations. These range from 212 – 300 kDa (Tables 21, 22 and 23).

1.7. Aims of the project.

As indicated in the introduction the study of MFEs in fish has received much less attention than their mammalian counterparts. Of particular interest for aquatic organisms is a group of nitrogen containing polycyclic aromatic hydrocarbons (NPAHs) and their metabolites that are found as aquatic environmental pollutants (Blumer *et al.*, 1977, Balch *et al.*, 1995, Osborne *et al.*, 1997, de Voogt and Laane. 2009) are AOX substrates that are cytotoxic, embryotoxic, teratogenic, genotoxic and carcinogenic (Southworth *et al.*, 1979, Balch *et al.*, 1995, Jung *et al.*, 2001, Barron *et al.*, 2004, Peddinghaus *et al.*, 2012, Brinkmann *et al.*, 2014). These include AOX substrates such as phenanthridine, quinoline, isoquinoline, hydroxyisoquinolines, cinchonine, phthalazine, hydroxyphthalazines, quinazoline, hydroxyquinazolines and acridine (Rajagopalan and Handler. 1964b, Palmer *et al.*, 1969, Krenitsky *et al.*, 1972, McCormack *et al.*, 1978, Stubley *et al.*, 1979, Stubley and Stell. 1980, McMurtrey and Knight. 1984, Beedham *et al.*, 1992, Robertson and Bland. 1993, Rashidi. 1996, Schofield *et al.*, 2000, Beedham. 2001, Al-Tayib. 2009, Pryde *et al.*, 2010, Barr and Jones. 2013, Mu *et al.*, 2014).

Despite NPAHs being important aquatic pollutants to date only one of these, phthalazine, has been investigated as an AOX substrate in a fish species (Nile tilapia juveniles (*Oreochromis niloticus))* (Hegazi *et al.*, 2010).

The species focussed on in this research project and aims of this study are as follows: Rainbow trout (*Oncorhynchus mykiss)* was the focus of this study for several reasons. Rainbow trout is a member of the Salmonidae family, are widely distributed fish species cultured in regions with cold and cool water temperatures around the world (Harvey. 2004). They are important food and sport fish and the most cultivated cold

freshwater fish in the US, Canada and European countries (Wolf and Rumsey. 1985). Due to its economic importance and ease of availability of tissue it is one of the most rigorously studied fishes in many research areas including carcinogenesis, toxicology, comparative immunology, disease ecology, physiology and nutrition (Behnke. 1992). With regards MFEs rainbow trout belongs to a class of fish Salmonidae, that have a single active AOX gene (AOXβ) that is the ancestral AOX gene that gave rise to AOX1 the predominant hepatic AOX in rodents and the only AOX in humans(Kurosaki *et al.*, 2013). Despite the aforementioned reasons for studying AOX in a Salmoniforme there has been no study to date (Tables 10, 11 and 12).

(a)   The initial aim was to compare the biotransformation of endogenous and exogenous substrates by AOX and XOR in rainbow trout, rat and human.

(b)   Up until now there has been no published work on any fish AOX and XOR with Km and Vmax measurements. An aim was therefore to determine the Km and Vmax for MFEs in rainbow trout and compare it with results in rat and human using spectrophotometric and HPLC assays.

(c)   An additional aim of this project was to determine if environmental pollutants, drugs and estrogens might inhibit AOX in fish.

(d)   As there has been no report of the purification of any piscine AOX to homogeneity, another goal was to purify the AOX enzyme from rainbow trout liver to examine its molecular characteristics.

2.0. Materials and methods.

All reagents and chemicals were obtained from Fisher Scientific and Sigma / Aldrich Chemical Company Ltd, Poole, UK. Solvents and mobile phase reagents were obtained from different companies but were all for HPLC grade purity. The control of substances hazardous to health (COSHH) risk assessment for all reagents and chemicals were prepared before experiments were initiated.

Male Wistar rats (*Rattus norvegicus*) and male New Zealand white rabbit liver cytosol were obtained from the biomedical services unit, University of Dundee (Dr D.J.Clarke). Pooled human liver cytosol was obtained from Invitrogen Ltd. Immature rainbow trout (*Oncorhynchus mykiss*) liver was obtained from Pennine Trout Farm and Fishery, Calderbrook Road, Littleborough OL15 9HL, UK.

2.1. *In vitro* analysis of molybdo-flavoenzyme activity.

2.1.1. Preparation of cytosol.

For the preparation of cytosol all steps were carried out at $0 - 4°C$. Approximately 10 g of liver, kidney and gill were weighed out and homogenised in 40 ml of cold buffer (0.25 M sucrose, 10 mM Tris HCL pH 7.4) with a motor-driven tissue mortar fitted with a Teflon pestle (clearance 0.15-0.23mm, speed 10000 rpm and 5 minute duration) to produce a 25% w/v homogenate. The homogenate was then centrifuged at $4°C$ for 15 minutes at 10,000 xg, to pellet out the nuclear/mitochondrial fractions of the homogenate. The supernatant was then removed and centrifuged for a further 60 minutes at $4°C$ at 105,000 xg to obtain the cytosolic fraction. This fraction was then collected and separated into 0.5 ml aliquots and stored at -80°C.

2.1.2. Gel filtration of cytosol.

Gel filtration of cytosol was carried out in order to remove endogenous small molecules, such as endogenous substrates and inhibitors, which may interfere with enzyme assays. A PD-10 gel filtration column was used (GE Healthcare Bio-Science, UK). Prior to use the column was allowed to drain before being equilibrated with 25 ml (5 column volumes) 50 mM Tris HCL pH 7.4. 2.5 ml of cytosol was then loaded onto the column and eluted with 3.5 ml of 50 mM Tris HCL pH 7.4, the protein containing fraction was then collected, pooled and aliquoted into 0.5 ml fractions in 1.5 ml polypropylene Eppendorf tubes to avoid repeated freeze/thawing and stored at - 80°C.

2.2. Protein determination.

The amount of protein in each sample was calculated using a modification of the method described by Smith *et al*. using bovine serum albumin (BSA) as standard (Smith *et al.*, 1985). The bicinchoninic acid (BCA) based assay is available as a kit from Sigma-Aldrich Co.

2.2.1. Bicinchoninic acid reagents.

a) 1000 ml solution containing bicinchoninic acid (40 g), sodium carbonate (Na_2CO_3) (8 g), sodium tartrate ($Na_2C_4H_4O_6$)(16 g) and sodium bicarbonate ($NaHCO_3$) (9.5 g) in 0.1N NaOH (final pH 11.25).Purchased from Sigma- Aldrich Co.

b) 25 ml solution containing 4% w/v copper sulphate pentahydrate ($CuSO_4.$ $5H_2O$).For preparing of a set protein standards a 1mg/ml stock solution of bovine serum albumin (BSA) was prepared. This was then used to make the dilutions for the calibration curve as shown in (Table 24).

Table 24. Preparation of protein calibration standards

Final protein concentration (mg/mL)	Volume BSA stock solution (µl)	Distilled water (µl)
0	0	100
0.2	20	80
0.4	40	60
0.6	60	40
0.8	80	20
1.0	100	0

2.2.2. Bicinchoninic acid methodology.

a) The required amount of protein determination reagent was prepared by adding 1 part $CuSO_4$. $5H_2O$ 4% w/v solution to 50 parts bicinchoninic acid solution.

b) Bovine serum albumin standards or 1 in 20 dilution gel-filtered cytosol (20 µl cytosol + 380 µl PBS) were prepared in duplicate.

c) 300 µl of freshly protein determination reagent was added to 15 µl of diluted cytosol or protein standard and vortexed.

d) All tubes were incubated at 37°C for 30 minutes.

e) The absorbance at 562 nm was then measured on a microplate reader and distilled water was used to zero the instrument.

2.3. Preparation of substrate stocks.

5 mM individual stock solution of AOX and XOR substrates and corresponding metabolites were prepared with appropriate solvent as indicated in (Table 25). After preparing the stock solutions, working standard solutions of 1 mM were prepared by dilution with water.

Table 25: List of stock substrates, products and solvent used to prepare them.

Substrate and product (5mM stock solution)	Comment	AOX and XOR	Solvent/treatment
Allopurinol	Hyperuricemia drug	AOX/XOR	10 mM NaOH /sonicating
Oxipurinol	Allopurinol metabolite	AOX/XOR	10 mM NaOH /sonicating
All-trans retinal	Vitamin A	AOX	Absolute ethanol
Retinoic acid	Vitamin A metabolite	AOX	Absolute ethanol
Cinchonine	Anti-malarial drug	AOX	dissolve in minimum volume of 0.1M HC then dH$_2$O added
DMAC	Colouring dye	AOX	Absolute ethanol
6-mercaptopurine	Anti-cancer drug	AOX/XOR	10 mM NaOH /sonicating
6-thiouric acid	6-mercaptopurine metabolite	AOX/XOR	10 mM NaOH /sonicating
1-methylxanthine	Purine metabolism	XOR	10 mM NaOH /sonicating
1-methyl uric acid	1-methylxanthine metabolite	XOR	10 mM NaOH /sonicating
N^1- methylnicotinamide	Endogenous vitamin metabolite	AOX	dH$_2$O /sonicating
Phenanthridine	Environmental pollutant	AOX	Absolute ethanol
Phenanthridone	Phenanthridine metabolite	AOX	Absolute ethanol
Phthalazine	Environmental pollutants	AOX	Absolute ethanol
Phthalazinone	Phthalazine metabolite	AOX	Absolute ethanol
Pyrazinamide	Tuberculosis drug	AOX/XOR	10 mM NaOH /sonicating
Pyridoxal	Vitamin B6	AOX	dissolve in minimum volume of absolute ethanol then dH$_2$O added
6-pyridoxic acid	Pyridoxal metabolite	AOX	dissolve in minimum volume of absolute ethanol then dH$_2$O added
Vanillin	Food constituent	AOX	dH$_2$O /heated to 70^{0}C
Vanillic acid	Vanillin metabolite	AOX	dH$_2$O /heated to 70^{0}C
Xanthine	Purine metabolism	XOR	10 mM NaOH /sonicating
Uric acid	Xanthine metabolite	XOR	10 mM NaOH/Sonicating

Abbreviation: DMAC – dimethylaminocinnamaldehyde.

2.4. Spectrophotometric determination of aldehyde oxidase activity.

AOX assays were performed with 40µl of gel filtered cytosol, 10µl of 1mM of substrate (dimethylaminocinnamaldehyde (DMAC), phenanthridine or vanillin) and 50µl Tris HCL pH 7.4 at 37°C. Spectrophotometric molybdo-flavoenzyme assays were conducted by using a microplate spectrophotometer (BioTek) at 37ºC. All assays

were executed in triplicate in 100 µl reaction volumes. All cytosol samples were frozen and thawed just once, and the spectrophotometric data were collected at 5 second intervals for 3 to 5 minutes utilizing Gen5™ software on the Windows XP PC connected to the microplate reader's spectrophotometer (BioTek), using the appropriate wavelength and molar absorption coefficient for each substrate / product as summarised in (Table 26).

Table 26: Wavelength and molar absorption coefficients used for the spectrophotometric measurement of aldehyde oxidase activity

Substrates	Principle of assay	Wavelength nm	Molar absorption, $\mathcal{E}$ (M^{-1} cm^{-1})	Reference
DMAC	Disappearance of substrate	398	30500	(Kurth and Kubiciel. 1984)
Phenanthridine	Appearance of product	322	6400	(Johnson *et al.*, 1984)
Vanillin	Disappearance of substrate	310	8854	(Panoutsopoulos and Beedham. 2004)

Abbreviation: DMAC – dimethylaminocinnamaldehyde.

2.5. Spectrophotometric determination of xanthine oxidoreductase activity.

The oxidation of xanthine to the uric acid and 1-methylxanthine to the 1-methyluric acid was assayed by monitoring the appearance of uric acid or 1-methyluric acid at 295 nm with the electron acceptors NAD^+ and O_2 (Waud and Rajagopalan. 1976). A summary of the assay conditions is given in (Table 27). The specific activity was calculated using the molar extinction coefficient for uric acid and 1-methyluric acid which is 9,600 M^{-1} cm^{-1}.

Table 27: Summary of xanthine oxidoreductase assay setup.

XO activity assay			XO activity blank		
Reagent	Volume	Final concentration	Reagent	Volume	Final concentration
Gel-filtered cytosol	60 µl		Gel-filtered cytosol	60 µl	
100 mM Tris HCL, pH 8.0	20 µl	20 mM Tris HCL pH 8.0	100 mM Tris HCL, pH 8.0	20 µl	30 mM
1.5 mM (X or 1-MX) in 10 mM NaOH	10 µl	0.15 mM (X or 1MX) 1mM NaOH	10 mM NaOH	10 µl	1 mM
dH$_2$O	10µl		dH$_2$O	10µl	
XOR activity assay			**XOR activity blank**		
Reagent	Volume	Final concentration	Reagent	Volume	Final concentration
Gel-filtered cytosol	60 µl		Gel-filtered cytosol	60 µl	
100 mM Tris HCL, pH 8.0	20 µl	20 mM Tris HCL pH 8.0	100 mM Tris HCL, pH 8.0	20 µl	20 mM
6.7 mM NAD$^+$	10 µl	0.67 mM NAD$^+$	6.7 mM NAD$^+$	10 µl	0.67 mM
1.5 mM (X or 1-MX) in 10 mM NaOH	10 µl	0.15 mM (X or 1MX) 1mM NaOH	10 mM NaOH	10 µl	1 mM

Abbreviation; Xanthine(X) and 1-methylxanthine (1-MX)

The total XOR activity was calculated following subtraction of the XOR blank. This gave the total XOR activity with both NAD$^+$ and O$_2$ as electron acceptors and was the total activity of the enzyme in the sample as both a dehydrogenase and oxidase. The XO activity was calculated following subtraction of the XO blank. This gave the activity with O$_2$ as an electron acceptor. In order to calculate the XDH activity in the sample, the XO activity was subtracted from the XOR activity to give the activity with NAD$^+$ as electron acceptor only. The percentage XDH activity in the sample was calculated by dividing the XDH activity by the total XOR activity and multiplying by 100. Similarly the percentage XO activity was calculated by dividing the XO activity by the total XOR activity and multiplying by 100.

2.6. Determination of specific activity from spectrophotometric data.

The number of nmoles of substrate biotransformed per minute was calculated using the absorbance change observed per minute using the relationship :$c = A/\mathcal{E}l$ where c = concentration (mM), A = absorbance, l = path length of absorbing solution in cm, $\mathcal{E}$ = molar extinction coefficient. The light path for 100µl in a 96-well microplate was 0.681cm. Specific activity was then calculated as the number of nmoles of substrate converted per minutes per mg of protein. The protein concentration of the sample was measured as described in the section 2.2.

2.7. Determination of optimum conditions of molybdo-flavoenzymes.

As enzyme activity changes according to the reaction conditions changes in pH, temperature and substrate concentration were investigated.

2.7.1. Determination of optimum pH of buffer.

The pH dependence of AOX and XDH were analyzed by assay of the enzymes at 37°C for 5 minutes at different pH values 5.6, 6.5, 7, 7.5 and 8.0 utilizing sodium phosphate buffers (50 mM final concentration).

2.7.2. Temperature dependence of AOX and XOR activities.

This assay was performed to study the effects of incubation temperature on reaction rates of enzyme activity at different incubation temperature. The aliquots of filtered cytosol were assayed at 25, 30, 37, 40, 45, 55°C and 60°C in a microplate reader with a final DMAC concentration of 100µM as substrate of AOX and a final xanthine concentration of 100µM as substrate of XOR and 0.67mM NAD^+ as an electron acceptor. As summarized in (Tables 26 and 27).

2.7.3. Heat stability study.

The aliquots of filtered cytosol were incubated at 55°C for 15, 30 and 60 minute in a thermocycler machine (PCR machine) with a heated lid. The heated lid of the PCR machine prevented evaporation and losses due to refluxing. The cytosols were removed from heating and cooled in ice for 5 min and cooled cytosol centrifuged at 13,000 xg for 5 min and any precipitate discarded. The assays were performed on the supernatant fraction using standard assay conditions for AOX activity with DMAC, as summarized in section 2.4.

2.8. Assay of molybdo-flavoenzyme activity using high pressure liquid chromatography.

All aldehydes and N- heterocyclic compounds mentioned before in section 2.3 (Table 25) were purchased from Sigma Aldrich and reagents required for the preparation of the HPLC mobile phases were all of HPLC grade purity from the same company.

The analysis of aldehyde and N-heterocyclic compounds and their corresponding metabolites were carried out by reverse phase HPLC. The system used comprised of a Beckman Coulter System Gold^{TM} 127 Solvent HPLC Module (dual pump) and a programmable UV detector (module 166) or a programmable diode array detector (module 168) along with injector designed with a 20 μl sample loop and auto sampler. The analytical columns used were either: a Kromasil (25 cm X 4. 6 mm, 5μm; RP-C18), Hypersil ODS (25 cm X 4. 6 mm, 5μm; RP-C18), LiChrosphere® (25 cm X 4 mm, 5μm; RP-C18) or Spherisorb® (5μm CNRP 4.6 X 15 cm; RP-C18). A guard column with same stationery phase as the main chromatography column was used upstream in the analytical column. These columns were from Phenomenex, UK and Capital HPLC limited, UK. The mobile phases were filtered through a 0.45μm filter

before use. Isocratic and gradient methods were utilized to develop the optimal conditions for the separation of analytes and the most highly sensitive method for the determination of the different compounds.

5 mM individual stock solutions of AOX and XOR substrates and corresponding metabolites were prepared within appropriate solvent as described in (Table 25) in section 2.3. After preparing the stock solutions 1mM working standard solutions were prepared by dilution along with water. Quantification was done using five standards prepared from stock solutions with distilled water, 0.01, 0.02, 0.03, 0.05 and 0.1mM. 20µl of these compounds were injected onto the HPLC instrument starting with the lowest concentration to give a range of 0.2 to 2 nmol, as documented in figures 1- 5 in the Appendix 3. All stock's solutions were stored at 4^0C for up to 3 months with the exception of vanillin and N^1-methylnicotinamide, which were stored at -20^0C.

Calibration standards injected on the same day were used to calculate intra-day accuracy and precision. This is a measure of the distribution of individual measurements around the mean. This parameter was assessed by repeated analysis of the same solution and expressed as the relative standard deviation (RSD) otherwise known as the coefficient of variation (CV). % RSD for retention time was calculated by dividing the standard deviation by the mean of retention time of three replicates in the same day (Miller and Miller. 2005, Ghassan *et al.*, 2010). The accuracy of the assay was calculated by comparison of the nominal analyte concentration to the actual concentration obtained from the linear regression line within the concentration investigated (0.01, 0.02, 0.03, 0.05, 0.1mM) (Accuracy = nominal concentration / actual concentration x 100). By using slope, intercept and the correlation coefficient (RSQ or r^2) for the linearity of the calibration curve was determined for each analyte. The lower limit of quantification (LOQ) and limit of detection (LOD) were

determined for each analyte. According to international conference on harmonisation (ICH) guidelines, the LOD is defined as the lowest concentration of an analyte in a sample that can be detected but not quantified. The LOQ is the lowest amount of analyte in a sample that can be quantitatively determined with suitable precision and accuracy under the standard operational conditions of the method (ICH. 1994). The lower LOQ and LOD of samples was defined as the lowest added analyte concentration that can be measured with a low RSD and an accuracy of $100 \pm 20\%$ that can be discriminated significantly from the basal concentration of analyte. The ICH has listed two options available to calculate both the LOD and the LOQ of an assay. One of these options are expressed as a concentration at a specified signal to noise ratio, usually 3:1 and 10:1 for the signal to noise ratio for LOD and LOQ respectively (ICH. 1994). The LOD and the lower of LOQ were calculated from the mean of the slope (S) and standard deviation of the intercept of three calibration curves using the linear regression method. The LOD and LOQ are calculated according to the following equations: The LOD = 3.3 (SD/S) and the LOQ = 10 (SD/S) (ICH. 1994, Miller and Miller. 2005). All mobile phases and HPLC methods for assay of MFE activity for allopurinol, 6-mercaptopurine, 1-methylxanthine, xanthine, pyridoxal, all-trans retinal, vanillin, cinchonine, N[1]-methylnicotinamide, phenanthridine, phthalazine and pyrazinamide are summarized in (Tables 28 and 29).

76

Analytes	Chromatograph column	Mobile phases	Gradient/ Isocratic	Flow rate ml/min	Wavelength	Reference
Cinchonine	Hypersil ODS 5µm (25 cm x 4.6 mm, C18)	A:0.4% w/v CH_3COONH_4, pH 3.27 B:Acetonitrile 35% v/v.	Isocratic	1.0	248 nm UV detector	(Beedham *et al.*, 1992)
Pyrazinamide	Kromasil 5µm (25cm x 4.6mm, C18) with guard column 5µm	A: 20 mM KH_2PO_4, pH 5.2 B:Acetonitrile 5% v/v	Isocratic	0.8	268 nm UV detector	(Kraemer *et al.*, 1998)
Pyridoxal	Kromasil 5µm (25cm x 4.6mm, C18) with guard column 5µm	A: 60 mM Na_2HPO_4, pH 6.5 B: Methanol 25% v/v.	Isocratic	0.8	315 nm UV detector	Modified from(Talwar *et al.*, 2003)
All-trans retinal	Kromasil 5µm (25cm x 4.6mm, C18) with guard column 5µm	A: 30 mM CH_3COONH_4, pH 4.5 B: Acetonitrile 70% v/v.	Isocratic	1.0	378 nm diode array detector	Modified from(Huang and Ichikawa. 1997)
Vanillin	Kromasil 5µm (25cm x 4.6mm, C18) with guard column 5µm	A: 0.22 M KH_2PO_4, pH 2.9 B: Acetonitrile 15% v/v.	Isocratic	1.5	285 nm UV detector	(Panoutsopoulos and Beedham. 2004)

Table 28: Isocratic HPLC protocols for the measurement of MFE activity

Analytes	Chromatograph column	Mobile phases	Gradient/ Isocratic	Flow rate ml/min	Wavelength	Reference
Allopurinol and oxipurinol	Kromasil 5μm (25cm x 4.6mm, C18) with guard column 5μm	A: water H_2O with addition of 0.1% v/v of glacial acetic acid. B: Acetonitrile.	Gradient see table 30	Flow rate was varied according to table 31	280 nm UV detector	This study
6-mercaptopurine and 6-thioxanthine	Kromasil 5μm (25cm x 4.6mm, C18) with guard column 5μm	A: water H_2O with addition of 0.1% v/v of glacial acetic acid. B: Acetonitrile.	Gradient see table 31	Flow rate was varied according to table 32	280 nm UV detector	This study
N^1- methylnicotinamide (2PY and 4PY)	Water Spherisorb® 5um (CNRP 4.6 x 150 mm; C18)	A: 0.1% v/v of formic acid B: Acetonitrile	Gradient see table 32	0.8	254 nm UV detector	(Szafarz *et al.*, 2010)
N^1- methylnicotinamide (2PY and 4PY)	Kromasil 5μm (25cm x 4.6mm, C18) with guard column 5μm	A: water H_2O with addition of 0.1% v/v of glacial acetic acid. B: Acetonitrile	Gradient see table 30	Flow rate was varied according to table 31	280 nm UV detector	This study
Phenanthridine and 6(5H)-phenanthridone	Kromasil 5μm (25cm x 4.6mm, C18) with guard column 5μm	A: water H_2O B: Acetonitrile	Gradient see table 33	1.5	254 nm UV detector	Modified from(LaVoie *et al.*, 1985)
Phthalazine and phthalazinone	Kromasil 5μm (25cm x 4.6mm, C18) with guard column 5μm	A: water H_2O with addition of 0.1% v/v of glacial acetic acid. B: Acetonitrile.	Gradient see table 31	Flow rate was varied according to table 32	280 nm UV detector	This study
Xanthine and 1-methylxanthine	Kromasil 5μm (25cm x 4.6 mm, C18) with guard column 5μm	A: water H_2O with addition of 0.1% v/v of glacial acetic acid. B: Acetonitrile	Gradient see table 31	Flow rate was varied according to table 32	280 nm UV detector	Modified from(Begas *et al.*, 2007)
Pyrazinamide 5-hydroxypyrazinamide	Kromasil 5μm (25cm x 4.6mm, C18) with guard column 5μm	A: water H_2O with addition of 0.1% v/v of glacial acetic acid. B: Acetonitrile	Gradient see table 31	Flow rate was time programmed with the variation in the solvent which was as follows see table 32	268 nm UV detector	This study

Abbreviations: (2-PY) -N^1-methyl-2-pyridone-5-carboxamide, (4-PY)-N^1-methyl-4-pyridone-5-carboxamide

Table 29: Gradient HPLC protocols for the measurement of MFE activity

Table 30: HPLC program for the separation of allopurinol, N1-methylnicotinamide and their metabolites

Time	Solvent A (%)	Solvent B (%)	Flow (mL/min)
0	100	0	0.8
16	100	0	0.8
16	85	15	1.2
20	85	15	1.2
20	100	0	0.8
24	100	0	0.8

Solvent A: water H_2O with addition of 0.1% v/v of glacial acetic acid, Solvent B: Acetonitrile.

Table 31: HPLC program for the separation of 6-mercaptopurine, 1-methylxanthine, xanthine, phthalazine, pyrazinamide and their metabolites

Time	Solvent A (%)	Solvent B (%)	Flow (mL/min)
0	100	0	0.8
7	100	0	0.8
7	100	0	1.5
15	90	10	1.5
15	90	10	1
19	85	15	1
22.5	85	15	1
22.5	100	0	1.2
25	100	0	1.2

Solvent A: water H_2O with addition of 0.1% v/v of glacial acetic acid, Solvent B: Acetonitrile.

Table 32: HPLC program for the separation of N^1-methylnicotinamide and its metabolites on a polar cyan column

Time	Solvent A (%)	Solvent B (%)	Flow (mL/min)
0	55	45	0.8
1	61	39	0.8
2	67	33	0.8
3	72	28	0.8
4	78	22	0.8
5	84	16	0.8
6	90	10	0.8
9	90	10	0.8
9	55	45	0.8
15	55	45	0.8

Solvent A: 0.1% v/v of formic acid, Solvent B: Acetonitrile.

Table 33: HPLC program for the separation of phenanthridine and 6(5H) phenanthridone

Time	Solvent A (%)	Solvent B (%)	Flow (mL/min)
0	95	5	1.5
1	90	10	1.5
6	50	50	1.5
12	0	100	1.5
15	0	100	1.5
15	90	10	1.5
20	90	10	1.5

Solvent A: water H_2O, Solvent B: Acetonitrile.

2.8.1. HPLC analysis of the *in vitro* metabolism of molybdo-flavoenzyme substrates.

HPLC assays of AOX and XOR were performed with a final volume of 100µl as following, 50µl of gel filtered cytosol, 10µl of 1mM stock of substrates (vanillin, pyridoxal, all-trans retinal, phenanthridine, phthalazine, N^1-methylnicotinamide, methotrexate, cinchonine, xanthine, 1-methylxanthine and 6-mercaptopurine and 40µl (40 mM Tris HCL pH 7.4) at 37°C. XDH assays were similar with the exception that 30µl of (40 mM Tris HCL pH 7.4) was used and 10µl of 6.7mM NAD^+ was added in addition to the substrate. Reactions were terminated with the addition of 60µl of acetonitrile and samples centrifuged at 12000 xg prior to chromatography of the supernatant on HPLC.

Validation that a compound was a substrate for AOX or XOR was achieved using enzyme specific inhibitors and electron acceptors.

2.9. Determination of K_m and V_{max} for molybdo-flavoenzymes.

The rate of oxidation of varying concentrations of substrate of AOX and XOR were monitored such that linear reaction rates were observed and used for Km and Vmax calculations. The volume of cytosol added was varied to provide suitable reaction rates over the range of substrate concentrations used. The substrates concentrations used were 25, 40, 55, 70, 85 and 100 μM for DMAC, vanillin, phenanthridine, xanthine, 1-methylxanthine, pyridoxal, all-trans retinal, allopurinol, phthalazine and 6-mercaptopurine. Specific activity was then calculated as described in section 2.6. Eadie Hofstee plots V/[S] versus [V] were then plotted (Figure 23). The intercept on the ordinate axis is Vmax and the slope is -K_m, the line of best fit through the points on plot was determined using linear regression by least squares method using Microsoft Excel (Microsoft Office).
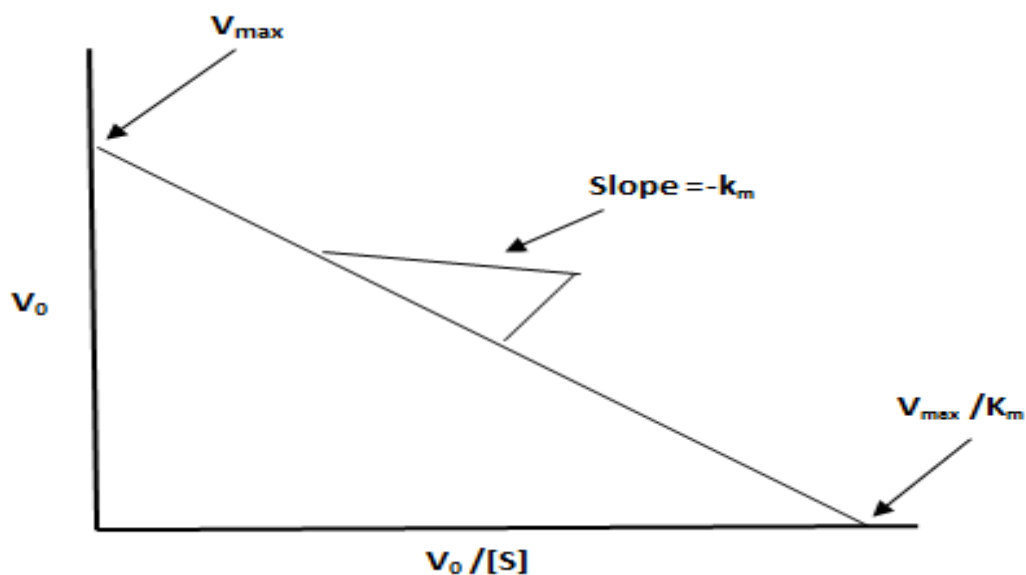
Figure 23: Eadie- Hofstee plot.

2.10. Determination of the mode of inhibition and inhibitor constant (Ki)

The effects of the AOX and XOR inhibitors were studied as summarized in (Table 34) using DMAC and xanthine in spectrophotometric assay. The stock inhibitors were prepared in different solvents as follows. A stock solution of menadione was prepared by dissolving 1mg in 1ml of dimethyl sulphoxide (DMSO). Estradiol, 17α-ethinyl estradiol and phenanthridine stock solutions were prepared by dissolving 1mg in 1ml of ethanol. 5μM, 10μM and 50μM inhibitor stock solutions were prepared from these by dilution in water and one tenth of these were added to assays to give final concentration 0.5, 1 and 5μM inhibitor. The XOR inhibitor oxipurinol was prepared as a stock solution by dissolving in 10mM NaOH. 0.25mM, 0.5mM and 1mM oxipurinol stock solutions were prepared from this by dilution in water and one tenth of these were added to assays to give final concentration of 25μM, 50μM and 100μM oxipurinol.

Table 34: Summary of AOX and XOR inhibitors assays

AOX inhibitor assay				
Substrate	stock concentration in assay	Inhibitor	Final concentration in assay	Mode of inhibition of mammalian enzyme
DMAC	25, 40, 55, 70, 85 and 100μM	Menadione	0.5, 1and 5μM	Non-competitive
		Estradiol	0.5, 1and 5μM	Uncompetitive
		17α-ethinyl estradiol	0.5, 1and 5μM	Uncompetitive
		Phenanthridine	0.5, 1and 5μM	Competitive
		Chlorpromazine	0.5, 1and 5μM	competitive
XOR inhibitor assay				
Substrate	stock concentration in assay	Inhibitor	Final concentration in assay	Mode of inhibition of mammalian enzyme
Xanthine NAD$^+$	25, 40, 55, 70, 85 and 100μM NAD$^+$ 0.67mM	Oxipurinol	25, 50 and 100μM	Non-competitive

Abbreviation; DMAC – dimethylaminocinnamaldehyde.

Determination of the mode of inhibition and subsequently the inhibitor constant was achieved by use of the method described for the determination of Michaelis-Menten constants with the addition of inhibitor to each cuvette. The initial rate of oxidation at varying substrate concentrations was measured alone and in the presence of a fixed concentration of inhibitor. This procedure was then repeated in the presence of a second inhibitor concentration. The type of inhibition was then determined by examination of double reciprocal plots of both non-inhibited and inhibited data (Cook and Cleland. 2007) and the inhibitor constant (Ki) was calculated by using this equation for the exhibited competitive inhibition. Ki = Km [I]/ (Km app-Km) where: Km = uninhibited Km, Km app= apparent inhibited Km and [I] = inhibitor concentration and for exhibited uncompetitive and non-competitive inhibition using

this equation. $Ki = [Vmax\ app][I]/Vmax$, where $Vmax$ = uninhibited $Vmax$, $Vmax$ app= apparent inhibited $Vmax$ and $[I]$ = inhibitor concentration. To determine Km and Vmax for these calculations Lineweaver-Burk plots $1/V$ versus $1/[S]$ were plotted. The intercept on the ordinate axis is $1/Vmax$ and the slope is $Km/Vmax$. From these plots the mode of inhibition was also determined. (Figure 24) illustrates the different plots expected for competitive (Figure 24 A), uncompetitive (Figure 24 B) and non-competitive (Figure 24 C).
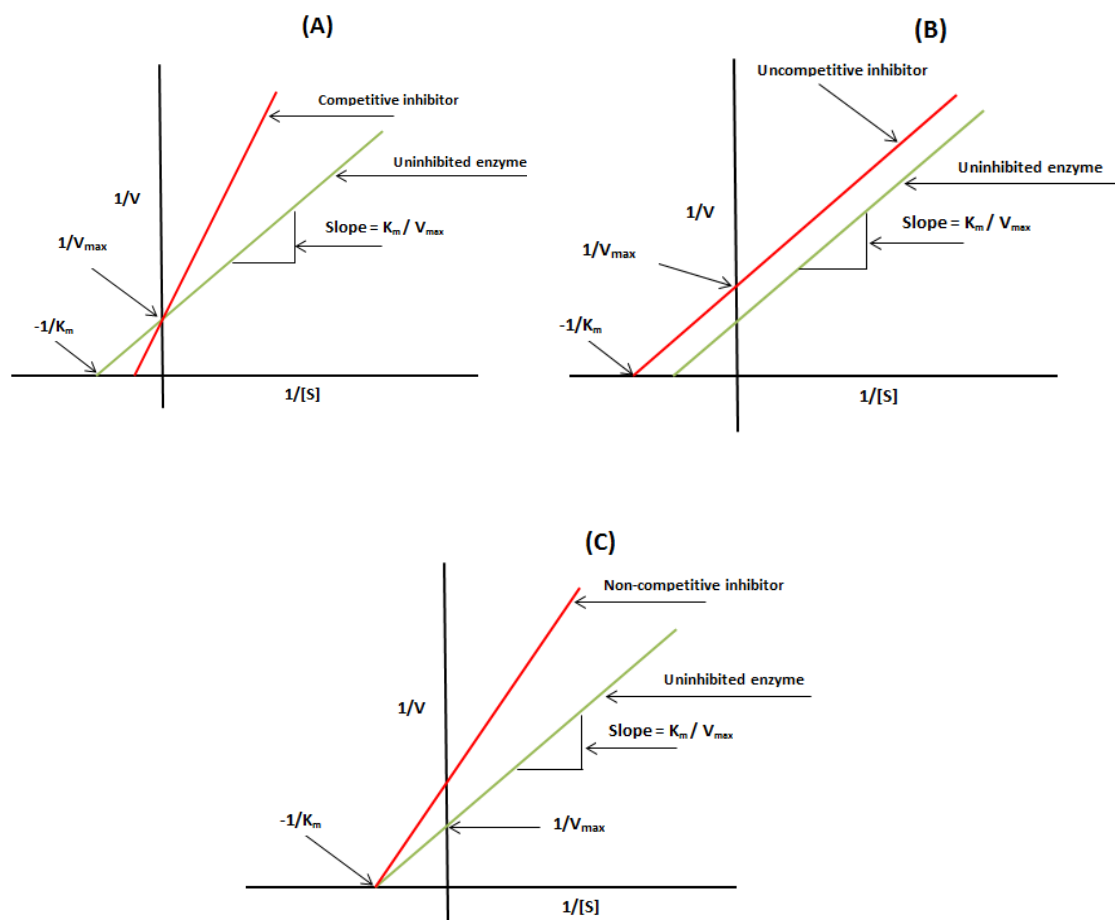
Figure 24: Lineweaver-Burk plots with different types of inhibitors.

2.11. Purification of aldehyde oxidase

2.11.1. Chromatography instruments media and concentrators used

The instrument used was a GE Healthcare AKTA FPLC System with dual pump and fraction collector operated with Unicorn 4.11 Software. Chromatography media used was Q Sepharose 30/100, Superose 6 prep grade XK 16/70, MonoQ 5/50 GL, benzamidine Sepharose 6B and Mono P HR 5/20 were purchased from VWR International Ltd .UK. The centrifugal concentrators used were Amicon Ultra-15, Ultracel-PL Membrane, purchased from Millipore (UK) Ltd. All mobile phases were of FPLC grade purity and were filtered through a 0.45µm filter before use. Isocratic and gradient chromatography methods were using to develop the optimal conditions for the purification of enzymes from original sample.

2.11.2. Buffers used in purification protocols.

The following buffers were used in the course of the purification:

Buffer A: 20mM Tris-HCL, 1mM cysteine, 5% (v/v) glycerol. The pH of this buffer was varied depending on chromatographic conditions required.

Buffer B: 20mM Tris-HCL, 1mM cysteine, 5% (v/v) glycerol, 0.3-0.6M KCL. The pH of this buffer was varied depending on chromatographic conditions required.

Buffer C: 0.075M Tris HCL pH 9.3.

Buffer D: 10% (v/v) polybuffer 96, adjusted to pH 6.0 with glacial acetic acid.

Buffer E: 0.1mM glycine pH 9.0, 0.1M NaCL.

Buffer F: 0.1mM glycine pH 9.0, 0.1M NaCL, 20mM benzamidine.

Buffer G: 20mM Tris-HCL pH8.0, 1mM cysteine, 5% (v/v) glycerol, 0.1M NaCL.

All buffers were prepared from ultrapure reagents dissolved in Milli Q grade water and filtered through 0.45µM filters (Millipore, U.K.).

2.11.3. Purification of AOX

Purification of enzyme activity was monitored throughout the purification procedure with DMAC as substrate. Protein elution was monitored at 280nm with an on-line spectrophotometric detection cell in the FPLC instrument. All procedure was carried out at 0 - 4°C. (Figure 25) summarises the protein purification protocols used.

2.11.3.1. Preparation of cytosol.

Cytosol was prepared as previously described in section 2.1.1. with 20 to 70 g of fresh liver.

2.11.3.2. Heat treatment step.

Cytosol was subjected to heat treatment in a water bath at 55°C for 15 minutes and after that cooled on ice for 10 minute then centrifuged at 10,000 xg for 15 minutes. The supernatant was then removed and used for subsequent experiments.

2.11.3.3. Ammonium sulphate fractionation step.

Cytosol or heat treated supernatant derived from cytosol were subjected to ammonium sulphate fractionation as follows. Finely ground ammonium sulphate was added slowly to the sample with stirring to a concentration of 13.82g/100ml. This solution was stirred for a further 20 minutes and then centrifuged at 15,000 xg for 15 minutes to pellet protein precipitated by a 25% ammonium sulphate saturation. The supernatant was then subjected to a further fractionation so that the final ammonium sulphate concentration was 14.91g/100ml (60% saturation) and after stirring and centrifuging as in the first ammonium sulphate fractionation step the pellet was resuspended in approximately 5ml of buffer A.

Procedure 1	**Procedure 2**	**Procedure 3**	**Procedure 4**
↓	↓	↓	↓
Cytosol preparation	Cytosol preparation	Cytosol preparation	Cytosol preparation
↓	↓	↓	↓
Heat treatmentat55°C	25-50% ammonium sulphate fractionation	25-50% ammonium sulphate fractionation	25-50% ammonium sulphate fractionation
↓	↓	↓	↓
25-50% ammonium sulphate fractionation	Q-sepharose 30/100 anion exchange chromatography	Q-sepharose 30/100 anion exchange chromatography	Q-sepharose 30/100 anion exchange chromatography
↓	↓	↓	↓
Q-sepharose 30/100 anion exchange chromatography	Benzamidine 6B affinity chromatography	Mono P HR 5/20 chromatography	Superose 6 16/70 gel filtration chromatography
↓	↓		↓
Benzamidine 6B affinity chromatography	MonoQ 5/50 anion exchange chromatography		MonoQ 5/50 anion exchange chromatography
↓			
MonoQ 5/50 anion exchange chromatography			

Figure 25: AOX purification protocols.

The sample was then dialysed against three changes of 100 volumes of buffer A over a 24 hour period and the dialysate centrifuged at 15,000 xg for 15 minutes to remove any undissolved material. The sample was then subjected to chromatography for further purification.

2.11.3.4. Q-Sepharose anion exchange fast flow chromatography.

In this case the pH of buffer A and B was varied from pH 8.0 to pH 8.6 in different chromatographic runs. The dimensions of the Q-Sepharose column were 2.5 x 55cm and the flow rate was 10ml/minute. Following ammonium sulphate fractionation 10ml of the sample was applied to the Q-Sepharose column which had previously been equilibrated with buffer A. Unbound protein was eluted with 140ml of buffer A and protein retained on the column was eluted with 150ml of a gradient of 0.6M KCL in buffer B. The fractions containing AOX activity were pooled and concentrated to 4-5ml by ultrafiltration using Amicon Ultra-15 centrifugal concentrator. Following this anion exchange chromatography step, pooled fractions were further purified by affinity chromatography or chromatofocusing or size exclusion followed by a further anion chromatographic step on MonoQ, as outlined in (Figure 25).

2.11.3.5. Affinity chromatography on benzamidine Sepharose 6B.

Benzamidine Sepharose 6B was used as an affinity matrix to bind AOX (Figure 25). In procedure 1 the AOX-active pooled fractions from the anion exchange columns Q-Sepharose were dialysed in 100 volumes of buffer E, with three changes over 24 hours and applied to a 15ml bed volume benzamidine Sepharose 6B column (2.5 x 10cm) at a flow rate was 0.5ml/minute. After application the flow was stopped for 30 minutes to facilitate binding of AOX to the benzamidine-ligands. Unbound material was then eluted at a flow rate of 1ml/minute by washing the column with 6 ml of buffer E. Bound AOX was eluted by sequential batch elution with 10ml of 5mM benzamidine,

10ml of 10mM benzamidine and 10ml of 20mM benzamidine in buffer F. The column was regenerated for further use by washing the column with 20 ml of 2M NaCL to remove any protein still bound and the re-equilibrated in buffer E.

2.11.3.6. Chromatofocusing on Mono P HR 5/20.

The pooled fractions from the Q-sepharose anion exchange step were passed through a Sephadex G25 column (PD 10; 9.1ml bed volume) equilibrated with buffer C for buffer exchange prior to chromatofocusing. 2ml of protein of the resultant sample was then applied to a Mono P HR 5/20 column fitted to an AKTA FPLC system which had previously been equilibrated with buffer C. The column was then washed with two column volumes of buffer C at flow rate of 1ml/minute followed by 35ml of buffer D to generate a pH gradient from pH 9.3 to pH 6.0 over 30ml. Any material still bound to the column was then removed by a 2M NaCL elution.

2.11.3.7. Gel filtration chromatography.

A Superose 6 16/70 column equilibrated with buffer G was used as a step to separate proteins on the basis of their differences in their native molecular mass (Figure 25). In procedure 4, 0.5ml of the AOX active concentrated fraction from Q-sepharose anion exchange chromatography was applied to the Superose column and eluted at a flow rate of 1ml/minute with 140ml of buffer G using 0.1M NaCL as isocratic elution. The column was then equilibrated with the buffer G for the next run.

2.11.3.8. MonoQ chromatography.

This was used as a final step for the purification of AOX as it has proved a suitable medium for the final purification step of AOX in other species (Table 22). In thiscase the pH buffer A and B were varied from pH 8.0 to pH 8.6 in different chromatographic runs, the column dimensions were 5 x 50 mm and the flow rate was 1ml/minute. Following equilibration with 2 bed volumes of buffer A, 0.3ml of concentrated protein sample containing AOX was eluted by washing the column with 2ml of buffer A to remove unbound protein and bound protein was eluted with 20ml of a linear gradient of 0-0.3M KCL in buffer B. Active AOX fractions eluted by the salt were pooled and concentrated to 1-2ml by ultrafiltration using Amicon Ultra-15 membrane. The column was then regenerated for further use by washing the column with one bed volume of each of the following: 1M NaCL, 1.5M NaOH, and 20% (v/v) ethanol. The column was the re-equilibrated in buffer A.

2.11.4. Sodium dodecyl sulphate polyacrylamide gel electrophoresis

Sodium dodecyl sulphate polyacrylamide gel electrophoresis (SDS-PAGE), a technique for separating of proteins according to their mass was used to monitor the purification of AOX(Laemmli. 1970). All SDS-PAGE gels and reagents were from Life Technologies Ltd, UK. The material for SDS-PAGE is described in the (Table 35) and the protocols used according to Life Technology (www.lifetechnologies.com).

Table 35: SDS-polyacrylamide gel electrophoresis reagents (SDS- PAGE)

Materials	
Gel used	NuPAGE® Novex® 3-8% Tris-Acetate Gel 1.5 mm
Running buffer	NuPAGE® Tris-Acetate SDS
Sample buffer	NuPAGE® LDS
Ladder	HiMark™ Unstained Protein Standard
Denaturing agent	DTT
Antioxidant agent	NuPAGE® Antioxidant (N,N-dimethylformarmide)

Abbreviations: LDS- Lithium dodecyl sulphate, DTT-Dithiothreitol, concentration DTT 5% (w/v), MOPS SDS- 3-(N-morpholino) propanesulfonic acid, concentration MOPS 0.6M, SDS 2% and pH 8.4±0.1.

2.11.4.1. Staining of SDS polyacrylamide gels

For the staining of SDS PAGE gels Coomassie blue and silver staining methods were used. All materials used purchased from Sigma Aldrich Company UK. The summary of the two methods are given in (Table 36).

Table 36: Summary of Coomassie Blue and Silver stains used for protein visualisation of SDS-PAGE.

Staining	Materials	Method
Coomassie blue	For 500ml of Coomassie blue stain. **1**) 1.25g Serva G blue. **2**) 228ml methanols. **3**) 46ml acetic acid. **4**) 226ml distilled H_2O Stir for 15 minute. **5**) Filter through general grade whatman filter paper.	**1**) Stain gels with gentle shaking for at least 30 minutes with Coomassie blue stain heated to 60^0C or two hours at room temperature. **2**) Destain overnight with 10% v/v methanol, 15% v/v acetic acid, 75% v/v distilled H_2O.
Reference	(Laemmli. 1970)	
Staining	Materials	Method
Silver	**1**) Oxidiser, 3.4mM potassium dichromate with 0.0032N Nitric Acid. **2**) Silver nitrate solution 0.012M silver nitrate. **3**) Developing agent 0.28M sodium carbonate+0.5ml/L formalin.	**1**) Soak gel 2 times for 10 minutes in 40% methanol+10% acetic acid (200ml/gel). **2**) Soak gel 2 times for 10 minutes with 10% ethanol+5% acetic acid(200ml/gel). **3**) Soak gel for 10minutes in oxidiser (200ml/gel at RT). **4**) Wash with distilled H_2O three times for 10 minutes or until gel colourless (200ml/gel at RT). **5**) Soak for 30 minute in 0.012M silver nitrate (200ml/gel) at RT. **6**) Wash with distilled $H_2O$for two minutes. **7**) Develop three times with developing reagent for 1, 5 and 3minutes respectively (200ml/gel at RT). **8**) Stop with 5% v/v acetic acid for 5 minutes, then immerses gel in deionised H_2O.
Reference	(De Moreno *et al.*, 1985)	

Abbreviations: room temperature (RT)

2.11.4.2. Determination of native molecular mass using Superose 6 chromatography.

The gel filtration marker kit for protein molecular masses 29,000-700,000 Da was obtained from Sigma Aldrich UK. A summary and concentration of the standards used in the calibration curve for the Superose 6 16/70 chromatography is shown in (Table 37). The buffer used for prepare the standard proteinswas20mM Tris HCl pH8.0, 1mM cysteine and 5% (v/v) glycerol with 0.1M NaCL. 1 ml of each prepared standard was injected onto the FPLC starting with the highest molecular mass standard Dextran blue 2,000,000 Da first followed by protein mixture containing all proteins listed in (Table 37). The method and sample preparation was according to (Whitaker. 1963, Andrews. 1964, Marshall. 1970)noting that the Blue Dextran was not mixed with other standards because many proteins bind to dextran. Blue dextran and the protein standards were applied in 1 ml volume and eluted with a 1 ml/minute flow rate.

Table 37: Summary of gel filtration standards used for native molecular mass determination

Standard protein	Approximate Molecular mass	Recommended concentration
Carbonic anhydrase from bovine erythrocytes	29000 Da	3mg/1ml
Albumin, bovine serum	66000 Da	10mg/1ml
Alcohol dehydrogenase from yeast	150000 Da	5mg/1ml
β-Amylase from sweet potato	200000 Da	4mg/1ml
Apoferritin from horse spleen	443000 Da	10mg/1ml
Thyroglobulin, bovine	669000 Da	8mg/1ml
Blue Dextran	2000000 Da	2mg/1ml

Absorbance was recorded at 280nm and a graph was drawn by plotting the logarithms of molecular mass of all standards versus to the elution volume of the standards. This graph was used to calculate the molecular mass of AOX.

2.12. Statistical analysis.

2.12.1. ANOVA-test

Each experiment was repeated at least three times. Statistical analysis was carried out using Microsoft Excel 2010 software. The result of each experiment was determined as the mean ± standard deviation. Data were then analysed for significance using one way ANOVA. Differences with p values ≤0.05 were considered statistically significant.

3. Results.

The section of results is divided into 6 main sections as follows. Firstly sections 3.1, 3.2 and 3.3 describe the quantification of molybdo-flavoenzyme activity in rainbow trout, human and rat using spectrophotometric and HPLC assays. In sections 3.4 and 3.5 the determination of the kinetic parameters and comparison different inhibitors of AOX and XOR in different species are described. The final section 3.6 covers the purification of AOX from rat and trout.

3.1. Quantification of molybdo-flavoenzyme activity

A number of spectrophotometric assays were used to measure the relative reaction rates of the AOX and XOR. Three spectrophotometric assays measured the rate of biotransformation of two aldehyde compounds vanillin and dimethylaminocinnamaldehyde (DMAC) and one N-heterocyclic AOX substrate phenanthridine with molecular oxygen as an electron acceptor. A further spectrophotometric XOR assay was performed using endogenous substrate xanthine and the caffeine metabolite, 1-methylxanthinewith O_2 or with NAD^+ plus O_2 as electron acceptors. These assays were carried out with $20 - 40$ µl of gel filtered cytosol at 37ºC as described in materials and methods section 2.4 to give linear reaction kinetics. As the majority of MFEs substrates and products cannot be quantified by spectrophotometry, HPLC assays were used to measure MFEs oxidation rates for 13 substrates. In order to optimise the experimental conditions for the assays a series of experiments were performed to assess the optimal pH and temperature. In addition prior to performing HPLC assays the methods were tested for accuracy and precision.

3.1.1. Effect of pH on trout, rat and human molybdo-flavoenzymes activity.

In order to test the effect of pH on trout, human and rat AOX these were assayed under standard assay condition, except that the reaction pH was varied between 5.7 and 8.0 as described in section 2.7.1. The maximum activity of AOX was found to be at pH 7.0 with all three species as shown (Figure 26).
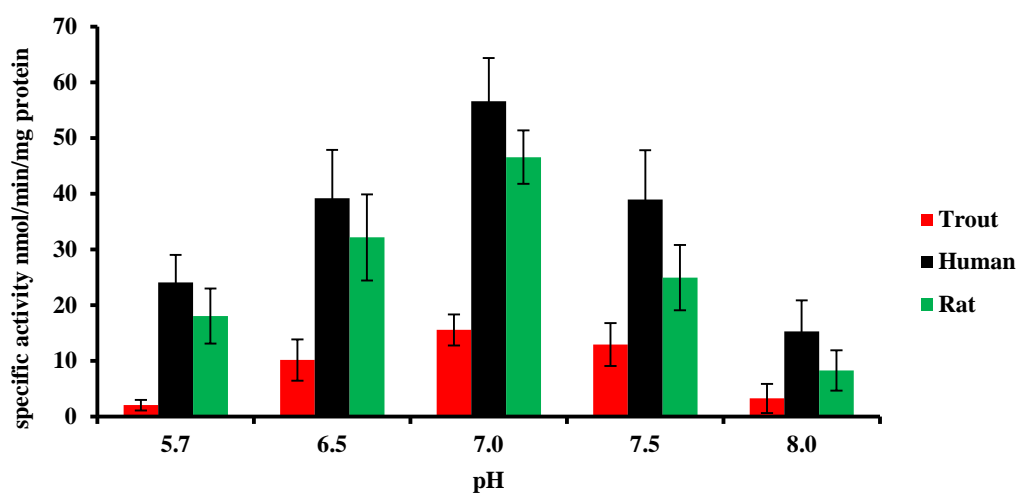
Figure 26: Effect of pH on of trout, human and rat AOX activity.

AOX activity was measured at 37°C. 0.1 mM DMAC was used as the substrate in AOX assay. Each point represents the mean ± S.D. of three experiments with liver cytosol from ~3 animals.

In order to test the effect of pH on of trout, human and rat XO and XDH these were assayed under standard assay condition, except that the reaction pH was varied between 5.7 and 8.0 as described in section 2.7.1 and 2.8.1. The maximum activities of XO and XDH were found to be pH 7.0 with the three species tested as shown (Figure 27a and b).

95
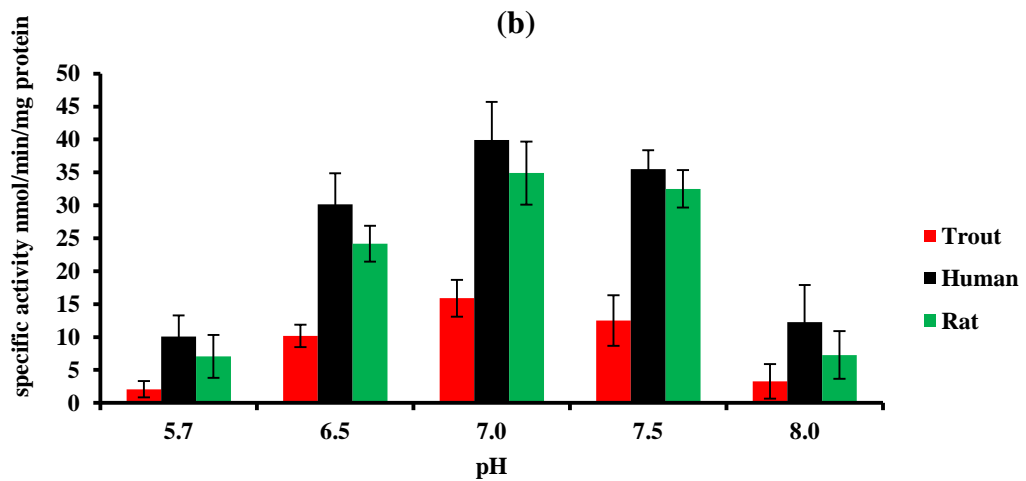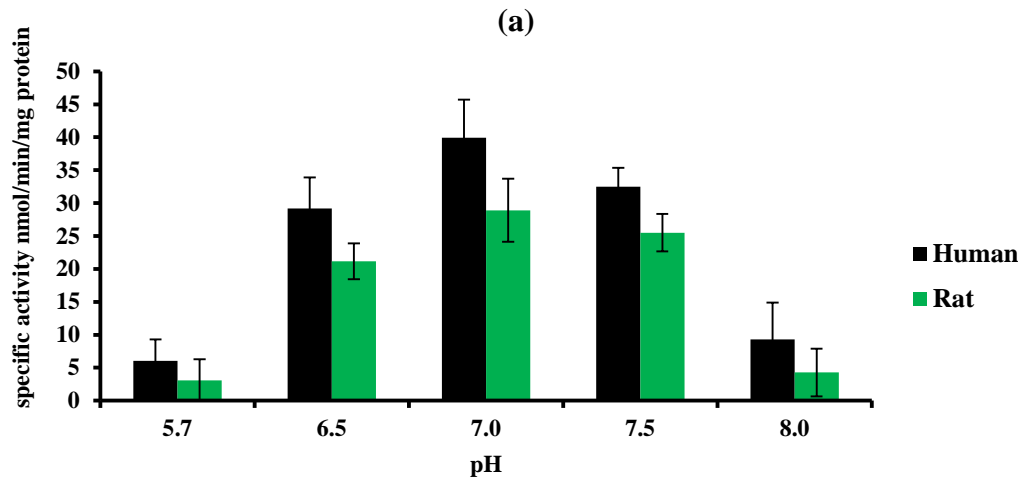
Figure 27: Effect of the pH on of trout, human and rat XOR activity.

The (a) XO activity was measured at 37˚C with 0.15 mM xanthine and O_2 as electron acceptor. (b) XDH activity was measured at 37˚C with 0.15 mM xanthine and 0.67 mM NAD^+ plus O_2 as electron acceptor. Each point represents the mean ± S.D. of three experiments with pooled cytosol from ~3 animals.

3.1.2. Effect of temperature on trout, rat and human molybdo-flavoenzymes activity.

In the initial assays 37˚C was used for assays but in order to determine if this was the optimum temperature to use a series of experiments were performed. In order to test effect of temperature on the activity of trout, rat and human AOX this was measured as at different incubation temperatures as described in section 2.7.2. The rate of reaction of trout AOX with DMAC increase gradually with increasing temperature from 25˚C to 37˚C then decreased gradually until it fell to < 10 % at 55˚C and 60˚C compared to the activity at 37°C as shown in (Figure 28). The activity at 60˚C was ~ 10% obtained at 37°C. The rate of reaction of human and rat AOX with DMAC increase gradually with increasing temperature from 25˚C to 37˚C then decrease gradually as shown in (Figure 28) and the activity of human and rat at 60°C was ~ 60% obtained at 37°C respectively. As the maximum reaction rate was obtained at 37˚C for AOX enzymes, this temperature was therefore selected for all assays.
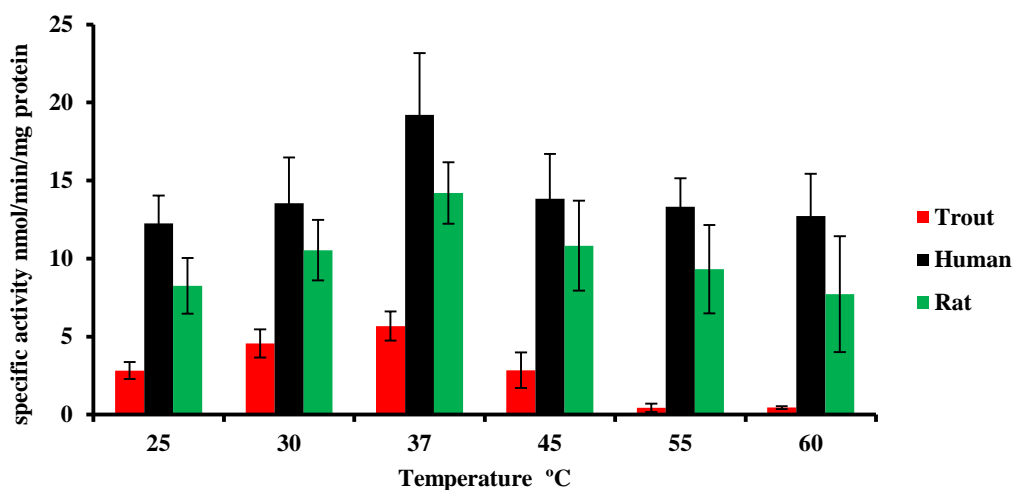
Figure 28: Effect of the assay incubation temperature on of trout, human and rat AOX activity.

Enzyme activity was measured with 0.1 mM DMAC was used as the substrate in AOX assays. Each point represents the mean ± S.D. of three experiments with pooled cytosol from 3 animals.

In order to test the effect of temperature on the activity of trout, human and rat XOR this was measured at different incubation temperatures. The rate of reaction of human and rat XO with xanthine and O_2 as an electron acceptor. Gradually increasing with increase temperature from 25°C to 37°C then decrease gradually as shown in figure 29a and the activity of human and rat at 60°C was ~ 60% obtained at 37°C respectively. The rate of reaction of trout XOR with xanthine and NAD^+ with O_2 as electron acceptors. Increasing gradually with increasing temperature from 25°C to 37°C then decreased gradually until fell to near zero at 55°C and 60°C as shown in (Figure 29b). The activity at 60°C was ~ 5% of that obtained at 37°C. The rate of reaction of human and rat XDH with xanthine and NAD^+ increase gradually with increasing temperature from 25°C to 37°C then gradually decrease as shown in (Figure 29b) the activity of human and rat at 60°C was ~ 60% obtained at 37°C respectively . As the maximum reaction rate was obtained at 37°C for XOR enzyme, this temperature was therefore selected for all assays.

(a)

(b)
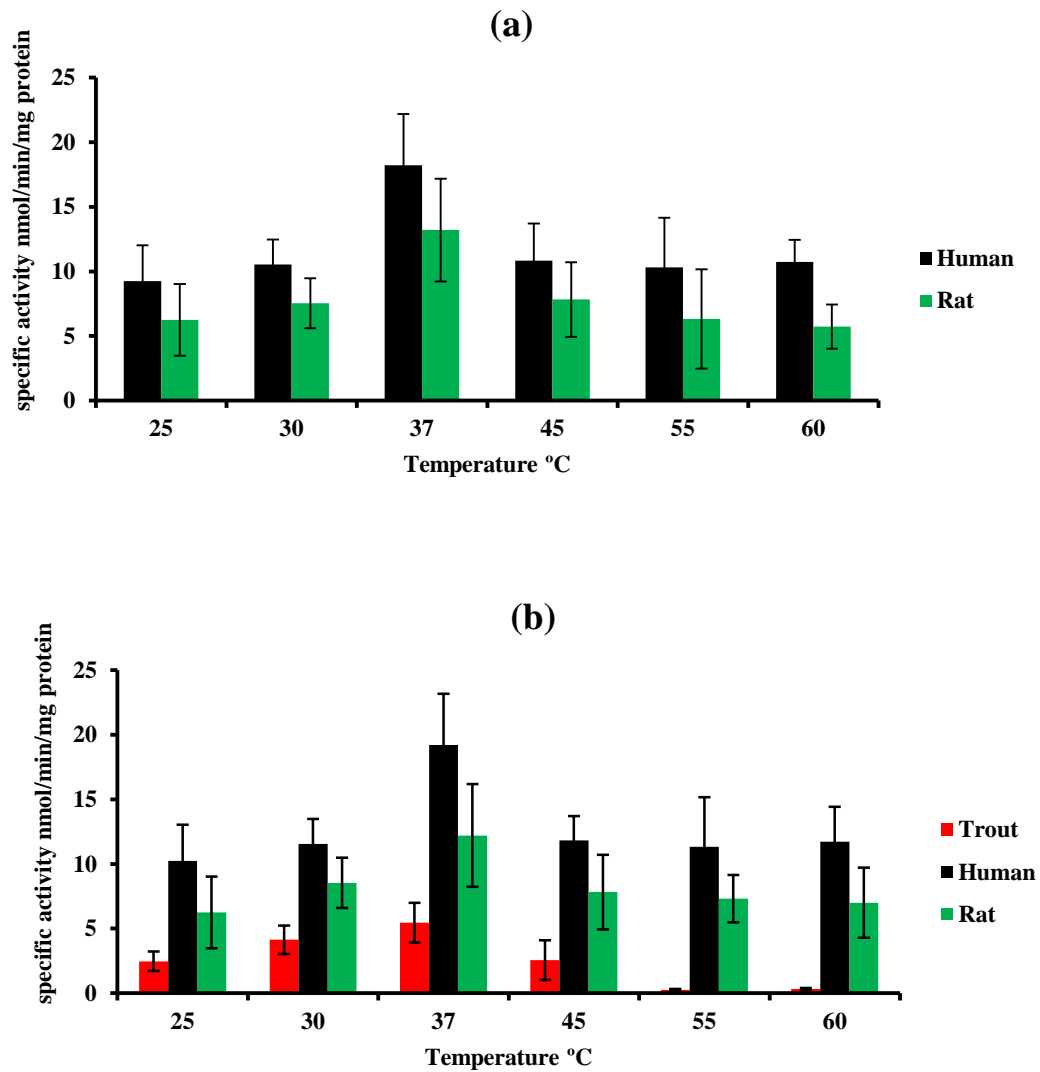
Figure 29: Effect of the assay incubation temperature on of trout, human and rat XOR activity.

Enzyme activity was measured with (a) 0.15 mM xanthine and O_2 as an electron acceptor. (b) 0.15 mM xanthine and 0.67 mM NAD^+ plus O_2 as an electron acceptors. Each point represents the mean $\pm$ S.D. of three experiments with pooled cytosol from ~3 animals.

3.1.3. Validation of the accuracy and precision of HPLC assays

The precision of the various HPLC assays was determined by injecting five concentrations (0.01, 0.02, 0.03, 0.05 and 0.1 mM) of all AOX and XOR substrates and the products listed in materials and methods section 2.8., three times on the same day to determine the intra-day variation. The intra-day variation assessed as the coefficient of variation in peak area ratio. The relative standard deviation (%RSD) calculation for retention time was described in section 2.8. The lower the value is the better the assay performance. At lower level it was below 3.5% for 3 replicates, see Appendix3 (Table 1). The accuracy of the assay was calculated by comparison of the nominal analyte concentration to the actual concentration obtained from the linear regression line within the concentration range investigated (0.01 mM to 0.1 mM), see Appendix3(Table 2). Appendix3 (Table 2) showed that the intra-day values ranged between 95.1-100.8%. The precision of all concentrations of analyte was approximately less than ± 5%. The calibration graphs obtained with these HPLC methods were linear over the concentration range used and the (r^2) values were 0.92 to 0.99 for each analyte when plotted for the mean peak area for three injections against the actual concentration (Figures 1- 5 in Appendix 3). This demonstrates that these HPLC methods are precise and repeatable and can be successfully used to analyse MFE catalysed biotransformations in this study. In addition to accuracy and precision tests, the limit of detection (LOD) and the limit of quantification (LOQ) were calculated for each of the analytes in section 2.5.2.3. The LOD of all substrates and products were ranged between 0.1-5.4 nmol and LOQ was ranged from 0.9 to 94 nmol. From these results, it can be concluded that the HPLC methods were sufficiently sensitive to detect low concentrations of substrates and products of

molybdo-flavoenzyme catalysed reactions enzymes. The results of linearity, limit of detection and limit of quantification are presented in Appendix3 (Table 3).

3.2. Screening of molybdo-flavoenzyme activities.

Following optimisation and validation of the assays, AOX and XOR activities in rainbow trout, Wistar rat and human cytosols were assessed using a multitude of spectrophotometric and HPLC assays prior to scrutinising the Km and Vmax for different substrates.

3.2.1. AOX activity with exogenous aldehydes in trout tissue and mammalian liver cytosol.

The substrates used to evaluate AOX activity in this research included the exogenous food flavouring agent vanillin (4-hydroxy-3-methoxybenzaldehyde) and artificial dye dimethylaminocinnamaldehyde (DMAC). (Figures 30 and 31) illustrate spectrophotometric assays with the two aldehyde substrates vanillin and DMAC. This demonstrated that liver cytosols from all three species had measurable AOX activity towards these two aromatic aldehydes. In contrast rainbow trout kidney and gill cytosols had no measurable activity towards these substrates (data not shown). In order to check unequivocally if there was no AOX activity towards vanillin in kidney and gill cytosols an HPLC assay was used. This showed that even following a 120 minute incubation with this substrate there was no vanillic acid formed in contrast to liver cytosol (Figure 32). (Figure 33) shows an HPLC chromatogram for all liver cytosol from trout, rat and human with vanillin.
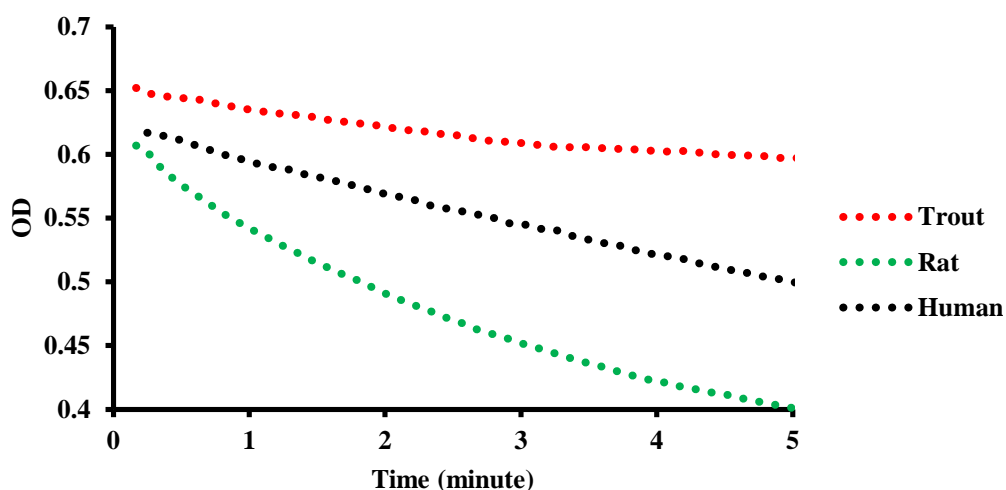
Figure 30: Spectrophotometric assays of aldehyde oxidase activities using rainbow trout, Wistar rat and human liver cytosol at 37˚C with AOX substrate DMAC. For assays using 50 µL rainbow trout [red], 30 µL Wistar rat [green] and 20 µL human [black] liver cytosol. 100 µM final substrate concentrations were used. For analysis conditions see section 2.4.
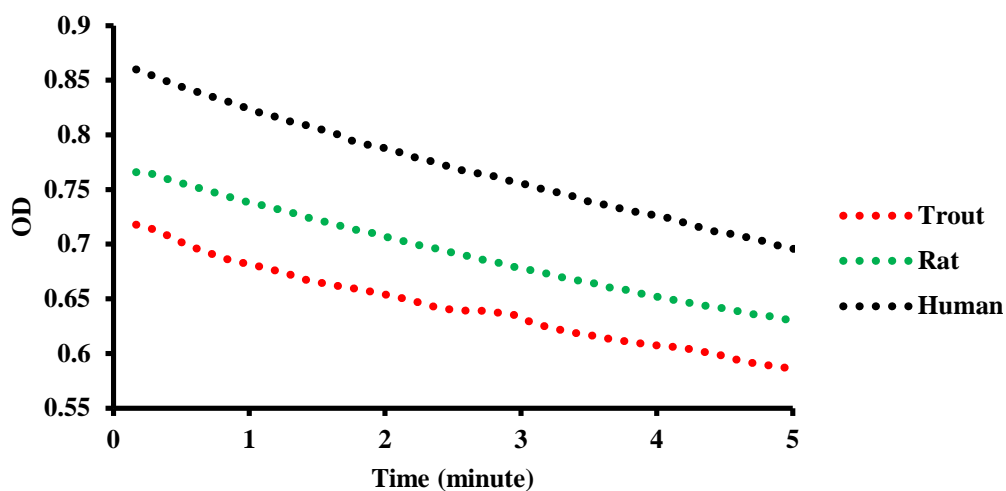
Figure 31: Spectrophotometric assays of aldehyde oxidase activities using rainbow trout, Wistar rat and human liver cytosol at 37˚C with AOX substrate vanillin. For assays using rainbow trout [red], Wistar rat [green] and human [black] liver cytosol. For all assays 100 µM final substrate concentrations were used. For analysis conditions see section 2.4.
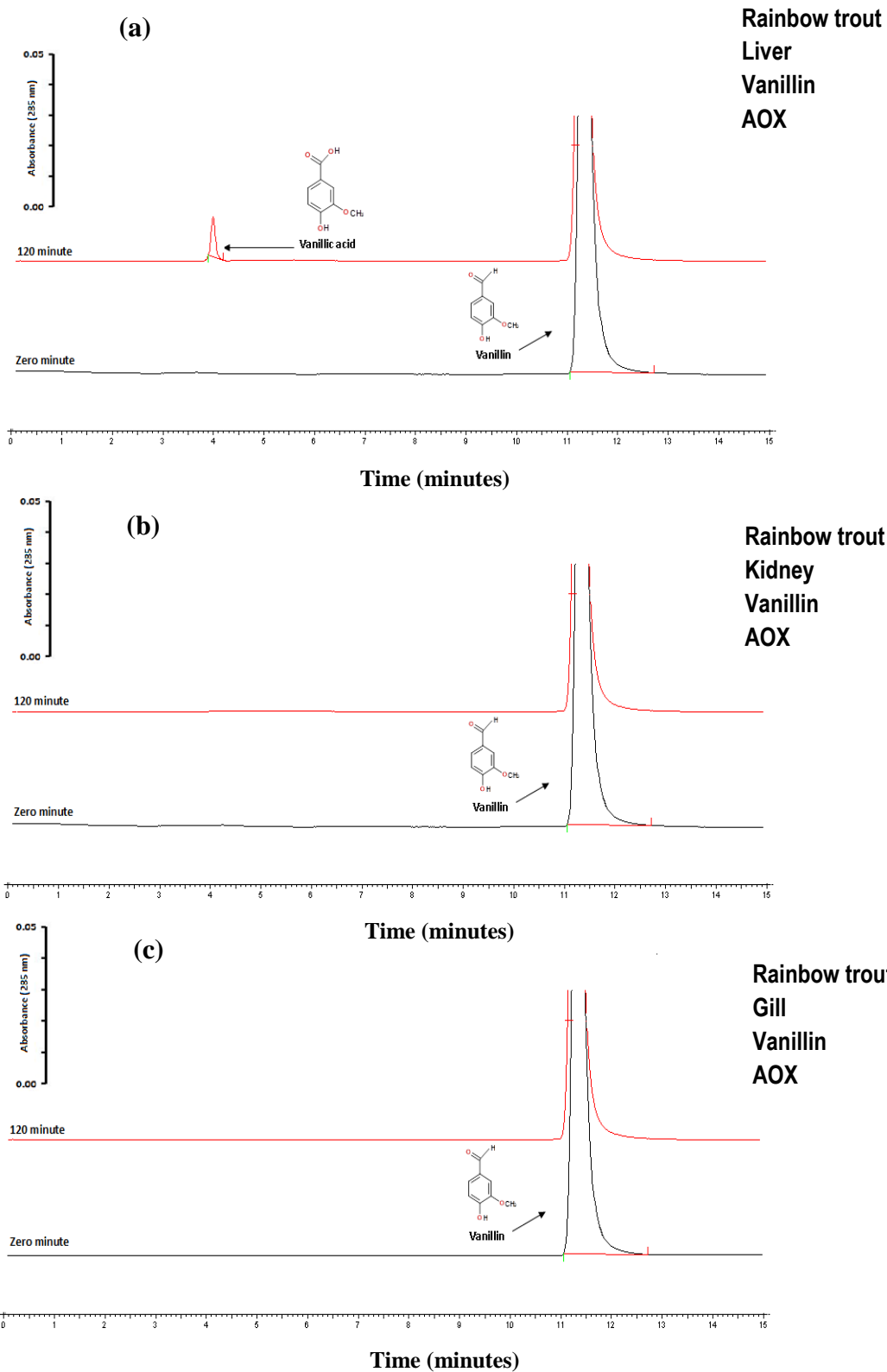
Figure 32: HPLC analysis of the *in vitro* biotransformation of vanillin by rainbow trout cytosol. (a) Liver, (b) kidney and (c) gill liver cytosol. Times at the left hand side of the chromatograms indicate incubation times. HPLC chromatograms are offset on the vertical axis to allow comparison between different incubation times. Analytes were injected onto a C-18 column (Kromasil 5 µm) and eluted with a 0.22 M KH2PO4: acetonitrile system (85: 15) as mobile phase. The wavelength of the detection was 285 nm.
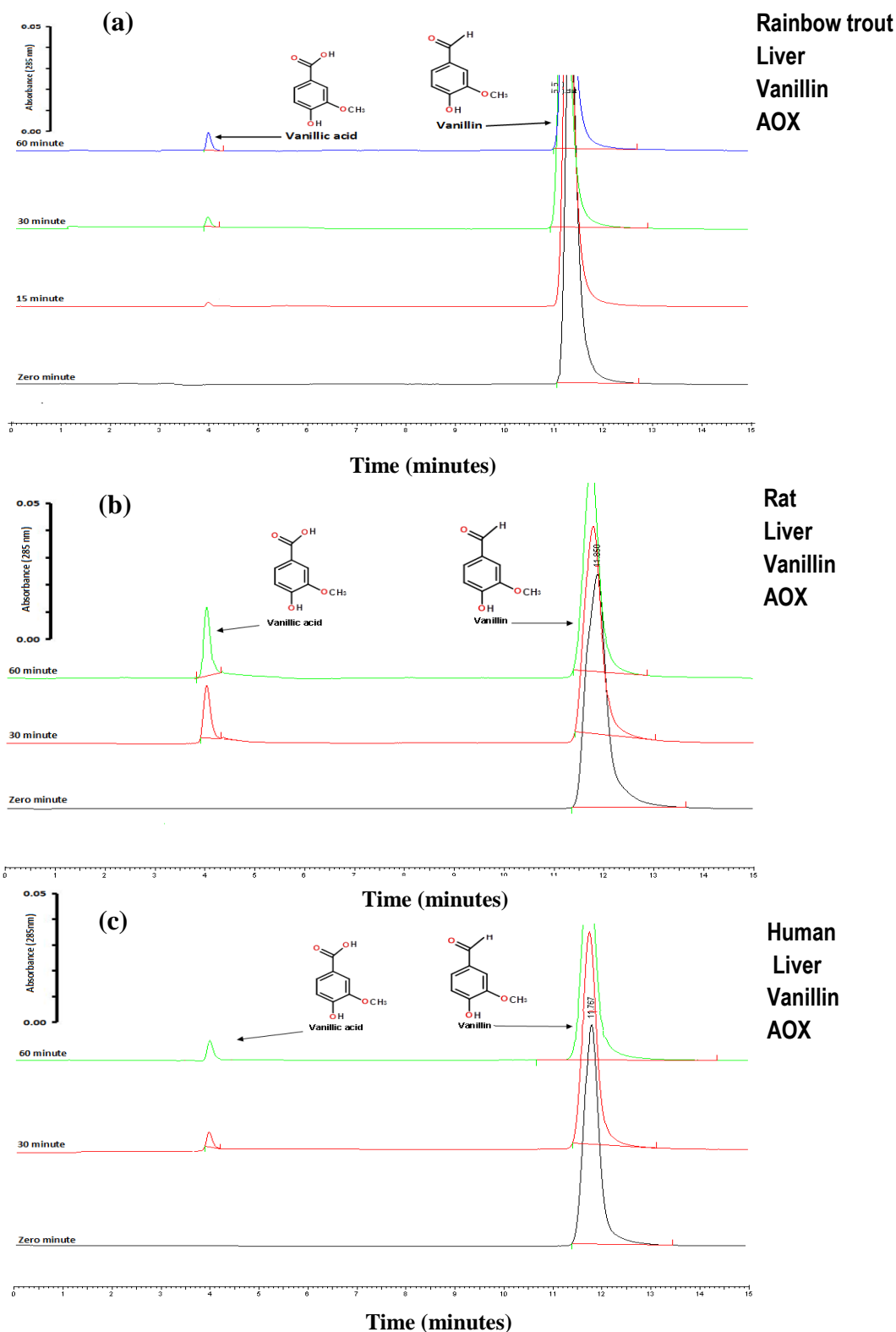
Figure 33: HPLC analysis of the *in vitro* biotransformation of vanillin by liver cytosol.

HPLC chromatogram of the *in vitro* oxidation of vanillin to vanillic acid by (a) rainbow trout, (b) Wistar rat and (c) human liver cytosol. Times at the left hand side of the chromatograms indicate incubation times. HPLC chromatograms are offset on the vertical axis to allow comparison between different incubation times. Analytes were injected onto a C-18 column (Kromasil 5 μm) and eluted with a 0.22 M KH_2PO_4: acetonitrile system (85: 15) as mobile phase. The wavelength of the detection was 285 nm.

3.2.2. HPLC analysis of AOX activity with endogenous vitamins and vitamin metabolites.

When the endogenous vitamin B6 (pyridoxal) was incubated with rainbow trout, Wistar rat and human liver cytosol its metabolite pyridoxic acid was generated with cytosols from all three species (Figure 34).
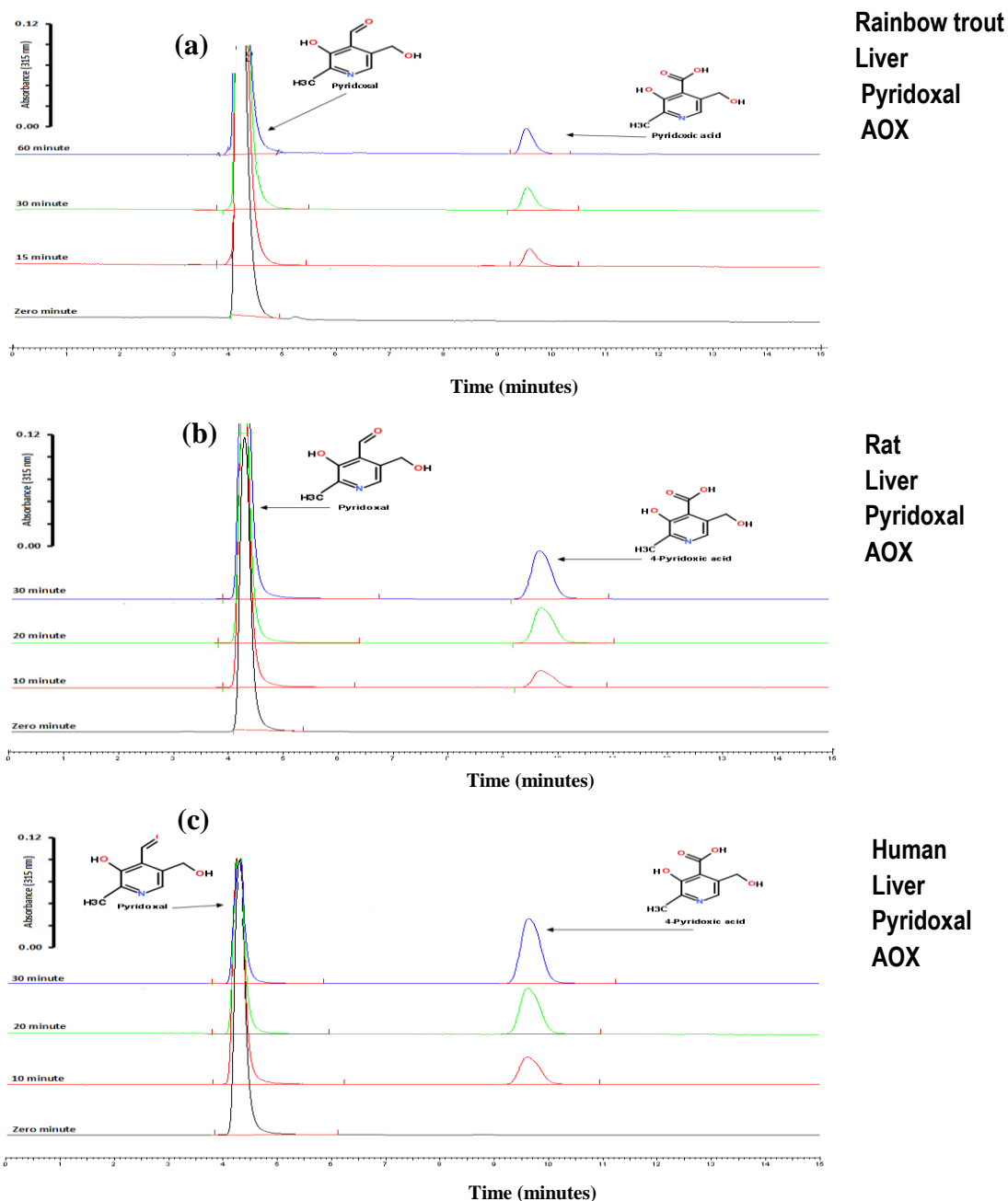
Figure 34: HPLC analysis of the *in vitro* biotransformation of endogenous compound pyridoxal by liver cytosol from different species. HPLC chromatogram of the *in vitro* oxidation of pyridoxal to pyridoxic acid by (a) rainbow Trout, (b) Wistar rat, (c) human liver cytosol. Times at the left hand side of the chromatograms indicate incubation times. HPLC chromatograms are offset on the vertical axis to allow comparison between different incubation times. Analytes were injected onto a C-18 column (Kromasil 5 µm) using methanol: 60 mM Na_2HPO_4 (25: 75) as mobile phase. The wavelength of the detection was 315 nm.

105

When all-trans retinal (vitamin A) was incubated with rainbow trout, Wistar rat and human liver cytosol, the AOX metabolite retinoic acid was generated with cytosols from all three species (Figure 35).
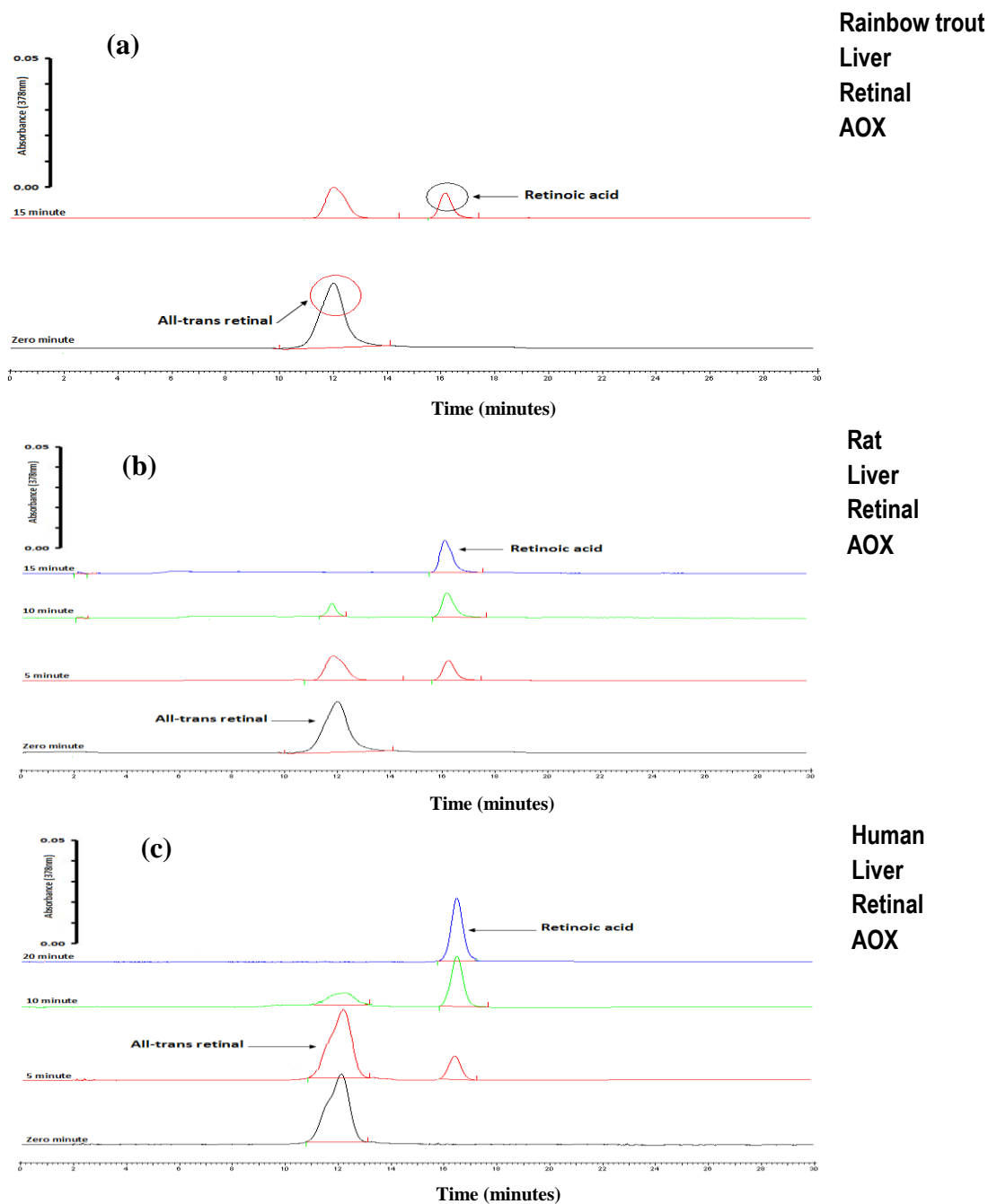
Figure 35: HPLC analysis of the *in vitro* biotransformation of endogenous compound all-trans retinal by liver cytosol from different species. HPLC chromatogram of the *in vitro* oxidation of all-trans retinal to retinoic acid by (a) rainbow Trout, (b) Wistar rat, (c) human liver cytosol. Times at the left hand side of the chromatograms indicate incubation times. HPLC chromatograms are offset on the vertical axis to allow comparison between different incubation times. Analytes were injected onto a C-18 column (Kromasil 5 µm) and eluted with a 30 mM CH_3COONH_4: acetonitrile (30: 70) as mobile phase. The wavelength of the detection was 378 nm.

106

When liver cytosol from rainbow trout, Wistar rat and human were incubated with N^1-methylnicotinamide (NMN)two products (Figure 36) were observed with retention times of (9 minute) N^1-methyl-2-pyridone-5-carboxamide (2-PY) and (12 minute) N^1-methyl-4-pyridone-5-carboxamide (4-PY) (Szafarz *et al.*, 2010).
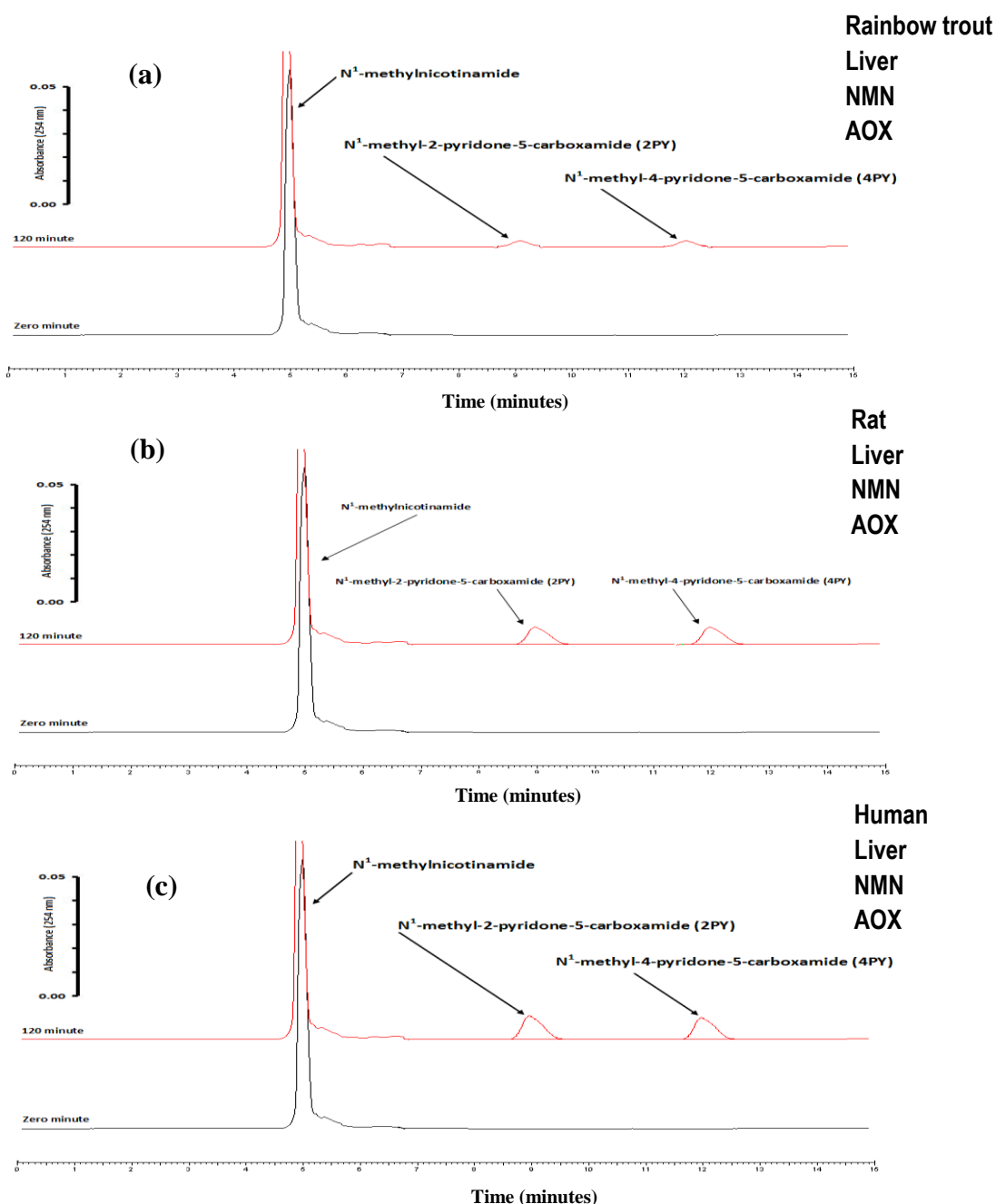
Figure 36: HPLC analysis of the *in vitro* biotransformation of N^1-methylnicotinamide by liver cytosol from different species. HPLC chromatogram of the *in vitro* oxidation of N^1-methylnicotinamide to (2-PY and 4-PY) by (a) rainbow Trout, (b) Wistar rat, (c) human liver cytosol. Times at the left hand side of the chromatograms indicate incubation times. HPLC chromatograms are offset on the vertical axis to allow comparison between different incubation times. Analytes were injected onto a C-18 column (Spherisorb; CNRP 5 μm) and eluted with a 0.8 % v/v formic acid: acetonitrile gradient as described in section 2.5.3 as mobile phase. The wavelength of the detection was 254 nm.

3.2.3. Spectrophotometric and HPLC analysis of AOX activity with exogenous N-heterocyclic compounds.

3.2.3.1. Phenanthridine.

When the prototypical N-heterocyclic AOX substrate phenanthridine was used as a substrate in a spectrophotometric assay (Beedham. 2001) (Figure 37) only Wistar rat and human liver cytosol had activity. Cytosols prepared from trout liver, kidney and gill had no detectable activity (Figure 37). As there is evidence that at least one fish, the carp, generates phenanthridone from phenanthridine *in vivo*, an HPLC assay was used to determine if any activity could be detected. This demonstrated that rainbow trout liver cytosol AOX was able to generate measurable phenanthridone (Figure 39). In contrast there was no detectable phenanthridone formed with extended incubation with rainbow trout kidney or gill cytosol (Figure 38). Rat and human liver cytosol were also able to carry out this biotransformation (Figure 39).
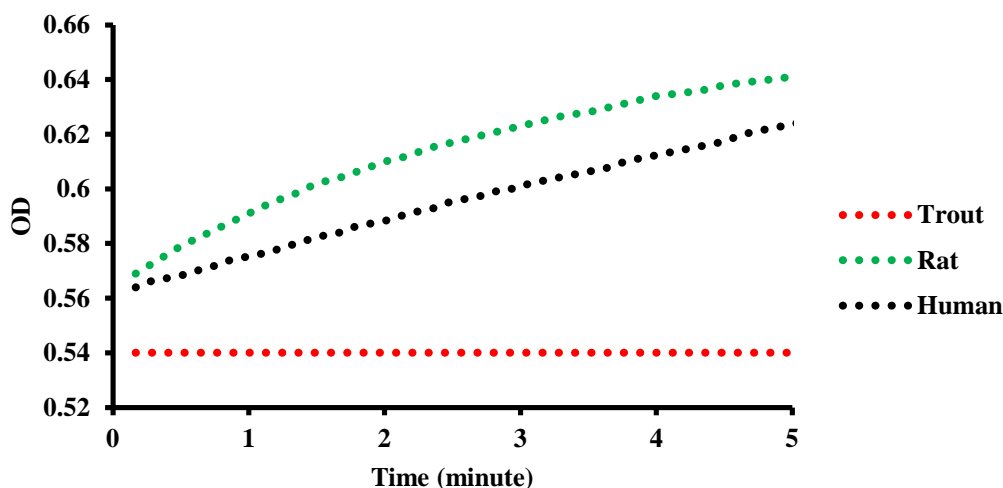

Figure 37: Spectrophotometric assays of aldehyde oxidase activities using rainbow trout, Wistar rat and human liver cytosol at 37°C with AOX substrate phenanthridine. For assays using rainbow trout [red], Wistar rat [green] and human [black] liver cytosol. For all assays 100 μM final substrate concentrations were used. For analysis conditions see section 2.4
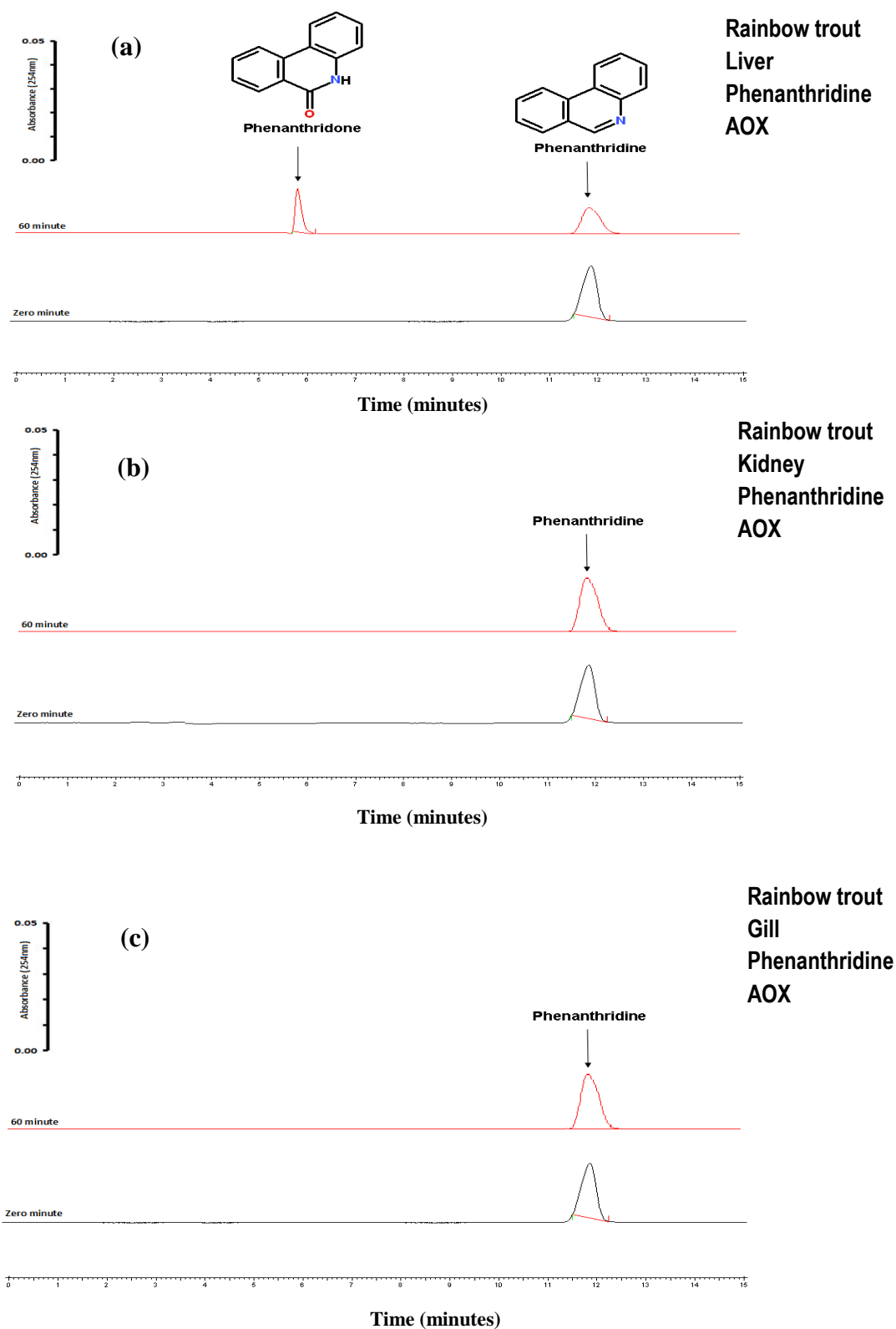
Figure 38: HPLC analysis of the *in vitro* biotransformation of phenanthridine by trout cytosol. (a) Liver, (b) kidney and (c) gill trout cytosol. Times at the left hand side of the chromatograms indicate incubation times. HPLC chromatograms are offset on the vertical axis to allow comparison between different incubation times. Analytes were injected onto a C-18 column (Kromasil 5 μm) and eluted with water: acetonitrile gradient system as described in section 2.5.3 as mobile phase. The wavelength of the detection was 254 nm.
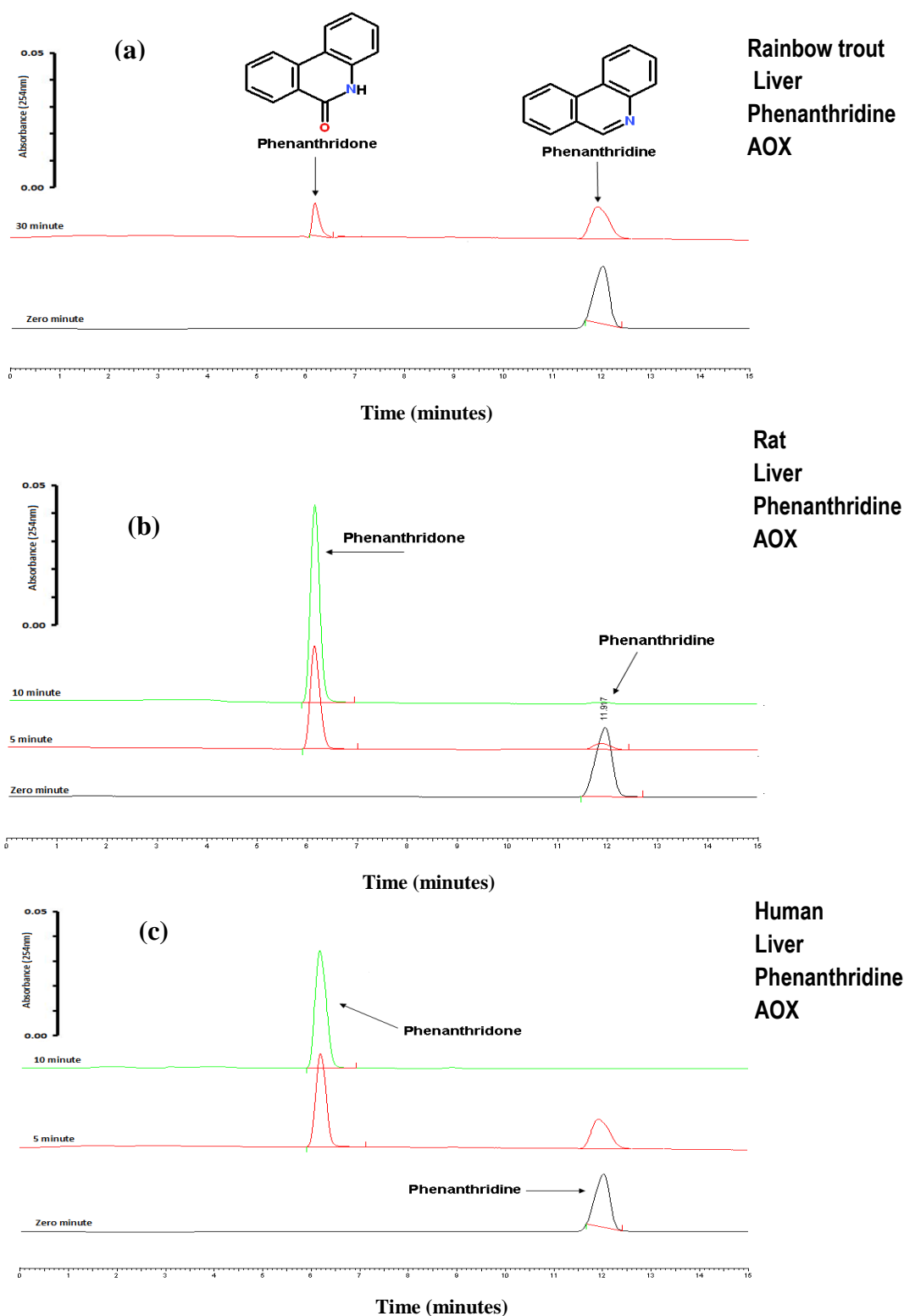
Figure 39: HPLC analysis of the *in vitro* biotransformation of phenanthridine by rainbow trout, Wistar rat, and human liver cytosol. (a) rainbow trout, (b) Wistar rat, (c) human liver cytosol. HPLC chromatogram of the *in vitro* oxidation of phenanthridine to phenanthridone. Times at the left hand side of the chromatograms indicate incubation times. HPLC chromatograms are offset on the vertical axis to allow comparison between different incubation times. Analytes were injected onto a C-18 column (Kromasil 5 µm) and eluted with water: acetonitrile gradient system as described in section 2.5.3 as mobile phase. The wavelength of the detection was 254 nm.

110

3.2.3.2. Phthalazine.

When the N-heterocyclic phthalazine was incubated with rainbow trout, Wistar rat and human liver cytosol, all were found to be capable of biotransforming it to the AOX product phthalazinone (Figure 40).
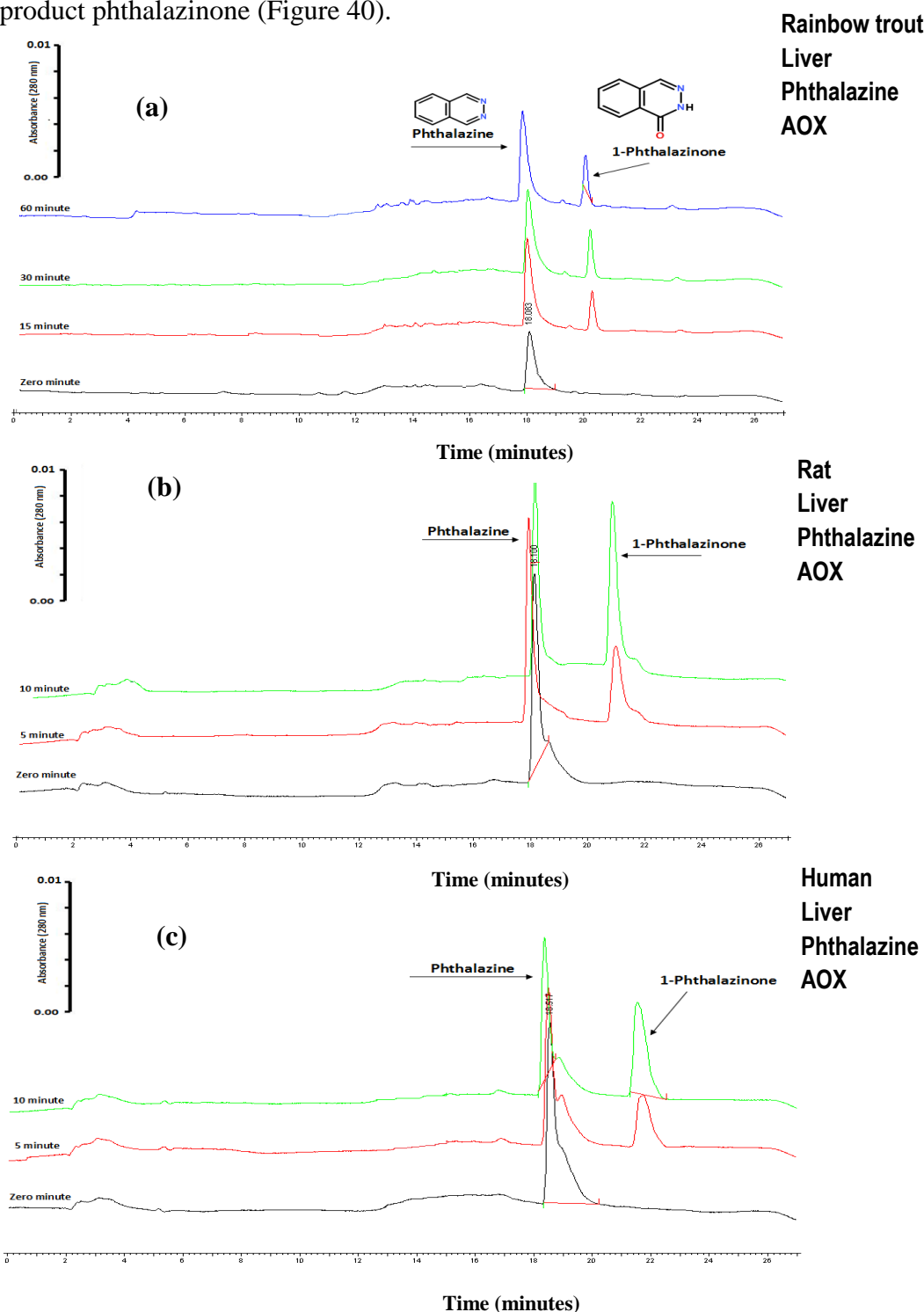
Figure 40: HPLC analysis of the *in vitro* biotransformation of phthalazine by rainbow trout, Wistar rat and human liver cytosol. (a) rainbow trout, (b) Wistar rat, (c) human liver cytosol. HPLC chromatogram of the *in vitro* oxidation of phthalazine to phthalazinone Times at the left hand side of the chromatograms indicate incubation times. HPLC chromatograms are offset on the vertical axis to allow comparison between different incubation times. Analytes were injected onto a C-18 column (Kromasil 5 µm) and eluted with a 0.1% v/v glacial acetic acid: acetonitrile gradient system as described in section 2.5.3 as mobile phase. The wavelength of the detection was 280 nm.

111

3.2.3.3. Cinchonine.

When anti-malaria drug N-heterocycle cinchonine was incubated with rainbow trout, Wistar rat and human liver cytosol, a metabolite of cinchonine was detected by HPLC with all samples (Figure 41) that had a retention time (12 minute) indicative of $2^{'}$-cinchoninone (Beedham *et al.*, 1992).
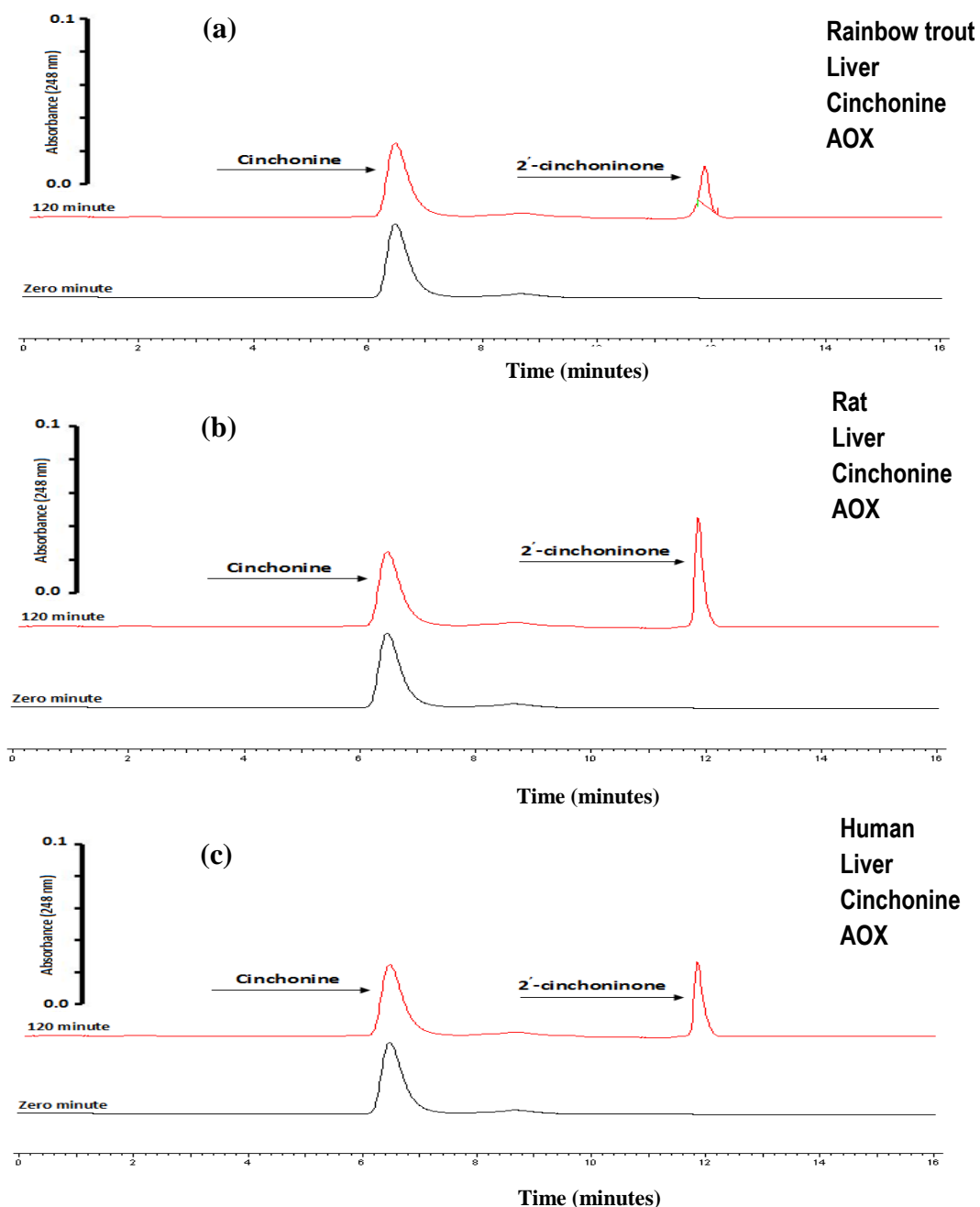
Figure 41: HPLC analysis of the *in vitro* biotransformation of cinchonine to 2-cinchoninone by rainbow trout, Wistar rat and human liver cytosol. (a) rainbow trout, (b) Wistar rat, (c) human liver cytosol. Times at the left hand side of the chromatograms indicate incubation times. HPLC chromatograms are offset on the vertical axis to allow comparison between different incubation times. Analytes were injected onto a C-18 column (Kromasil 5 μm) and eluted with a 0.4% w/v CH_3COONH_4: acetonitrile (65: 35) as mobile phase. The wavelength of the detection was 248 nm.

3.2.3.4. Pyrazinamide.

In mammals the tuberculosis drug pyrazinamide is biotransformed by AOX and XOR. Pyrazinamide was incubated with rainbow trout, Wistar rat and human liver cytosol with O_2 or with NAD^+ as electron acceptor and HPLC analysis were carried out. After incubation with rainbow trout liver cytosol with O_2 or with NAD^+ (Figure 42). The incubation of rainbow trout liver cytosol with pyrazinamide in the presence of O_2 as an electron acceptor for 240 minute incubation time did not show the production of any metabolite peak as seen in (Figure 42a). In contrast, the incubation of trout liver cytosol with pyrazinamide with NAD^+ as an electron acceptor generated 5-hydroxypyrazinamide (Figure 42b). In contrast Wistar rat and human liver cytosol displayed activity with both O_2 and NAD^+ as electron acceptor (Figure 43 and 44), indicating that in these species pyrazinamide was a substrate for both oxidase and dehydrogenase enzymes.
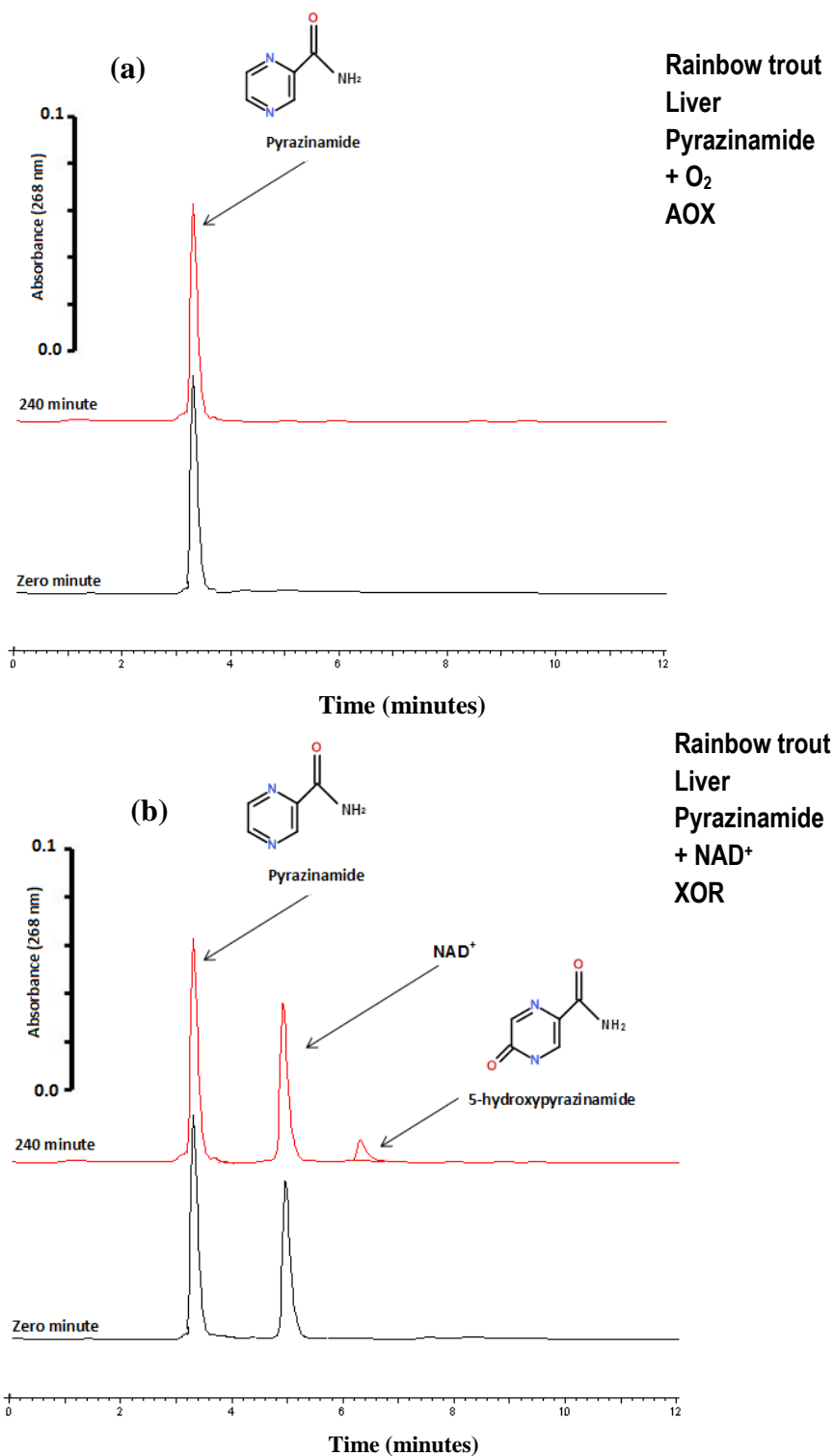
Figure 42: HPLC analysis of the *in vitro* biotransformation of pyrazinamide by rainbow trout liver cytosol at 37˚C. Incubation (a) with O_2(b) with NAD^+ as an electron acceptor. Times at the left hand side of the chromatograms indicate incubation times. HPLC chromatograms are offset on the vertical axis to allow comparison between different incubation times. Analytes were injected onto a C-18 column (Kromasil 5 μm) and eluted with a 20 mM KH_2PO_4: acetonitrile (95: 5) as mobile phase. The wavelength of the detection was 268 nm.
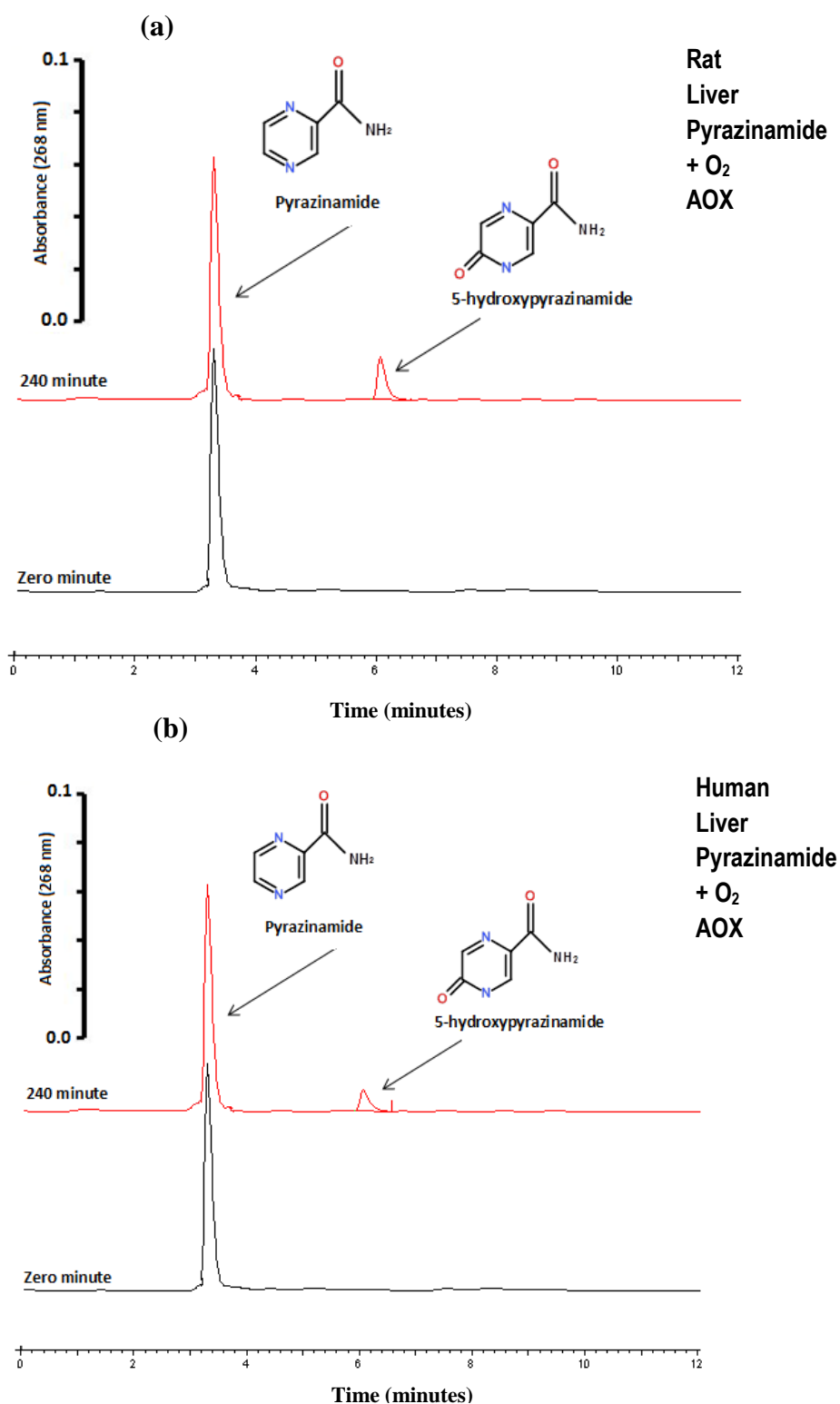
Figure 43: HPLC analysis of the *in vitro* biotransformation of pyrazinamide by Wistar rat and human liver cytosol at 37°C. Incubation with O_2 as an electron acceptor. (a) Wistar rat, (b) human liver cytosol. Times at the left hand side of the chromatograms indicate incubation times. HPLC chromatograms are offset on the vertical axis to allow comparison between different incubation times. Analytes were injected onto a C-18 column (Kromasil 5 μm) and eluted with a 20 mM KH_2PO_4: acetonitrile (95: 5) as mobile phase. The wavelength of the detection was 268 nm.
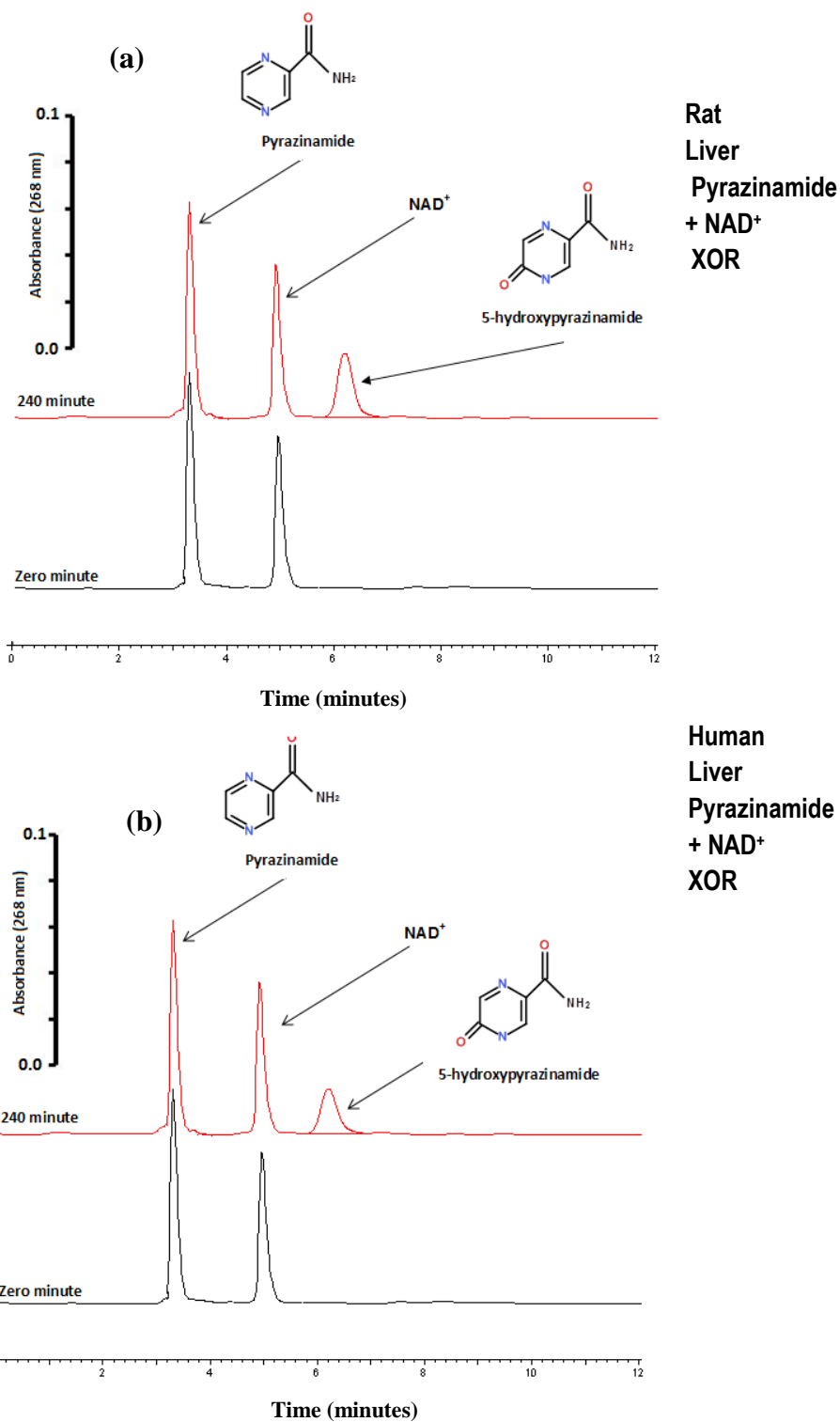
Figure 44: HPLC analysis of the *in vitro* biotransformation of pyrazinamide by Wistar rat and human liver cytosol at 37°C. Incubation with NAD [+] as an electron acceptor. (a) Wistar rat, (b) human liver cytosol. Times at the left hand side of the chromatograms indicate incubation times. HPLC chromatograms are offset on the vertical axis to allow comparison between different incubation times. Analytes were injected onto a C-18 column (Kromasil 5 μm) and eluted with a 20 mM KH_2PO_4: acetonitrile (95: 5) as mobile phase. The wavelength of the detection was 268 nm.

The rainbow trout AOX activity were tested in liver, kidney and gill cytosol and it was found exclusively in the liver using HPLC and spectrophotometric assays. Hepatic aldehyde oxidase in cytosols of rainbow trout, human and rat (Table 38) were able to catalyse the oxidation of a range of MFE substrates to varying degrees. These included the exogenous aldehydes (DMAC and vanillin), endogenous vitamin substrates (all-trans retinal, pyridoxal and N^1-methylnicotinamide), NPAH environmental pollutants (phenanthridine, phthalazine and cinchonine), and drug (pyrazinamide). The activity of rainbow trout with DMAC as AOX substrate in spectrophotometric assay were found lower compared to that other species (Table 38). The activity of Wistar rat with vanillin as AOX substrate was greater compared than that with human and trout respectively. The activity of human with endogenous vitamin substrates (all-trans retinal, pyridoxal and N^1-methylnicotinamide) was greater than that with Wistar rat and trout respectively (Table 38). The lowest activity found of NPAH environmental pollutants (phenanthridine, phthalazine and cinchonine) was in trout compared with that of Wistar rat and human and the highest activity found was with human for phthalazine as AOX substrate and the highest activity with Wistar rat was for phenanthridine and cinchonine (Table 38). The highest activity found for pyrazinamide as substrate was with human and the lowest activity was found with trout (Table 38).

Table 38: Summary of *in vitro* studies of hepatic aldehyde oxidase activity in different species using HPLC and spectrophotometric assays with different substrates

Substrate	Species	Activity
DMAC	Rainbow trout	+++
	Wistar rat	++++
	Human	+++++
Vanillin	Rainbow trout	++
	Wistar rat	+++++
	Human	+++
Pyridoxal	Rainbow trout	++
	Wistar rat	++++
	Human	+++++
All-trans retinal	Rainbow trout	++
	Wistar rat	++++
	Human	+++++
N^1-methylnicotinamide	Rainbow trout	+
	Wistar rat	++++
	Human	+++++
Phenanthridine	Rainbow trout	+
	Wistar rat	+++++
	Human	++++
Phthalazine	Rainbow trout	++
	Wistar rat	++++
	Human	+++++
Cinchonine	Rainbow trout	++
	Wistar rat	+++++
	Human	++++
Pyrazinamide	Rainbow trout	+
	Wistar rat	+++++
	Human	++++

(+++++ = ultra-high activity,++++ =high activity, +++ = intermediate activity, ++ = low activity,
 + = very low activity).

3.3. Spectrophotometric and HPLC analysis of molybdo-flavoenzyme activity with endogenous purine and purine analogue substrates.

3.3.1. Xanthine and 1-methylxanthine.

For XOR activity two substrates were assessed using spectrophotometry. These were the endogenous purine catabolite xanthine and the major caffeine metabolite 1-methylxanthine. (Figure 45) illustrates spectrophotometric assays with the xanthine demonstrating that liver cytosols from Wistar rat and human had measurable XOR activity with and without NAD^+. In contrast rainbow trout liver cytosol only had measurable XOR activity in presence of NAD^+ (Figure 45b). Similar spectrophotometric results were obtained with 1-methylxanthine (data not shown). Rainbow trout kidney and gill cytosols had no measurable activity towards either of these substrates.

In order to check unequivocally if there was no XDH activity towards xanthine and 1-methylxanthinein kidney and gill cytosols a sensitive HPLC assay was used, this showed that even following a 120 minute incubation with these substrates there was no uric acid metabolite formed in contrast to liver cytosol (Figures 46 and 47).Reflecting the results from the spectrophotometric assay even after an extended 2 hour incubation no uric acid metabolite was formed with O_2 as an electron acceptor. When xanthine and 1-methylxanthine were incubated with rainbow trout liver cytosol (Figures 48 and 49) there were appreciable levels of uric acid produced with NAD^+ as electron acceptor. This was in contrast to that found when rat and human liver cytosol was incubated with these substrates where both electron acceptors were utilised resulting in uric acid metabolite being formed with both the endogenous and exogenous purine (Figures 50, 51, 52 and 53).
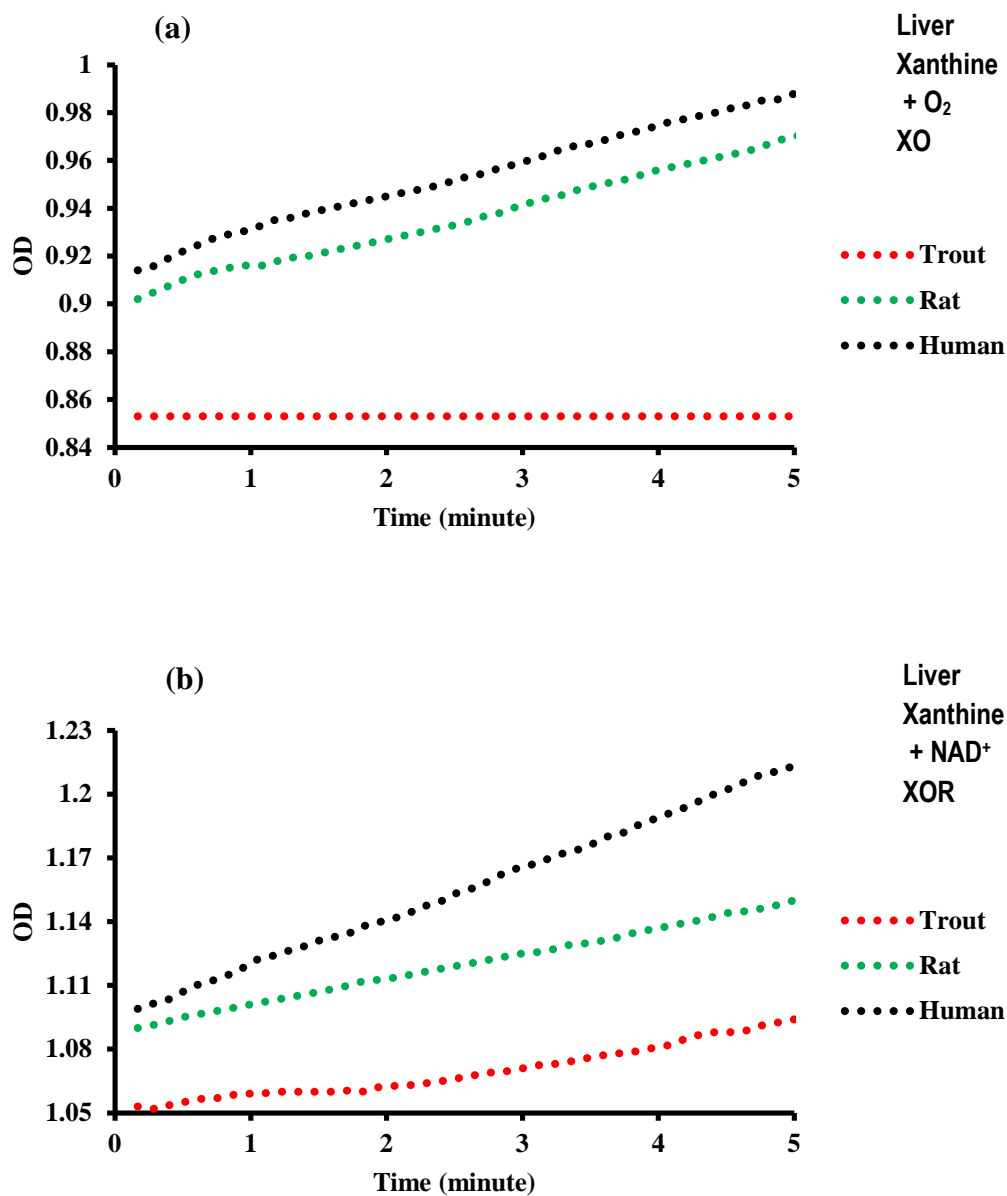
Figure 45: Spectrophotometric assays of xanthine oxidoreductase activities using rainbow trout, Wistar rat and human liver cytosol at 37°C with XOR substrates. (a) xanthine oxidase activity assay. (b) xanthine oxidoreductase activity assay. Rainbow trout [red], Wistar rat [green] and human [black] liver cytosol. For all assays 100 µM final xanthine concentrations were used. For the XOR assay 670 µM NAD+ was used as the electron acceptor. For analysis conditions see section 2.5.
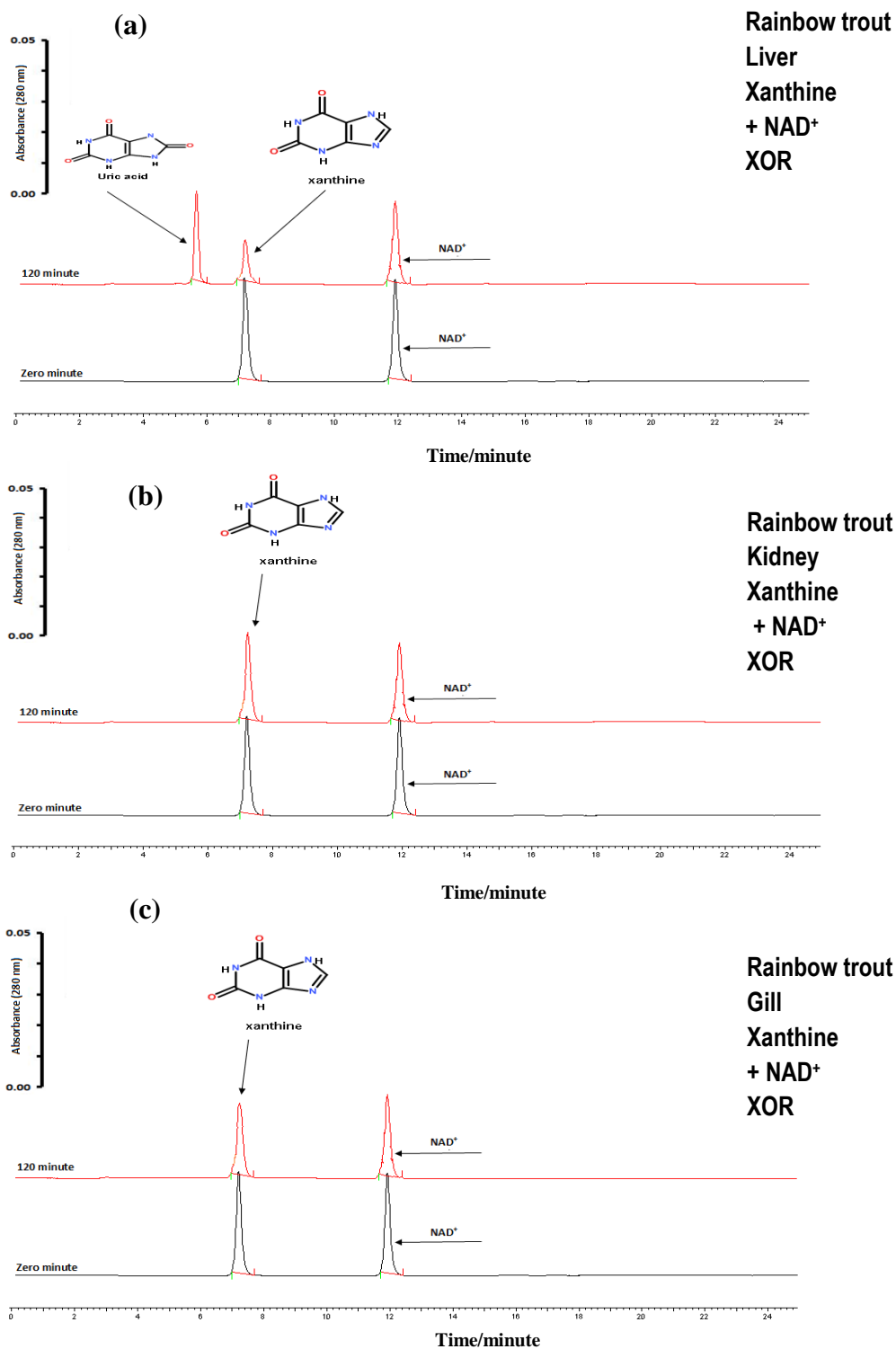
Figure 46: HPLC analysis of the in vitro biotransformation of xanthine + NAD^+ by rainbow trout cytosol. The chromatogram(a) Liver, (b) Kidney and (c) Gill trout cytosol with xanthine and NAD^+. Times at the left hand side of the chromatograms indicate incubation times. HPLC chromatograms are offset on the vertical axis to allow comparison between different incubation times .Analytes were injected onto a C-18 column (Kromasil 5 μm) and eluted with a 0.1% v/v glacial acetic acid: acetonitrile gradient system as described in section 2.5.3 as mobile phase. The wavelength of the detection was 280 nm.
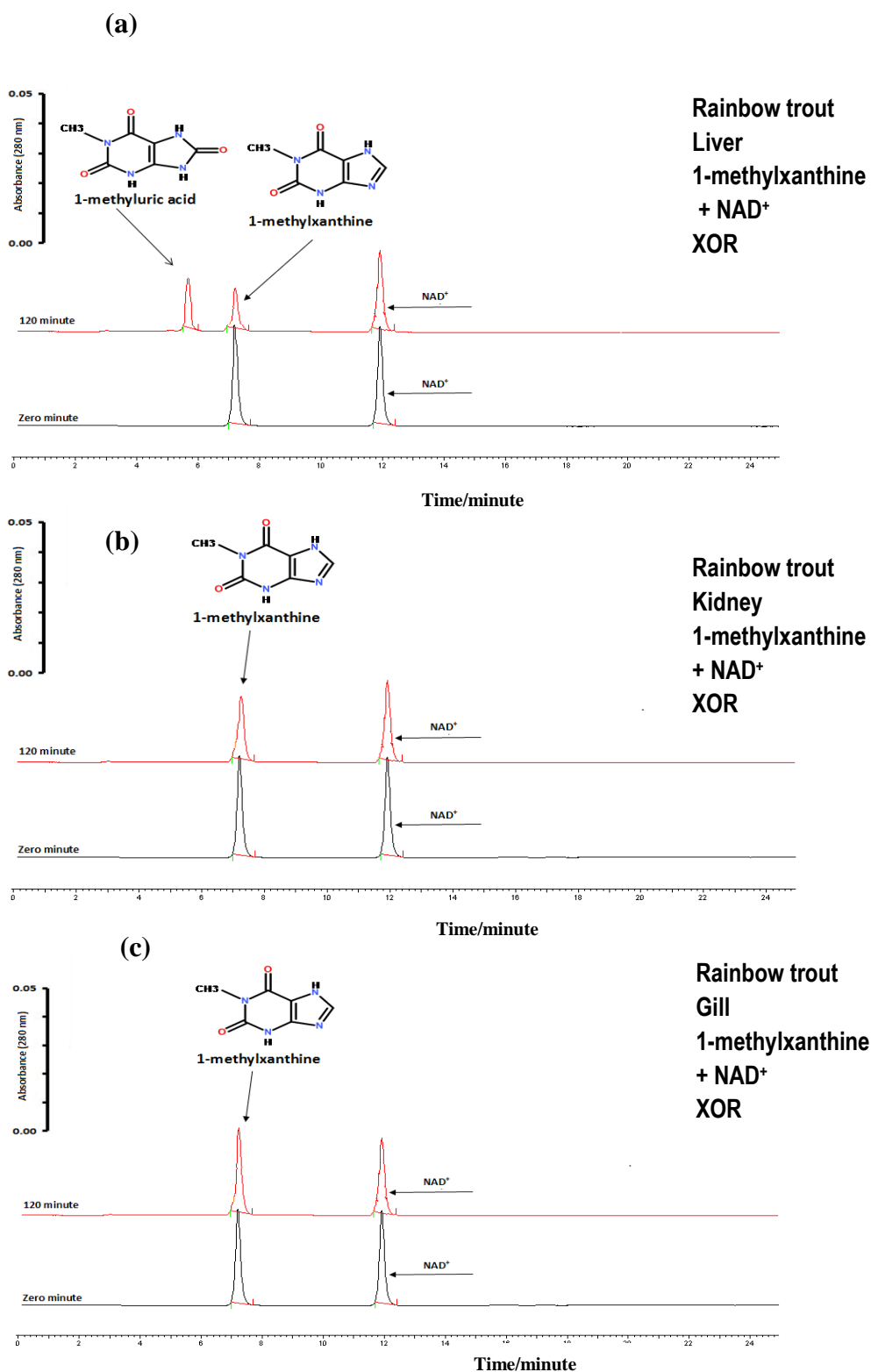
Figure 47: HPLC analysis of the in vitro biotransformation of 1-methylxanthine + NAD$^+$ by rainbow trout cytosol. The chromatogram (a) Liver, (b) Kidney and (c) Gill trout cytosol with xanthine and NAD$^+$. Times at the left hand side of the chromatograms indicate incubation times. HPLC chromatograms are offset on the vertical axis to allow comparison between different incubation times .Analytes were injected onto a C-18 column (Kromasil 5 μm) and eluted with a 0.1% v/v glacial acetic acid: acetonitrile gradient system as described in section 2.5.3 as mobile phase. The wavelength of the detection was 280 nm.

(a)

(b)
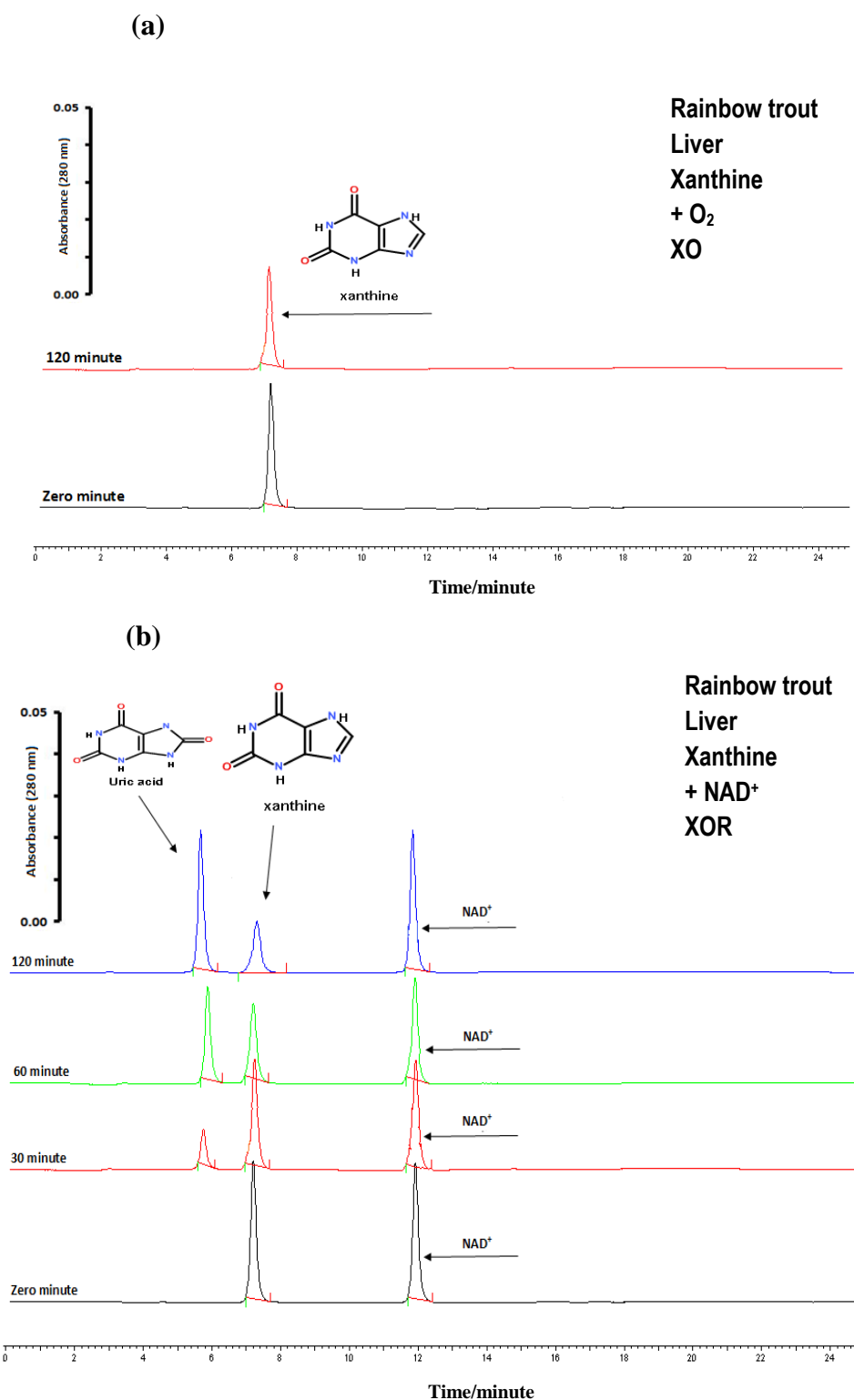
Figure 48: HPLC analysis of the *in vitro* biotransformation of xanthine by rainbow trout liver cytosol. The chromatogram (a) HPLC analytes generated by rainbow trout liver cytosol with xanthine in presence of O_2 as an electron acceptor. The chromatogram (b) HPLC analytes generated by rainbow trout liver cytosol with xanthine and NAD^+. Times at the left hand side of the chromatograms indicate incubation times. HPLC chromatograms are offset on the vertical axis to allow comparison between different incubation times .Analytes were injected onto a C-18 column (Kromasil 5 µm) and eluted with a 0.1% v/v glacial acetic acid: acetonitrile gradient system as described in section 2.5.3 as mobile phase. The wavelength of the detection was 280 nm.

123
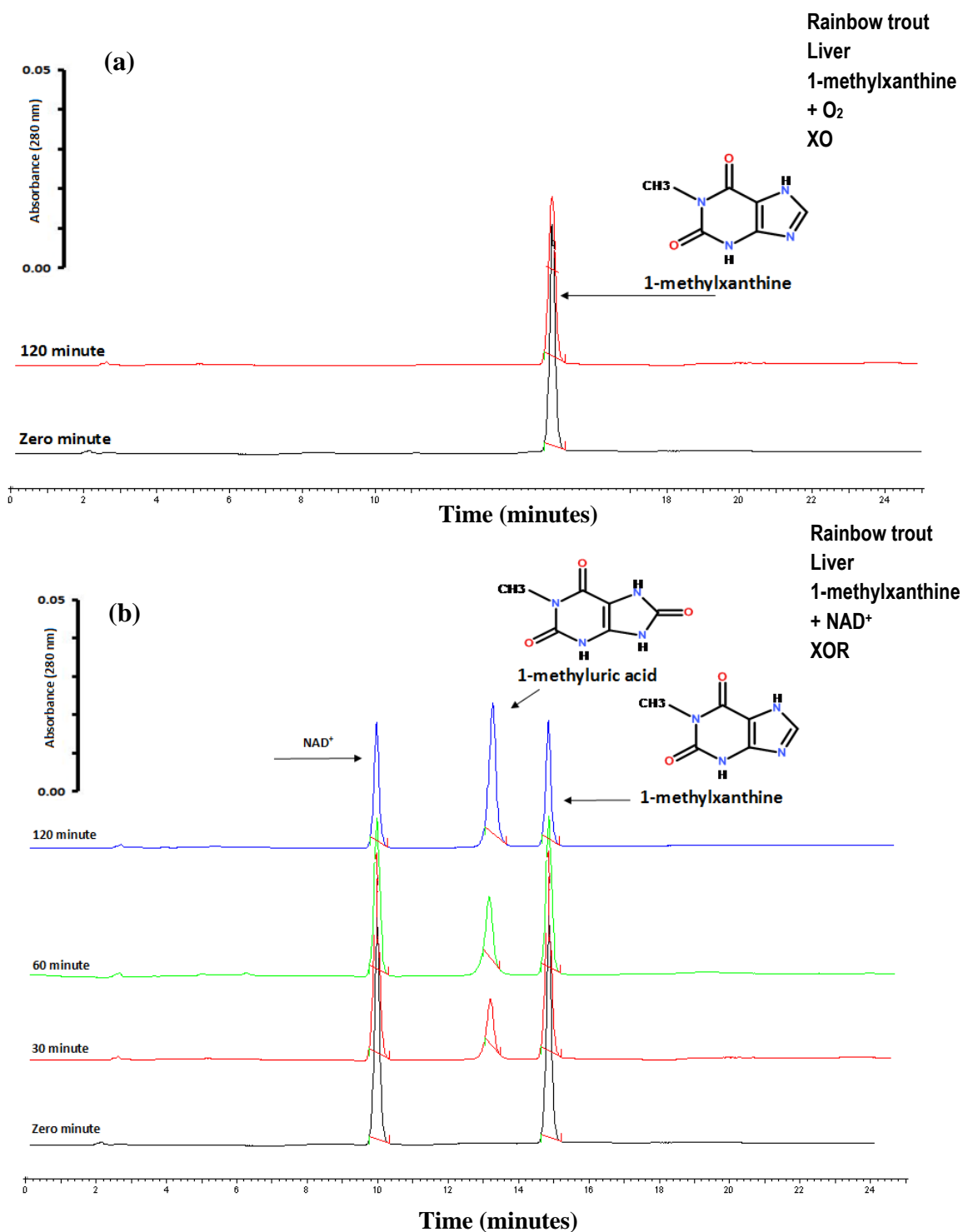
Figure 49: HPLC analysis of the *in vitro* biotransformation of 1-methylxanthine by rainbow trout liver cytosol at 37°C. The chromatogram (a) HPLC analytes generated by rainbow trout liver cytosol with 1-methylxanthine in the presence of O_2 as an electron acceptor. The chromatogram (b) HPLC analytes generated by trout liver cytosol with 1-methylxanthine and NAD^+ as an electron acceptor. Times at the left hand side of the chromatograms indicate incubation times. HPLC chromatograms are offset on the vertical axis to allow comparison between different incubation times. Analytes were injected onto a C-18 column (Kromasil 5 μm) and eluted with a 0.1% v/v glacial acetic acid: acetonitrile gradient system as described in section 2.5.3 as mobile phase. The wavelength of the detection was 280 nm.

(a)

Absorbance (280 nm)

Uric acid

xanthine

Rat
Liver
Xanthine
+ O$_2$
XO

15 minute

10 minute

5 minute

8.300

Zero minute

Time (minutes)

(b)

Absorbance (280 nm)

Uric acid

xanthine

Rat
Liver
Xanthine
+ NAD$^+$
XOR

NAD$^+$

5 minute

NAD$^+$

Zero minute

Time (minutes)
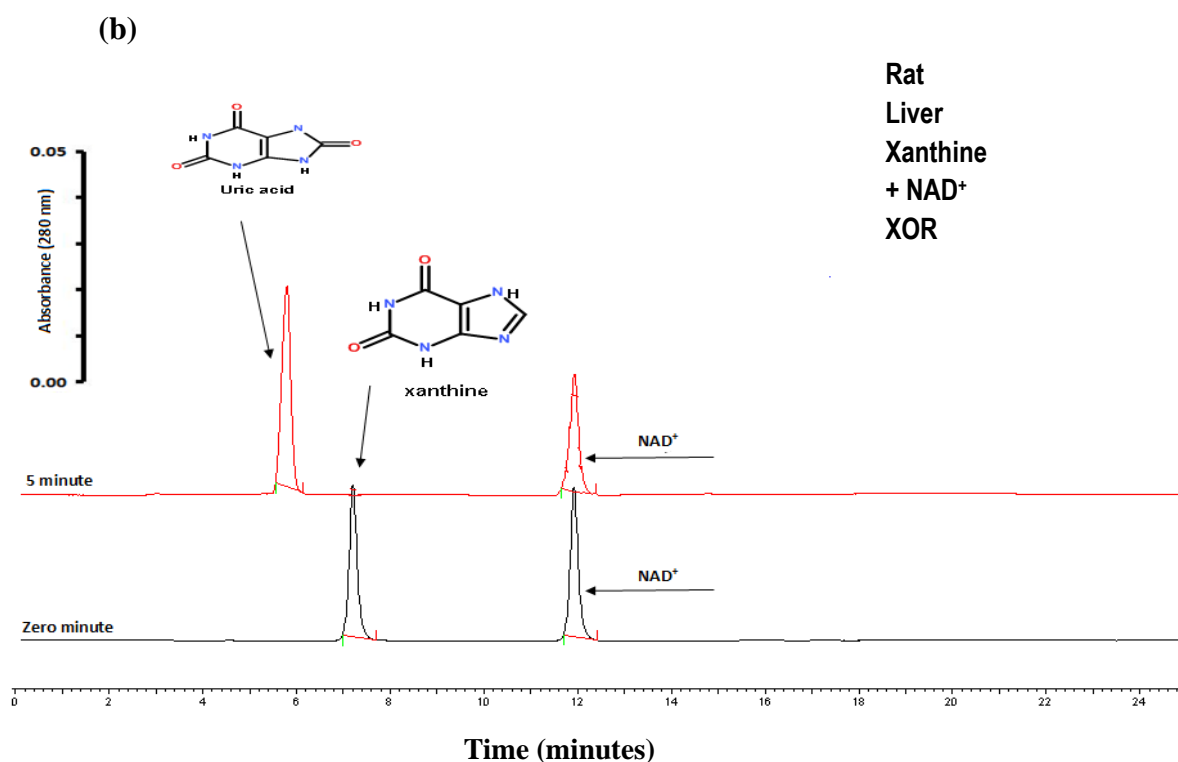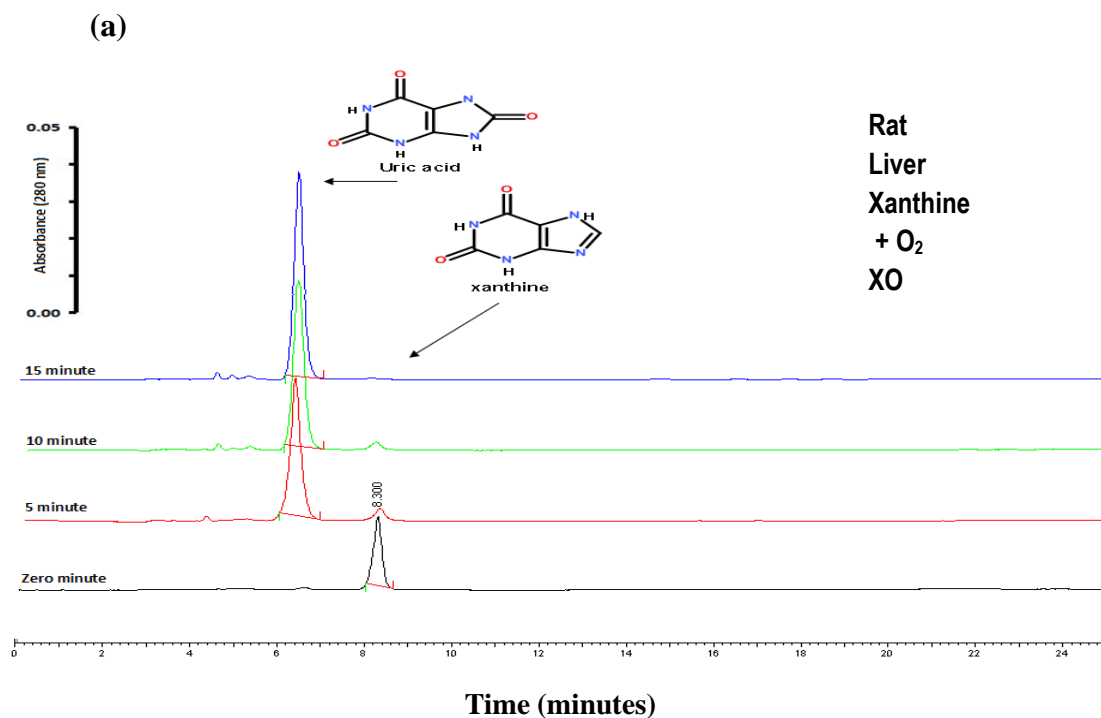
Figure 50: HPLC analysis of the *in vitro* biotransformation of xanthine by Wistar rat liver cytosol. The chromatogram (a) HPLC analytes generated by rat liver cytosol with xanthine and O$_2$ as electron acceptor. The chromatogram (b) HPLC analytes generated by Wistar rat liver cytosol with xanthine and NAD$^+$. The amount of NAD$^+$ added to incubation 675µM. Times at the left hand side of the chromatograms indicate incubation times. HPLC chromatograms are offset on the vertical axis to allow comparison between different incubation times. Analytes were injected onto a C-18 column (Kromasil 5 µm) and eluted with a 0.1% v/v glacial acetic acid: acetonitrile gradient system as described in section 2.5.3 as mobile phase. The wavelength of the detection was 280 nm.
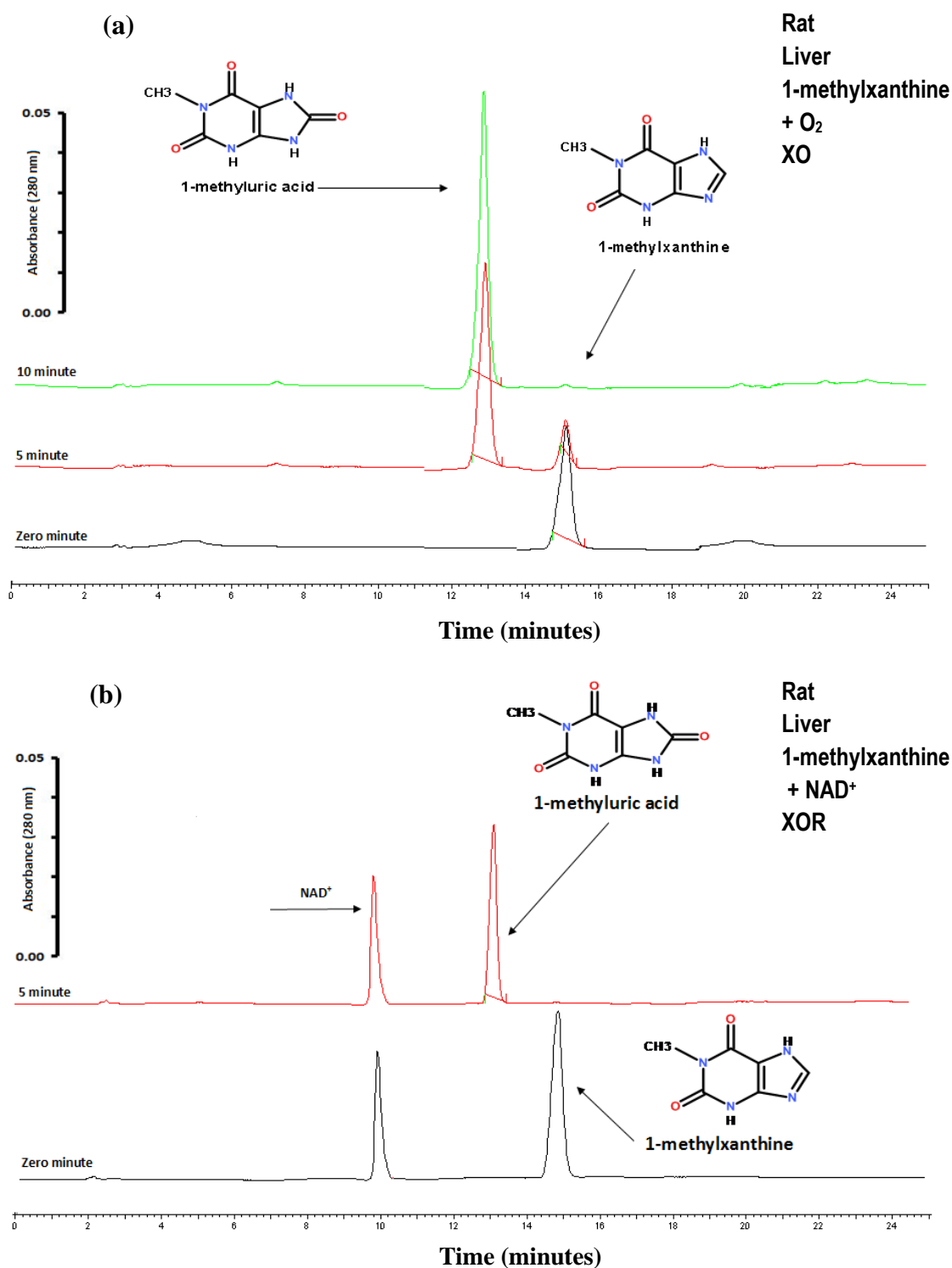
Figure 51: HPLC analysis of the *in vitro* biotransformation of 1-methylxanthine by Wistar rat liver cytosol at 37^{0}C. The chromatogram (a) HPLC analytes generated by Wistar rat liver cytosol with 1-methylxanthine and O$_2$ as an electron acceptor. The chromatogram (b) HPLC chromatogram for incubation of Wistar rat liver cytosol with 1-MX and NAD$^+$ as an electron acceptor. Times at the left hand side of the chromatograms indicate incubation times. HPLC chromatograms are offset on the vertical axis to allow comparison between different incubation times .Analytes were injected onto a C-18 column (Kromasil 5 µm) and eluted with a 0.1% v/v glacial acetic acid: acetonitrile gradient system as described in section 2.5.3 as mobile phase. The wavelength of the detection was 280 nm.
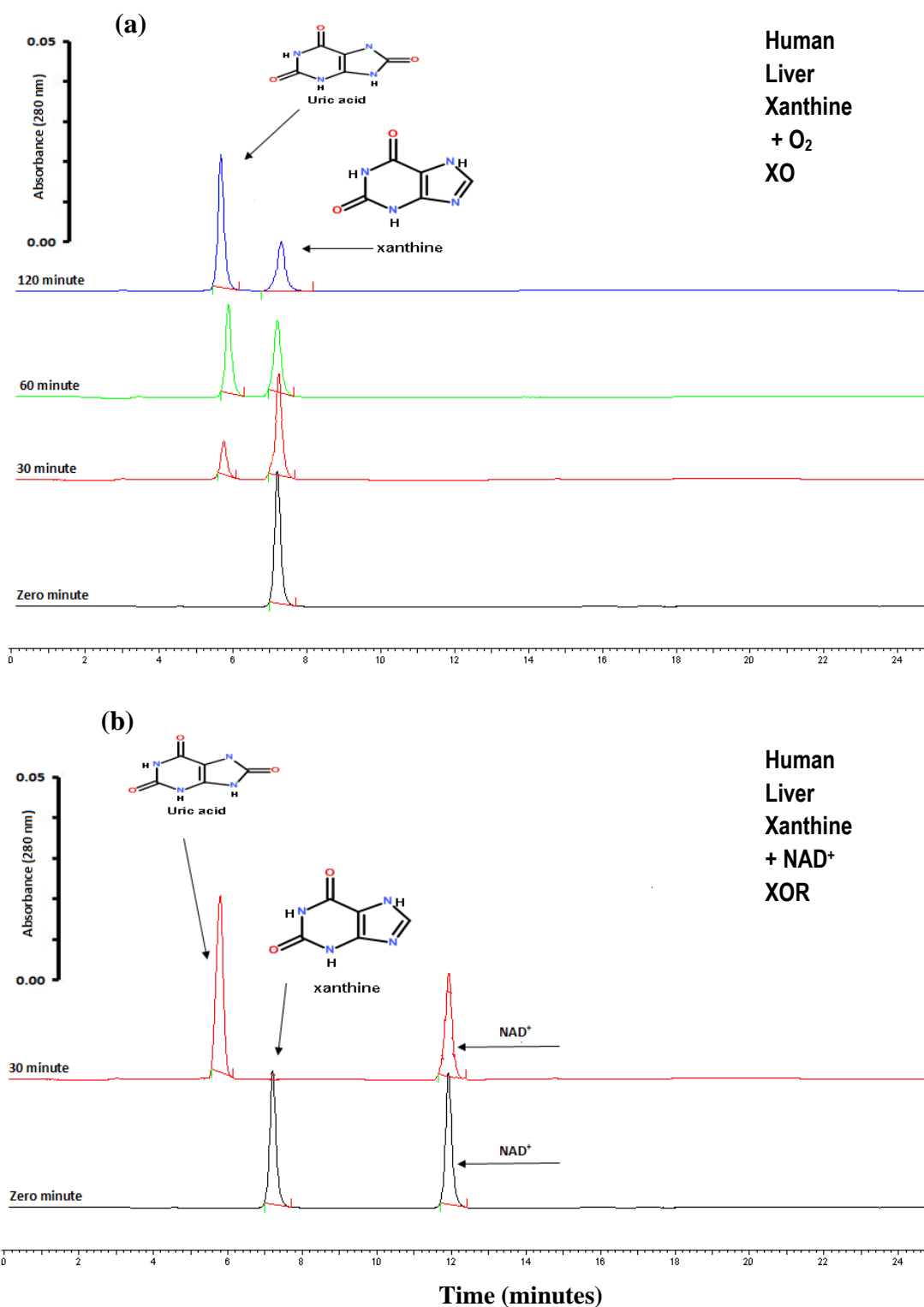
Figure 52: HPLC analysis of the *in vitro* biotransformation of xanthine by human liver cytosol. The chromatogram (a) HPLC analytes generated by human liver cytosol with xanthine and O_2 as electron acceptor. The chromatogram (b) HPLC analytes generated by human liver cytosol with xanthine and NAD^+. The amount of NAD^+ added to incubation 675µM. Times at the left hand side of the chromatograms indicate incubation times. HPLC chromatograms are offset on the vertical axis to allow comparison between different incubation times Analytes were injected onto a C-18 column (Kromasil 5 µm) and eluted with a 0.1% v/v glacial acetic acid: acetonitrile gradient system as described in section 2.5.3 as mobile phase. The wavelength of the detection was 280 nm.

127

Figure 53: HPLC analysis of the *in vitro* biotransformation of 1-methylxanthine to 1-methyluric acid by human liver cytosol at 37^0C. The chromatogram (a) HPLC analytes generated by human liver cytosol with 1-methylxanthine using O_2 as an electron acceptor. The chromatogram (b) HPLC analytes generated by human liver cytosol with 1-methylxanthine (1-MX) and NAD^+. Times at the left hand side of the chromatograms indicate incubation times. HPLC chromatograms are offset on the vertical axis to allow comparison between different incubation times .Analytes were injected onto a C-18 column (Kromasil 5 μm) and eluted with a 0.1% v/v glacial acetic acid: acetonitrile gradient system as described in section 2.5.3 as mobile phase. The wavelength of the detection was 280 nm.

When the liver cytosol from all three species was incubated with the XOR inhibitor oxipurinol and AOX inhibitor menadione, oxipurinol gave 100% inhibition while the menadione did not have any effect (Figures 54, 55, 56, 57, 58 and 59), this illustrates that XOR is responsible for biotransformation of xanthine and 1-methylxanthine to their metabolites in these species.
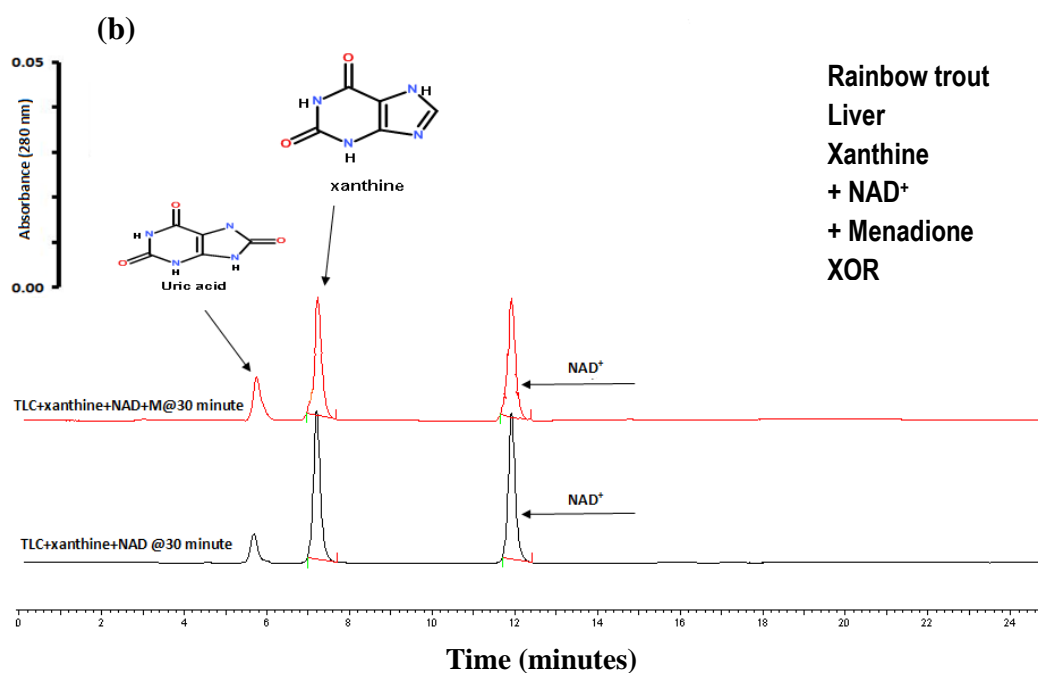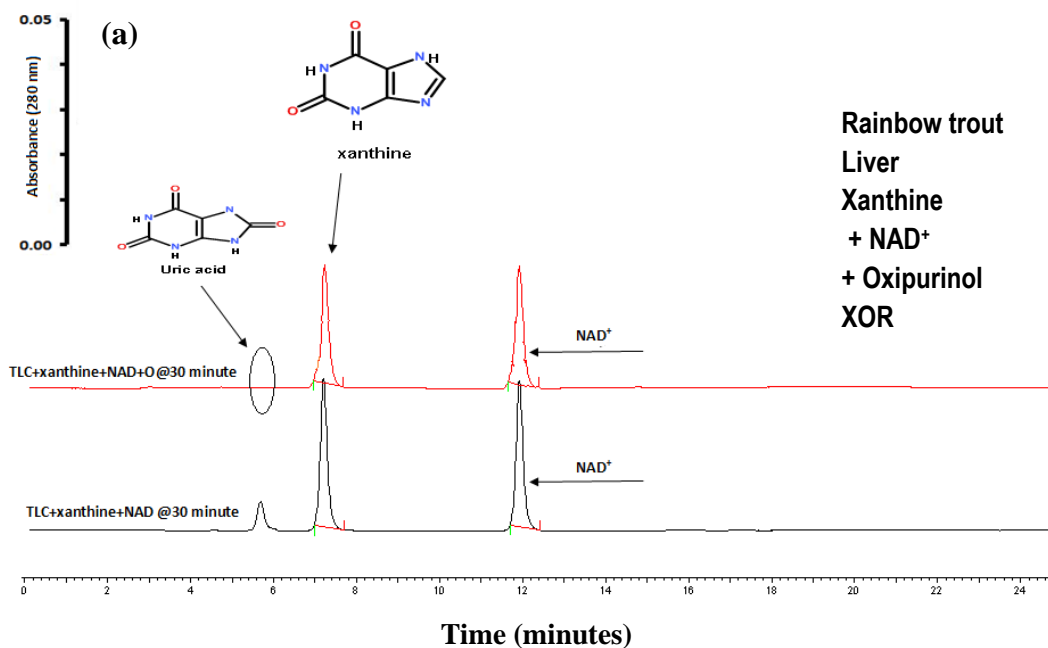
Figure 54: HPLC analysis of the in vitro biotransformation of xanthine by rainbow trout liver cytosol with and without enzyme inhibitors. The chromatogram of xanthine, NAD^+ plus (a) oxipurinol and (b) menadione. Red line with inhibitor and black line without inhibitor. The amount of inhibitor added to incubation its $100\mu M$. Times at the left hand side of the chromatograms indicate incubation times. HPLC chromatograms are offset on the vertical axis to allow comparison between different incubation times. Analytes were injected onto a C-18 column (Kromasil 5 μm) and eluted with a 0.1% v/v glacial acetic acid: acetonitrile gradient system as described in section 2.5.3 as mobile phase. The wavelength of the detection was 280 nm.
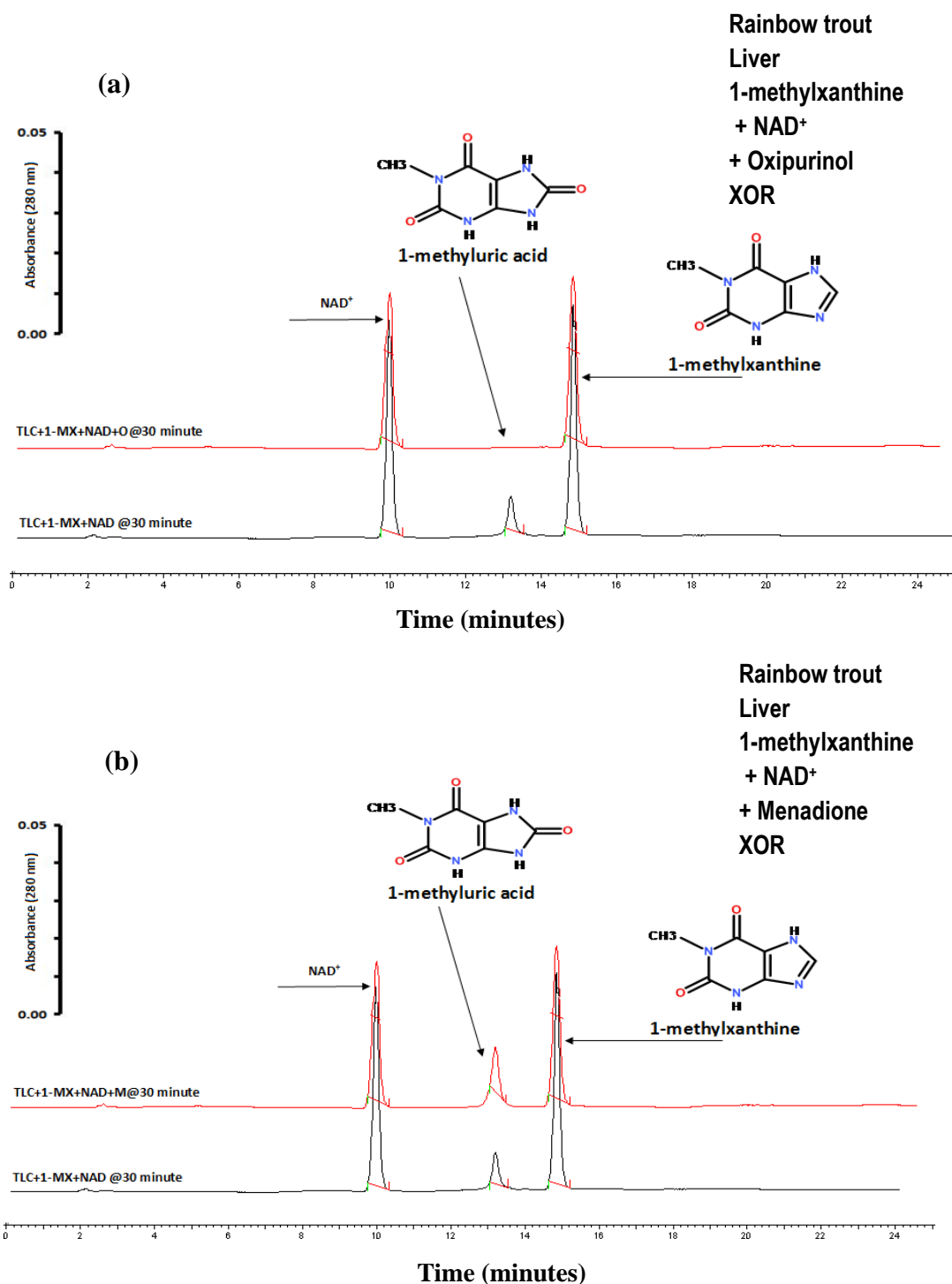
Figure 55: HPLC analysis of the *in vitro* biotransformation of 1-methylxanthine by rainbow trout liver cytosol with and without xanthine oxidoreductase and aldehyde oxidase inhibitors. HPLC chromatogram for incubation of trout liver with (1-MX), NAD^+ with (a) oxipurinol, (b) menadione. Red lines with inhibitors and black lines without inhibitors. The amount of inhibitors added to incubation its 100μM. Times at the left hand side of the chromatograms indicate incubation times. HPLC chromatograms are offset on the vertical axis to allow comparison between different incubation times. Analytes were injected onto a C-18 column (Kromasil 5 μm) and eluted with a 0.1% v/v glacial acetic acid: acetonitrile gradient system as described in section 2.5.3 as mobile phase. The wavelength of the detection was 280 nm.

(a)

(b)

Time (minutes)

Figure 56: HPLC analysis of the *in vitro* biotransformation of xanthine by Wistar rat liver cytosol with and without enzyme inhibitors. HPLC chromatogram for incubation of Wistar rat liver cytosol with xanthine and (a) oxipurinol, (b) menadione. Red lines with inhibitors and black lines without inhibitors. The amount of inhibitor added to incubation its 100μM. Times at the left hand side of the chromatograms indicate incubation times. HPLC chromatograms are offset on the vertical axis to allow comparison between different incubation times. Analytes were injected onto a C-18 column (Kromasil 5 μm) and eluted with a 0.1% v/v glacial acetic acid: acetonitrile gradient system as described in section 2.5.3 as mobile phase. The wavelength of the detection was 280 nm.

Figure 57: HPLC analysis of the *in vitro* biotransformation of 1-methylxanthine by Wistar rat liver cytosol with and without enzyme inhibitors. HPLC chromatogram for incubation of rat with 1-MX and (a) oxipurinol, (b) menadione. Red lines with inhibitors and black lines without inhibitors. The amount of inhibitors added to incubation its 100μM. Times at the left hand side of the chromatograms indicate incubation times. HPLC chromatograms are offset on the vertical axis to allow comparison between different incubation times. Analytes were injected onto a C-18 column (Kromasil 5 μm) and eluted with a 0.1% v/v glacial acetic acid: acetonitrile gradient system as described in section 2.5.3 as mobile phase. The wavelength of the detection was 280 nm.

133

(a)

(b)
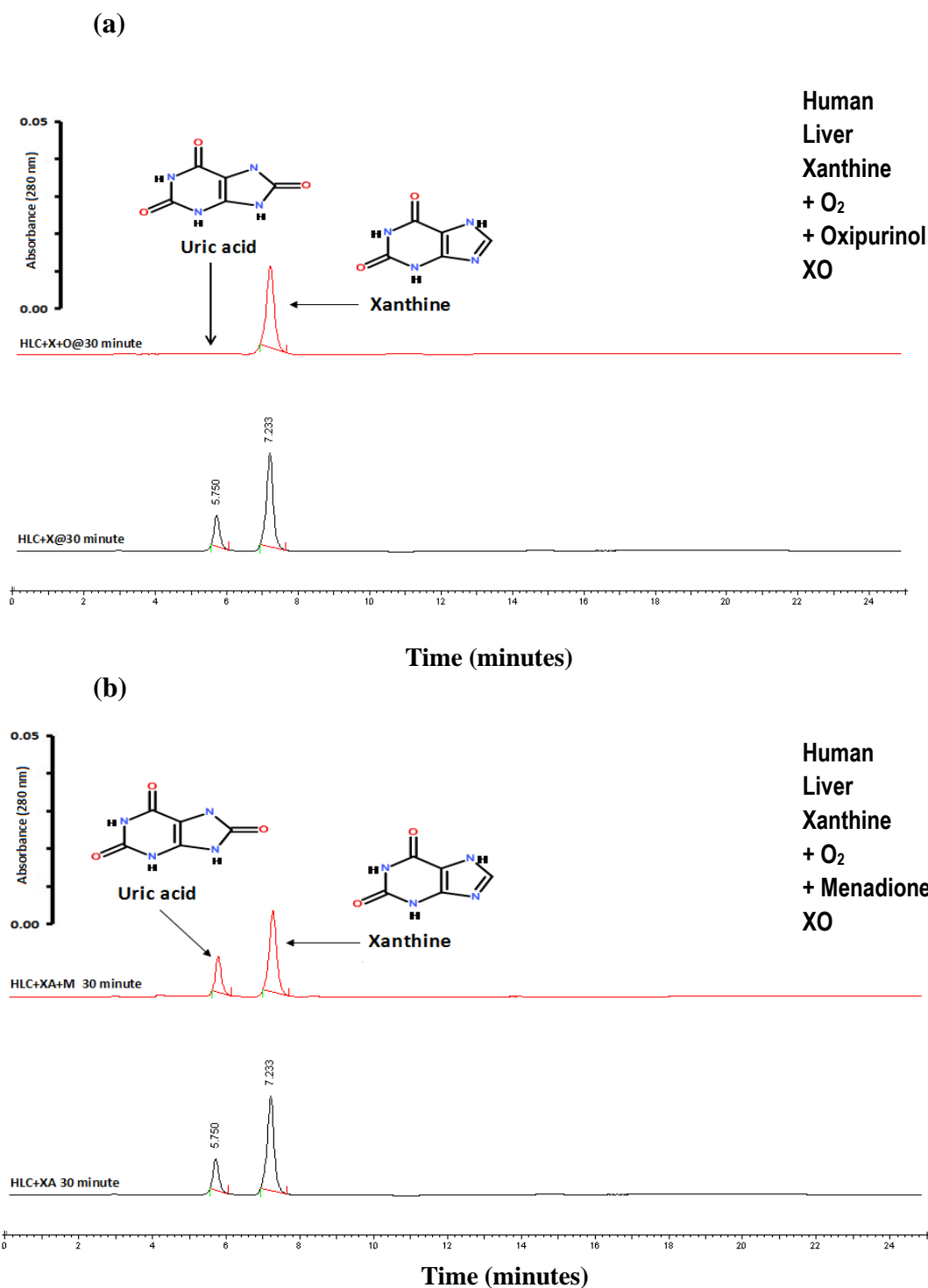
Figure 58: HPLC analysis of the *in vitro* biotransformation of xanthine by human liver cytosol with and without enzyme inhibitors. The chromatogram of human liver cytosol with xanthine and (a) oxipurinol, (b) menadione. Red lines with inhibitors and black lines without inhibitors The amount of inhibitor added to incubation its 100μM. Times at the left hand side of the chromatograms indicate incubation times. HPLC chromatograms are offset on the vertical axis to allow comparison between different incubation times. Analytes were injected onto a C-18 column (Kromasil 5 μm) and eluted with a 0.1% v/v glacial acetic acid: acetonitrile gradient system as described in section 2.5.3 as mobile phase. The wavelength of the detection was 280 nm.
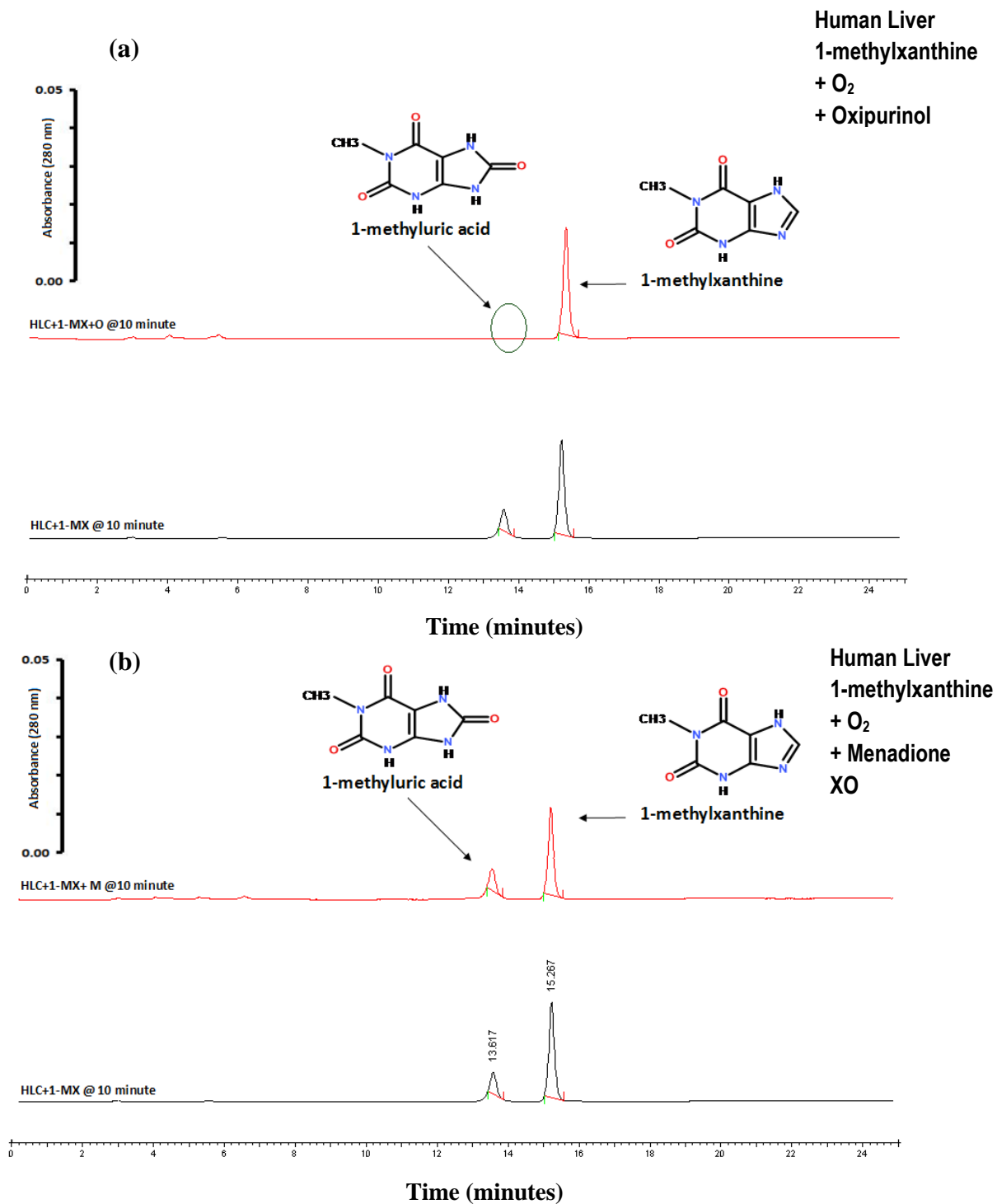
Figure 59: HPLC analysis of the *in vitro* biotransformation of 1-methylxanthine by human liver cytosol with and without enzyme inhibitors. HPLC chromatogram for incubation of human liver with 1-MX and (a) oxipurinol, (b) menadione. Red lines with inhibitors and black lines without inhibitors. The amount of inhibitors added to incubation its 100μM. Times at the left hand side of the chromatograms indicate incubation times. HPLC chromatograms are offset on the vertical axis to allow comparison between different incubation times. Analytes were injected onto a C-18 column (Kromasil 5 μm) and eluted with a 0.1% v/v glacial acetic acid: acetonitrile gradient system as described in section 2.5.3 as mobile phase. The wavelength of the detection was 280 nm.

3.3.3. 6-mercaptopurine.

6-mercaptopurine (6-MP) is a thiopurine anti-leukemia drug in which carbon 6 of purine has been substituted with a sulphur atom. In mammals 6-MP is oxidized to 6-thiouric acid via 6-thioxanthine or 8-oxo-6-mercaptopurine by AOX or XOR (Figure 17) although there is some controversy over the *in vitro* studies (Krenitsky *et al.*, 1972, Hall and Krenitsky. 1986, Rashidi *et al.*, 2007). In order to validate the assay in this study, rabbit liver cytosol was incubated with 6-MP and the products generated analysed by HPLC. This demonstrated that when rabbit cytosol was incubated with 6-MP with O_2 as sole electron acceptor it was biotransformed to 6-thiouric acid via 6-thioxanthine (Figure 60). This confirmed that the HPLC procedure and incubation conditions had successfully detected and resolved the expected 6-MP metabolites confirming the lack of detectable activity in rainbow trout liver cytosol towards this substrate was not due to experimental conditions. According to the *in vitro* experiments with rainbow trout, Wistar rat and human in this study, trout liver cytosol incubated with 6-MP with and without NAD^+ as an electron acceptor for 60 minute incubation time no peak of 6-thiouric acid formed (Figure 61). In contrast Wistar rat and human liver cytosol incubated with 6-mercaptopurine is a substrate for either XOR or AOX using O_2 or NAD^+ as electron acceptors (Figures 62 and 63). On the other hand as in the (Figures 64 and 65), in the Wistar rat and human liver cytosol incubated with XOR inhibitor oxipurinol and AOX inhibitor menadione it was found that oxipurinol produced 100% inhibition while menadione did not have any effect. This shows that XOR was responsible for biotransformation of 6-mercaptopurine (6-MP) to 6-thiouric acid. Due to the 6-MP not being a substrate for rainbow trout it was decided to test 6-thioxanthine as a substrate for either XOR or AOX of rainbow trout liver cytosol without and with NAD^+ as electron acceptors (Figure 66). On the other

hand, as in (Figure 67), trout liver cytosol incubated with XOR inhibitor oxipurinol and AOX inhibitor menadione found that oxipurinol produced 100% inhibition while the menadione does not have any effect, this shows that XOR is responsible for biotransformation of 6-thioxanthine to 6-thiouric acid.

Time (minute)
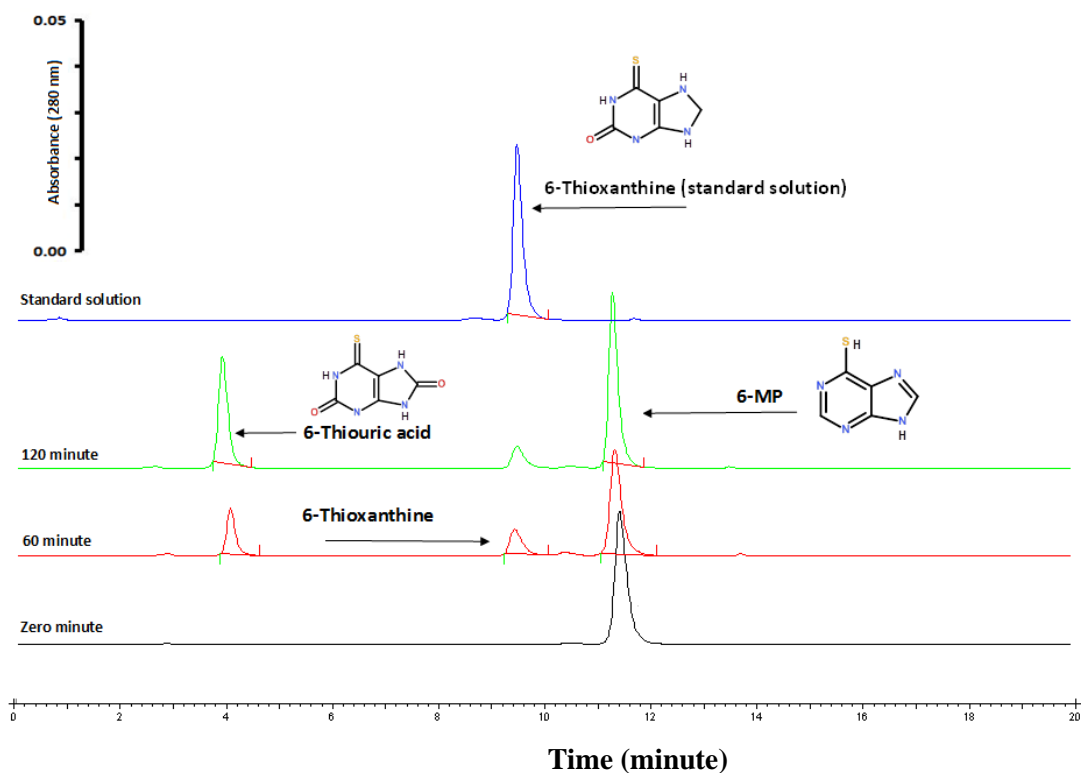
Figure 60: HPLC analysis of the *in vitro* biotransformation of 6-mercaptopurine by rabbit liver cytosol. Times at the left hand side of the chromatograms indicate incubation times. HPLC chromatograms are offset on the vertical axis to allow comparison between incubation times. Analytes were injected onto a C-18 column (Kromasil 5 µm) and eluted with a 0.1% v/v glacial acetic acid: acetonitrile gradient system as described in section 2.5.3 as mobile phase. The wavelength of the detection was 280 nm.
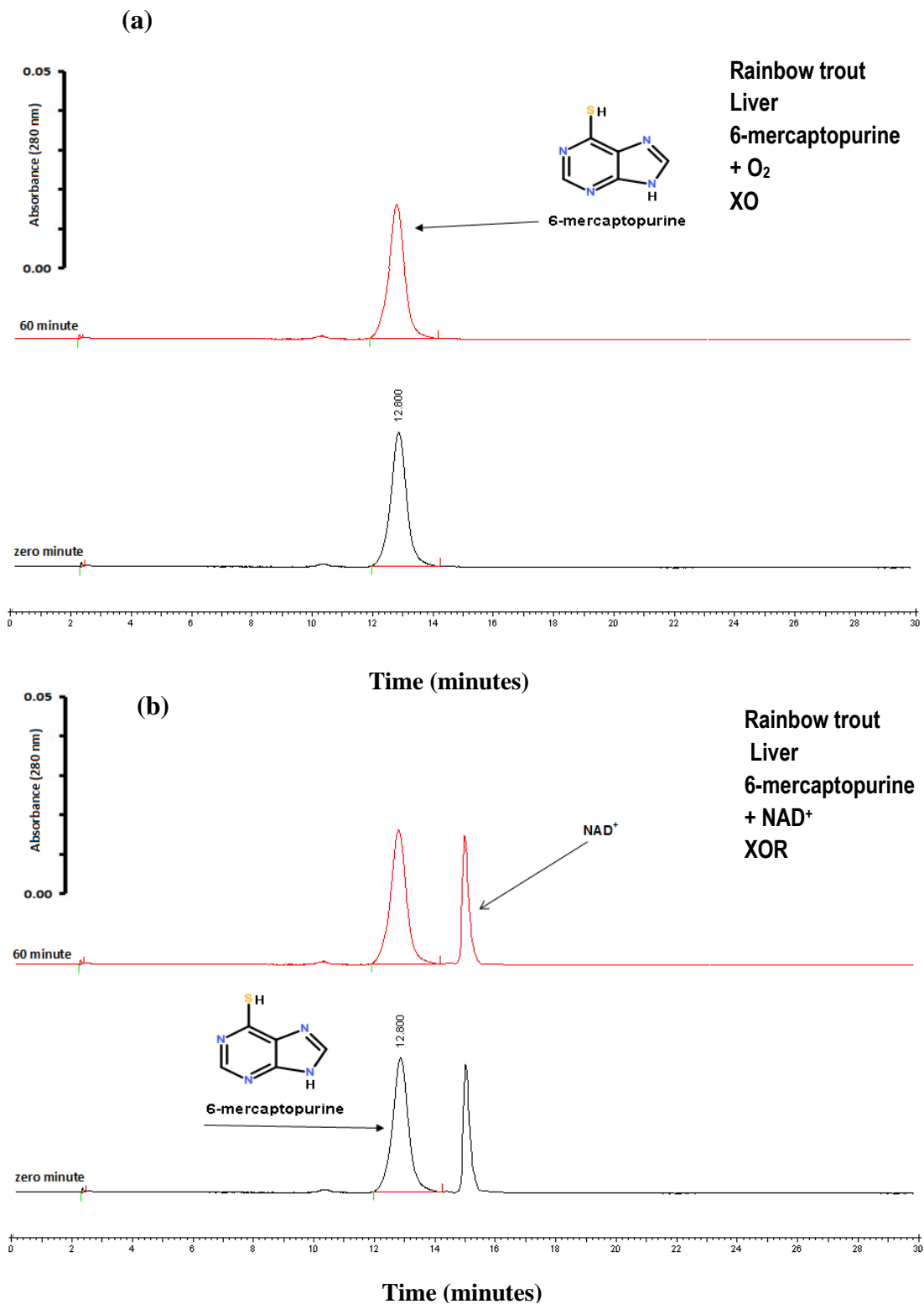
Figure 61: HPLC analysis of analytes produced following the *in vitro* incubation of 6-mercaptopurine with rainbow trout liver cytosol at 37°C. HPLC chromatogram (a) of analytes generated following incubation of 6-MP with trout liver cytosol and O_2 as an electron acceptor. HPLC chromatogram (b) of analytes generated following incubation of 6-MP with trout liver cytosol and NAD^+ as an electron acceptor. Times at the left hand side of the chromatograms indicate incubation times. HPLC chromatograms are offset on the vertical axis to allow comparison between different incubation times. Analytes were injected onto a C-18 column (Kromasil 5 µm) and eluted with a 0.1% v/v glacial acetic acid: acetonitrile gradient system as described in section 2.5.3 as mobile phase. The wavelength of the detection was 280 nm.
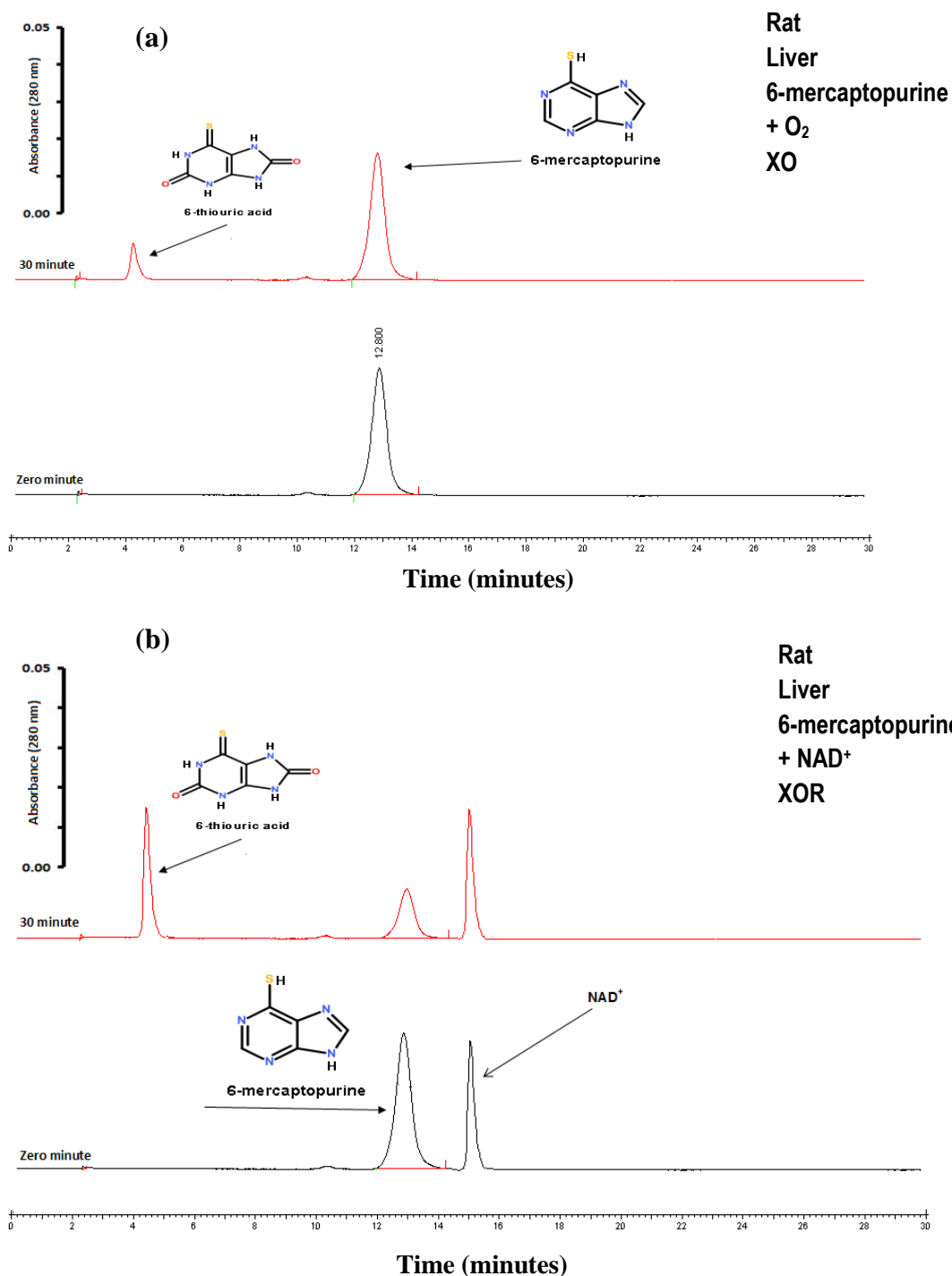
Figure 62: HPLC analysis of analytes produced following the *in vitro* incubation of 6-mercaptopurine with Wistar rat liver cytosol at 37°C. HPLC chromatogram (a) of analytes generated following incubation of 6-MP and O_2 as an electron acceptor. HPLC chromatogram (b) of analytes generated following incubation of 6-MP and NAD^+. Times at the left hand side of the chromatograms indicate incubation times. HPLC chromatograms are offset on the vertical axis to allow comparison between different incubation times .Analytes were injected onto a C-18 column (Kromasil 5 µm) and eluted with a 0.1% v/v glacial acetic acid: acetonitrile gradient system as described in section 2.5.3 as mobile phase. The wavelength of the detection was 280 nm.
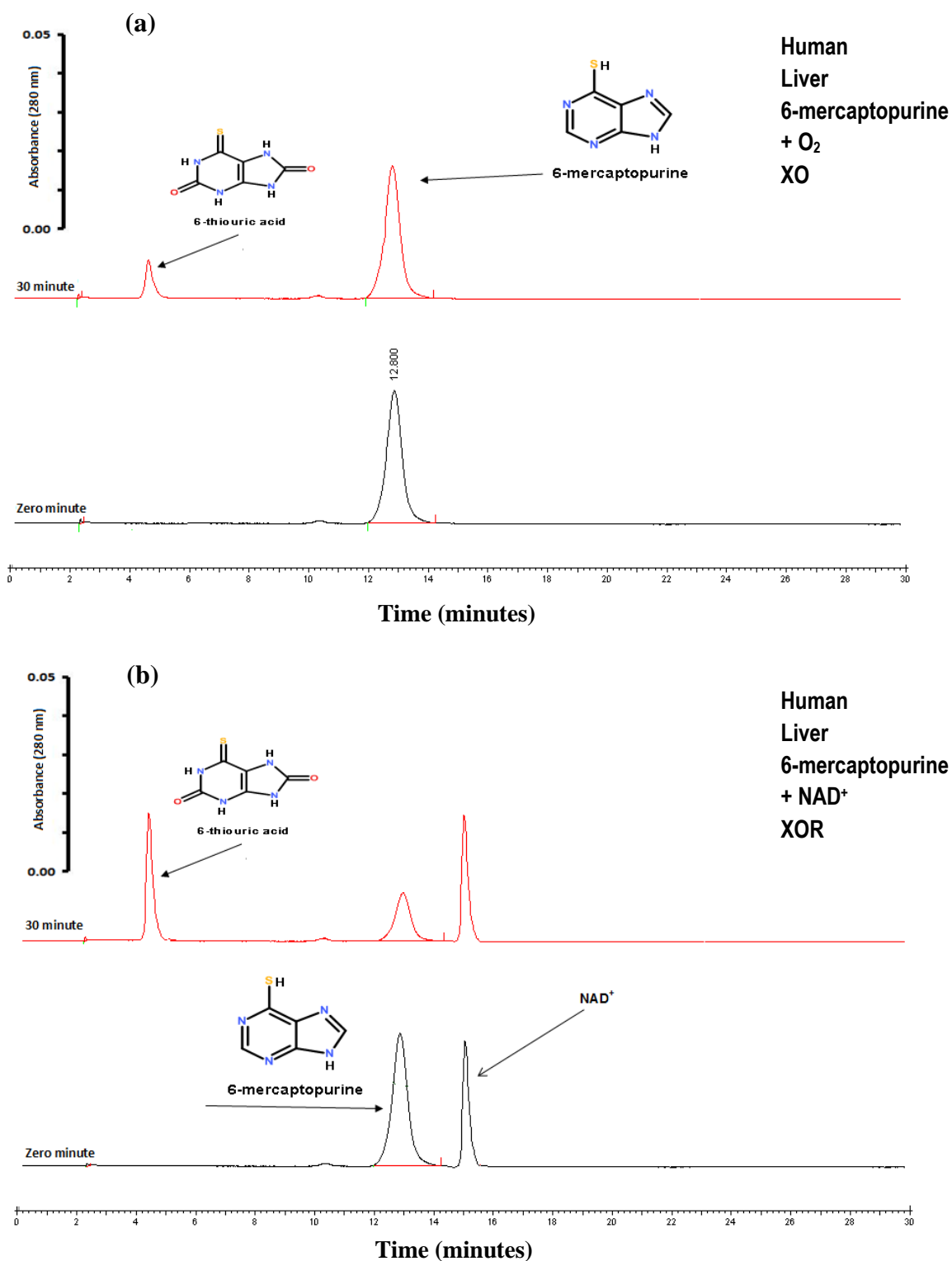
Figure 63: HPLC analysis of the *in vitro* biotransformation of 6-mercaptopurine by human liver cytosol. HPLC chromatogram (a) for incubation of human liver with 6-MP and O_2 as an electron acceptor. HPLC chromatogram (b) for incubation of human liver with 6-MP and NAD^+ as an electron acceptor. Times at the left hand side of the chromatograms indicate incubation times. .HPLC chromatograms are offset on the vertical axis to allow comparison between different incubation times. Analytes were injected onto a C-18 column (Kromasil 5 µm) and eluted with a 0.1% v/v glacial acetic acid: acetonitrile gradient system as described in section 2.5.3 as mobile phase. The wavelength of the detection was 280 nm.

140
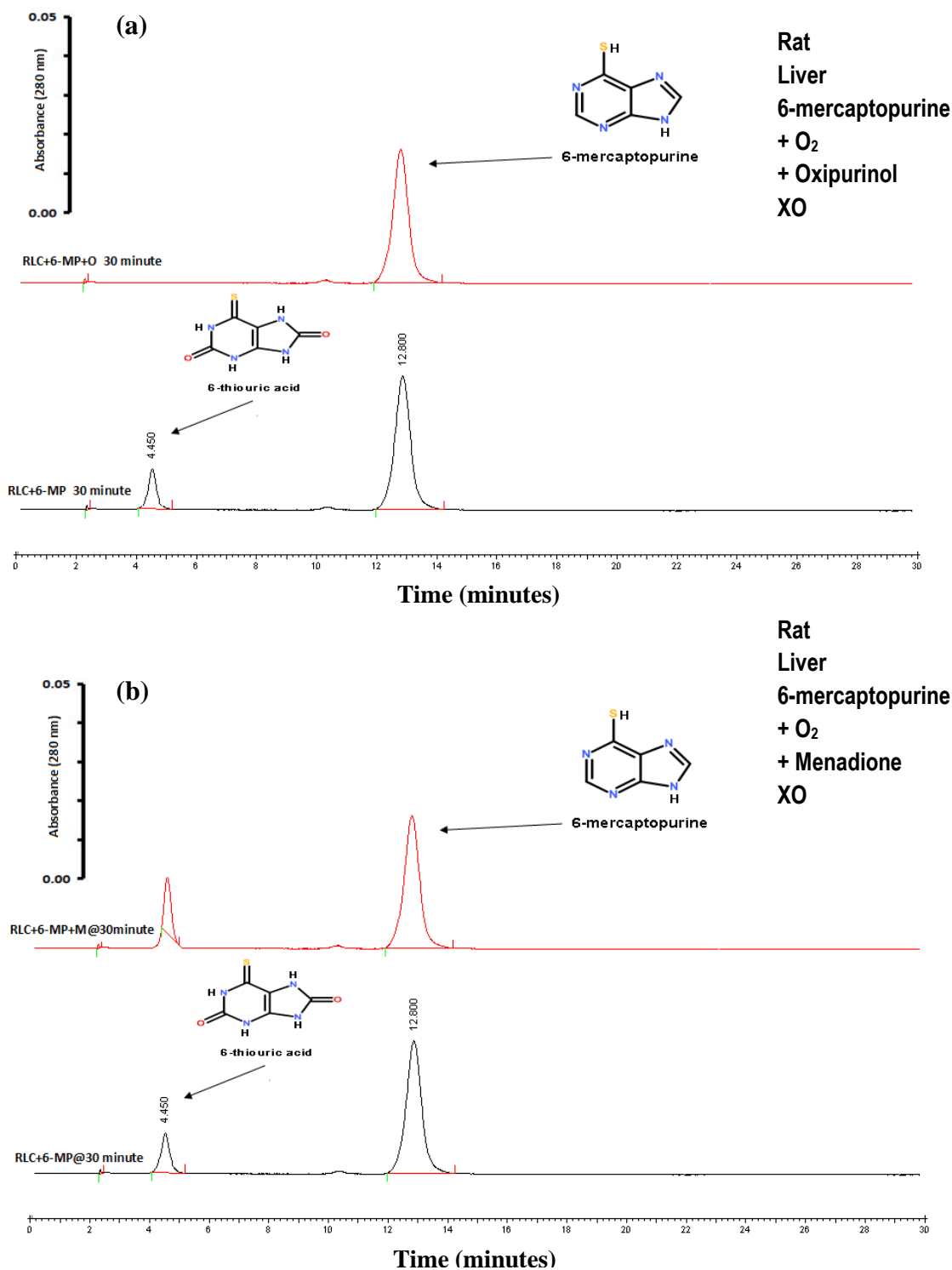
Figure 64: HPLC analysis of the *in vitro* biotransformation of 6-mercaptopurine by Wistar rat liver cytosol with and without enzyme inhibitors. HPLC chromatogram for incubation of Wistar rat with 6-MP and (a) oxipurinol, (b) menadione. Red lines with inhibitors and black lines without inhibitors. The amount of inhibitor added to incubation its 100μM. Times at the left hand side of the chromatograms indicate incubation times. HPLC chromatograms are offset on the vertical axis to allow comparison between different incubation times. Analytes were injected onto a C-18 column (Kromasil 5 μm) and eluted with a 0.1% v/v glacial acetic acid: acetonitrile gradient system as described in section 2.5.3 as mobile phase. The wavelength of the detection was 280 nm.

141
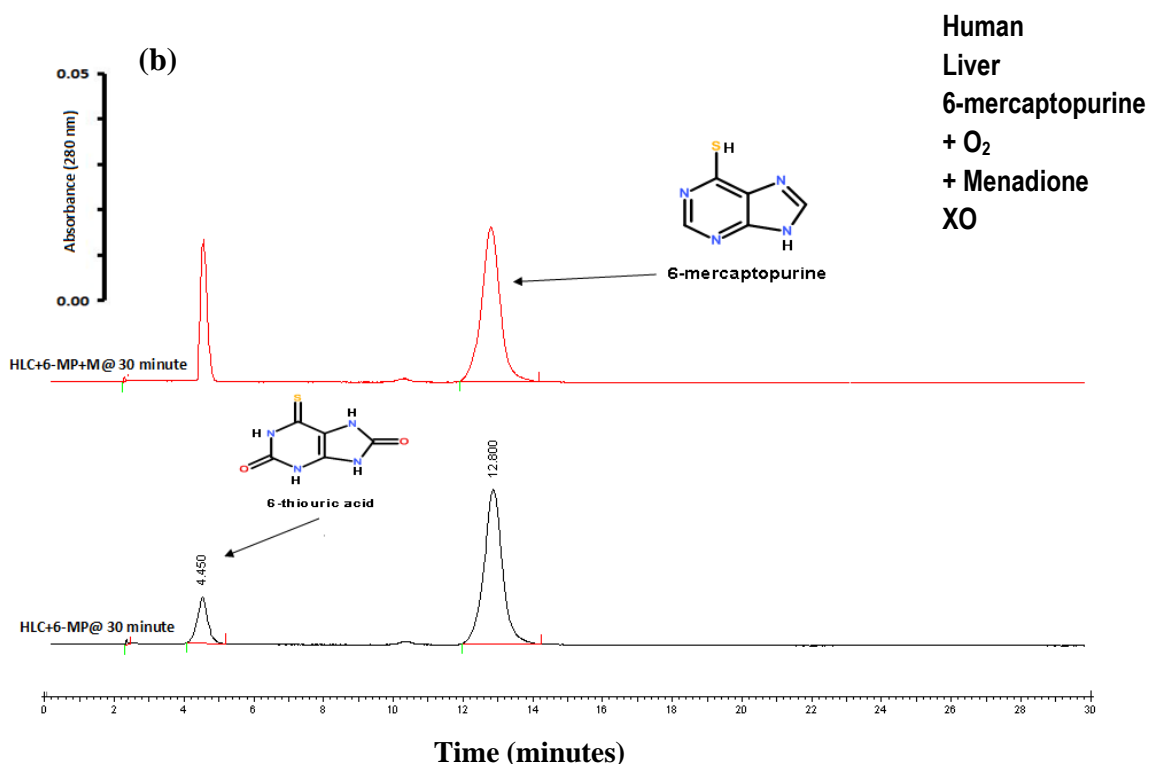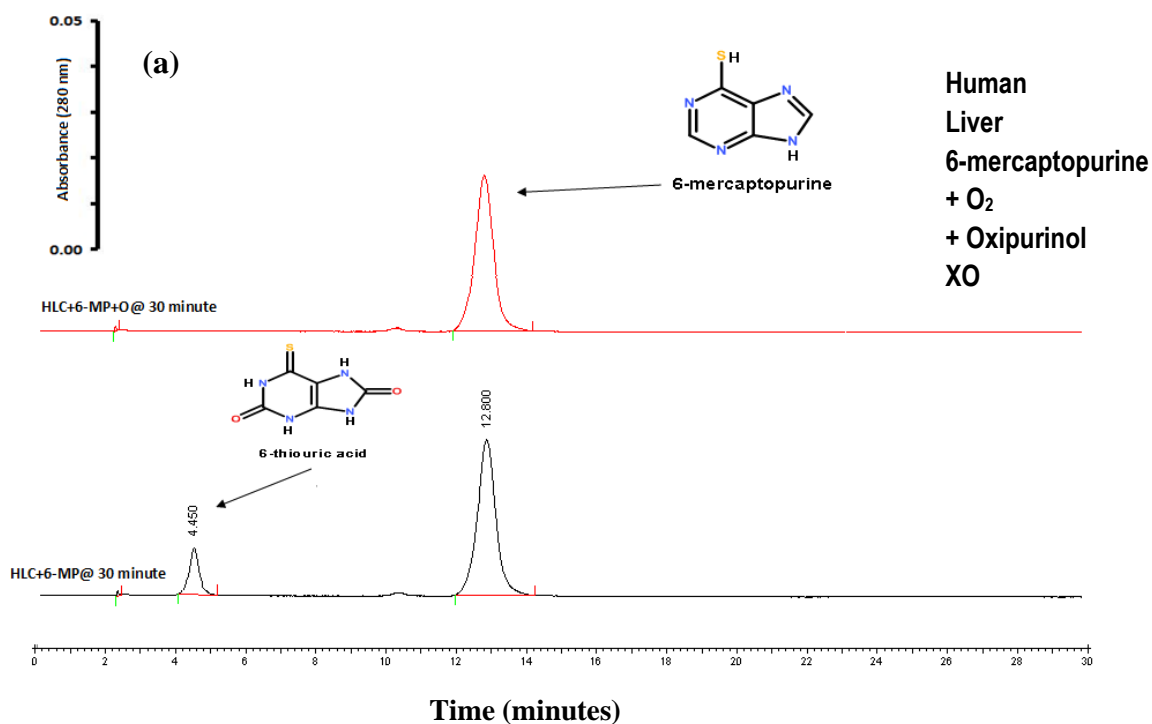
Figure 65: HPLC analysis of the *in vitro* biotransformation of 6-mercaptopurine by human liver cytosol with and without enzyme inhibitors. Human liver with 6-MP and (a) oxipurinol, (b) menadione. Red lines with inhibitors and black lines without inhibitors. The amount of inhibitor added to incubation its 100μM. Times at the left hand side of the chromatograms indicate incubation times. HPLC chromatograms are offset on the vertical axis to allow comparison between different incubation times. Analytes were injected onto a C-18 column (Kromasil 5 μm) and eluted with a 0.1% v/v glacial acetic acid: acetonitrile gradient system as described in section 2.5.3 as mobile phase. The wavelength of the detection was 280 nm.
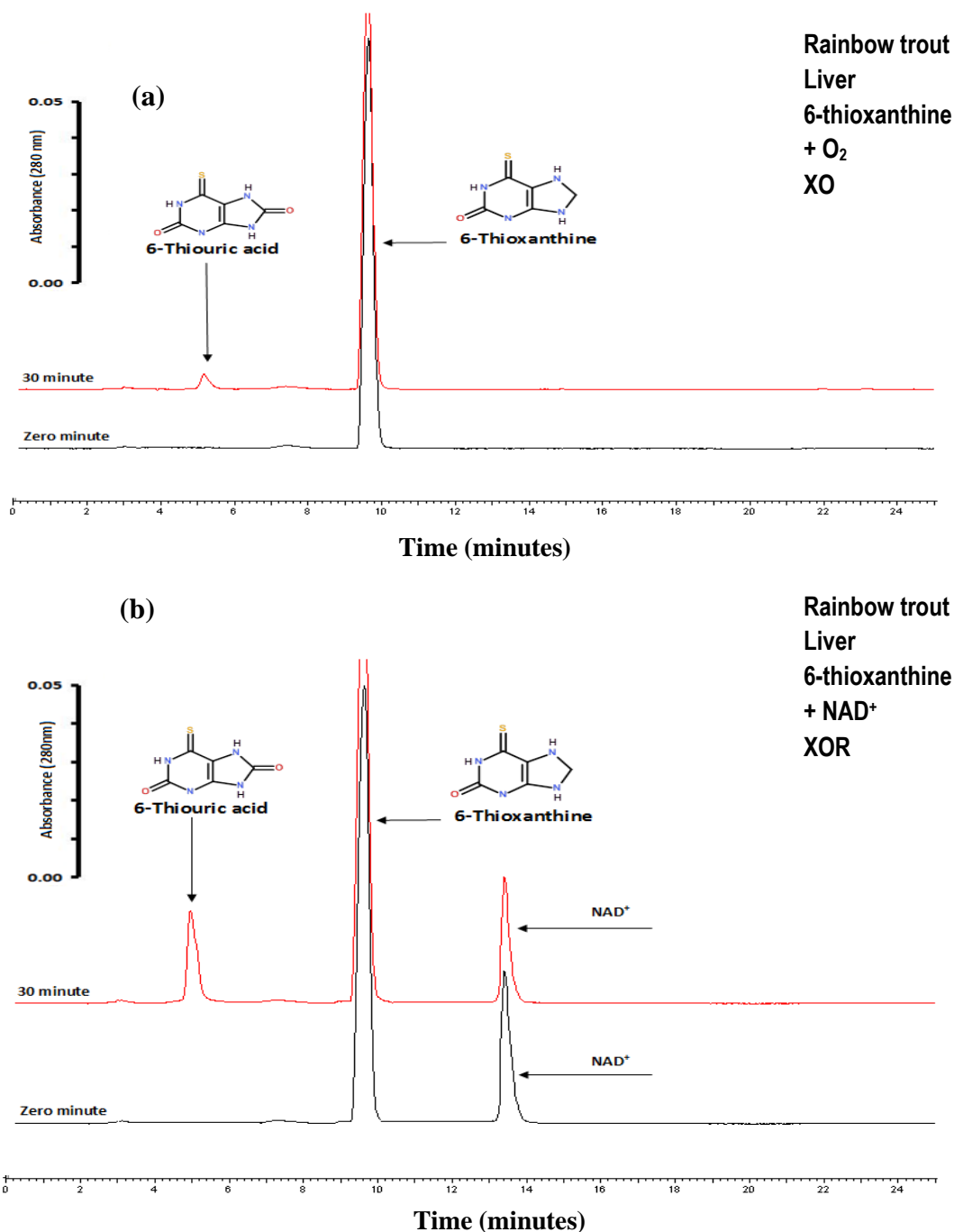
Figure 66: HPLC analysis of the *in vitro* biotransformation of 6-thioxanthine by rainbow trout liver cytosol at 37°C. HPLC chromatograms (a) generated by rainbow trout liver cytosol with 6-thioxanthine and O_2 as electron acceptor. HPLC chromatograms (b) generated by Trout liver cytosol with 6-thioxanthine and NAD^+ as electron acceptor. Times at the left hand side of the chromatograms indicate incubation times. HPLC chromatograms are offset on the vertical axis to allow comparison between different incubation times .Analytes were injected onto a C-18 column (Kromasil 5 μm) and eluted with a 0.1% v/v glacial acetic acid: acetonitrile gradient system as described in section 2.5.3 as mobile phase. The wavelength of the detection was 280 nm.
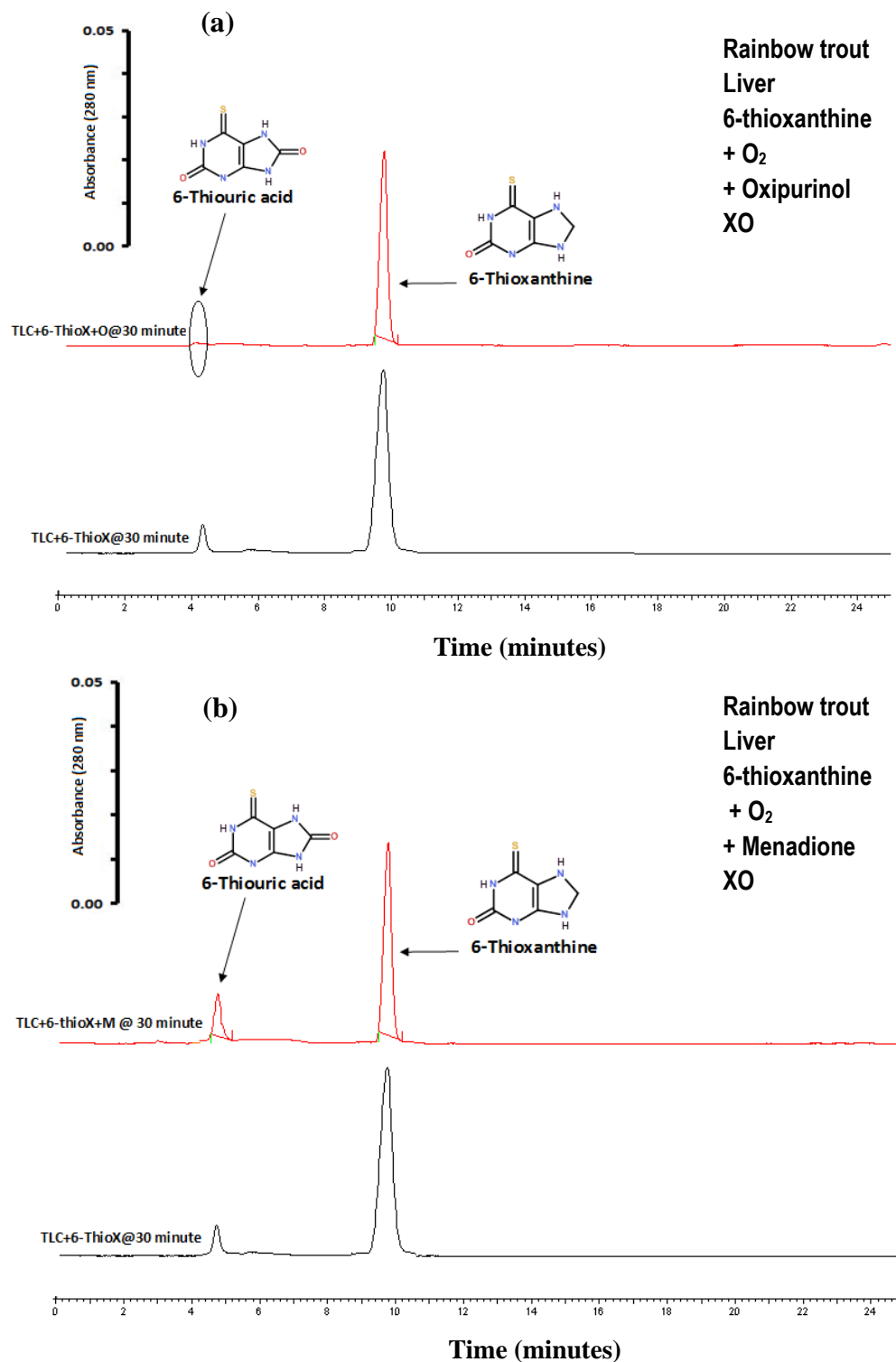
Figure 67: HPLC analysis of the *in vitro* biotransformation of 6-thioxanthine by rainbow trout liver cytosol with and without enzyme inhibitors. The chromatogram of rainbow trout with 6-thioxanthine and (a) oxipurinol, (b) menadione. Red lines with inhibitors and black lines without inhibitors. Times at the left hand side of the chromatograms indicate incubation times. The amount of inhibitor added to incubation its 100μM. HPLC chromatograms are offset on the vertical axis to allow comparison between different incubation times. Analytes were injected onto a C-18 column (Kromasil 5 μm) and eluted with a 0.1% v/v glacial acetic acid: acetonitrile gradient system as described in section 2.5.3 as mobile phase. The wavelength of the detection was 280 nm.

3.3.4. Allopurinol.

When liver cytosol from rainbow trout, Wistar rat and human were incubated with hyperuricemia drug allopurinol the two mammalian species exhibited activity with both the O_2 and NAD^+ as electron acceptor indicative of both oxidase and dehydrogenase activity (Figures 68 and 69). In contrast the piscine XOR enzyme was only active as a dehydrogenase as no activity was present even after prolonged incubation times without NAD^+ figure 71.
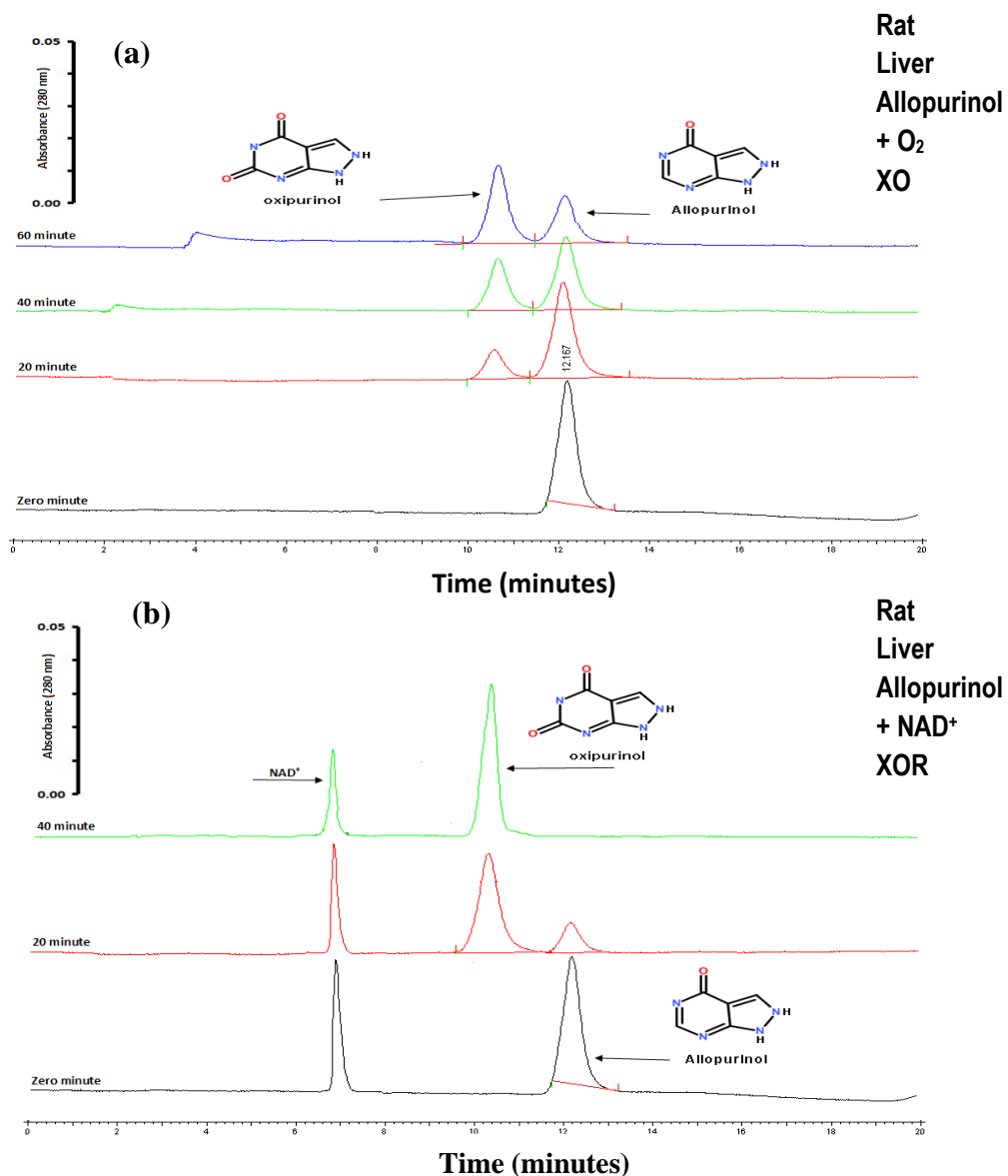
Figure 68: HPLC analysis of the *in vitro* biotransformation of allopurinol to oxipurinol by Wistar rat liver cytosol at 37°C. (a) HPLC chromatograms of incubation of Wistar rat and allopurinol with O_2 as an electron acceptor. (b) HPLC chromatograms of incubation of Wistar rat and allopurinol with NAD^+ as an electron acceptor. Times at the left hand side of the chromatograms indicate incubation times. HPLC chromatograms are offset on the vertical axis to allow comparison between different incubation times. Analytes were injected onto a C-18 column (Kromasil 5 μm) and eluted with a 0.1% v/v glacial acetic acid: acetonitrile gradient as described in section 2.5.3 as mobile phase. The wavelength of the detection was 280 nm.

145
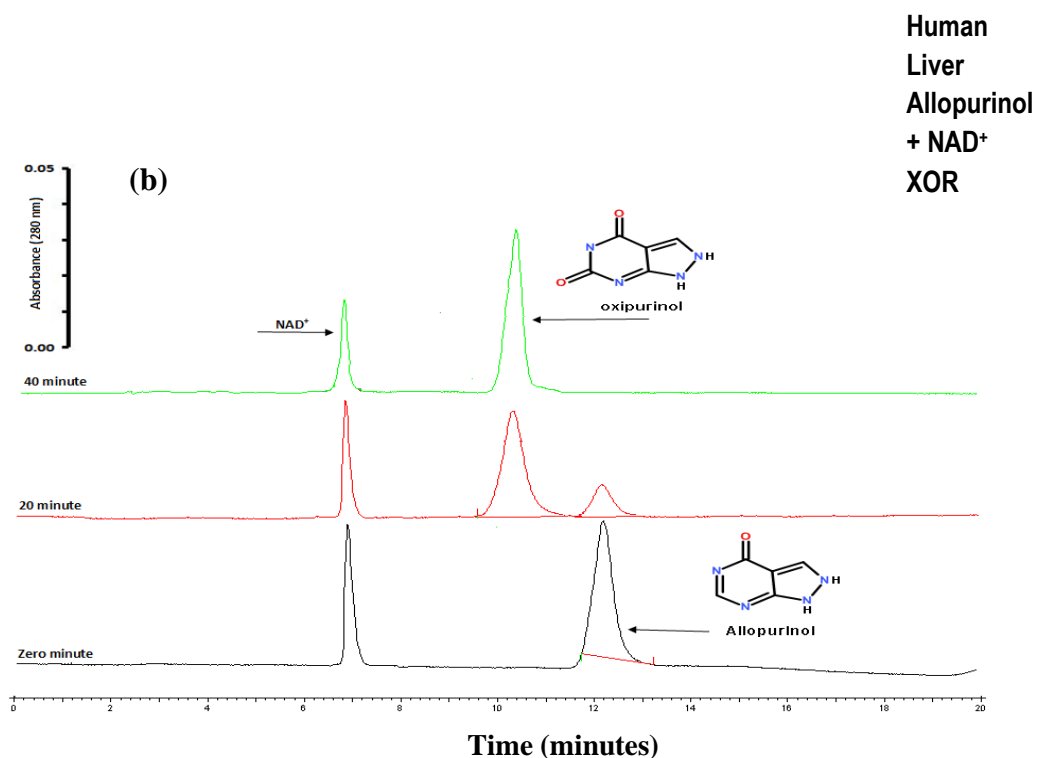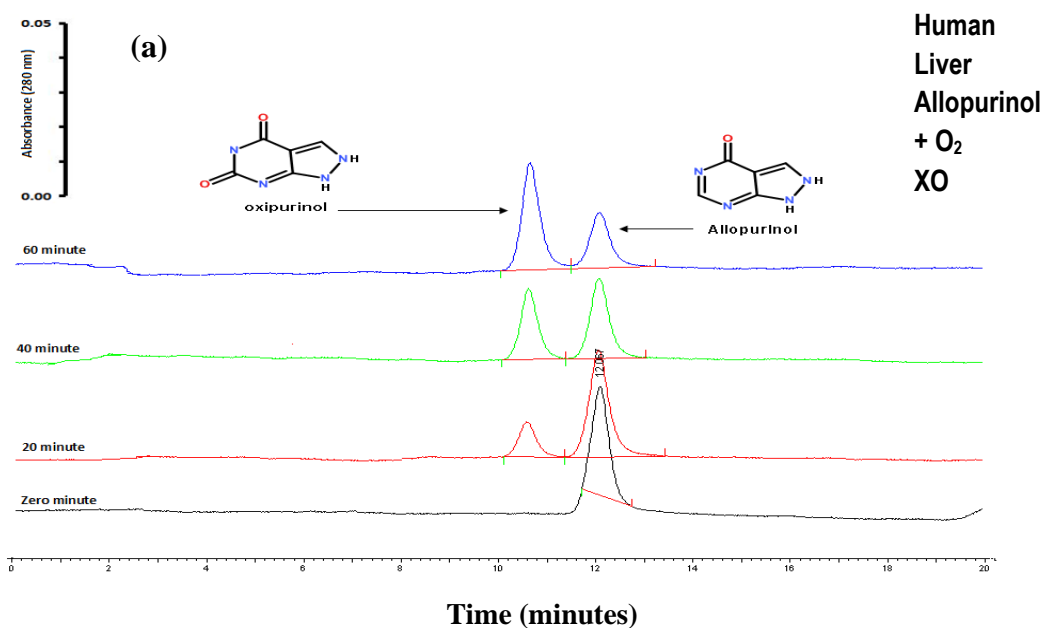
Figure 69: HPLC analysis of the *in vitro* biotransformation of allopurinol by human liver cytosol at 37°C. (a) HPLC chromatograms of incubation of human and allopurinol with O_2 as an electron acceptor. (b) HPLC chromatograms of incubation of human and allopurinol with NAD^+ as an electron acceptor. Times at the left hand side of the chromatograms indicate incubation times. HPLC chromatograms are offset on the vertical axis to allow comparison between different incubation times. Analytes were injected onto a C-18 column (Kromasil 5 μm) and eluted with a 0.1% v/v glacial acetic acid: acetonitrile gradient as described in section 2.5.3 as mobile phase. The wavelength of the detection was 280 nm.
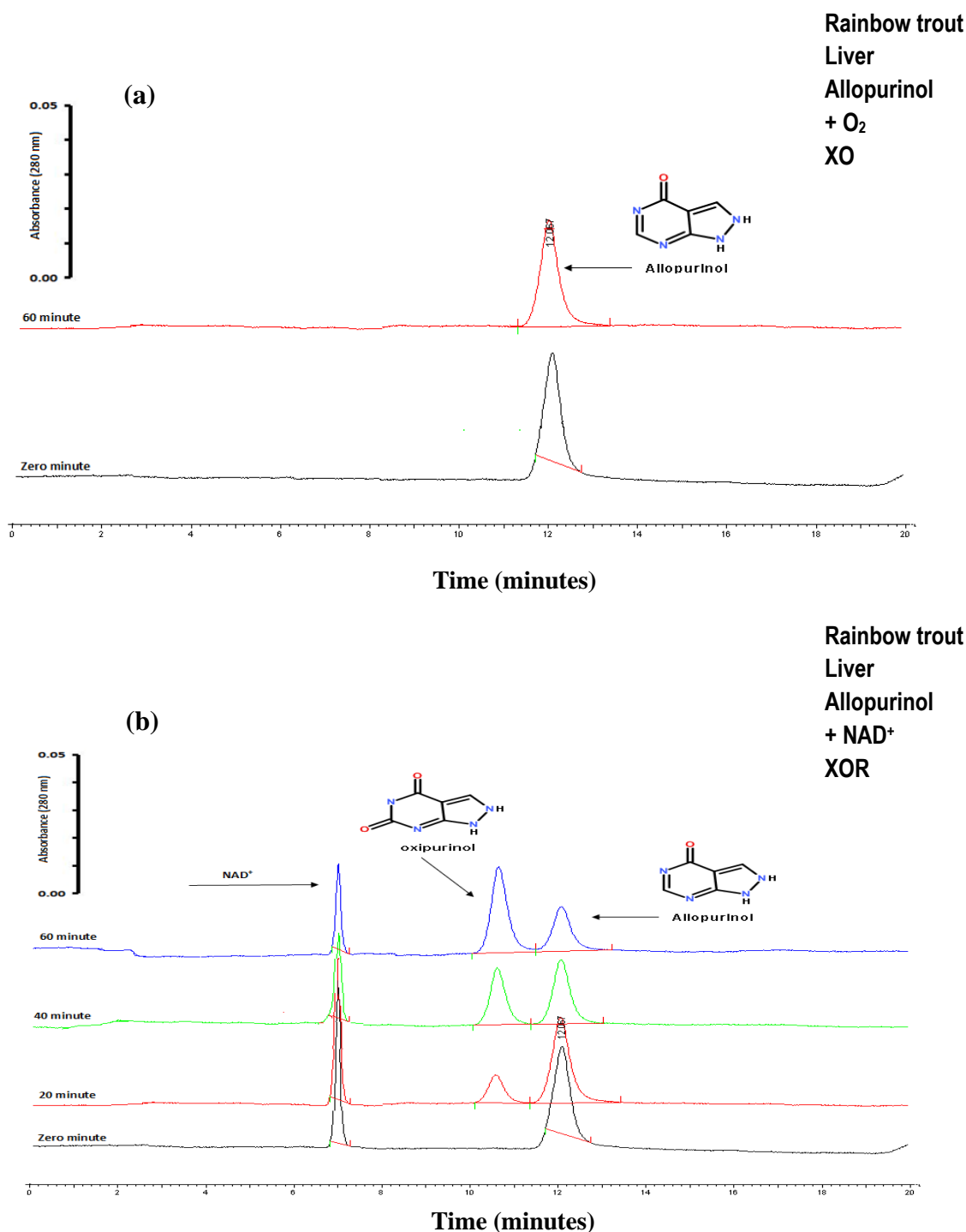
Figure 70: HPLC analysis of the *in vitro* biotransformation of allopurinol by rainbow trout liver cytosol at 37°C. (a) HPLC chromatograms of analytes from incubation of rainbow trout with allopurinol using O_2 as an electron acceptor. (b) HPLC chromatograms from analytes from incubation of rainbow trout and allopurinol with NAD^+ as an electron acceptor. Times at the left hand side of the chromatograms indicate incubation times. HPLC chromatograms are offset on the vertical axis to allow comparison between different incubation times. Analytes were injected onto a C-18 column (Kromasil 5 μm) and eluted with a 0.1% v/v glacial acetic acid: acetonitrile gradient as described in section 2.5.3 as mobile phase. The wavelength of the detection was 280 nm.

147

3.4. Determination of the kinetic parameters for aldehyde oxidase and xanthine oxidoreductase in trout, rat and human

Km and Vmax were calculated for the oxidation of exogenous aldehydes, endogenous vitamin and purines and exogenous N-heterocycles as substrates for AOX and XOR as described in methods section 2.8. Mean values of Km, Vmax and substrate efficiency (Ks = Vmax/Km) of AOX and XOR were determined using Eadie-Hofstee plots that gave good correlation coefficients $(r^2) > 0.97$ Appendix 3 (Figures 6 – 25). The advantage of this linearization method is that it tends to distribute the points more evenly so that it gives equal weight to data points in any range of substrate concentration or reaction rate.

3.4.1. Exogenous aldehydes as substrates for AOX

The Km and Vmax were calculated for two exogenous aromatic aldehyde compounds, vanillin and dimethylaminocinnamaldehyde (DMAC) by AOX.

The results obtained in the present study shows that DMAC and vanillin were good substrates of trout AOX. The enzyme kinetic parameters for AOX for all species are listed in table 38. K_m values for DMAC and vanillin were 21.5 ± 1.05 μM and 53.2 ± 2.1 μM respectively for trout liver cytosols. V_{max} values obtained 0.69 ± 0.13 nmol/min/mg protein and 1.51 ± 0.18 nmol/min/mg protein respectively. The K_m values for DMAC in trout were approximately 4 and 7-fold higher than that in rat and human. The K_m value of vanillin in the trout was approximately 5 and 10-fold higher compared with that in rat and human respectively in spectrophotometric assay and Vmax value was similar for both mammalian species. The substrate efficiency (Ks) value of DMAC and vanillin in the trout was lower compared with that in rat and human respectively see Appendix3(figures 6 - 25) (Table 39).

Table 39: Kinetic constants for trout, rat and human liver AOX substrates in spectrophotometric and HPLC assays

Species	Substrates	K_m^{**} (μM)	V_{max} (nmol/min/mg protein)	$K_s = (V_{max}/K_m)$ (ml/min/mg protein)
Rainbow trout	DMAC	21.5 ± 1.05^a	0.69 ± 0.13^a	0.032
	Vanillin	53.2 ± 2.11^a	1.51 ± 0.18^a	0.028
	Vanillin	54.2 ± 0.64	1.89 ± 0.27	0.035
	Pyridoxal	121.9 ± 3.69	1.41 ± 0.69	0.012
	All-trans retinal	124.7 ± 2.27	2.22 ± 0.62	0.017
	N^1-methylnicotinamide	273.9 ± 2.89	1.63 ± 1.33	0.006
	Phenanthridine	55.0 ± 1.63	1.78 ± 0.55	0.032
	Phthalazine	61.2 ± 1.41	2.02 ± 0.46	0.033
	Cinchonine	174.7 ± 2.55	1.63 ± 1.33	0.009
Wistar rat	DMAC	5.4 ± 1.62^a	2.24 ± 0.07^a	0.415*
	Vanillin	9.7 ± 1.56^a	3.77 ± 0.21^a	0.388
	Vanillin	$10.2 \pm 0.55^*$	5.97 ± 0.05	0.585*
	Pyridoxal	46.4 ± 2.51	6.28 ± 0.59	0.135
	All-trans retinal	30.9 ± 1.23	5.16 ± 0.56	0.166
	N^1-methylnicotinamide	156.2 ± 3.68	$5.92 \pm 0.68^*$	0.037
	Phenanthridine	$5.60 \pm 0.65^*$	2.43 ± 0.14	0.433*
	Phthalazine	10.5 ± 0.55	5.79 ± 0.08	0.551
	Cinchonine	37.3 ± 1.99	4.53 ± 0.52	0.121
Human	DMAC	3.4 ± 1.21^a	3.14 ± 0.07^a	0.923
	Vanillin	5.5 ± 1.83^a	4.65 ± 0.10^a	0.845
	Vanillin	8.1 ± 0.36	$6.29 \pm 0.04^*$	0.776*
	Pyridoxal	$34.1 \pm 1.97^*$	9.16 ± 0.56	0.268
	All-trans retinal	12.6 ± 0.58	8.32 ± 0.06	0.660*
	N^1-methylnicotinamide	139.5 ± 2.86	6.69 ± 0.74	0.047
	Phenanthridine	3.2 ± 0.23^a	4.16 ± 0.14^a	1.300
	Phthalazine	$9.8 \pm 0.59^*$	$9.43 \pm 0.07^*$	0.962*
	Cinchonine	43.8 ± 1.62	8.69 ± 0.53	0.198

Values shown are the mean ± S.D. The typical results are from three independent experiments. (*$P < 0.05$ one way ANOVA are marked with asterisks) compared with the rainbow trout, **n = 3. (a)-Spectrophotometric assays,

3.4.2. Endogenous vitamin aldehydes as substrates for AOX

Two endogenous vitamin aldehydes, pyridoxal (vitamin B6), all-trans retinal (vitamin A) and N^1-methylnicotinamide (NMN) (a vitamin B3 metabolite) were used as AOX substrates. The Km value of endogenous vitamin was measured using an HPLC assays with trout, rat and human liver cytosols, Km, Vmax and Ks values are summarized in (Table 39).

3.4.2.1. Vitamin B6 (pyridoxal)

The Km value of trout AOX with pyridoxal its 121.9 ± 3.6 µM was approximately 3-fold more than that for mammalian AOX with Wistar rat and human of 46.4 ± 0.55 µM and 34.1 ± 1.97 µM respectively (Table 39). The Vmax value of trout AOX with pyridoxal found to be 1.41 ± 0.69 nmol/min/mg protein and was approximately 6 and 9-fold lower than that Wistar rat and human respectively. The substrate efficiency (Ks) value of trout AOX was lower compared than that of human and rat respectively (Table 39).

3.4.2.2. Vitamin A (all-trans retinal)

The Km value of trout AOX with all-trans retinal was 124.7 ± 2.27 µM was approximately 4-fold greater than that measured with Wistar rat with all-trans retinal and ~ 10 fold more than that of human AOX (Table 39). The Vmax value of trout AOX with all-trans retinal was 2.22 ± 0.62 nmol/min/mg protein and was approximately 3 and 4-fold lower than that Wistar rat and human respectively. The substrate efficiency (Ks) value of trout with all-trans retinal was lower than that of rat and human respectively (Table 39).

3.4.2.3. N^{1}-methylnicotinamide

The Km value of N^{1}-methylnicotinamide was measured and it was found to be 273.9 ± 2.89 µM with trout AOX, 156.2 ± 3.68 µM with Wistar rat AOX and 139.5 ± 2.86 µM with human AOX. The activity of trout AOX with N^{1}-methylnicotinamide approximately 1.5-fold more than that of mammalian AOX with N^{1}-methylnicotinamide table 38. The Vmax value of Wistar rat and human with N^{1}-methylnicotinamide was approximately 5 and 6-foldgreaterrespectivelythan the piscine AOX. The substrate efficiency (Ks) value of trout AOX with N^{1}-methylnicotinamide was lower than that both mammalian species (Table 39).

3.4.3. Exogenous N-heterocycles as substrates for AOX

The Km, Vmax and Ks values were calculated for three exogenous NPAHs that are environmental pollutants (phenanthridine, phthalazine and cinchonine) are shown in (Table 39).

3.4.3.1. Phenanthridine

Phenanthridine oxidation by trout cytosol was below detection limits of the spectrophotometric assay at all substrate concentrations used. However the activity was measurable with a sensitive HPLC assay. The Km value of exogenous N-heterocyclic phenanthridine with trout it was 55.0 ± 1.63µM. On other hand, the Km value of mammalian enzyme Wistar rat and human with exogenous N-heterocyclic phenanthridine were 5.60 ± 0.65 µM, 3.20 ± 0.23 µM respectively (Table 39). The Km of the piscine AOX with phenanthridine was approximately 10 times greater than that with mammalian AOX. The Vmax value of Wistar rat and human with phenanthridine was approximately 2 and 4 times respectively more than that with trout AOX. The substrate efficiency (Ks) value of Wistar rat and human with phenanthridine was greater than that with trout AOX (Table 39).

3.4.3.2. Phthalazine

The Km value of exogenous N-heterocyclic phthalazine with trout it was 61.2 ± 1.41 µM. On other hand, the Km value of mammalian enzyme Wistar rat and human with exogenous N-heterocyclic phthalazine was 10.50 ± 0.55 µM and 9.8 ± 0.59 µM (Table 39). The Km of the piscine AOX with exogenous N-heterocyclic phthalazine was approximately 6 times higher than that with rat and human AOX activity. The Vmax value of trout AOX with phthalazine found to be 2.02 ± 0.46 nmol/min/mg protein and was approximately 2 and 4 times lower than that Wistar rat and human respectively. The substrate efficiency (Ks) value of trout AOX with phthalazine was lower compared with Wistar rat and human respectively (Table 39).

3.4.3.3. Cinchonine

The Km value of exogenous N-heterocyclic cinchonine with rainbow trout AOX approximately 4-fold higher than that two mammalian AOX with cinchonine (Table 39). The Vmax value of Wistar rat and human with cinchonine was approximately 4 and 8-fold greater than that trout AOX. The substrate efficiency (Ks) value of human AOX was greater compared than that Wistar rat and trout respectively (Table 39).

3.4.4. Endogenous and exogenous purines and purine analogs as substrates for XOR

The Km, Vmax and Ks values of purines and purine analogs were measured using spectrophotometric and HPLC assays with rainbow trout, Wistar rat and human as in (Table 40).

3.4.4.1. Xanthine.

The Km value for O_2-dependent xanthine oxidase assay for human was approximately 2-fold lower than that of rat in spectrophotometer and HPLC assay (Table 40). The Km value of NAD-dependent xanthine dehydrogenase with trout in spectrophotometric assay was 2-fold and 3-fold higher than that Wistar rat and human respectively (Table 40). The Km value of NAD-dependant xanthine dehydrogenase with trout in HPLC assay were 3 times higher than that with Wistar rat and human (Table 40). The NAD-dependant Vmax value for xanthine dehydrogenase with Wistar rat and human was approximately 5 and 7-fold greater than that O_2-dependant respectively (Table 40). The substrate efficiency (Ks) value of NAD-dependent xanthine dehydrogenase with trout in spectrophotometer was lower compared with that in Wistar rat and human respectively (Table 40).

3.4.4.2. 1-methylxanthine.

The NAD-dependent K_m value for 1-methylxanthine as an XDH substrate for trout was approximately 2-fold higher than that of other species as in (Table 40). The O_2-dependant Km value for 1-methylxanthine as substrate for both mammals was similar, and the NAD-dependant Vmax value for 1-methylxanthine dehydrogenase with Wistar rat and human was approximately 5 and 8-fold greater than the O_2-dependantactivity respectively (Table 40). The NAD-dependent substrate efficiency (Ks) value for 1-methylxanthine as an XDH substrate for trout was lower than that of

other species (Table 40). The O_2-dependant substrate specificity (Ks) value for 1-methylxanthine as substrate for human was greater compared with that Wistar rat (Table 40).

Table 40: Kinetic constants for trout, rat and human liver XOR substrates in spectrophotometric and HPLC assays

Species	Substrates	K_m^{**} (µM)	V_{max} (nmol/min/mg protein)	$Ks = V_{max} / K_m$ (ml/min/mg protein)
Rainbow trout	Xanthine+NAD$^+$	13.5 ± 1.9[a]	0.56 ± 0.15[a]	0.041
	Xanthine+NAD$^+$	15.8 ± 0.58	0.77 ± 0.03	0.048
	1-MX+NAD$^+$	17.6 ± 1.23[a]	0.52 ± 0.14[a]	0.029
	1-MX+NAD$^+$	18.2 ± 0.55	0.51 ± 0.05	0.028
	6-Thioxanthine + O$_2$	39.9 ± 0.85	1.67 ± 0.30	0.026
	6-Thioxanthine+NAD$^+$	30.9±1.52	5.01 ± 0.98	0.099
	Allopurinol +NAD$^+$	63.2 ± 0.98	0.56 ± 0.75	0.008
	Pyrazinamide + O$_2$	ND	ND	ND
	Pyrazinamide +NAD$^+$	209.5 ± 2.40	1.21 ± 0.74	0.005
Wistar rat	Xanthine	13.2 ± 1.7[a]	1.69 ± 0.11[a]	0.128
	Xanthine	9.2 ± 0.45	1.27±0.17	0.138
	Xanthine+NAD$^+$	5.5 ± 1.45[a]	4.27 ± 0.87[a]	0.776*
	Xanthine+NAD$^+$	6.4 ±0.81	5.17 ± 0.15*	0.807
	1-MX + O$_2$	10.7 ± 0.56*	1.01 ± 0.04	0.094
	1-MX+NAD$^+$	9.2 ± 0.62[a]	5.31 ± 0.10[a]	0.577*
	1-MX+NAD$^+$	8.2 ± 0.62	5.13 ± 0.95	0.625
	6-MP + O$_2$	29.1 ± 0.85	1.61 ± 0.06*	0.055
	6-MP+NAD$^+$	24.6±0.85*	3.68±0.45	0.149
	Allopurinol + O$_2$	20.9 ± 0.76	1.19 ± 0.08	0.056
	Allopurinol +NAD$^+$	15.30±1.05	3.53±0.27	0.230*
	Pyrazinamide + O$_2$	163.3 ± 1.46	1.30 ± 1.33*	0.007
	Pyrazinamide +NAD$^+$	92.2 ± 1.20*	4.25 ± 1.06	0.046
Human	Xanthine	3.0 ± 0.65[a]	1.41 ± 0.01[a]	0.470
	Xanthine	5.5 ± 0.50*	1.97±0.05	0.358
	Xanthine+NAD$^+$	1.9 ± 0.20[a]	5.48 ± 0.07[a]	2.884*
	Xanthine+NAD$^+$	2.4 ± 0.35	7.25 ± 0.17*	3.021*
	1-MX + O$_2$	7.0 ± 0.58*	1.02 ± 0.15	0.145
	1-MX+NAD$^+$	6.6 ± 1.05[a]	8.31 ± 0.96[a]	1.259*
	1-MX+NAD$^+$	5.7 ± 0.30	8.18 ± 0.85	1.435*
	6-MP + O$_2$	25.7 ± 0.51	1.73 ± 0.04*	0.067
	6-MP+NAD$^+$	20.80±0.41	6.62±0.64	0.318
	Allopurinol + O$_2$	16.7 ± 0.62*	1.73 ± 0.05	0.103
	Allopurinol+NAD$^+$	15±0.25	5.52± 1.07*	0.368*
	Pyrazinamide + O$_2$	153.1 ± 2.05	1.07 ± 0.37	0.006
	Pyrazinamide +NAD$^+$	90.7 ± 1.00	6.41 ± 0.94	0.070

The values shown are the mean ± S.D. The typical results are from three independent experiments. (*$P < 0.05$ one way ANOVA are marked with asterisks) compared with the rainbow trout, **n = 3. (a)-Spectrophotometric assays.

3.4.4.3. Allopurinol

The NAD-dependant Km values for allopurinol as an XDH substrate with trout was approximately 4-fold greater than that both mammalian species (Table 40). The O_2-dependant Km value for allopurinol as XO substrate with Wistar rat and human are similar as in (Table 40). The NAD-dependant Vmax value for allopurinol as XDH substrate with Wistar rat and human was approximately 3 and 5-fold more than that O_2-dependant Vmax value respectively (Table 40). The NAD-dependant substrate efficiency (Ks) values for allopurinol as an XDH substrate with trout was lower compared than that with Wistar rat and human respectively (Table 40). The O_2-dependant substrate efficiency (Ks) value for allopurinol as XO substrate with human was lower than that with Wistar rat (Table 40).

3.4.4.4. 6-mercaptopurine (6MP).

The NAD-dependant Km value for 6-MP as an XDH substrate with both mammalian are similar as in (Table 40).The NAD-dependant Vmax value for 6-MP with Wistar rat and human was approximately 3 and 6-fold greater than that O_2-dependant Vmax value (Table 40).The NAD and O_2- dependent substrate efficiency (Ks) value for 6-MP with Wistar rat was lower than that with human (Table 40).

3.4.4.4. 6-thioxanthine.

 The NAD-dependant Vmax value for 6-thioxanthine as an XOR substrate with trout was approximately 2-fold greater than that O_2-dependant Vmax value (Table 40). The O_2-dependant substrate efficiency (Ks) value for 6-thioxanthine as an XOR substrate with trout was lower than that with NAD-dependent (Table 40).Due to time constraints activities were not measured for the mammalian species.

3.4.3.4. Pyrazinamide

With the anti-tuberculosis drug pyrazinamide no activity was found with O_2 as an electron acceptor with rainbow trout cytosol. In contrast, pyrazinamide was biotransformed in the presence of O_2 with the both mammalian enzymes with Km values for both Wistar rat and human being similar as in (Table 40). When NAD^+ was used as an electron acceptor both Wistar rat and human had approximately 4 and 6-fold enhanced Vmax respectively and the trout cytosol had measurable NAD-dependent activity. The Km value for the trout enzyme was approximately 2-fold higher than two mammalian enzymes (Table 40). The NAD-dependent substrate efficiency (Ks) value of trout with pyrazinamide as XDH substrate was found to be lower compared with that Wistar rat and human respectively (Table 40). The O_2-dependent substrate efficiency (Ks) value for both mammalians with pyrazinamide as substrate was similar (Table 40).

3.5. Comparison of menadione, benzamidine and oxipurinol as molybdo-flavoenzyme inhibitors in different species.

Inhibition of AOX was determined with menadione and benzamidine, whereas inhibition of XOR was determined with oxipurinol (Figure 72). Enzyme activity was measured spectrophotometrically and inhibitor concentrations used were from 0.5 μM to 5 μM menadione and from 25μM to 100μM for benzamidine and oxipurinol respectively. As seen in (Figure 71a), the AOX inhibitor 5μM menadione strongly inhibited AOX in trout liver with approximately 80% inhibition, while with rat and human enzymes were inhibited ~ 90%. Another AOX inhibitor tested was benzamidine which has been shown to be an inhibitor of AOX in rabbit and rat (Stell *et al.*, 1989, Maia and Mira. 2002) and has been found to be a good affinity ligand for

the purification of AOXs in rabbit, rat, mouse, bovine and chicken (Tables 21 and 22). Benzamidine inhibition is pH dependent with higher pH giving stronger inhibition. Whereas 100µM benzamidine inhibited rat and human AOX ~ 80% at pH 7.4 and by ~ 90% for both rat and human at pH 9.0, in contrast 100µM benzamidine did not inhibit trout AOX either pH (Figures 71b and 71c). The XOR inhibitor oxipurinol at 100µM inhibited XDH in trout, rat and human liver cytosol with ~ 60%, ~ 92% and~ 95% inhibition respectively.

(a)

(b)

(c)
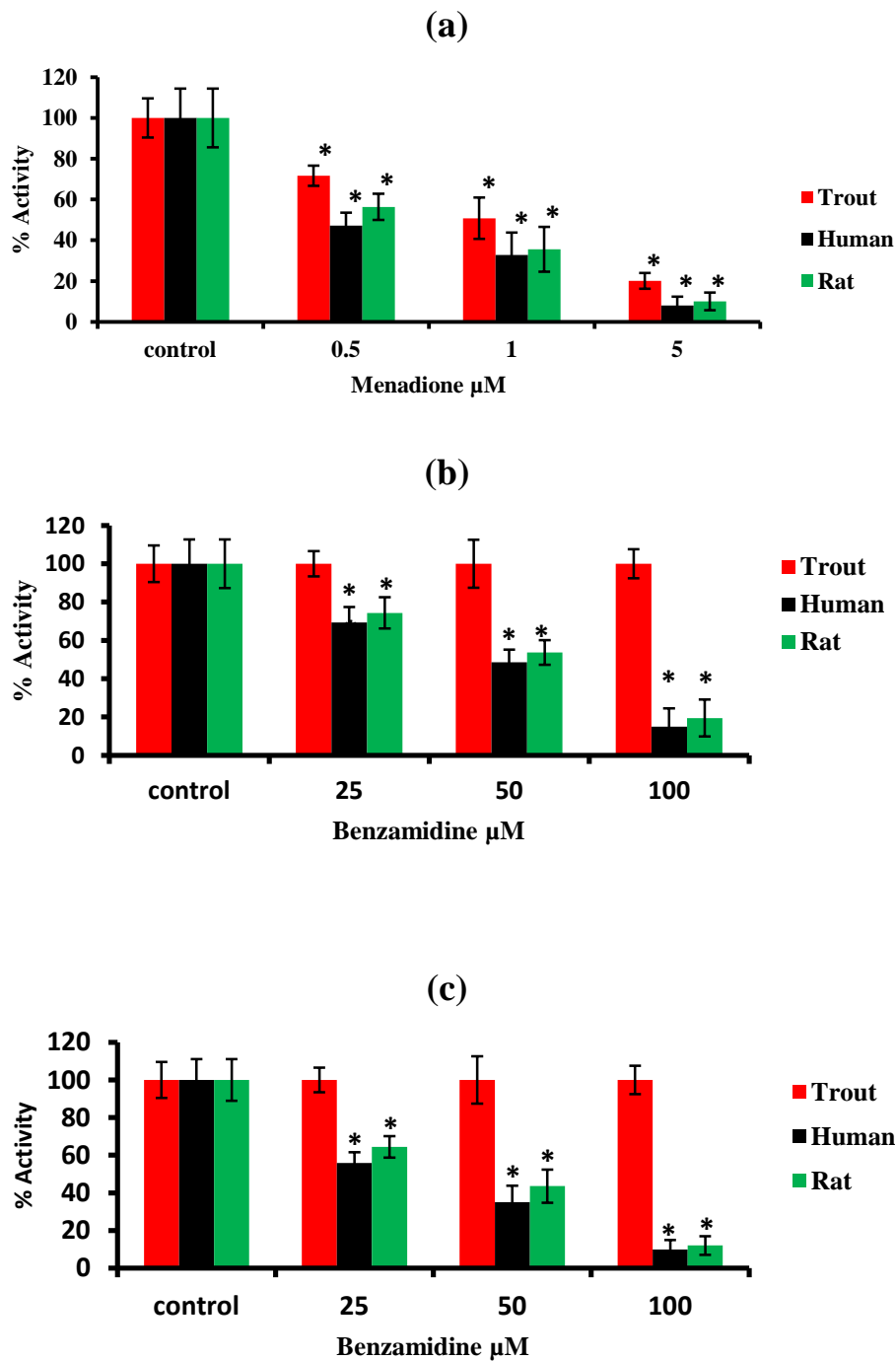
Figure 71: Inhibition of trout, human and rat aldehyde oxidase by menadione and benzamidine.

(a) Menadione (b) benzamidine at pH 7.4 (c) benzamidine at pH 9.0. AOX assays were carried out with 100μM DMAC final concentration. The bar graph shows the mean ± S.D. (*) signify a statistically significant difference (one way ANOVA p. ≤ 0.05) compared with the control. The typical results are from three independent experiments.

(a)

(b)
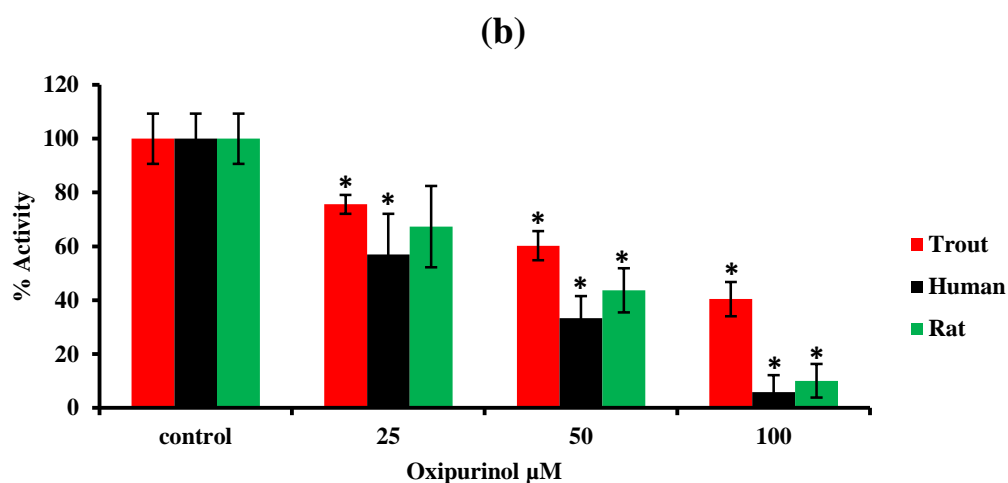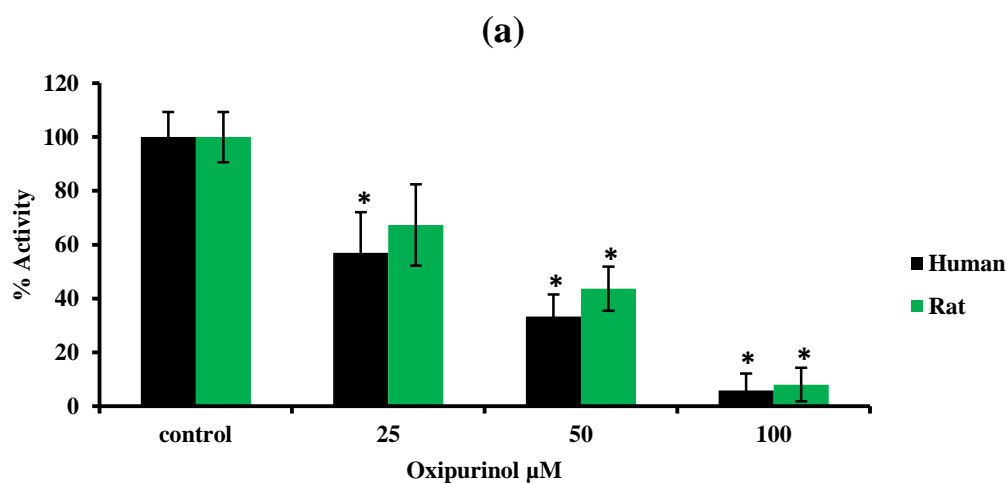
Figure 72: Inhibition of trout, human and rat xanthine oxidoreductase by oxipurinol at pH 7.4.

(a) oxipurinol. XO assays were carried out with 100µM xanthine final concentration (b) oxipurinol. XOR assays were carried out with 100µM xanthine final concentration and670µM NAD$^+$ final concentration as electron acceptor. The bar graph shows the mean ± S.D. (*) signify a statistically significant difference (one way ANOVA p. ≤ 0.05) compared with the control. The typical results are from three independent experiments.

3.5.1. Determination of Ki for molybdo-flavoenzyme inhibitors in trout liver cytosol.

In order to determine the Ki for AOX and XOR inhibitors with the trout liver molybdo-flavoenzymes a series of experiments were conducted with menadione, ethinyl estradiol, estradiol, chlorpromazine, phenanthridine and oxipurinol with $25\mu M$ to $100\mu M$ substrate concentration and $0.5\mu M$ to $5\mu M$ inhibitor concentration except oxipurinol concentration from $25\mu M$ to $100\mu M$. Lineweaver-Burk plots from this data were used to determine the inhibitor constant Ki. (Figures 73 to 84) show the effect of these inhibitors on trout liver AOX and XDH. (Table 41) summarises the inhibition constants (Ki) and mode of inhibition of different inhibitors with trout AOX and XDH.
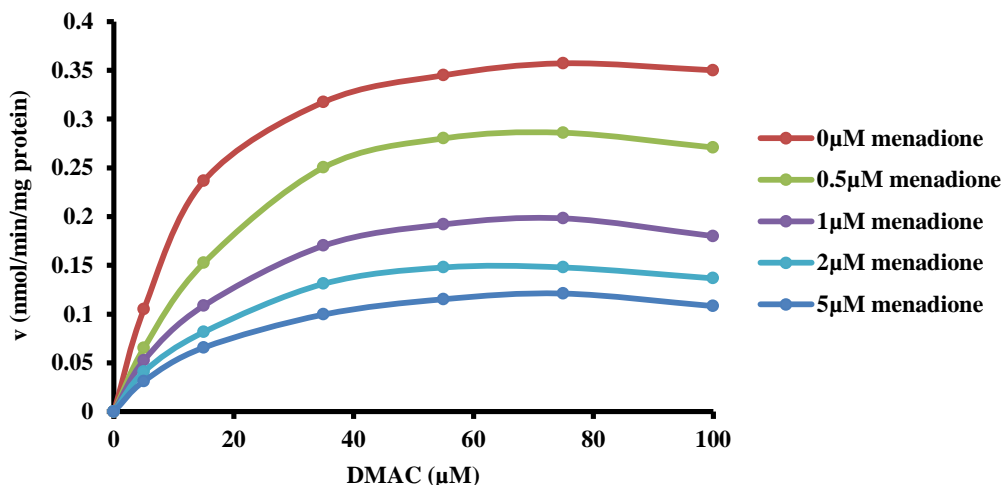
Figure 73: Saturation kinetics plot for menadione inhibition with DMAC as an AOX substrate in trout liver cytosol.

The concentration of DMAC as aldehyde oxidase substrate was varied from 25μM to 100μM and menadione concentration ranged from 0.5μM to 5μM. The typical results are from three independent experiments.
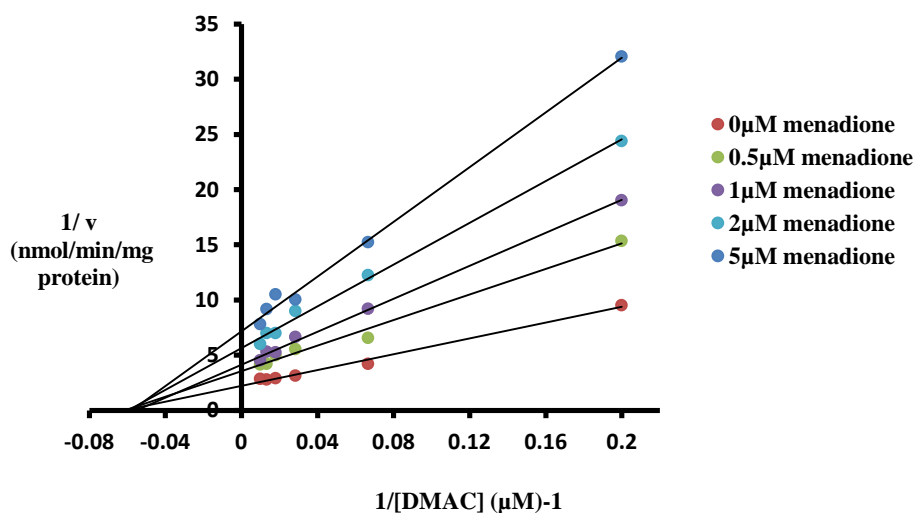
Figure 74: Lineweaver-Burk plot for menadione inhibition with DMAC as an AOX substrate in trout liver cytosol.

The concentration of DMAC as aldehyde oxidase substrate varied from 25μM to 100μM and menadione concentration ranged from 0.5μM to 5μM. The typical results are from three independent experiments.
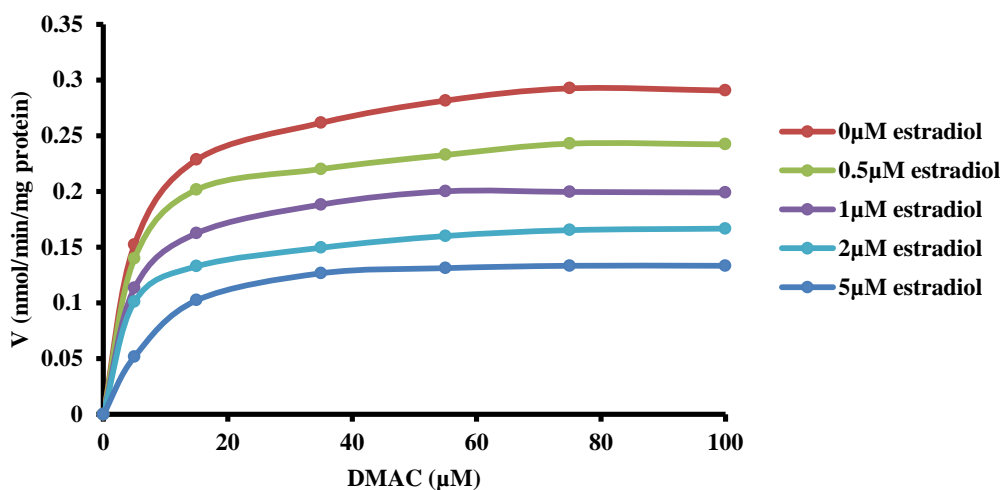
Figure 75: Saturation kinetics plot for estradiol inhibition with DMAC as an AOX substrate in trout liver cytosol.

The concentration of DMAC as aldehyde oxidase substrate was varied from 25μM to 100μM and estradiol concentration ranged from 0.5μM to 5μM. The typical results are from three independent experiments.
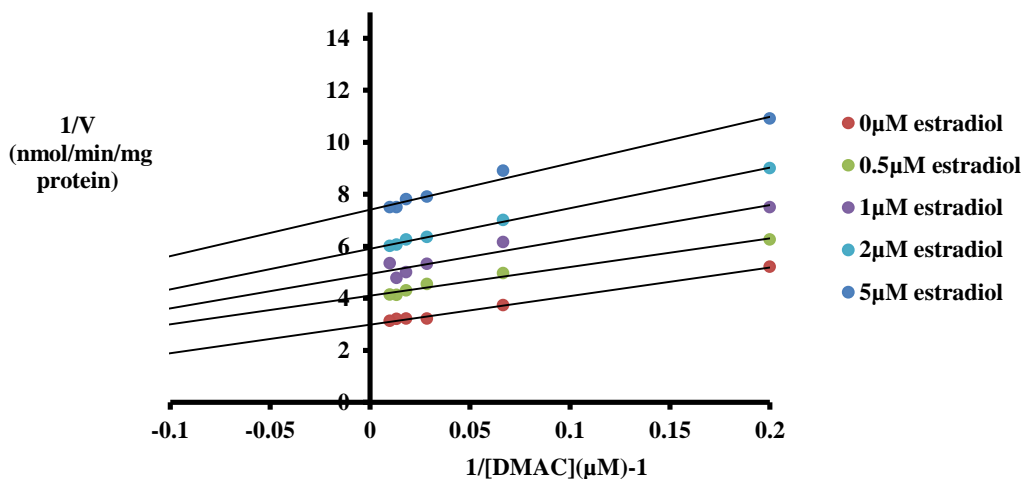
Figure 76: Lineweaver-Burk plot for estradiol inhibition with DMAC as an AOX substrate in trout liver cytosol.

The concentration of DMAC as aldehyde oxidase substrate was varied from 25μM to 100μM and estradiol concentration ranged from 0.5μM to 5μM. The typical results are from three independent experiments.

163
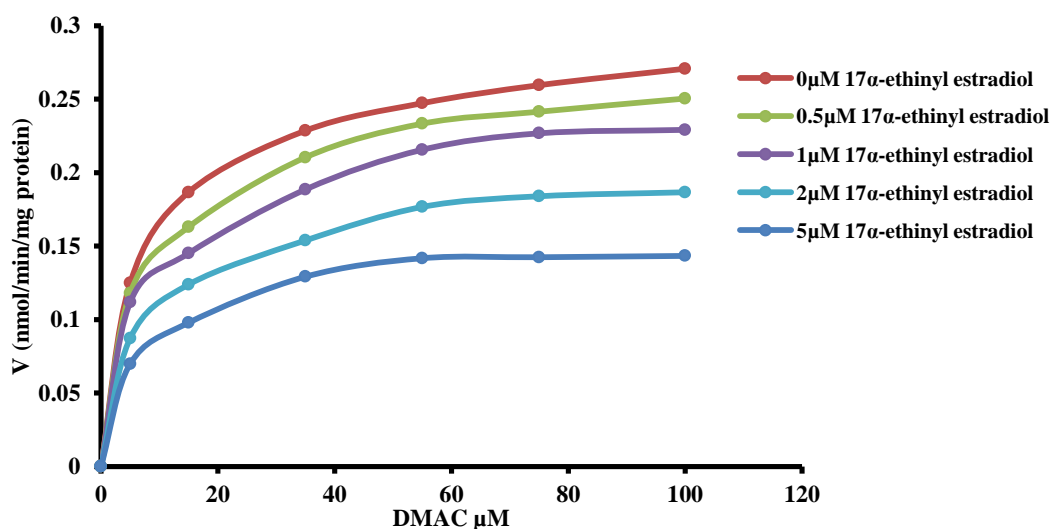
Figure 77: Saturation kinetics plot for 17α-ethinyl estradiol inhibition with DMAC as an AOX substrate in trout liver cytosol.

The concentration of DMAC as aldehyde oxidase substrate was varied from 25μM to 100μM and 17α-ethinyl estradiol concentration ranged from 0.5μM to 5μM. The typical results are from three independent experiments.
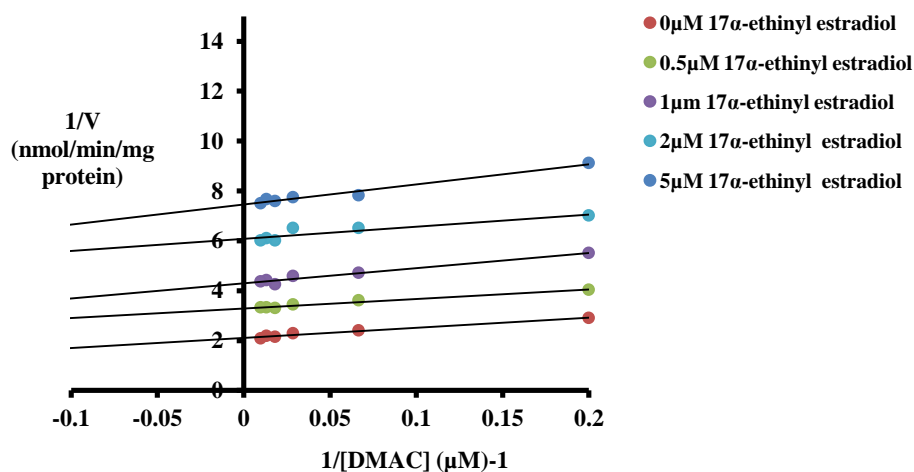
Figure 78: Lineweaver-Burk plot for 17α-ethinyl estradiol inhibition with DMAC as an AOX substrate in trout liver cytosol.

The concentration of DMAC as aldehyde oxidase substrate was varied from 25μM to 100μM and 17α-ethinyl estradiol concentration ranged from 0.5μM to 5μM. The typical results are from three independent experiments.

164
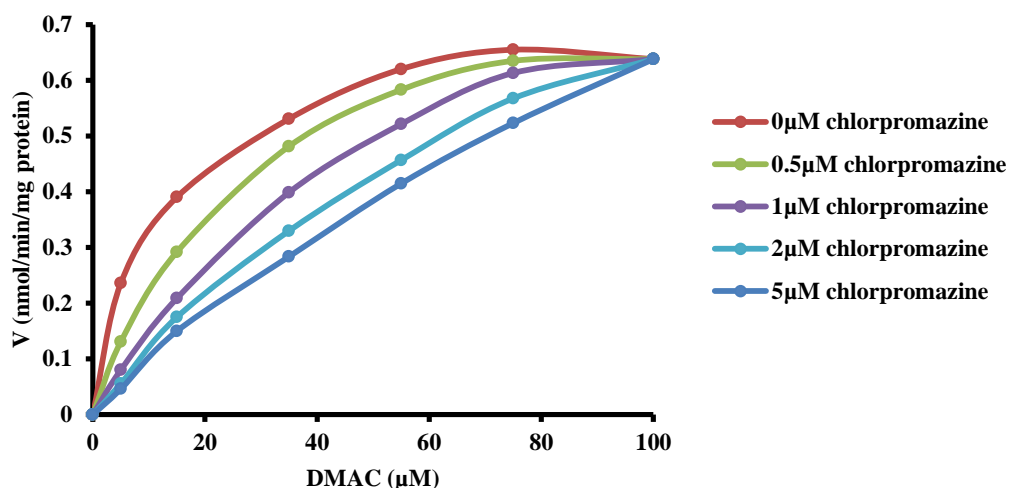
Figure 79: Saturation kinetics plot for chlorpromazine inhibition with DMAC as an AOX substrate in trout liver cytosol.

The concentration of DMAC as aldehyde oxidase substrate was varied from 25μM to 100μM and chlorpromazine concentration ranged from 0.5μM to 5μM. The typical results are from three independent experiments.
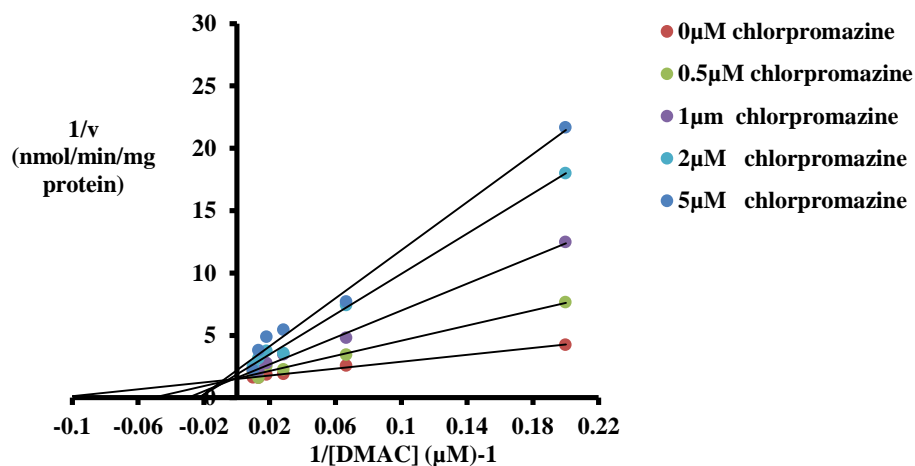
Figure 80: Lineweaver-Burk plot for chlorpromazine inhibition with DMAC as an AOX substrate in trout liver cytosol.

The concentration of DMAC as aldehyde oxidase substrate was varied from 25μM to 100μM and chlorpromazine concentration ranged from 0.5μM to 5μM. The typical results are from three independent experiments.
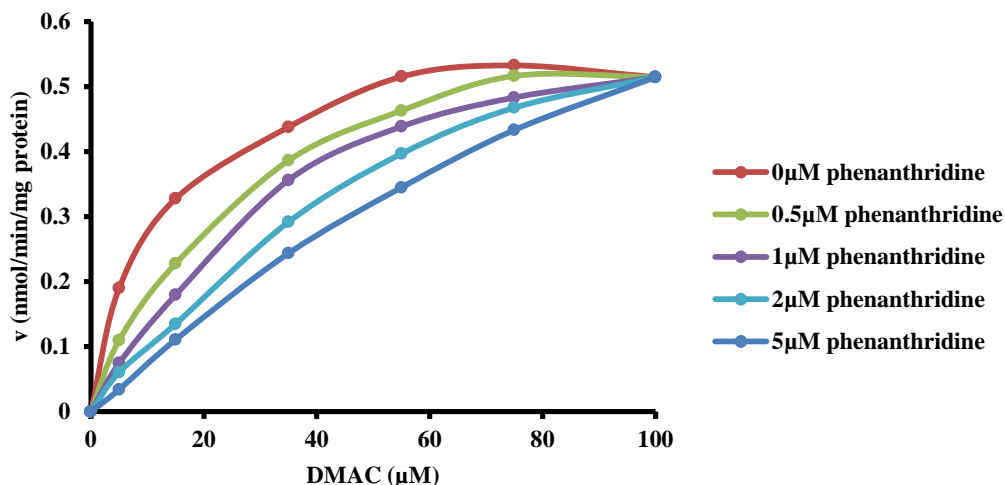
Figure 81: Saturation kinetics plot for phenanthridine inhibition with DMAC as an AOX substrate in trout liver cytosol.

The concentration of DMAC as aldehyde oxidase substrate was varied from 25μM to 100μM and phenanthridine concentration ranged from 0.5μM to 5μM. The typical results are from three independent experiments.
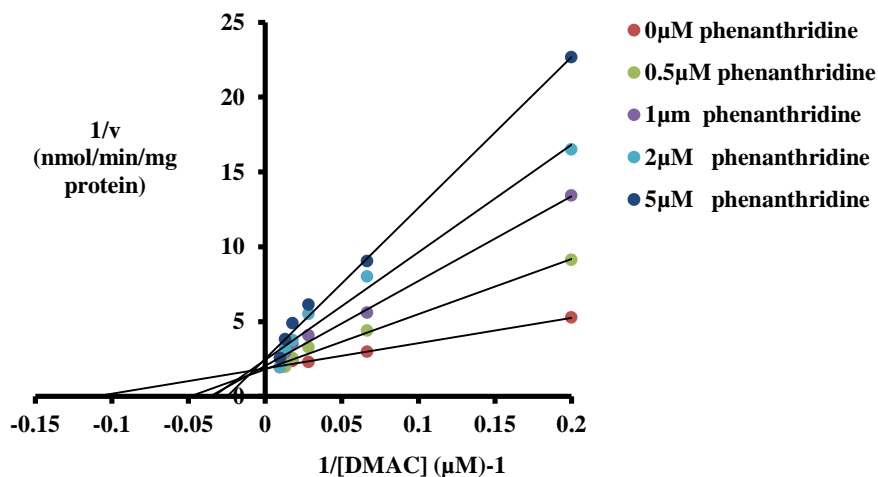
Figure 82: Lineweaver-Burk plot for phenanthridine inhibition with DMAC as an AOX substrate in trout liver cytosol.

The concentration of DMAC as aldehyde oxidase substrate was varied from 25μM to 100μM and phenanthridine concentration ranged from 0.5μM to 5μM. The typical results are from three independent experiments.
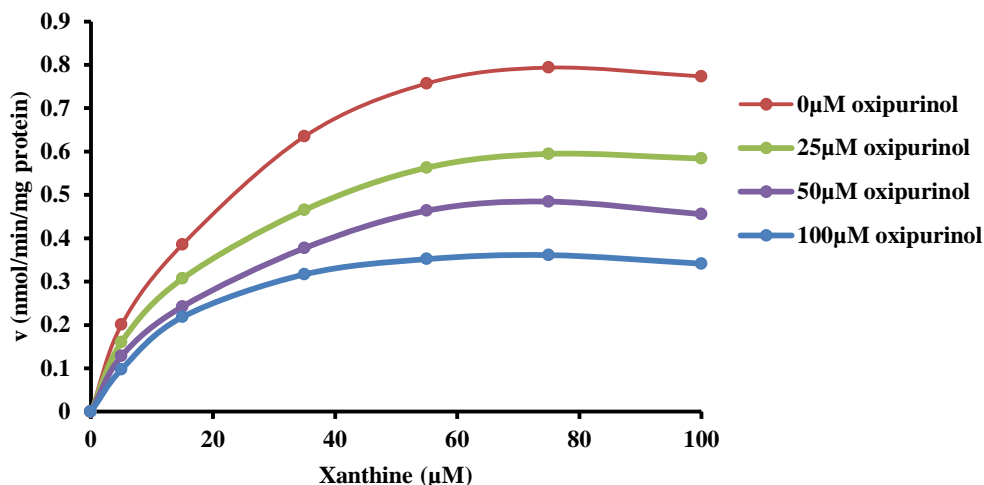
Figure 83: Saturation kinetics plot for oxipurinol inhibition with xanthine as an XOR substrate in trout liver cytosol.

The concentration of xanthine + NAD^+ as xanthine dehydrogenase substrate was varied from 25μM to 100μM with 6.7mM NAD^+ and oxipurinol concentration ranged from 25μM to 100μM. The typical results are from three independent experiments.
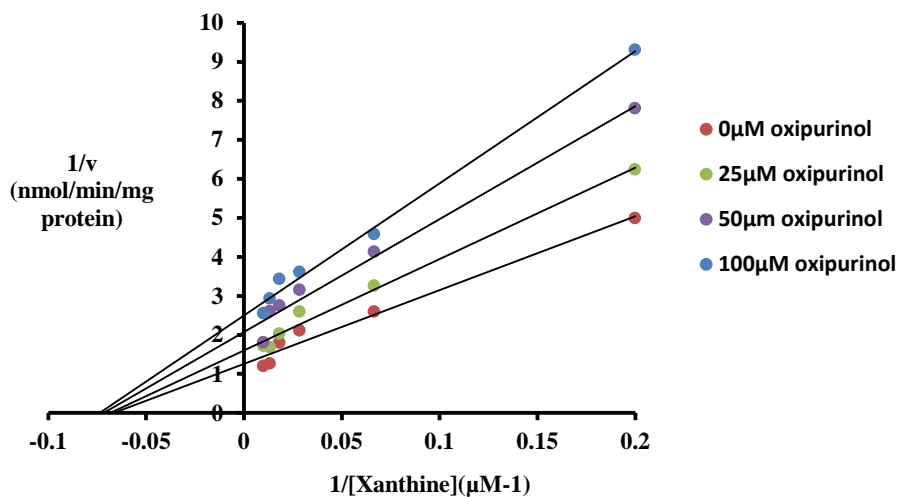
Figure 84: Lineweaver-Burk plot for oxipurinol inhibition with xanthine as an XOR substrate in trout liver cytosol.

The concentration of xanthine + NAD^+ as xanthine dehydrogenase substrate was varied from 25μM to 100μM with 6.7mM NAD^+ and oxipurinol concentration ranged from 25μM to 100μM. The typical results are from three independent experiments.

167

Table 41: Summary of inhibition constant (Ki) and mode of inhibition of different inhibitors with trout AOX and XDH.

AOX inhibitor	Ki (μM)[**]	Mode of inhibition
Menadione	0.17 ± 0.03	Non-competitive
Estradiol	0.34 ± 0.05	Uncompetitive
Ethinyl estradiol	0.44±0.05	Uncompetitive
Chlorpromazine	0.76 ±0.06	Competitive
Phenanthridine	0.77±0.07	Competitive
XOR inhibitor	Ki (μM)[**]	Mode of inhibition
Oxipurinol	0.37±0.06	Non-competitive

The values shown are the (average ± S.D[**]), obtained from three separate liver cytosol fractions for each trout.

It was found that all AOX inhibitors had a Ki values between 0.1μM to 1μM with the lowest Ki value with menadione. The weakest AOX inhibitors found were phenanthridine and chlorpromazine. Lineweaver-Burk plot analysis revealed that the inhibitors had different modes of inhibition. Menadione was a non-competitive inhibitor, while estradiol and 17α-ethinyl estradiol were uncompetitive inhibitors. In contrast, chlorpromazine and phenanthridine were competitive inhibitors. Despite its structural similarity to XOR substrates xanthine and hypoxanthine, oxipurinol was found to be a non-competitive inhibitor.

3.6. Purification of aldehyde oxidase.

Purification of AOX from rat and fish was monitored throughout the purification procedure with DMAC as substrate. Protein elution was monitored at 280nm with an on-line spectrophotometric detection cell in the FPLC instrument. All procedures were carried out at 0 - 4°C. For preliminary experiments AOX was purified from Wistar rat as known protocols existed in published literature.

3.6.1.Purification of AOX from Wistar rat liver.

AOX was purified from Wistar rat liver with a series of purification steps as described in material and method section 2.11. (Figure 25), procedure 1.The first step of purification was heat treatment of liver cytosol at 55ºC for 15 minutes and this step which gave~ 80% yield with a 2-fold purification as seen in (Table 42). The second step of purification was ammonium sulphate precipitation. 0-25%, 50-60% and 70-100% ammonium sulphate fractions had no activity. In contrast the 25-50% fraction had DMAC oxidase activity. This fraction retained 78 % yield of the initial cytosolic activity and there was an overall 3-fold purification of the enzyme. The third step of purification was Q-sepharose anion exchange chromatography which gave a 37 % yield and 12-fold purification as seen in (Table 42) and (Figure 85) and which gave two peaks. The later eluting DMAC oxidase activity peak had activity towards the both substrates DMAC and phenanthridine.
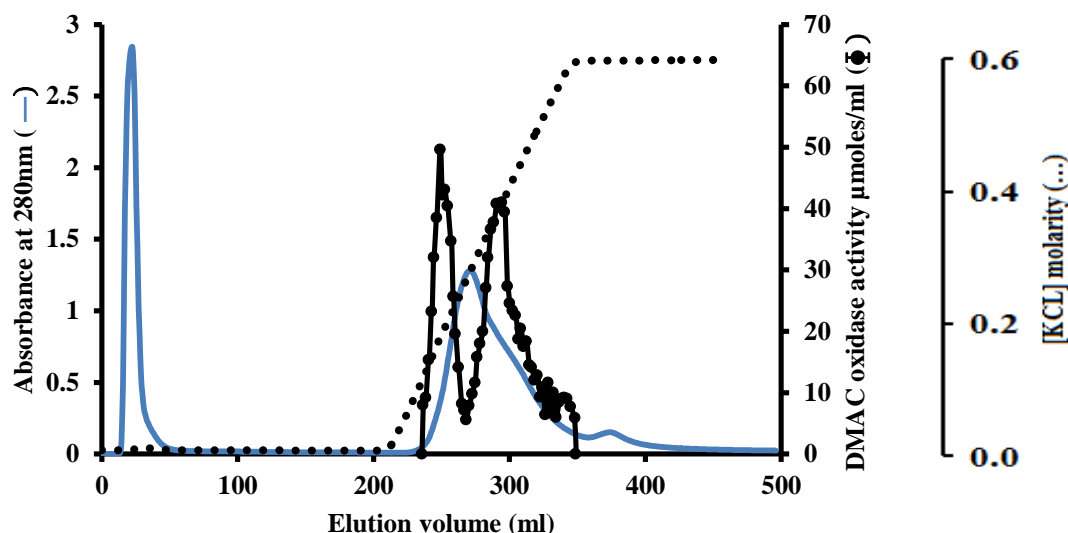
Figure 85: Chromatography of heat treated ammonium sulphate fractionated rat liver cytosol on a Q-sepharose column at pH 8.0. Using 20mM Tris HCL pH8.0 with 1mM cysteine and 5% (v/v) glycerol. Following elution of unbound proteins a linear 0 – 600 mM KCL gradient was applied. Fractions were collected at 1ml/minute and assayed for DMAC oxidase activity. Protein was monitored at 280 nm with an online detector. The result was typical from three independent experiments.

Following concentration using an Amicon concentrator, the peak eluting with high salt (DMAC oxidase peak 2) was further purified by affinity chromatography using benzamidine sepharose 6B as described in materials and methods and following elution of unbound proteins, AOX containing fractions were batch eluted with 10ml of 5mM benzamidine. Pooled and dialysed AOX-active fractions from this step were then subjected to chromatography on a Mono-Q 5/10 anion exchange column (Figure 86). Overall this last step in the purification gave a 22% yield and 227-fold purification of AOX from Wistar rat liver cytosol as seen in (Table 42).
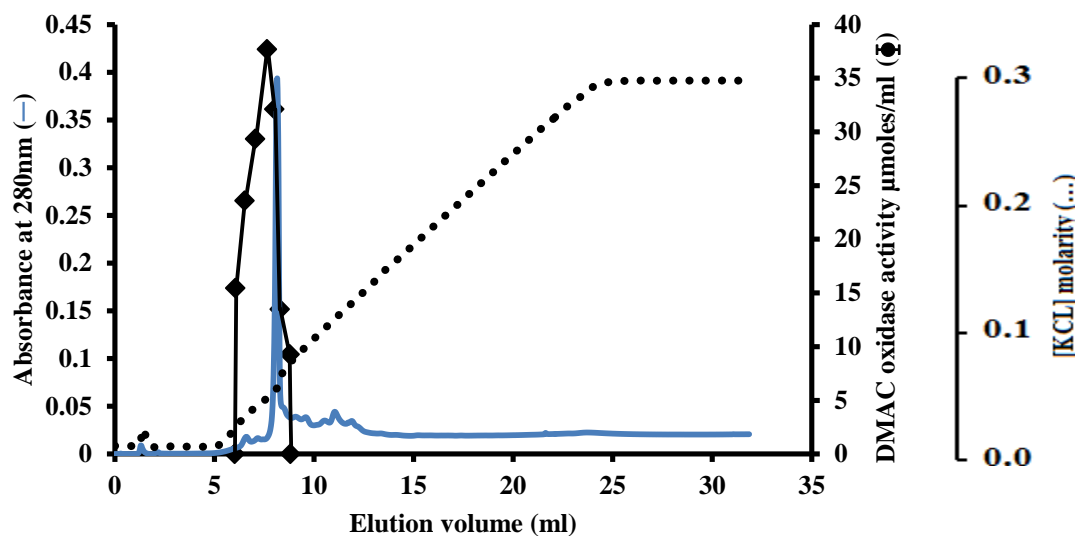
Figure 86: Mono-Q 5/10 anion exchange chromatography column of pooled fractions from affinity chromatography step. Using 20mM Tris HCL pH8.6 with 1mM cysteine and 5% (v/v) glycerol. Following elution of unbound proteins a linear 0 – 300 mM KCL gradient was applied. Fractions were collected at 5ml/minute and assayed for DMAC oxidase activity. Protein was monitored at 280 nm with an online detector. The result from three independent experiments.

A summary of purification of Wistar rat AOX is given in (Table 42).

Table 42: Summary of Wistar rat AOX purification.

Purification stage	Volume [ml]	Total protein [mg]	Total activity [nmol/min]	Specific activity [nmol/min/mg protein]	Yield %	Purification fold
Cytosol preparation	36.6	7593.3	21109.4	2.78	100	1
Heat treatment at 55ºC	26.9	3037.3	16887.5	5.56	80	2
25-50% Ammonium sulphate precipitation	6.8	1895.1	16676.3	8.80	79	3
Qsepharose ion exchange chromatography	1.5	235.8	7873.8	33.39	37.3	12
Benzamidine Sepharose 6B affinity chromatography	0.5	32.2	5973.9	185.15	28.3	67
MonoQ ion Exchange chromatography	0.3	7.4	4686.3	631.83	22.2	227

The data shown is from a typical experiment.

3.6.2. SDS PAGE analysis of Wistar rat AOX

The SDS PAGE was used as described in materials and methods section 2.11.4 to analyse purified fractions figure 87 demonstrates that the purified preparations contained several polypeptide bands < 66kDa indicating that the enzyme had undergone proteolysis.
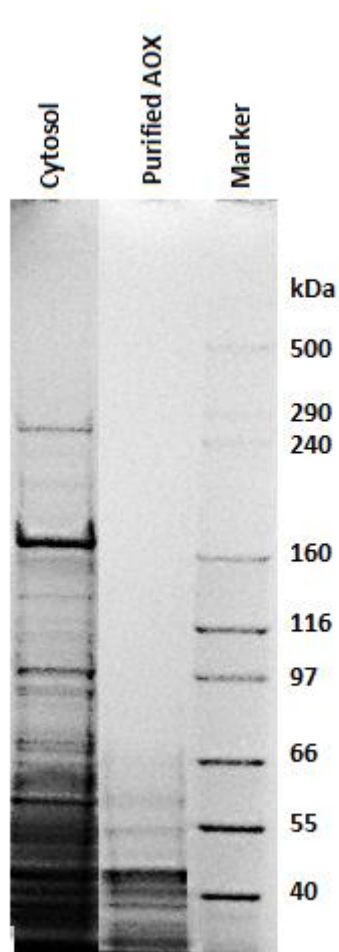
Figure 87: SDS PAGE of purified hepatic AOX from Wistar rat liver.

The lane [1] cytosol 20µg, lane [2] purified AOX 5µg from Mono Q, lane [3] molecular mass markers.

The principle and procedure of SDS PAGE and staining as described in method and material section 2.10.1 table 14. The result obtained represents a typical result from three independent purification experiments.

3.6.3. Purification of AOX from rainbow trout liver.

AOX was purified from rainbow trout liver with a series of purification steps as described in materials and methods section 2.11. (Figure 25), procedure 4.In order to determine if heat treatment that is used for the initial purification of mammalian AOX (Table 21 and 22) could be used for the trout enzyme the thermal stability of the trout enzyme was tested at 55°C for 15-60 minutes as described in section 2.7.3. These experiments with the trout enzyme indicated that it was much more heat labile than the rodent or human enzyme with 80% activity lost after a brief 15 minute incubation at the standard temperature used for many mammalian AOX purifications (Figure 88) and (Table 21 and 22). This indicated that this procedure could not be used as a purification step for the piscine enzyme.
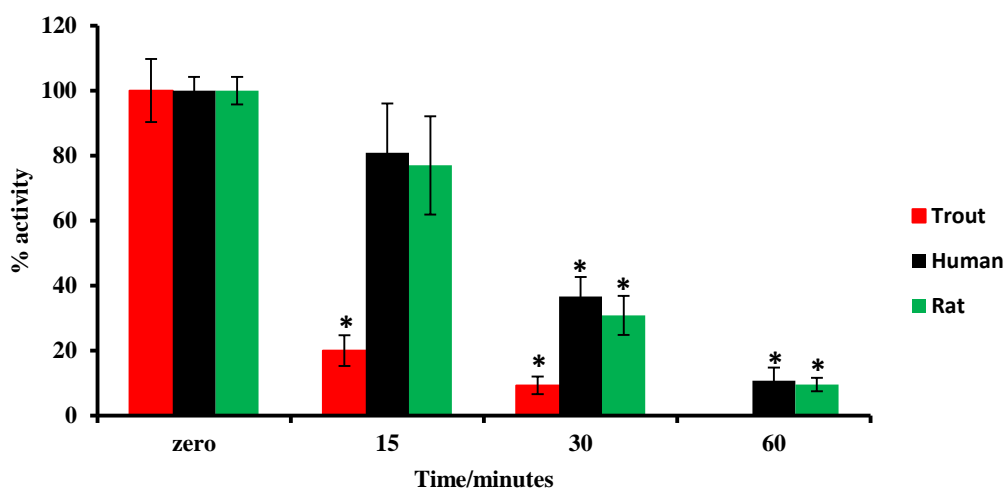
Figure 88: Thermal stability of rainbow trout, human and rat liver AOX activity at 55°C.

Enzyme activity was measured at 37˚C, pH 7.5 with 0.1 mM DMAC as the substrate in AOX assays. The bar graph shows the AOX activity mean ± S.D.(*) signify a statistically significant difference (one way ANOVA p. ≤ 0.05) compared with the control of three experiments with pooled cytosol from ~3 animals.

Rather than use heat treatment as for the mammalian enzyme the first step used for purification of the trout enzyme was ammonium sulphate precipitations. 0-25%, 50-60% and 70-100% ammonium sulphate precipitations had no AOX activity. In contrast, the 25-50% fraction had ~90% of AOX activity of the initial cytosol and there was an overall 3-fold purification of the enzyme. The 25-50% ammonium sulphate fraction was then subjected to Q-Sepharose anion chromatography. Both buffer pH and salt gradient used were optimised in a series of experiments to obtain good resolution of the AOX-active fraction. (Figure 89) illustrates a typical chromatographic profile obtained using pH 8.6 and a 75 ml 0-1.2M KCL gradient. Following selective pooling of AOX-active fractions this gave a51-fold and 15.4% yield purification as seen in (Table 43 and Figure 89).
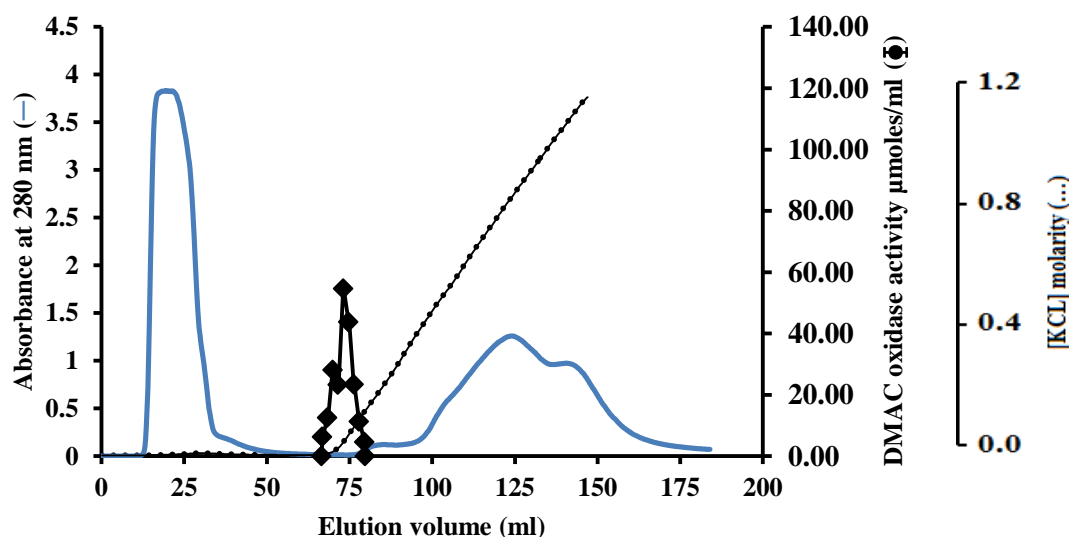
Figure 89: Chromatography of ammonium sulphate fractionated trout liver cytosol on a Q-sepharose column at pH 8.6.

Proteins were dialysed in 20mM Tris HCL pH8.6 with 1mM cysteine and 5% (v/v) glycerol and injected onto column. Following elution of unbound proteins a linear 0 – 1200 mM KCL gradient was applied. Fractions were collected at 1ml/minute and assayed for DMAC oxidase activity. Protein was monitored at 280 nm with an online detector. The result shown is representative from three independent experiments.

The third step of purification step was Superose 6 gel filtration chromatography that gave 14.6% yield and 70-fold purification as seen in (Table 43 and Figure 90).
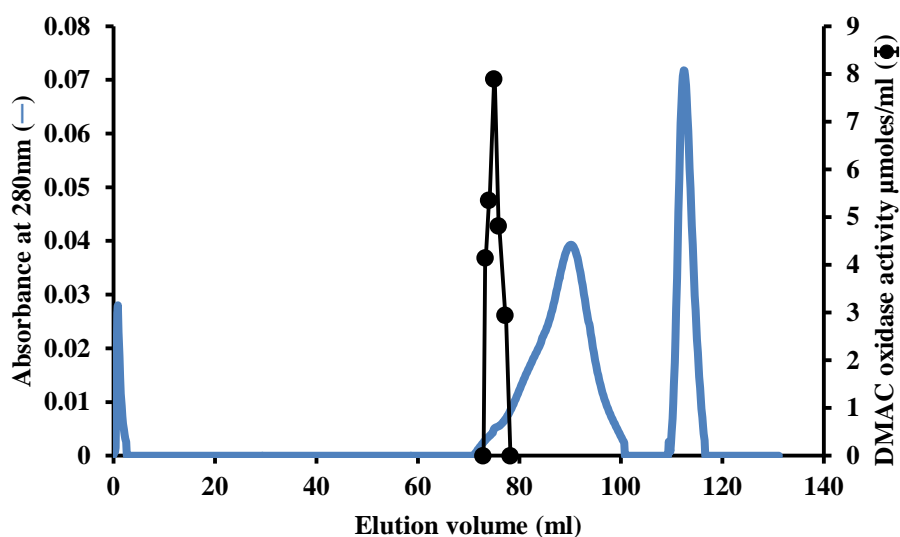
Figure 90: Superose 6 16/70 gel filtration chromatography column of pooled active fractions from Q-sepharose chromatography step.

The proteins were chromatographed using 20mM Tris HCL pH8.0, 100mM NaCL with 1mM cysteine and 5% glycerol. Fraction were collected at 1ml/minute and assayed for DMAC oxidase activity. Protein was monitored at 280 nm with an online detector. The result shown is representative from three independent experiments.

The fourth step of the purification was using a Mono-Q 5/10 anion exchange chromatography of the AOX-active fraction collected from the gel filtration chromatography step. This resulted in the chromatogram in (Figure 91). This last step in the purification resulted in an overall 12% yield and 210-fold purification of AOX from rainbow trout liver cytosol as seen in (Table 43).

The summary of the purification of rainbow trout AOX is given in the (Table 43).
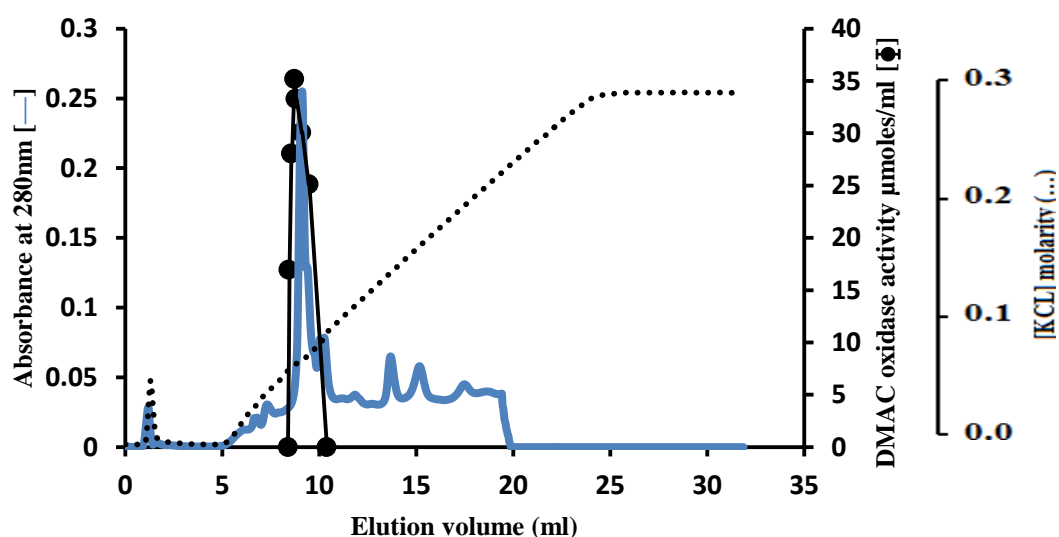
Figure 91: Mono-Q 5/10 anion exchange chromatography column of pooled active fractions from gel filtration chromatography step.

The proteins were chromatographed using 20mM Tris HCL pH 8.6 with 1mM cysteine and 5% (v/v) glycerol. Following elution of unbound proteins a linear 0 – 300 mM KCL gradient was applied. Fractions were collected at 1ml/minute and assayed for DMAC oxidase activity. Protein was monitored at 280 nm with an online detector. The result shown is representative from three independent experiments.

Table 43: Summary of rainbow trout AOX purification.

Purification stage	Volume [ml]	Total protein [mg]	Total activity [nmol/min]	Specific activity [nmol/min/mg protein]	Yield %	Purification fold
Cytosol preparation	27.4	1138.91	1161.7	1.02	100	1
25-50% ammonium sulphate fractionation	5.3	344.03	1073.4	3.12	92.4	3
Q-sepharose anion exchange chromatography	1.5	3.38	178.9	52.96	15.4	51
Superose 6 gel filtration chromatography	0.5	2.36	169.6	71.76	14.6	70
Mono Q anion Exchange chromatography	0.3	0.71	149.8	214.61	12.9	210

The data shown is from a single representative experiment from typical data from three independent experiments.

3.6.4. Determination of the native molecular mass of rainbow trout liver AOX using Superose 6 gel filtration chromatography.

In order to determine the native molecular mass of rainbow trout liver AOX a Superose 6 chromatography column (16 x 70 cm) was calibrated using protein molecular mass standards with the same buffer used for the AOX chromatography. The elution volume of each of the standards is shown in (Table 44) and a calibration graph was constructed from this data (Figure 92).

Table 44: Elution volume and relative molecular mass of the proteins standards on Superose 6 16/70 gel filtration chromatography

Molecular mass marker	Elution volume [ml]	Relative molecular mass [kDa]
Thymoglobulin	65	669
Apoferritin	72.5	443
β-amylase	77.5	200
Alcohol dehydrogenase	81	150
Bovine serum albumin	85	66
Carbonic anhydrase	94.6	29
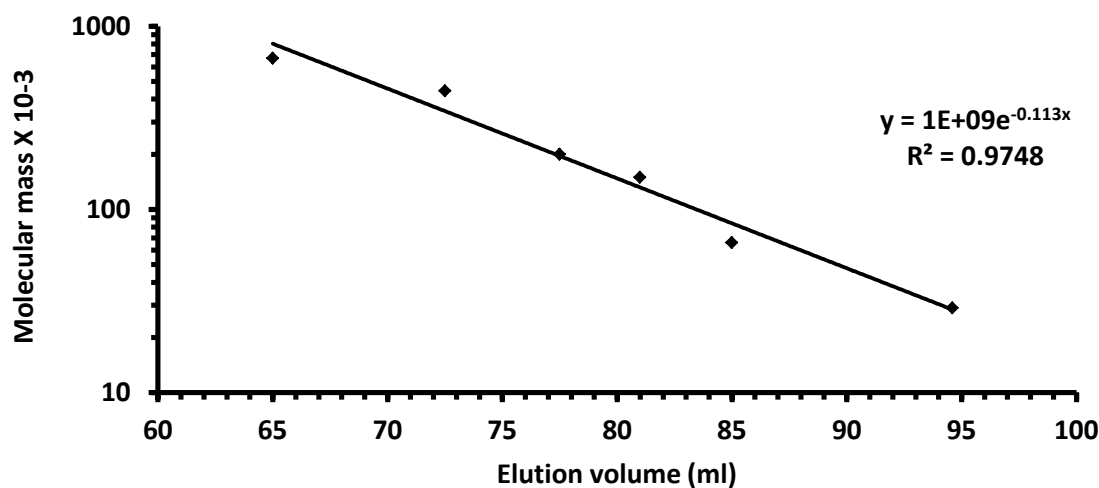
Figure 92: Calibration curve for determination of molecular mass of AOX by gel filtration chromatography.

As the elution volume of the peak of rainbow trout liver AOX activity in Superose 6 16/70 was 75ml, the native molecular mass of the fish AOX was calculated from the equation ($y = 1E+09e^{-0.113x}$) derived from the calibration curve. The mass calculated was 295 kDa. This suggests that the enzyme was a homodimer of ~ 150 kDa subunits as has been shown in mammals, however the SDS-PAGE gel analysis did not have any band of this mass. Instead the final purified preparation was composed of many polypeptides less than 150 kDa. This suggests that the trout AOX retained activity in a proteolysed form. Such as phenomenon is also found with proteolysed mammalian XOR that also retains activity and an overall native mass similar to the intact enzyme estimated by gel filtration chromatography (Engerson *et al.*, 1987).

3.6.5. SDS PAGE analysis of rainbow trout AOX.

The SDS PAGE used its described in method and material section 2.11.4 to analyse purified fractions (Figure 93) demonstrates that the purified preparations contained several polypeptide bands < 55kDa. This suggests that the enzyme had undergone significant proteolysis as the expected single subunit mass was 150 kDa.
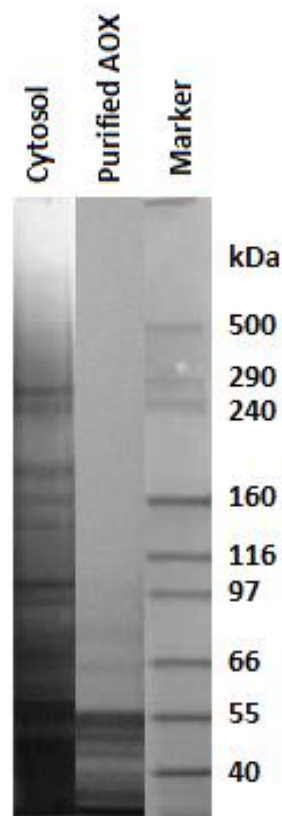

Figure 93: SDS PAGE of purified hepatic AOX from rainbow trout liver.

The lane [1] cytosol 20μg, lane [2] purified AOX5μg from Mono Q, lane [3] molecular mass markers.

The principle and procedure of SDS PAGE and staining as described in method and material section 2.10.1 table 14. The result obtained represents a typical result from three independent purification experiments.

As well as the aforementioned methods outlined above two others were tested. In order to determine if chromatofocusing could be used as a purification step following concentration of the fraction from Q-sepharose anion exchange column, chromatofocusing was performed on a Mono P HR 5/20 column with 0.075M Tris HCL pH 9.3 and a pH 9.3 to pH 6.0 gradient was generated with 10% (v/v) polybuffer 96, adjusted to pH 6.0 with glacial acetic acid. Following chromatography fractions were assayed for DMAC oxidase activity. No activity was found in any fraction. In addition as benzamidine sepharose is frequently used as an affinity matrix for the purification of mammalian AOX this was tested with partially purified trout liver AOX. This was unsuccessful and not entirely unexpected as benzamidine was not an effective inhibitor of the trout enzyme (Figure 71).

4. Discussion.

This discussion section follows the order of the results section.

4.1. Quantification of molybdo-flavoenzyme activities in trout, human and rat.

Both spectrophotometric and HPLC assays were used for the quantification of molybdo-flavoenzyme activities. For oxidation reactions, substrates in this study were classified into two structure types: aldehydes, which undergo oxidation to carboxylic acids and aromatic azaheterocyclic compounds, which undergo oxidation to lactams. Prior to testing with a number of substrates, the optimal conditions of the activities of both molybdo-flavoenzymes were studied in trout, human and rat using spectrophotometric assays with dimethylaminocinnamaldehyde (DMAC) for AOX and xanthine for XOR as substrates. The effect of pH on trout AOX and XOR was assayed under standard assay condition for trout, human and rat. The maximum activity of AOX and XOR with all species was achieved at a similar pH optimum of pH 7.0 as shown (figures 26 and 27). The pH optimum characteristics are similar to the pH-dependent kinetic study of XOR by Choi *et al*. who demonstrated that the steady-state and reductive half-reaction kinetics of the enzyme exhibits a bell-shaped profile with the pK_as of 6.6 and 7.4. These were assignable respectively to an active site base and the first ionization of substrate (Choi *et al.*, 2004). In contrast, Stripe and Della Corte (1969) found that the optimum pH of rat liver XO pH 8.0 (Stirpe and Della Corte. 1969). The optimum pH for AOX from trout, human and rat was observed in the present study is similar to that found by Stoddart and Levine (1992) who found the optimal pH of rabbit AOX was 7.5. (Stoddart and Levine. 1992). In order to test the effect of temperature the activity of AOX and XOR of trout was measured at different incubation temperatures for 5 minutes as described in section

2.7.2. The rate of reaction of trout AOX and XOR gradually increased with increase temperature from 25˚C up to 37˚C, and the activity dramatically decreased after 45°C with less than 10% remaining at 60°C (Figure 28). In contrast the rate of reaction of human and rat AOX and XOR gradually increased with increase temperature from 25ºC up to 37ºC, then the activity decreased gradually until 60°C with approximately 50% activity remaining at highest temperature. These results resemble those with most animal enzymes that become denatured at temperatures above 40˚C (Figure 28). This present result showed that the assay temperature of 37˚C is suitable for use with the trout, human and rat MFE. The contrast in the thermolability of the piscine and mammalian AOXs may reflect differences in the primary amino acid sequence of mammalian AOXs that may have increased hydrophobic, ionic and hydrogen bonding that are known to stabilise proteins at elevated temperatures. At present it is not known which amino acid residues are involved in this.

As well as optimising incubation conditions all HPLC protocols for analytes were tested for method linearity, accuracy and precision were checked. Regression for calibration (r^2) standards injected were more than 0.997 for all analytes tested. Accuracy for the method was more than 95% and precision < 3.5%, calculated by using three injections on the same day as calibration standards (intraday) (Tables 1 and 2 in Appendixes 3). For the linearity for the results, the lower limit of Quantification (LOQ) and limit of detection (LOD) were determined for each analyte (Table 3 in Appendix 3). According to (Miller and Miller. 2005) these methods have acceptable limits for both accuracy and precision and were therefore used to analyzed samples from this study.

4.1.1. Exogenous aldehydes as substrates for AOX

Two exogenous aromatic aldehyde compounds, vanillin and (DMAC), were used as substrates of AOX. Enzyme activity of AOX was measured spectrophotometrically using two different substrates (DMAC and vanillin) with O_2 as electron acceptor as follows. These were chosen for the following reasons. DMAC is a specific substrate for rat AOX (Kurth and Kubiciel. 1984, Moriwaki *et al.*, 1998, Maia and Mira. 2002). Vanillin has also been shown to be a good substrate with a high affinity for AOX (Panoutsopoulos and Beedham. 2004).

4.1.1.1. Vanillin and DMAC

Vanillin is an aromatic aldehyde found in food material as an additive and it can be biotransformed to its carboxylic metabolite with O_2 as an electron acceptor primarily by AOX. In the presence of NAD^+, aldehyde dehydrogenase (ALDH) plays a significant role (Beedham. 2001, Obach *et al.*, 2004, Sahi *et al.*, 2008, Pryde *et al.*, 2010, Garattini and Terao. 2013). Only two studies have directly measured the kinetics of a substrates disappearance or product generation spectrophotometrically on mammals, mollusks, crustaceans, insects and fish AOX. Wurzinger and Hartenstein (1974) used vanillin as substrate of fish and mammalian AOX with O_2 as an electron acceptor in a spectrophotometric assay measuring vanillic acid production (Wurzinger and Hartenstein. 1974). Using (DMAC) and vanillin substrates of fish AOX with O_2 as an electron acceptor (Wurzinger and Hartenstein. 1974, Maia and Mira. 2002, Kitamura *et al.*, 2003, Choughule *et al.*, 2013).

K_m and V_{max} were determined from the Eadie- Hofstee plot of V versus V/[S] as described in the section materials and methods using simple rapid spectrophotometric assays. The lowest K_m value for an AOX substrate was found with DMAC being 21.5 ± 1.05 µM (mean ± SD) with trout and 3.4 ± 1.2 µM with human and 5.4 ± 1.6 µM

with rat. In agreement with the present result Li *et al*. (2009) found that the DMAC is an excellent substrate for rat liver AOX with a low K_m value (9.6 µM) (Liu *et al.*, 2009). The results of this study indicated that DMAC is a better substrate of trout AOX than vanillin with a K_m value 2-fold higher (53.2 ± 2.1 µM). The K_m values for DMAC in trout were approximately 4 and 7-fold higher than that in rat and human. The K_m value of vanillin in the trout was approximately 5 and 10-fold higher compared with that in rat and human respectively in spectrophotometric assay and Vmax value was similar for both mammalian species (see Appendix 3 Figures 6 - 24) (Table 39). The K_m value for trout AOX with vanillin was approximately two times more than that found guinea pig liver AOX that has a K_m value of 29 µM (Panoutsopoulos *et al.*, 2005). Obach, (2004) found vanillin is an excellent substrate for human liver AOX with a low K_m of 2.7 µM (Obach. 2004). Vanillin has also been used to study species variation of aldehyde oxidase occurrence in 79 species. Wurzinger and Hartestein (1974) found vanillin to be a substrate of aldehyde oxidase from mollusks, crustaceans, insects and fish. Panoutsopoulos and Beedham (2004) incubated guinea pig AOX with vanillin and as shown by HPLC its metabolite vanillic acid formed quickly (Panoutsopoulos and Beedham. 2004). In this study trout liver, kidney and gill cytosol were incubated with vanillin and products analysed by HPLC. With trout kidney and gill cytosol no vanillic acid peak formed, while when incubated with trout liver cytosol the vanillic acid peak formed (Figure 34a). The trout kidney and gill lack AOX activity and the activity are found only in the liver. The lack of measurable AOX activity in kidney and gill contrasts that found by Krenitsky et al 1974 who measured AOX in the kidney of a Cypriniformes goldfish (*Carassius auratus*) and Asagba et al 2010 who found AOX activity in the kidney and gill of a Siluriforme African catfish (*Clarias gariepinus*). The Km of vanillin with trout liver

AOX determined using HPLC was found to be 57.20 ± 0.6 µM, which is ~ two times more than that found with human and rat AOX (Table 39).

4.1.2. Endogenous vitamin aldehydes as substrates for AOX

Two endogenous vitamin aldehydes, pyridoxal (vitamin B6), all-trans retinal (vitamin A) and the vitamin B3 metabolite N^1-methylnicotinamide (NMN) were used as aldehyde substrates of AOX.

4.1.2.1. Vitamin B6 pyridoxal

Vitamin B6 is a water-soluble compound that contains a pyridine ring that is present in nature as several different forms such as pyridoxal , pyridoxine (PN), pyridoxamine and the active form is pyridoxal 5'-phosphate (PLP) (Fitzpatrick *et al.*, 2007). PLP is the coenzymatically active form of vitamin B6 and plays an important role in maintaining the biochemical homeostasis of the body (Meister. 1990, Snell. 1990). There are more than 100 PLP-dependent enzymes in a cell that perform essential roles in various metabolic pathways including amino acid metabolism (such as amino acid synthesis and degradation), fatty acid metabolism (such as the synthesis of polyunsaturated fatty acids) and carbohydrate metabolism (such as the breakdown of glycogen) (Mooney *et al.*, 2009). The preferred degradation route from PLP to 4-pyridoxic acid involves the dephosphorylation of PLP by a phosphatase followed separately by the actions of AOX and β-nicotinamide adenosine dinucleotide-dependent dehydrogenase (Schwartz and Kjeldgaard. 1951, Stanulovic and Chaykin. 1971). When pyridoxal was incubated with trout, rat and human cytosol pyridoxic acid was produced (Figures 35) with Km value for trout AOX 121.9 ± 3.6 µM, rat AOX Km value of 46.4 ± 2.51 µM and human AOX Km value of 34.1 ± 1.97 µM respectively (Table 39). The Km value of trout AOX with pyridoxal is three times

more than that with human and rat AOX activity with pyridoxal. The Vmax value of trout AOX with pyridoxal found to be 1.41 ± 0.69 nmol/min/mg protein and was approximately 6 and 9-fold lower than that Wistar rat and human respectively.

4.1.2.2. Vitamin A all-trans retinal

Another potential substrate of AOX of physiological importance is all-trans-retinaldehyde which it oxidised to retinoic acid (Haung *et al.*, 1999). Retinoic acid is a key regulator of the homoeostasis of keratinized epithelia and a recognized morphogen of the vertebrate organisms (Chambon. 1996), although its role in fish is less well understood. All-trans retinal congeners are components of rhodopsin visual system in all vertebrate and invertebrates including fish (Lee *et al.*, 1996, Seki *et al.*, 1998). Interestingly the all-trans retinal determination network that is responsible for controlling eye development is one of the most extensively studied gene regulatory networks in both invertebrate and vertebrate species (Datta *et al.*, 2011) . The first report of fish AOX being involved in the biotransformation of all-trans retinal was by Lakshamanan *et al*. (1964) who examined the oxidation of the aldehydes of both vitamin A1 (all-trans retinal) and vitamin A2 (3, 4-dehydro-all-trans retinal) to the corresponding acids by AOX enzyme in the liver of several freshwater-fish (*Ophiocephalus muralius*, *Labeo calbasu* and *Cyprinus carpio communis*) as shown in (Table 10). The study also found that the enzyme from these freshwater fish livers was inhibited by the AOX inhibitor menadione (Lakshmanan *et al.*, 1964). Although the genes and proteins that control eye development are fully understood proteins that might regulate the levels of all-trans retinal and retinoic acid in fish are poorly understood. In this study, it was important to establish if trout AOX is capable of oxidizing all-trans retinaldehyde to its metabolite retinoic acid like vertebrate AOX (Huang and Ichikawa. 1994, Haung *et al.*, 1999, Kitamura *et al.*, 2006, Garattini *et al.*,

2008, Terao *et al.*, 2009, Garattini and Terao. 2011, Garattini and Terao. 2012).

Incubation of trout cytosol with all-trans retinaldehyde generated retinoic acid (Figure 36a). This indicated that all-trans retinal is a substrate for trout AOX. These finding are consistent with Lakshamanan *et al*. (1964) who first observed the role of AOX in the oxidation of all-trans retinaldehyde to retinoic acid in fish by liver AOX (Lakshmanan *et al.*, 1964) and Huang and Ichikawa, (1994) and Tsujita *et al*. (1994) who first observed the role of AOX in the oxidation of all-trans retinaldehyde to retinoic acid without NAD^+ in rabbit by liver cytosol AOX (Huang and Ichikawa. 1994, Tsujita *et al.*, 1994). The Km value for trout, rat and human with all-trans retinal was determined using HPLC and it was found that Km value of trout AOX with all-trans retinal of 124.7 ± 2.27 µM, rat AOX Km value of 30.9 ± 1.23 µM and human AOX Km value of 12.6 ± 0.58 µM (Table 39). The Km value of trout AOX with all-trans retinal was ten and four times more than that human and rat AOX activity with all-trans retinal respectively. The Vmax value of trout AOX with all-trans retinal was 2.22 ± 0.62 nmol/min/mg protein and it found to be approximately 3 and 4-fold lower than that Wistar rat and human respectively (Table 39).The Km values found in this study were of a similar magnitude to those found by Schumann *et al*., 2009 it found the Km value of all-trans retinaldehyde (vitamin A) with mouse AOX1 of 55.8 ± 8.8 µM (Schumann *et al.*, 2009).

4.1.2.3. N^1-methylnicotinamide (NMN)

Another vitamin tested in this study was N^1-methylnicotinamide (NMN) which is often used as a marker for aldehyde oxidase (Felsted and Chaykin. 1967, Stanulovic and Chaykin. 1971, Beedham. 1987, Sugihara *et al.*, 2006). NMN is formed from nicotinamide by nicotinamide N-methyltransferase which is widely distributed in animals (Yan *et al.*, 1997) . Many findings are consistent with the role of AOX in the

conversion of NMN to N[1]-methyl-2-pyridone-5-carboxamide (2-PY) and N[1]-methyl-4-pyridone-5-carboxamide (4-PY) in the final steps of the nicotinamide degradation pathway (Felsted and Chaykin. 1967, Stanulovic and Chaykin. 1971, Beedham. 1987, Sugihara *et al.*, 2006, Peretz *et al.*, 2012). Previously Kitamura *et al*, (2003) examined the activity of AOX from sea bream (*Pagrus major*) and goldfish (*Carassius auratus*), while using N[1]-methylnicotinamide as electron donor and organothiophosphate insecticide fenthion sulphoxide as an electron acceptor as shown in (Table 10)(Kitamura *et al.*, 2003). Rather than measure NMN metabolites Kitamura's study measured fenthion. In this study when NMN was incubated with trout, rat and human cytosol two product peaks were found (Figures 36) suggesting that there was AOX activity towards this compound. Based on what is found in mammals it is assumed that these might be N[1]-methyl-2-pyridone-5-carboxamide (2-PY) and N[1]-methyl-4-pyridone-5-carboxamide (4-PY) (Figure 36). The metabolism of NMN to 2-PY and 4-PY has been reported to be catalysed by AOX in a number of mammals including humans (Felsted and Chaykin. 1967, Stanulovic and Chaykin. 1971, Sugihara *et al.*, 2006). NMN showed different metabolic profiles in mice and humans by AOX *in vivo* and *in vitro*; for example the major product was 2-PY in humans, whereas in mice were 2-PY and 4-PY (Kitamura *et al.*, 2008). The ratio of 2-PY/4-PY from NMN differs and varies among species (Kitamura *et al.*, 2006, Garattini *et al.*, 2008, Kitamura *et al.*, 2008, Garattini and Terao. 2011). Krenitsky *et al*. (1986) reported that the N[1]-methylnicotinamide is substrate of human liver XO with very high Km value of 48 mM (Krenitsky *et al.*, 1986). In contrast, Krenitsky *et al*. (1972) reported that N-methylnicotinamide is an excellent substrate of rabbit liver AOX with low Km value of 1 mM (Krenitsky *et al.*, 1986). Hall and Krenitsky (1986) reported that the N-methylnicotinamide is a substrate of rabbit AOX with Km value of 7.9 mM (Hall and

Krenitsky 1986). In contrast, Rajagopalan and Handler (1964) incubated the N^1-methylnicotinamide with rabbit liver AOX and found that the Km value at pH 10 was 80 µM and at pH 7.8 was 300 µM respectively. These studies measured N^1-methynicotinamide indirectly using 2, 6-dichlorophenolindol (2, 6-DCPIP) as electron acceptor. In this study for the first time N^1-methylnicotinamide oxidation by AOX was assayed in trout liver cytosol using sensitive a HPLC method as a new direct assay for evaluating the AOX activity in trout. This indicated that N^1-methylnicotinamide is a substrate for trout AOX. The Km value of N^1-methylnicotinamide measured was found of 273.9 ± 2.89 µM with trout AOX, 156.2 ± 3.68 µM with Wistar rat AOX and 139.5 ± 2.86 µM with human AOX and Vmax 1.63 ± 1.33 nmol/min/mg protein, 5.92 ± 0.68 nmol/min/mg protein and 6.69 ± 0.74 nmol/min/mg protein with trout, rat and human respectively as in (Table 39). The Km of trout AOX with N^1-methylnicotinamide ~ 1.5-fold more than that of mammalian AOX with N^1-methylnicotinamide.The Km measured in this study were of the same magnitude as that found with N^1-methylnicotinamide with mouse AOX3 128.5 ± 5.8 µM (Coelho *et al.*, 2012, Mahro *et al.*, 2013).The Vmax value of Wistar rat and human with N^1-methylnicotinamide was approximately 5 and 6-fold greater respectively than the piscine AOX (Table 39).

4.1.3. Exogenous N-heterocycles as substrates for AOX.

Four exogenous N-heterocycles, phenanthridine, phthalazine, pyrazinamide, cinchonine were used as N-heterocycles substrates of AOX.

4.1.3.1. Phenanthridine.

Phenanthridine is an NPAH pollutant found in terrestrial and aquatic environments from industrial activities associated with fossil fuels (Blumer *et al.*, 1977). NPAHs are therefore a cause for concern both to humans and aquatic wildlife. Several papers

reported that the phenanthridine is a good substrate and has a very high affinity towards AOX (Stubley and Stell. 1980, Rashidi. 1996, Beedham. 2001). In the AOX spectrophotometric assays one N-heterocyclic compound, phenanthridine was used as a substrate. Enzyme activity of AOX was measured spectrophotometrically using phenanthridine as substrate with O_2 as electron acceptor as follows. These were chosen for the following reasons, phenanthridine has been shown to be a good specific substrate for monitoring mammalian AOX activity in many studies (Lake *et al.*, 2002, Pirouzpanah *et al.*, 2006, Sorouraddin *et al.*, 2008) . Phenanthridine is a specific substrate of mammalian AOX (Table 1). At present it is not known whether AOX in aquatic species such as fish can metabolise phenanthridine to a more polar metabolite (phenanthridone) aiding its excretion. However, Bleeker *et al*, (2001) examined the metabolism of the environmental pollutant phenanthridine in carp (*Cyprium carpio*) liver and bile into its metabolite 6(5H)-phenanthridinone (phenanthridone) suggesting that fish AOX catalyses this biotransformation. NPAHs are derivatives of polycyclic aromatic hydrocarbons in which one carbon atom is substituted by a nitrogen atom. Phenanthridine has been identified in air, marine and freshwater environments, and in ground water. High environmental concentrations in the field result from human activities such as combustion of fossil fuels. The presence of the electronegative nitrogen atom makes NPAHs more water soluble than their homocyclic analogues; this increase their mobility and bioavailability in aquatic environments (Bleeker *et al.*, 2001). The activity with phenanthridine was not detectable with trout liver cytosol using the standard spectrophotometric assay. It was a good substrate with both rat and human in my study and with a Km value of 5.6 ± 0.65 μM with rat and Km value of 3.2 ± 1.23μM with human. This agreement with phenanthridine as a specific substrate of AOX has been used in several papers and Km previously has been estimated were

< 1 μM with rabbit and guinea pig liver AOX enzyme and 6 μM and 14 μM with rat and human liver AOX respectively (Stubley and Stell. 1980, Rashidi *et al.*, 1997, Beedham. 2001). In this study trout liver, kidney and gill cytosol incubated with phenanthridine and product analysed by HPLC, with trout kidney and gill cytosol no 6(5H)-phenanthridinone (phenanthridone) metabolite peak found. This indicated no AOX activity in trout kidney and gill, while in trout liver cytosol the 6(5H)-phenanthridinone (phenanthridone) metabolite formed (Figure 39a) with a Km value of 55.0 ± 1.63 μM. The Km values of trout AOX with phenanthridine it found seven and six times more than that human and rat AOX activity respectively. The Vmax value of Wistar rat and human with phenanthridine was approximately 2 and 4 times respectively more than that with trout AOX (Table 38).In contrast, Hartmann et al., (2012) it found the Km value of phenanthridine with pure human AOX of 3.9 ± 0.8 μM. On other hand, Coelho *et al*., (2012) and Mahro *et al*., (2013) it found the Km value of phenanthridine with mouse AOX3 32.3 ± 1.4 μM and 32 ± 1 μM respectively (Coelho *et al.*, 2012, Mahro *et al.*, 2013).

4.1.3.2. Phthalazine.

Phthalazine an aromatic heterocyclic compounds which have a CH=N- group, which its biotransformed to its corresponding metabolite 1-phthalazinone by mammalian AOX (Stubley *et al.*, 1979, Beedham *et al.*, 1990, Obach. 2004, Panoutsopoulos and Beedham. 2004, Barr and Jones. 2011). In this study phthalazine was incubated with trout, rat and human liver cytosol and its metabolite was formed (Figure 40). The Km value determined for trout, rat and human AOX with phthalazine was 61.2 ± 1.41 μM, 10.5 ± 0.55 μM and 9.80 ± 0.59 μM respectively (Table 39). The Km value for trout AOX activity was therefore six and two times more than that human and rat AOX respectively. The Vmax value of trout AOX with phthalazine found to be 2.02 ± 0.46

nmol/min/mg protein and was approximately 2 and 4 times lower than Wistar rat and human respectively (Table 39).study by Beedham *et al*., (1995) which incubated human, rabbit, guinea pig and baboon liver cytosol with phthalazine, determined the Km for human AOX was41µM (Beedham *et al.*, 1995). This result is similar with trout and was ~ 4-fold higher than that with rat and human in this study. Barr and Jones (2011 and 2013) incubated human liver cytosol with phthalazine, identified its metabolite formed 1-phthalazinone using HPLC and determined the Km of human AOX with phthalazine and it found it to be 8.0 ± 0.4 µM (Barr and Jones. 2011, Barr and Jones. 2013). This result is similar what was found with human cytosol in this study. On other hand Hartmann et al., (2012) measured the activity of phthalazine spectrophotometrically with pure human AOX using 2,6-dichlorophenol-indophenol (2,6-DCIP) as electron acceptor and it found the Km value of phthalazine with human AOX of 1.3 ± 0.3 µM; this result was ~ 10-fold lower than human in this study due to use of an artificial electron transport. On other hand Schumann *et al.,* 2009 found the Km value of phthalazine with mouse AOX1 of 11.4 ± 4.0 µM (Schumann *et al.*, 2009) and this agrees with the Km value of phthalazine with human in this study. In contrast Coelho *et al.,* 2012 and Mahro *et al.*, 2013 found the Km value of phthalazine with mouse AOX3 was 1.4 ± 0.2 µM (Coelho *et al.*, 2012, Mahro *et al.*, 2013); this result was ~ 10-fold lower than human and rat in this study.

4.1.3.3. Cinchonine.

Cinchonine is a cinchona alkaloid a widely used in the treatment of malaria (Hunter. 1988). All four cinchona alkaloids, quinine, quinidine, cinchonine and cinchonidine, are oxidised by AOX to the 2'-quinolone derivatives in mammals (Palmer *et al.*, 1969, Stubley *et al.*, 1979, Beedham *et al.*, 1992, Zhao and Ishizaki. 1997, Al-Tayib. 2009). When cinchonine was incubated with trout, rat and human cytosol a metabolite of

194

cinchonine was produced (Figures 41) suggesting AOX plays an role in the metabolism of cinchonine in these species. The Km value of cinchonine with rainbow trout AOX was ~ 4-fold higher than that of two mammalian AOXs (Table 39).The Vmax value of Wistar rat and human AOX with cinchonine was approximately 4 and 8-fold greater than that of trout AOX (Table 39). A study by Fukiya *et al*., 2010, found the Km value of cinchonidine with rabbit of 124 ± 2.44 μM (Fukiya *et al.*, 2010) this was similar to that found with trout and was ~ 3-fold higher than that found with rat and human AOX in this study.

4.1.3.4. Pyrazinamide.

Pyrazinamide is a drug used to treat tuberculosis that is metabolised to 5-hydroxypyrazinamide by the action of XOR and AOX in mammals (Moriwaki *et al.*, 1993, Mehmedagic *et al.*, 1997, Mehmedagic *et al.*, 2002, Kitamura *et al.*, 2006). When pyrazinamide was incubated with trout in the presence of O_2 as an electron acceptor there was no production of 5-hydroxypyrazinamide (Figure 42a), but when pyrazinamide was incubated with trout in the presence of NAD^+, 5-hydroxypyrazinamide was produced (Figures 42b). This was in contrast with that found when pyrazinamide was incubated with both rat and human liver cytosol as 5-hydroxy pyrazinamide was formed both in presence of NAD^+ and without of NAD^+(Figures 44a, 44b, 45a and 45b). The Km value for the NAD^+-dependent trout enzyme was approximately 2-fold higher than that two mammalian enzyme (Table 40). With the addition of NAD^+ to the assay the Vmax of the rat and human activities were increased about 4 and 6-fold respectively than when oxygen was the sole electron acceptor. This result was consistent with finding in previous *in vitro* study, which confirmed that both AOX and XOR can oxidise pyrazinamide to 5-hydroxypyrazinamide in humans and rats (Yamamoto *et al.*, 1987, Moriwaki *et al.*,

1993). As in (table 38) the AOX substrate specificity is different from different substrate with the same species as well as with different species tested in this study. For more affinity of substrate to trout AOX found DMAC the best followed with vanillin and the lowest affinity found with N^1-methylnicotinamide as it have high Km value and lower substrate efficiency (Ks) value. On other hand, the substrate specificity with two mammalian species rat and human AOX have high specificity with DMAC and vanillin with lowest Km value and highest substrate efficiency (Ks) value and lowest specificity with N^1-methylnicotinamide as high Km value and lowest substrate efficiency (Ks) value. These different in specificity due to differentiation in amino acid sequence with different species as mentioned with (Pryde *et al.*, 2010) it used modelling of different AOX substrates to expect its reaction with enzyme and measured by using X-ray crystallography to find the activity of different substrates with the AOX.

4.1.4. Endogenous and exogenous purines and purine analogs as substrates for XOR

4.1.4.1. Xanthine.

Kinetic analyses of XOR enzymes revealed that the endogenous purine xanthine is the preferred substrate for XOR(Moriwaki *et al.*, 1993). In this study using the standard spectrophotometric assay the Km value of rat and human for XO with xanthine using O_2 as an electron acceptor was 13.2 ± 1.7 μM (mean $\pm$ SD) and 3.0 ± 0.65 μM (mean $\pm$ SD), respectively, while the Km value of rat and human for XDH with xanthine using NAD^+ as an electron acceptor was 5.5 ± 1.45 μM (mean $\pm$ SD) and 1.9 ± 0.2 μM (mean $\pm$ SD), respectively. The NAD-dependant Vmax value for xanthine dehydrogenase with Wistar rat and human was approximately 5 and 7-fold greater than that O_2-dependant respectively (Table 40). In contrast the trout XOR enzyme

only displayed activity in the presence of NAD^+ as an electron acceptor as no activity with O_2 was detected even after prolonged 120 minute incubations using a sensitive HPLC assay (Figure 48 b). The Km value of trout for XDH with xanthine using NAD^+ as an electron acceptor was 2-3-fold higher than the mammalian enzymes (13.5 ± 1.9 µM (mean $\pm$ SD) (Table 40). This Km value is similar to that obtained by Kaminski and Jezewska (1985) who found that the Km of the carp (*Cyprinus carpio)* enzyme was 24.7 µM. The Km value obtained with the piscine enzyme using xanthine as a XDH substrate was about 2.5 and 6-fold higher than those obtained with rat and human respectively. The activity of XOR in the three species was inhibited by the XOR inhibitor oxipurinol (Figures 54, 56 and 58).These finding agree with Kaminski and Jezewska, (1985) who observed that XDH of carp (*Cyprinus carpio*) converted xanthine to uric acid only with NAD^+ present and reported that allopurinol is a potent inhibitor of carp (*Cyprinus carpio*) XOR (Kamiński and Jeżewska. 1985). On other hand, Schumann *et al*., (2009) examined the activity of xanthine with mouse XDH and it measured its Km value and it found of 59 ± 10 µM (Schumann *et al.*, 2009)this result was ~ 4-fold greater than trout and was~ 10-fold greater than rat and was ~ 25-fold higher than human in this study. The Km value of mouse XDH was ~ 10-fold greater than rat which may be due to species variation in molybdo-flavoenzyme activity. Krenitsky *et al*. (1986) reported that the xanthine is an substrate of human liver XO that have low Km value of 7.0 µM (Krenitsky *et al.*, 1986). This result is similar to that with found with human in this study.

The lack of detectable XO activity is similar to that found by other investigators with fish XOR (Krenitsky *et al.*, 1974, Wurzinger and Hartenstein. 1974, Cleare *et al.*, 1976, Kamiński and Jeżewska. 1985). However in their assays a much less sensitive spectrophotometric assay was used which might not detect XO activity. The current

study which used a 120 minute incubation and a sensitive HPLC assay therefore unequivocally proves no XO activity exists with trout liver XOR. These results contrast with these by a number of investigators that have seemingly measured XO activity (Sastry and Rao. 1984, Basha and Rani. 2003, Pandey *et al.*, 2003, Asagba *et al.*, 2010, Hegazi *et al.*, 2010, Hari and Neeraja. 2012). In these studies where XO has been apparently measured it important to note that either crude homogenates or crude post nuclear or mitochondrial supernatants were used and additionally gel filtered was not carried out to remove small molecules that may interfere with the assay. This would therefore result in erroneous measurement of XOR activities. As the study describe in this thesis and other studies have used cytosol that has been gel filtered do not detect any activity with O_2 as an electron acceptor it is likely that studies that detect XO with crude non-gel filtered extracts gave false positive results. This is backed up by the fact that all studies that have used the correct procedure with non-mammalian species have consistently not found measurable XO activity. These included fish, amphibians, reptiles and birds where the enzyme exists as a non-convertible XDH form (Kamiński and Jeżewska. 1985, Frost *et al.*, 1986, Zakrzewska and Jeżewska. 1989, Nishino *et al.*, 2008). In addition XORs in non-mammalian species lack the cysteines required for the XO conversion. Protein sequence information from chicken and Drosophila XOR revealed that these NAD-dependant XDHs lack a cysteines (cysteine 535 and cysteine 992) necessary for this XO conversion (Nishino and Nishino. 1997, Nishino *et al.*, 2008). Similarly fish XORs also lack these cysteines (D. J. Clarke personal communication).

4.1.4.2. 1-methylxanthine.

Previous studies with bovine milk xanthine oxidase demonstrated it catalyses the oxidation of 1-methylxanthine, 7-methylxanthine and theophylline, to varying degrees with the 1-methylxanthine being the best substrate (Krenitsky *et al.*, 1972). In this study the caffeine metabolite 1-methylxanthine was tested as a substrate for trout, rat and human XOR. Trout cytosolic XOR was also able to convert 1-methylxanthine to 1-methyluric acid when NAD^+ was present as an electron acceptor (Figure 49b), but no product was formed without NAD^+ (Figure 49a). The Km value of trout for XDH with 1-methylxanthine using NAD^+ as an electron acceptor was $17.6 \pm 1.23\mu M$ (mean $\pm$ SD) (Table 40). The Km value obtained with the piscine enzymes using 1-methylxanthine as XDH substrate was about 2-fold higher than those obtained with human and rat respectively (Table40). The NAD-dependant Vmax value for 1-methylxanthine dehydrogenase with Wistar rat and human was approximately 5 and 8-fold greater respectively than the O_2-dependant (Table 40). The Km value of rat and human XOR in my study with 1-methylxanthine using NAD^+ as an electron acceptor were similar being 9.2 ± 0.62 μM (mean $\pm$ SD) and 8.6 ± 1.05 μM (mean $\pm$ SD), respectively (Table 40). 1-methylxanthine oxidation was inhibited in the presence of XOR inhibitor oxipurinol in all three species tested (Figures 55a, 57a and 59a). These results agree with Reinke *et al.* (1987) who found the XDH of rat can catalyse the oxidation of 1-methylxanthine to 1-methyluric acid (Reinke *et al.*, 1987).

4.1.4.3. Allopurinol

The exogenous purine, allopurinol, is a prodrug that is metabolised to oxipurinol by the action of both AOX and XOR (Reiter *et al.*, 1990, Ichida *et al.*, 1998, Pacher *et al.*, 2006, Yu *et al.*, 2009).When allopurinol was incubated with trout liver cytosol with O_2 as an electron acceptor no activity was detected indicating it was not a

substrate for AOX or XO in this species. Similar to the two xanthine substrates when NAD$^+$ was included in the incubation allopurinol was biotransformed to oxipurinol indicating that trout XDH was capable of this biotransformation. In contrast when the two mammalian liver cytosols were incubated with allopurinol, oxipurinol was formed with O$_2$ and NAD$^+$ (Figures 67 and 68) indicating AOX/XO and XDHs involvement in this drug biotransformation as has been previously shown by others (Reiter *et al.*, 1990, Yamamoto *et al.*, 1991, Moriwaki *et al.*, 1993) . The Km value of allopurinol with trout cytosol in presence of NAD$^+$ as an electron acceptor was 63.2 ± 0.98 μM with a Vmax value of 2.06 ± 0.75 nmol/min/mg protein, in contrast, the rat and human liver cytosol metabolise allopurinol as XO in presence of O$_2$ as an electron acceptor and with Km value of 20.9 ± 0.76 μM and 16.7 ± 0.05 μM respectively, and as XDH in presence of NAD$^+$ as an electron acceptor and with Km value of 15.30 ± 1.05 μM and 15.0 ± 0.25 μM respectively with rat and human. The Km value of trout XDH was four times more than that of rat and human XDH activity (Table 40). The NAD-dependant Vmax value for allopurinol as XDH substrate with Wistar rat and human was approximately 3 and 5-fold respectively more than that O$_2$-dependant Vmax value(Table 40).The Km results are in higher than that reported by Krenitsky *et al*. (1986) who reported that the allopurinol is an substrate of human liver XO with a low Km value of 1.7 μM (Krenitsky *et al.*, 1986).

4.1.4.4. 6-mercaptopurine (6MP)

In the present study, the anti-cancer drug 6-mercaptopurine (6-MP) was incubated with the cytosolic fraction of trout, rat and human. Both rat and human cytosolic fraction biotransformed 6-MP directly to 6-thiouric acid in the presence of NAD$^+$ or without NAD$^+$ (Figures 62a, 62b, 64a and 64b) and this activity was inhibited by the XOR inhibitor oxipurinol (Figures 63a and 65a) but was not inhibited by menadione

an AOX inhibitor (Figures 63b and 65b). This suggests XOR was the major enzyme responsible for 6-MP to 6-thiouric acid conversion in the two mammalian species. The NAD-dependant Km value for 6-MP as an XDH substrate with both mammalian are similar as in (Table 40). The NAD-dependant Vmax value for 6-MP with Wistar rat and human was approximately 3 and 6-fold greater than that O_2-dependant Vmax value (Table 40).In contrast no metabolites were formed when 6-MP was incubated with trout liver cytosol with or without NAD^+ (Figure 60) indicating this was not a substrate for trout AOX or XOR.

In order to determine if the structurally related metabolite of 6-MP, 6-thioxanthine was also not a substrate for the trout enzyme; 6-thioxanthine was incubated with trout liver cytosol with and without NAD^+. 6-thiouric acid was formed with both O_2 and NAD^+ as electron acceptors, with enhanced activity with NAD^+ (Figure 66). This activity was inhibited by the XOR inhibitor oxipurinol but not by the AOX inhibitor menadione (Figure 67).The NAD-dependant Vmax value for 6-thioxanthine as an XOR substrate with trout was approximately 3-fold greater than that O_2-dependant Vmax value (Table 40). Due to time constraints 6-thioxanthine was not used as a substrate for the mammalian species. The substrate specificity and species differences between 6-mercaptopurine and 6-thioxanthine in trout, rat and human XOR may be due to amino acid differences at the active site of the enzymes.

4.2. Determination of kinetic parameters for aldehyde oxidase and xanthine oxidoreductase inhibitors for trout, rat and human.

In this study preliminary experiments were performed with three well documented inhibitors of AOX and XOR. In this study the AOX inhibitor benzamidine did not have any effect with trout liver cytosol at two pH 7.4 and 9.0 as seen in (Figures 71a and 71b), while with human and rat liver cytosol it resulted in 80-90% inhibition using 100µM benzamidine. When the prototypical AOX inhibitor menadione was used the AOX activity was inhibited 80-92% in the three species tested using a 5 µM final concentration (Figure 70). The XOR inhibitor oxipurinol inhibited the two mammalian XORs 90-95% whereas the trout XOR was inhibited ∼ 60% with 100µM final concentration of this inhibitor (Figure 72).

In order to further understand the mode and kinetics of inhibition with trout AOX and XOR this was scrutinised with six different inhibitors and the mode of inhibition and Ki determined using Lineweaver-Burk plots. Menadione had a Ki of 0.17 ± 0.03µM and mode of inhibition non-competitive inhibition as seen in (Figures 73 and 74) and (Table 41). The inhibition effect of estradiol and 17α-ethinyl estradiol as inhibitors with trout AOX was uncompetitive with Ki values of 0.34 ± 0.05 µM and 0.44 ± 0.05 µM respectively (Figures 75, 76, 77 and 78). The mode of inhibition and Ki value of chlorpromazine as AOX inhibitor with trout was also tested and a Ki value of 0.76 ± 0.06 µM was obtained and mode of inhibition as competitive (Figures 79 and 80), the environmental pollutant NPAH phenanthridine was found to be competitive inhibitor of trout AOX with a Ki value of 0.77 ± 0.7 µM as in (Figures 81 and 82) which is 3-fold higher than that found with bovine AOX (Table 5). When the XOR inhibitor oxipurinol was tested with trout XOR the mode of inhibition was non-competitive

202

inhibition with Ki value of 0.37 ± 0.06 µM as in (Figures 84 and 85) as similar that it found with bovine in introduction (Table 6).

In conclusion all six different inhibitors tested displayed similar modes of inhibition in trout to that found in mammals (Table 4, 5 and 6).

4.3. Purification of AOX from rainbow trout and Wistar rat liver cytosol.

Prior to the purification of AOX from rainbow trout and Wistar rat liver a literature survey was carried out to establish the best methodologies to use to purify AOX.

AOX has been purified from many different species with different methodologies as summarised in the (Tables 21 and 22). Reviewing the literature on the subject reveals that the initial step of purification of AOX is generally subcellular fractionation to generate cytosol where the enzyme resides. A popular subsequent purification method used for AOX is heat precipitation as mammalian AOXs are thermotolerant. In some purification protocols buffers used to purify AOX contain dithiothreitol and cysteine to protect proteins containing sulfhydryl groups. (Rajagopalan and Handler. 1967, Felsted *et al.*, 1973, Andres. 1976, MacGibbon *et al.*, 1979, Yoshihara and Tatsumi. 1985, Stell *et al.*, 1989, Hughes *et al.*, 1994, Calzei *et al.*, 1995, Turner *et al.*, 1995, McManaman *et al.*, 1996, Yoshihara and Tatsumi. 1997, Sugihara *et al.*, 1999, Terao *et al.*, 2001, Maia and Mira. 2002, Kitamura *et al.*, 2003, Kurosaki *et al.*, 2004, Vila *et al.*, 2004, Terao *et al.*, 2006, Terao *et al.*, 2009, Mahro *et al.*, 2011). Prior to initiating experiments to purify AOX from the piscine species, in order to check procedures were operating successfully initially AOX was purified from Wistar rat liver cytosol using procedure 1 in materials and methods section (Figure 25). Heat treatment, Q-sepharose anion exchange chromatography, affinity chromatography using benzamidine 6B Sepharose column and MonoQ anion exchange chromatography successfully gave a 227-fold purification and a 22 % yield. The fold purification was about 4-fold lower than Maia and Mira (2002) found. When AOX was purified from rainbow trout a different procedure was used, as the piscine enzyme was more heat liable than that rodent enzyme with 80% activity lost after a brief 15 minute incubation at the 55°C standard temperature used for mammalian AOX purification

(Tables 21 and 22 and Figure 88). The heat treatment step was therefore omitted from the procedure for purification of AOX from rainbow trout. In addition the affinity chromatography step was also not useful for purification of AOX from rainbow trout, due to the benzamidine not being an effective inhibitor of rainbow trout AOX (Figure 71). The alternative procedure used to purify the AOX from rainbow trout liver started with the second step of the purification of AOX from rat liver, this was ammonium sulphate precipitation that successfully purified the piscine enzyme 3-fold. Subsequently a series of chromatography steps were carried out including Q-sepharose anion exchange chromatography, gel filtration chromatography on Superose 6 16/70 and the final step was MonoQ anion exchange chromatography. This resulted in a 210-fold purification and 12.9 % yield. The native molecular mass of rainbow trout AOX estimated using gel filtration was found to be similar to its mammalian, avian and insect counterparts being ~ 295 kDa (Table 22). SDS PAGE indicated the trout AOX had undergone extensive proteolysis as several low molecular mass polypeptides were apparent at less than the expected monomeric mass of the enzyme of 150 kDa. This result is in agreement with other researchers that purified AOX from another fish the Sea bream *(Pagrus major)* that also suggested proteolysis had occurred during purification (Kitamura *et al.*, 2003). Despite this the procedure used in this laboratory had a much enhanced success compared with Kitamura *et al*. (2003) in that the partially purified AOX from Sea bream liver was only purified 33-fold with a 5.5 % yield. A possible solution to the problems of purification of piscine AOX might be to add a protease inhibitors such as phenylmethylsulfonyl fluoride (PMSF).

Another solution to characterising purified AOX in fish is to use a recombinant protein expression system in which piscine AOX cDNA is expressed in bacteria and subsequently purified using a simple protocol that would avoid the proteases that are

found in animal liver. Such a system has been used successfully to study mouse, monkey, rat and human AOX (Kane *et al.*, 2006, Schumann *et al.*, 2009).

4.4. Conclusions.

This study aimed to determine whether a fish rainbow trout (*Oncorhynchus mykiss*) can biotransform AOX and XOR substrates like their mammalian counterparts. To date there has been no study of AOX in any Salmoniforme despite their commercial and scientific importance.

Rainbow trout AOX and XOR activities were tested in liver, kidney and gill cytosol and it was found exclusively in the liver using HPLC and spectrophotometric assays.

Hepatic cytosols of rainbow trout, human and rat were able to catalyse the oxidation of a range of MFE substrates to varying degrees. These included the exogenous aldehydes (DMAC and vanillin), endogenous vitamin substrates (all-trans retinal, pyridoxal and N^1-methylnicotinamide), NPAH environmental pollutants (phenanthridine, phthalazine and cinchonine), and drugs (allopurinol and pyrazinamide). The exogenous purine and purine analogues xanthine, 1-methylxanthine, 6-mercaptopurine, 6-thioxanthine were also biotransformed by XOR in all species tested (Table 1). The study also demonstrated that the XOR activity of rainbow trout was exclusively NAD^+-dependant activity unlike that in the two mammalian species tested (Table 40). When Eadie-Hofstee plots were used to determine kinetic values of rainbow trout MFE activities with different substrates and compared with human and rat and it was found that the Km was higher and the Vmax lower in rainbow trout. This study therefore demonstrated that a piscine AOX has the ability to metabolise several NPAH environmental pollutants and is capable of the oxidative biotransformation of several endogenous vitamin substrates like its mammalian counterparts. With regards to the physiological role of NPAH biotransformation by AOX this is an important detoxication mechanism as several studies *in vivo* and *ex vivo* have demonstrated that NPAHs are harmful. AOX

substrates phenanthridine, phthalazine, isoquinoline and acridine together with several benzoacridine and dibenzoacridine have been shown to be cytotoxic in cultured cell lines such as H4IIE rat hepatoma and mouse embryonic carcinoma P19/A15 cell lines (Sovadinova *et al.*, 2006, Beníšek *et al.*, 2011). Bleeker *et al* (1999) also demonstrated that NPAH compounds acridine, benzo[c]acridine, benzo[a]acridine, quinoline, benzo[f]quinoline, benzo[h]quinoline and phenanthridine were toxic to *Chironomus riparius* (midge) (Bleeker *et al.*, 1999). Benzoquinoline-diones have also been shown to be teratogenic to cricket embryos resulting in extra heads and legs (Walton *et al.*, 1983). Many of the harmful effects of NPAHs have also been documented in fish species. Baylock *et al*., (1985) found that acridine was toxic to fathead minnows (*Pimephales promelas*) (Blaylock *et al.*, 1985),whilst acridine and quinoline have also been shown to cause embryotoxicity in rainbow trout (*Salmo gairdneri=Oncorhynchus mykiss*) (Black *et al.*, 1983), largemouth bass (*Micropterus salmoides*) (Black *et al.*, 1983) and zebrafish (*Danio rerio*) (Peddinghaus *et al.*, 2012). As well as *in vivo* studies *ex vivo* work using the fish hepatoma PLHC-1 cell line (derived from *Poeciliopsis lucida*) has also shown that benzo[a]acridine and dibenz[a, h]acridine are cytotoxic (Jung *et al.*, 2001). Very recently research utilising the rainbow trout liver cell line RTL-W1 has shown that acridine is genotoxic in micronucleus assays (Brinkmann *et al.*, 2014). With regards compounds that interfere with AOX biotransformation several compounds were tested in these studies that have physiological importance. Endogenous steroids (estradiol) and drugs (menadione and chlorpromazine) and exogenous environmental pollutants (phenanthridine and 17α-ethinyl estradiol) were inhibitors of the piscine AOX enzyme. These results may therefore have important physiological consequences for fish that live in an aquatic environment exposed to pollutants such as NPAHs, estrogens and drugs(Furlong and

Carpenter. 1982, Jobling *et al.*, 1996, Schultz *et al.*, 2001, Schultz *et al.*, 2003, Vulliet and Cren-Olivé. 2011, Brulik *et al.*, 2013)as it may have effects on vitamin A, B3 or B6 metabolism (Spinneker *et al.*, 2007, Van der Sluijs *et al.*, 2011). With regards compounds that effect XOR biotransformation the compounds tested were of less physiological importance to a fish, but the results reveal species similarities and differences exist. Whereas oxipurinol was a potent inhibitor of XOR in all species tested, in contrast to the mammalian AOXs benzamidine did not inhibit the piscine AOX.

In order to further characterise trout AOX protein purification was carried out. In contrast to mammalian AOX, the piscine enzyme was not thermotolerant at 55°C nor was it inhibited by benzamidine, thus heat treatment and affinity chromatography could not be used as a purification steps. Trout AOX was purified 210-fold using ammonium sulphate fractionation, together with ion exchange and gel filtration chromatography. The native molecular mass of the piscine AOX was 295 kDa, which is similar to mammalian AOXs.

In conclusion this study yields new insight into groups of anthropogenic environmental pollutants, drugs and vitamins that are substrates and inhibitors of piscine AOX that is an ancestral vertebrate AOX.

4.5. Recommendations for future work.

This study could be expanded to analyse a wider range of xenobiotics including drugs that are potential piscine MFE substrates. A particular focus could be NPAHs which are well documented aquatic environmental pollutants (Blumer *et al.*, 1977, Balch *et al.*, 1995, Osborne *et al.*, 1997, de Voogt and Laane. 2009) that are cytotoxic, embryotoxic, teratogenic, genotoxic and carcinogenic (Southworth *et al.*, 1979, Balch *et al.*, 1995, Jung *et al.*, 2001, Barron *et al.*, 2004, Peddinghaus *et al.*, 2012, Brinkmann *et al.*, 2014).

Another set of compounds that could be tested are MFEs reductase substrates such as acetophenone oxime, salicylaldoxime, benzamidoxime, aromatic and heterocyclic hydroxamic acids, fenthion sulfoxide, sulindac sulfoxide and zonisamide (Table 2) some of which are found in aquatic environment.

Another area that could be researched is the induction of MFEs by NPAHs.

Although cytochrome P450 have been well documented to be induced by PAHs including NPAHs in mammals (Sovadinova *et al.*, 2006, Beníšek *et al.*, 2011) the effect of such compounds on MFEs have received scant attention. There have been the only two studies with two environmental polycyclic aromatic hydrocarbons (PAHs) demonstrating that such compounds can induce MFEs. Johnson *et al*., (1984) found that oral administration of the NPAH phthalazine (50mg/kg/day) to female rabbits caused an 2 to 3-fold increase in the activity of the hepatic AOX and XOR, whereas there was no effect on microsomal cytochrome P-450 activity (Johnson *et al.*, 1984). Sugihara *et al.*, (2001) demonstrated that 2, 3, 7, 8-tetrachlorodibenzo-p-dioxin (TCDD) induced hepatic XOR and AOX in liver of mice about 3-fold and 1.5-fold respectively (Sugihara *et al.*, 2001). This suggests that induction of MFEs in fish

might be a useful monitor for NPAH pollution to complement the use of CYP1A induction in environmental monitoring (Stagg *et al.*, 2000, Basu *et al.*, 2001, Tom *et al.*, 2001). In order to determine the extent of NPAHs induction of MFEs in fish, investigations could be conducted by treating fish in laboratory conditions with a range of NPAHs to determine if MFE induction occurs. MFEs could also be measured in fish from polluted environments to determine if there is a correlation between NPAHs levels and MFEs activity.

5. References

Al-Tayib, Y. 2009. *In vitro* hepatic metabolism of cinchona antimalarials by hamster enzymes. *J.B Ap Sci* 5**,** 17-25.

Andres, R. Y. 1976. Aldehyde oxidase and xanthine dehydrogenase from wild-type *Drosophila melanogaster* and immunologically cross-reacting material from *ma-1* mutants. Purification by immunoadsorption and characterization. *Eur J Biochem,* 62**,** 591-600.

Andrews, P. 1964. Estimation of the molecular weights of proteins by Sephadex gel-filtration. *Biochem J,* 91**,** 222-33.

Arnaud, M. J. 2011. Pharmacokinetics and metabolism of natural methylxanthines in animal and man. *Handb Exp Pharmacol,* 200**,** 33-91.

Asagba, S. O.,G. E. Eriyamremu,J. O. T. Emudainohwo & I. Okoro 2010. Oxidative enzymes in tissues of the catfish (Clarias gariepinus) exposed to varying levels of cadmium. *Environ,* 30**,** 260-266.

Balch, G.,C. Metcalfe & S. Huestis 1995. Identification of potential fish carcinogens in sediment from Hamilton Harbour, Ontario, Canada. *Environ Toxicol Chem,* 14**,** 79-91.

Barnabe, N.,J. A. Zastre,S. Venkataram & B. B. Hasinoff 2002. Deferiprone protects against doxorubicin-induced myocyte cytotoxicity. *Free Radic Biol Med,* 33**,** 266-75.

Barr, J. T. & J. P. Jones 2011. Inhibition of human liver aldehyde oxidase: implications for potential drug-drug interactions. *Drug Metab Dispos,* 39**,** 2381-6.

Barr, J. T. & J. P. Jones 2013. Evidence for substrate-dependent inhibition profiles for human liver aldehyde oxidase. *Drug Metab Dispos,* 41**,** 24-9.

Barron, M. G.,R. Heintz & S. D. Rice 2004. Relative potency of PAHs and heterocycles as aryl hydrocarbon receptor agonists in fish. *Mar Environ Res,* 58**,** 95-100.

Baselt, R. C. & R. H. Cravey 1996. *Disposition of toxic drugs and chemicals in man* Year Book medical Publishers, Inc.USA.

Basha, P. S. & A. U. Rani 2003. Cadmium-induced antioxidant defense mechanism in freshwater teleost *Oreochromis mossambicus* (Tilapia). *Ecotoxicol Environ Saf,* 56**,** 218-21.

Basu, N.,S. Billiard,N. Fragoso,A. Omoike,S. Tabash,S. Brown & P. Hodson 2001. Ethoxyresorufin-O-deethylase induction in trout exposed to mixtures of polycyclic aromatic hydrocarbons. *Environ Toxicol Chem,* 20**,** 1244-51.

Bean, R. M.,D. D. Dauble,B. L. Thomas,R. William Hanf Jr & E. K. Chess 1985. Uptake and biotransformation of quinoline by rainbow trout. *Aquatic Toxicology,* 7**,** 221-239.

Beedham, C. 1985. Molybdenum hydroxylases as drug metabolising enzymes. *Drug Metab. Rev. ,* 16**,** 11-156.

Beedham, C. 1987. Molybdenum hydroxylases: biological distribution and substrate-inhibitor specificity. *Prog Med Chem,* 24**,** 85-127.

Beedham, C. 1998. Oxidation of carbon via molybdenum hydroxylases. *Drug metab***,** 39-52.

Beedham, C. 2001. *Molybdenum hydroxylase, In: Enzyme Systems that Metabolise Drugs and Other Xenobiotics* C. Ioannides (Ed.),John Wiley & Sons Ltd

Beedham, C. 2010. *Xanthine oxidoreductase and aldehyde oxidase*, Comprehensive Toxicology Copyright, 2010 Elsevier Ltd. All rights reserved.

Beedham, C.,Y. Al-Tayib & J. A. Smith 1992. Role of guinea pig and rabbit hepatic aldehyde oxidase in oxidative *in vitro* metabolism of cinchona antimalarials. *Drug Metab Dispos,* 20**,** 889-95.

Beedham, C.,S. E. Bruce,D. J. Critchley & D. J. Rance 1990. 1-substituted phthalazines as probes of the substrate-binding site of mammalian molybdenum hydroxylases. *Biochem Pharmacol,* 39**,** 1213-21.

Beedham, C.,D. J. Critchley & D. J. Rance 1995. Substrate specificity of human liver aldehyde oxidase toward substituted quinazolines and phthalazines: a comparison with hepatic enzyme from guinea pig, rabbit, and baboon. *Arch Biochem Biophys,* 319**,** 481-90.

Begas, E.,E. Kouvaras,A. Tsakalof,S. Papakosta & E. K. Asprodini 2007. *In vivo* evaluation of CYP1A2, CYP2A6, NAT-2 and xanthine oxidase activities in a Greek population sample by the RP-HPLC monitoring of caffeine metabolic ratios. *Biomed Chromatogr,* 21**,** 190-200.

Behnke, R. J. 1992. Native trout of western North America. *American Fisheries Society monograph (USA). no. 6.*

Beníšek, M.,P. Kubincová,L. Bláha & K. Hilscherová 2011. The effects of PAHs and N-PAHs on retinoid signaling and Oct-4 expression *in vitro*. *Toxicology letters,* 200**,** 169-175.

Black, J. A.,W. J. Birge,A. G. Westerman & P. C. Francis 1983. Comparative aquatic toxicology of aromatic hydrocarbons. *Fundam Appl Toxicol,* 3**,** 353-8.

Blaylock, B.,M. Frank & J. McCarthy 1985. Comparative toxicity of copper and acridine to fish, Daphnia and algae. *Environ Toxicol Chem,* 4**,** 63-71.

Bleeker, E. A.,L. Noor,M. H. Kraak,P. de Voogt & W. Admiraal 2001. Comparative metabolism of phenanthridine by carp (*Cyprinus carpio*) and midge larvae (*Chironomus riparius*). *Environ Pollut,* 112**,** 11-7.

Bleeker, E. A. J.,H. A. Leslie,D. Groenendijk,M. Plans & W. Admiraal 1999. Effects of exposure to azaarenes on emergence and mouthpart development in the midge Chironomus riparius (Diptera : Chironomidae). *Environ Toxicol Chem,* 18**,** 1829-1834.

Blumer, M.,T. Dorsey & J. Sass 1977. Azaarenes in recent marine sediments. *Science,* 195**,** 283-5.

Bonner, P. L. R. 2007. *Protein Purification*, Taylor & Francis.

Borges, F.,E. Fernandes & F. Roleira 2002. Progress towards the discovery of xanthine oxidase inhibitors. *Curr Med Chem,* 9**,** 195-217.

Brinkmann, M.,H. Blenkle,H. Salowsky,K. Bluhm,S. Schiwy,A. Tiehm & H. Hollert 2014. Genotoxicity of heterocyclic PAHs in the micronucleus assay with the fish liver cell line RTL-W1. *PLoS One,* 9**,** e85692.

Brondino, C. D.,M. G. Rivas,M. J. Romao,J. J. Moura & I. Moura 2006. Structural and electron paramagnetic resonance (EPR) studies of mononuclear molybdenum enzymes from sulfate-reducing bacteria. *Acc Chem Res,* 39**,** 788-96.

Brondino, C. D.,M. J. Romao,I. Moura & J. J. G. Moura 2005 Molybdenum and tungsten enzymes: the xanthine oxidase family. *Curr. Opin. Chem. Biol.,* 10**,** 1-6.

Brulik, J.,Z. Simek & P. de Voogt 2013. A new liquid chromatography–tandem mass spectrometry method using atmospheric pressure photo ionization for the simultaneous determination of azaarenes and azaarones in Dutch river sediments. *J Chromatogr A,* 1294**,** 33-40.

Calzei, L.,C. Raviolo,E. Ghibaudi,L. de Gioia,M. Salmona,G. Cazzaniga,M. Kurosaki,M. Terao & G. E. 1995. Purification, cDNA cloning, and tissue distribution of bovine liver aldehyde oxidase. *J Biol Chem,* 270**,** 31037-45.

Chambon, P. 1996. A decade of molecular biology of retinoic acid receptors. *FASEB J,* 10**,** 940-54.

Chen, Q.,H. C. Park,M. S. Goligorsky,P. Chander,S. M. Fischer & S. S. Gross 2012. Untargeted plasma metabolite profiling reveals the broad systemic consequences of xanthine oxidoreductase inactivation in mice. *PLoS One,* 7**,** e37149.

Chen, Y. & D. H. Reese 2013. A screen for disruptors of the retinol (vitamin A) signaling pathway. *Birth Defects Res B Dev Reprod Toxicol,* 98**,** 276-82.

Chiamvimonvat, N.,B. O'Rourke,T. J. Kamp,R. G. Kallen,F. Hofmann,V. Flockerzi & E. Marban 1995. Functional consequences of sulfhydryl modification in the

pore-forming subunits of cardiovascular Ca2+ and Na+ channels. *Circ Res,* 76**,** 325-34.

Chladek, J.,J. Martinkova & L. Sispera 1997. An *in vitro* study on methotrexate hydroxylation in rat and human liver. *Physiol Res,* 46**,** 371-9.

Choi, E. Y.,A. L. Stockert,S. Leimkuhler & R. Hille 2004. Studies on the mechanism of action of xanthine oxidase. *J Inorg Biochem,* 98**,** 841-8.

Choughule, K. V.,J. T. Barr & J. P. Jones 2013. Evaluation of rhesus monkey and guinea pig hepatic cytosol fractions as models for human aldehyde oxidase. *Drug Metab & Dispos,* 41**,** 1852-1858.

Cleare, W. F.,S. Bree & M. P. Coughlan 1976. Urate oxidase and xanthine dehydrogenase activities in liver extracts from fish caught in Irish waters. *Comp Biochem Physiol B,* 54**,** 117-9.

Coelho, C.,M. Mahro,J. Trincao,A. T. Carvalho,M. J. Ramos,M. Terao,E. Garattini,S. Leimkuhler & M. J. Romao 2012. The first mammalian aldehyde oxidase crystal structure: insights into substrate specificity. *J Biol Chem,* 287**,** 40690-702.

Cook, P. F. & W. W. Cleland 2007. *Enzyme kinetics and mechanism*, Garland Sci New York.

Datta, R. R.,T. Cruickshank & J. P. Kumar 2011. Differential selection within the Drosophila retinal determination network and evidence for functional divergence between paralog pairs. *Evol Dev,* 13**,** 58-71.

De Moreno, M. R.,J. F. Smith & R. V. Smith 1985. Silver staining of proteins in polyacrylamide gels - increased sensitivity through a combined coomassie blue silver stain procedure. *Anal Biochem,* 151**,** 466-470.

de Voogt, P. & R. W. Laane 2009. Assessment of azaarenes and azaarones (oxidized azaarene derivatives) in the Dutch coastal zone of the North Sea. *Chemosphere,* 76**,** 1067-74.

Derbre, F.,B. Ferrando,M. C. Gomez-Cabrera,F. Sanchis-Gomar,V. E. Martinez-Bello,G. Olaso-Gonzalez,A. Diaz,A. Gratas-Delamarche,M. Cerda & J. Viña 2012. Inhibition of xanthine oxidase by allopurinol prevents skeletal muscle atrophy: role of p38 MAPKinase and E3 ubiquitin ligases. *PloS one,* 7**,** e46668.

Diamond, S.,J. Boer,T. P. Maduskuie, Jr.,N. Falahatpisheh,Y. Li & S. Yeleswaram 2010. Species-specific metabolism of SGX523 by aldehyde oxidase and the toxicological implications. *Drug Metab Dispos,* 38**,** 1277-85.

Dick, R. A.,D. B. Kanne & J. E. Casida 2005. Identification of aldehyde oxidase as the neonicotinoid nitroreductase. *Chem Res Toxicol,* 18**,** 317-323.

Dick, R. A.,D. B. Kanne & J. E. Casida 2007. Nitroso-imidacloprid irreversibly inhibits rabbit aldehyde oxidase. *Chem Res Toxicol,* 20**,** 1942-6.

Dickinson, W. J. 1970. The genetics of aldehyde oxidase in Drosophila melanogaster. *Gene,* 66**,** 487-96.

Dickinson, W. J. 1971. Aldehyde oxidase in *Drosophila melanogaster*: a system for genetic studies on developmental regulation. *Dev Biol,* 26**,** 77-86.

Duggan, D. E. 1981. Sulindac: therapeutic implications of the prodrug/pharmacophore equilibrium. *Drug Metab Rev,* 12**,** 325-37.

Elion, G. B. 1966. Enzymatic and metabolic studies with allopurinol. *Ann Rheum Dis,* 25**,** 608-14.

Engerson, T. D.,T. G. McKelvey,D. B. Rhyne,E. B. Boggio,S. J. Snyder & H. P. Jones 1987. Conversion of xanthine dehydrogenase to oxidase in ischemic rat tissues. *J Clin Invest,* 79**,** 1564-70.

Enroth, C.,B. T. Eger,K. Okamoto,T. Nishino & E. F. Pai 2000. Crystal structures of bovine milk xanthine dehydrogenase and xanthine oxidase: structure-based mechanism of conversion. *Proc Natl Acad Sci U S A,* 97**,** 10723-8.

Epifanio, J. & D. Philipp 1993. Linkage Analysis of 10 Enzyme Loci in the Genus Pomoxis (*Pisces: centrarchidae*). *Journal of Heredity,* 84**,** 116-121.

Epifanio, J. M. & D. P. Philipp 1994. Ontogeny of gene expression in Pomoxis (Pisces: Centrarchidae). *Developmental genetics,* 15**,** 119-128.

Falciani, F.,M. Terao,S. Goldwurm,A. Ronchi,A. Gatti,C. Minoia,M. Li Calzi,M. Salmona,G. Cazzaniga & E. Garattini 1994. Molybdenum(VI) salts convert the xanthine oxidoreductase apoprotein into the active enzyme in mouse L929 fibroblastic cells. *Biochem J,* 298 69-77.

Felsted, R. L. & S. Chaykin 1967. N1-methylnicotinamide oxidation in a number of mammals. *J Biol Chem,* 242**,** 1274-1279.

Felsted, R. L.,A. E. Chu & S. Chaykin 1973. Purification and properties of the aldehyde oxidases from hog and rabbit livers. *J Biol Chem,* 248**,** 2580-7.

Feng, G.-P.,P. Zhuang,L.-Z. Zhang,J.-Y. Liu,M. Duan,F. Zhao & W.-G. Yan 2012. Effects of water temperature on metabolic enzyme and antioxidase activities in juvenile Chinese sturgeon (*Acipenser sinensis*). *Acta Hydrobiologica Sinica,* 36**,** 137-142.

Fitzpatrick, T.,N. Amrhein,B. Kappes,P. Macheroux,I. Tews & T. Raschle 2007. Two independent routes of de novo vitamin B6 biosynthesis: not that different after all. *Biochem. J,* 407**,** 1-13.

Fridovich, I. & P. Handler 1962. Xanthine oxidase v. differential inhibition of the reduction of various electron acceptors. *J Biol Chem,* 237**,** 916-921.

Frost, S. K.,M. E. Borchert & S. Thorsteinsdottir 1986. Rapid and sensitive thin-layer chromatographic assay procedure for measuring xanthine dehydrogenase activity from tissue extracts. *J Chromatogr,* 382**,** 314-20.

Fukiya, K.,K. Itoh,S. Yamaguchi,A. Kishiba,M. Adachi,N. Watanabe & Y. Tanaka 2010. A single amino acid substitution confers high cinchonidine oxidation activity comparable with that of rabbit to monkey aldehyde oxidase 1. *Drug Metab Dispos,* 38**,** 302-7.

Furlong, E. T. & R. Carpenter 1982. Azaarenes in Puget Sound Sediments. *Geochimica Et Cosmochimica Acta,* 46**,** 1385-1396.

Garattini, E.,M. Fratelli & M. Terao 2008. Mammalian aldehyde oxidases: genetics, evolution and biochemistry. *Cell Mol Life Sci,* 65**,** 1019-48.

Garattini, E.,M. Fratelli & M. Terao 2009. The mammalian aldehyde oxidase gene family. *Hum Genomics,* 4**,** 119-30.

Garattini, E.,R. R. Mendel,M. J. Romao,R. Wright & M. Terao 2003. Mammalian molybdo-flavoenzymes, an expanding family of proteins: structure, genetics, regulation, function and pathophysiology. *Biochem J,* 372**,** 15-32.

Garattini, E. & M. Terao 2011. Increasing recognition of the importance of aldehyde oxidase in drug development and discovery. *Drug Metab Rev,* 43**,** 374-86.

Garattini, E. & M. Terao 2012. The role of aldehyde oxidase in drug metabolism. *Expert Opin Drug Metab Toxicol,* 8**,** 487-503.

Garattini, E. & M. Terao 2013. Aldehyde oxidase and its importance in novel drug discovery: present and future challenges. *Expert Opin Drug Discov,* 8**,** 641-54.

Ghassan, Z. A.,F. A. Muthanna,M. S. Ibrahim,Z. Omar,C. Mallikarjun,S. M. Elrashid,F. Y. Mun,H. Sakeena,B. Mahiran,A. S. Munavvar & M. N. Azmin 2010. HPLC method modification and validation for quantification of Ibuprofen. *Int J Pharm Sci,* 4**,** 404-409.

Glatigny, A. & C. Scazzocchio 1995. Cloning and molecular characterization of hxA, the gene coding for the xanthine dehydrogenase (purine hydroxylase I) of *Aspergillus nidulans*. *J Biol Chem,* 270**,** 3534-50.

Gustafson, D. L. & C. A. Pritsos 1992. Bioactivation of mitomycin C by xanthine dehydrogenase from EMT6 mouse mammary carcinoma tumors. *J Natl Cancer Inst,* 84**,** 1180-5.

Hall, W. W. & T. A. Krenitsky 1986. Aldehyde oxidase from rabbit liver: specificity toward purines and their analogs. *Archives Biochem Biophysic,* 251**,** 36-46.

Hamelin, B. A.,K. Xu,F. Valle,L. Manseau,M. Richer & M. LeBel 1994. Caffeine metabolism in cystic fibrosis: enhanced xanthine oxidase activity. *Clin Pharmacol Ther,* 56**,** 521-9.

Hari, P. & P. Neeraja 2012. Ambient ammonia stress on certain detoxifying enzymes in kidney tissues of fish, *Cyprinus carpio*. *Int J Pharm Biochem Sci,* 4**,** 213-217.

Harris, C. M. & V. Massey 1997. The oxidative half-reaction of xanthine dehydrogenase with NAD; reaction kinetics and steady-state mechanism. *J Biol Chem,* 272**,** 28335-41.

Hartmann, T.,M. Terao,E. Garattini,C. Teutloff,J. F. Alfaro,J. P. Jones & S. Leimkuhler 2012. The impact of single nucleotide polymorphisms on human aldehyde oxidase. *Drug Metab Dispos,* 40**,** 856-64.

Harvey, D. J. 2004. Aquaculture outlook. *Electronic Outlook report from the Economic Research Service LDP-AQS-20.*

Haung, D.,A. Furukawa & Y. Ichikawa 1999. Molecular cloning of retinal oxidase/aldehyde oxidase cDNAs from rabbit and mouse livers and functional expression of recombinant mouse retinal oxidase cDNA in Escherichia coli. *Arch Biochem Biophys. ,* 364(2):264-72.

Hegazi, M. M.,Z. I. Attia & O. A. Ashour 2010. Oxidative stress and antioxidant enzymes in liver and white muscle of Nile tilapia juveniles in chronic ammonia exposure. *Aquat Toxicol,* 99**,** 118-25.

Hille, R. 2005. Molybdenum-containing hydroxylases. *Arch Biochem Biophys,* 433**,** 107-16.

Hille, R. & T. Nishino 1995. Flavoprotein structure and mechanism. 4. Xanthine oxidase and xanthine dehydrogenase. *FASEB J,* 9**,** 995-1003.

Hille, R. & H. Sprecher 1987. On the mechanism of action of xanthine oxidase. Evidence in support of an oxo transfer mechanism in the molybdenum-containing hydroxylases. *J Biol Chem,* 262**,** 10914-10917.

Hirao, Y.,S. Kitamura & K. Tatsumi 1994. Epoxide reductase activity of mammalian liver cytosols and aldehyde oxidase. *Carcinogenesis,* 15**,** 739-43.

Holmes, R. S. 1979. Genetics, ontogeny, and testosterone inducibility of aldehyde oxidase isozymes in the mouse: evidence for two genetic loci (Aox-I and Aox-2) closely linked on chromosome 1. *Biochem Genet,* 17**,** 517-27.

Holmes, R. S. & J. L. Vandeberg 1986. Aldehyde dehydrogenases, aldehyde oxidase and xanthine oxidase from baboon tissues: phenotypic variability and subcellular distribution in liver and brain. *Alcohol,* 3**,** 205-14.

Huang, D. Y. & Y. Ichikawa 1994. Two different enzymes are primarily responsible for retinoic acid synthesis in rabbit liver cytosol. *Biochem Biophys Res Commun,* 205**,** 1278-83.

Huang, D. Y. & Y. Ichikawa 1997. Purification and characterization of a novel cytosolic NADP(H)-dependent retinol oxidoreductase from rabbit liver. *Biochim Biophys Acta,* 1338**,** 47-59.

Hughes, R. K.,B. Bennett & R. C. Bray 1994. Xanthine Dehydrogenase from Drosophila-Melanogaster - Purification and Properties of the Wild-Type

Enzyme and of a Variant Lacking Iron-Sulfur Centers (Vol 31, Pg 3073, 1992). *Biochem,* 33**,** 8384-8384.

Hunter, C. 1988. Cinchona spp.: micropropagation, and the in vitro production of quinine and quinidine. *Med Arom Plant I.* Springer.

ICH 1994. Validation of analytical methods: definitions and terminology. ICH Q2 A.

Ichida, K.,M. Yoshida,R. Sakuma & T. Hosoya 1998. Two siblings with classical xanthinuria type 1: significance of allopurinol loading test. *Intern Med,* 37**,** 77-82.

Idle, J. R. & F. J. Gonzalez 2007. Metabolomics. *Cell Metab,* 6**,** 348-51.

Isamah, G. K. & S. O. Asagba 2004. A comparative study on the archives of xanthine oxidase and aldehyde oxidase in different fish species from two rivers in the Western Niger-Delta. *Environ Monit Assess,* 91**,** 293-300.

Itoh, K.,M. Yamamura,W. Takasaki,T. Sasaki,A. Masubuchi & Y. Tanaka 2006. Species differences in enantioselective 2-oxidations of RS-8359, a selective and reversible MAO-A inhibitor, and cinchona alkaloids by aldehyde oxidase. *Biopharm Drug Dispos,* 27**,** 133-9.

Jobling, S.,J. P. Sumpter,D. Sheahan,J. A. Osborne & P. Matthiessen 1996. Inhibition of testicular growth in rainbow trout (Oncorhynchus mykiss) exposed to estrogenic alkylphenolic chemicals. *Environ Toxicol Chem,* 15**,** 194-202.

Johns, D. G. 1967. Human liver aldehyde oxidase: differential inhibition of oxidation of charged and uncharged substrates. *J Clin Invest,* 46**,** 1492-505.

Johnson, C.,C. Stubley-Beedham & J. G. Stell 1984. Elevation of molybdenum hydroxylase levels in rabbit liver after ingestion of phthalazine or its hydroxylated metabolite. *Biochem Pharmacol,* 33**,** 3699-705.

Johnson, M.,D. Hebbert & M. Moran 1993. Genetic analysis of populations of north-western Australian fish species. *Mar Freshwater Res,* 44**,** 673-685.

Jordan, C. G.,M. R. Rashidi,H. Laljee,S. E. Clarke,J. E. Brown & C. Beedham 1999. Aldehyde oxidase-catalysed oxidation of methotrexate in the liver of guinea-pig, rabbit and man. *J Pharm Pharmacol,* 51**,** 411-8.

Jung, D. K.,T. Klaus & K. Fent 2001. Cytochrome P450 induction by nitrated polycyclic aromatic hydrocarbons, azaarenes, and binary mixtures in fish hepatoma cell line PLHC-1. *Environ Toxicol Chem,* 20**,** 149-59.

Kamiński, Z. W. & M. M. Jeżewska 1985. Xanthine:NAD+ oxidoreductase in the liver of the teleostean fish *Cyprinus carpio. Comp Biochem Phys B,* 80**,** 371-375.

Kane, C. D.,O. L. Francone & K. A. Stevens 2006. Differential regulation of the cynomolgus, human, and rat acyl-CoA oxidase promoters by PPARalpha. *Gene,* 380**,** 84-94.

Katsura, H.,S. Kitamura & K. Tatsumi 1993. Purification and characterization of salicylhydroxamic acid reductase from rat liver. *Arch Biochem Biophys,* 302**,** 356-61.

Kawashima, K.,K. Hosoi,T. Naruke,T. Shiba,M. Kitamura & T. Watabe 1999. Aldehyde oxidase-dependent marked species difference in hepatic metabolism of the sedative-hypnotic, Zaleplon, between monkeys and rats. *Drug Metab Dispos,* 27**,** 422-428.

Kelley, E. E.,N. K. Khoo,N. J. Hundley,U. Z. Malik,B. A. Freeman & M. M. Tarpey 2010. Hydrogen peroxide is the major oxidant product of xanthine oxidase. *Free Radical Biology and Medicine,* 48**,** 493-498.

Kikuchi, H.,H. Fujisaki,T. Furuta,K. Okamoto,S. Leimkuhler & T. Nishino 2012. Different inhibitory potency of febuxostat towards mammalian and bacterial xanthine oxidoreductases: insight from molecular dynamics. *Sci Rep,* 2**,** 331.

Kisker, C. 1997. Molecular basis of sulfite oxidase deficiency from the structure of sulfite oxidase. *Cell,* 91**,** 973-983.

Kitamura, S.,K. Nakatani,K. Sugihara & S. Ohta 1999. Strain differences of the ability to hydroxylate methotrexate in rats. *Comp Biochem Physiol C Pharmacol Toxicol Endocrinol,* 122**,** 331-6.

Kitamura, S.,K. Nitta,Y. Tayama,C. Tanoue,K. Sugihara,T. Inoue,T. Horie & S. Ohta 2008. Aldehyde oxidase-catalyzed metabolism of N1-methylnicotinamide *in vivo* and *in vitro* in chimeric mice with humanized liver. *Drug Metab Dispos,* 36**,** 1202-5.

Kitamura, S.,K. N. K. Ohashi,K. Sugihara,R. Hosokawa,Y. Akagawa & S. Ohta 2001. Extremely high drug-reductase activity based on aldehyde oxidase in monkey liver. *Biol Pharm Bull,* 24**,** 856-9.

Kitamura, S.,K. Sugihara & S. Ohta 2006. Drug-metabolizing ability of molybdenum hydroxylases. *Drug Metab Pharmacokinet,* 21**,** 83-98.

Kitamura, S.,T. Suzuki,T. Kadota,M. Yoshida,K. Ohashi & S. Ohta 2003. In vitro metabolism of fenthion and fenthion sulfoxide by liver preparations of sea bream, goldfish, and rats. *Drug Metab Dispos,* 31**,** 179-86.

Kitamura, S. & K. Tatsumi 1983. Azoreductase activity of liver aldehyde oxidase. *Chem Pharm Bull (Tokyo),* 31**,** 3334-7.

Kitamura, S. & K. Tatsumi 1984. Involvement of liver aldehyde oxidase in the reduction of nicotinamide N-oxide. *Biochem Biophys Res Commun,* 120**,** 602-6.

Klecker, R. W.,R. L. Cysk & J. M. Collins 2006. Zebularine metabolism by aldehyde oxidase in hepatic cytosol from humans, monkeys, dogs, rats, and mice: influence of sex and inhibitors. *Bioorg Med Chem,* 14**,** 62-6.

Kraemer, H. J.,U. Feltkamp & H. Breithaupt 1998. Quantification of pyrazinamide and its metabolites in plasma by ionic-pair high-performance liquid chromatography. Implications for the separation mechanism. *J Chromatogr B Biomed Sci Appl,* 706**,** 319-28.

Krenitsky, T. A.,S. M. Neil,G. B. Elion & G. H. Hitchings 1972. A comparison of the specificities of xanthine oxidase and aldehyde oxidase. *Arch Biochem Biophys,* 150**,** 585-99.

Krenitsky, T. A.,T. Spector & W. W. Hall 1986. Xanthine oxidase from human liver: purification and characterization. *Arch Biochem Biophys,* 247**,** 108-19.

Krenitsky, T. A.,J. V. Tuttle,E. L. Cattau, Jr. & H. D. Wang 1974. A comparison of the distribution and electron acceptor specificities of xanthine oxidase and aldehyde oxidase. *Comp Biochem Physiol B,* 49**,** 687-703.

Kundu, T. K.,R. Hille,M. Velaytham & J. L. Zweier 2007. Characterization of superoxide production from aldehyde oxidase: an important source of oxidants in biological tissues. *Arch Biochem Biophys,* 460**,** 113-21.

Kuroisaki, M.,M. Terao,L. Calzi,S. Zanotta & E. Garattini 1996. Expression of xanthine oxidoreductase in mouse mammary epithelium during pregnancy and lactation: regulation of gene expression by glucocorticoids and prolactin. *Biochem J,* 319**,** 801-10.

Kurosaki, M.,M. Bolis,M. Fratelli,M. M. Barzago,L. Pattini,G. Perretta,M. Terao & E. Garattini 2013. Structure and evolution of vertebrate aldehyde oxidases: from gene duplication to gene suppression. *Cell Mol Life Sci,* 70**,** 1807-30.

Kurosaki, M.,S. Demontis,M. M. Barzago,E. Garattini & M. Terao 1999. Molecular cloning of the cDNA coding for mouse aldehyde oxidase: tissue distribution and regulation in vivo by testosterone. *Biochem J,* 341 71-80.

Kurosaki, M.,M. Li Calzi,E. Scanziani,E. Garattini & M. Terao 1995. Tissue- and cell-specific expression of mouse xanthine oxidoreductase gene *in vivo*: regulation by bacterial lipopolysaccharide. *Biochem J,* 306 225-34.

Kurosaki, M.,M. Terao,M. M. Barzago,A. Bastone,D. Bernardinello,M. Salmona & E. Garattini 2004. The aldehyde oxidase gene cluster in mice and rats. Aldehyde oxidase homologue 3, a novel member of the molybdo-flavoenzyme family with selective expression in the olfactory mucosa. *J Biol Chem,* 279**,** 50482-98.

Kurth, J. & A. Kubiciel 1984. Method for the photometric determination of aldehyde oxidase activity. *Biomed Biochim Acta,* 43**,** 1223-6.

Kurzawski, M.,K. Dziewanowski,K. Safranow & M. Drozdzik 2012. Polymorphism of genes involved in purine metabolism (XDH, AOX1, MOCOS) in kidney transplant recipients receiving azathioprine. *Ther Drug Monit,* 34**,** 266-74.

Laemmli, U. K. 1970. Cleavage of structural proteins during the assembly of the head of bacteriophage T4. *Nature,* 227**,** 680-5.

Lake, B.,S. Ball,J. Kao,A. Renwick,R. Price & J. Scatina 2002. Metabolism of zaleplon by human liver: evidence for involvement of aldehyde oxidase. *Xenobiotica,* 32**,** 835-847.

Lakshmanan, M. R.,C. S. Vaidyanathan & H. R. Cama 1964. Oxidation of vitamin A1 aldehyde and vitamin A2 aldehyde to the corresponding acids by aldehyde oxidase from different species. *Biochem J,* 90**,** 569-73.

LaVoie, E. J.,A. Shigematsu & D. Hoffmann 1985. Metabolites of phenanthridine formed by rat liver homogenate. *Drug Metab Dispos,* 13**,** 71-5.

Lee, R. D.,C. F. Thomas,R. G. Marietta & W. S. Stark 1996. Vitamin A, visual pigments, and visual receptors in Drosophila. *Microsc Res Tech,* 35**,** 418-430.

Lenfant, P. 2003. Demographic and genetic structures of white sea bream populations (*Diplodus sargus*, Linnaeus, 1758) inside and outside a Mediterranean marine reserve. *C R Bio,* 326**,** 751-760.

Leoni, C.,F. M. Buratti & E. Testai 2008. The participation of human hepatic P450 isoforms, flavin-containing monooxygenases and aldehyde oxidase in the biotransformation of the insecticide fenthion. *Toxicol Appl Pharmacol,* 233**,** 343-52.

Lindsley, D. & G. Zimm 1992 *The genome of Drosophila melanogaster.* , Academic Press, New York.

Liu, P.,S. Liang,B. J. Wang & R. C. Guo 2009. Construction of expression system of rabbit aldehyde oxidase cDNA for the clarification of species differences. *Eur J Drug Metab Pharmacokinet,* 34**,** 205-11.

MacGibbon, A. K.,R. L. Motion,K. E. Crow,P. D. Buckley & L. F. Blackwell 1979. Purification and properties of sheep-liver aldehyde dehydrogenases. *Eur J Biochem,* 96**,** 585-95.

Mahro, M.,N. F. Brás,N. M. Cerqueira,C. Teutloff,C. Coelho,M. J. Romão & S. Leimkühler 2013. Identification of Crucial Amino Acids in Mouse Aldehyde Oxidase 3 That Determine Substrate Specificity. *PloS one,* 8**,** e82285.

Mahro, M.,C. Coelho,J. Trincao,D. Rodrigues,M. Terao,E. Garattini,M. Saggu,F. Lendzian,P. Hildebrandt,M. J. Romao & S. Leimkuhler 2011. Characterization and crystallization of mouse aldehyde oxidase 3: from mouse liver to Escherichia coli heterologous protein expression. *Drug Metab Dispos,* 39**,** 1939-45.

Maia, L. & L. Mira 2002. Xanthine oxidase and aldehyde oxidase: a simple procedure for the simultaneous purification from rat liver. *Arch Biochem Biophys,* 400**,** 48-53.

Marshall, J. J. 1970. Comments on the use of Blue Dextran in gel chromatography. *J Chrom A,* 53**,** 379-380.

McCormack, J.,B. Allen & C. Hodnett 1978. Oxidation of quinazoline and quinoxaline by xanthine-oxidase and aldehyde oxidase. *J Heterocyclic Chem,* 15**,** 1249-1254.

McManaman, J. L.,M. C. Neville & R. M. Wright 1999. Mouse mammary gland xanthine oxidoreductase: purification, characterization, and regulation. *Arch Biochem Biophys,* 371**,** 308-16.

McManaman, J. L.,C. A. Palmer,R. M. Wright & M. C. Neville 2002 Functional regulation of xanthine oxidoreductase expression and localization in the mouse mammary gland: evidence of a role in lipid secretion. *J Physiol. ,* 1;545**,** 567-79.

McManaman, J. L.,V. Shellman,R. M. Wright & J. E. Repine 1996. Purification of rat liver xanthine oxidase and xanthine dehydrogenase by affinity chromatography on benzamidine-sepharose. *Arch Biochem Biophys,* 332**,** 135-41.

McMurtrey, K. D. & T. J. Knight 1984. Metabolism of acridine by rat-liver enzymes. *Mutat Res,* 140**,** 7-11.

Mehmedagic, A.,P. Verite,S. Menager,C. Tharasse,C. Chabenat,D. Andre & O. Lafont 1997. Determination of pyrazinamide and its main metabolites in rat urine by high-performance liquid chromatography. *J Chromatogr B Biomed Sci Appl,* 695**,** 365-72.

Mehmedagic, A.,P. Verite,S. Menager,C. Tharasse,C. Chabenat,D. Andre & O. Lafont 2002. Investigation of the effects of concomitant caffeine administration on the metabolic disposition of pyrazinamide in rats. *Biopharm Drug Dispos,* 23**,** 191-5.

Meister, A. 1990. On the transamination of enzymes. *Ann N Y Acad Sci,* 585**,** 13-31.

Mendel, R. R. 2013. The molybdenum cofactor. *J Biol Chem,* 288**,** 13165-72.

Mendel, R. R. & F. Bittner 2006a. Cell biology of molybdenum. *Biochimica. Et. Biophysica. Acta,* 1763**,** 621-635.

Mendel, R. R. & F. Bittner 2006b. Cell biology of molybdenum. . *Biochimica. Et. Biophysica. Acta,* 1763**,** 621-635.

Miller, J. & J. C. Miller 2005. *Statistics and Chemometrics for Analytical Chemistry*, Person education limited; Fifth edition.

Minoshima, S.,Y. Wang,K. Ichida,T. Nishino & N. Shimizu 1995. Mapping of the gene for human xanthine dehydrogenase (oxidase) (XDH) to band p23 of chromosome 2. *Cytogenet Cell Genet,* 68**,** 52-3.

Miyajima, M.,I. Sagami,S. Daff,C. T. Migita & T. Shimizu 2000. Azo reduction of methyl red by neuronal nitric oxide synthase: The important role of FMN in catalysis. *Biochem Biophysi R Com,* 275**,** 752-758.

Mooney, S.,J. E. Leuendorf,C. Hendrickson & H. Hellmann 2009. Vitamin B6: a long known compound of surprising complexity. *Molecules,* 14**,** 329-51.

Moriwaki, Y.,T. Yamamoto,Y. Nasako,S. Takahashi,M. Suda,K. Hiroishi,T. Hada & K. Higashino 1993. In vitro oxidation of pyrazinamide and allopurinol by rat liver aldehyde oxidase. *Biochem Pharmacol,* 46**,** 975-981.

Moriwaki, Y.,T. Yamamoto,S. Takahashi,Z. Tsutsumi & T. Hada 2001. Widespread cellular distribution of aldehyde oxidase in human tissues found by immunohistochemistry staining. *Histol Histopathol,* 16**,** 745-53.

Moriwaki, Y.,T. Yamamoto,K. Yamaguchi,S. Takahashi & K. Higashino 1996. Immunohistochemical localization of aldehyde and xanthine oxidase in rat tissues using polyclonal antibodies. *Histochem Cell Biol,* 105**,** 71-9.

Moriwaki, Y.,T. Yamamoto,J. Yamakita,S. Takahashi & K. Higashino 1998. Comparative localization of aldehyde oxidase and xanthine oxidoreductase activity in rat tissues. *Histochem J,* 30**,** 69-74.

Moura, J. J.,A. V. Xavier,M. Bruschi,J. Le Gall,D. O. Hall & R. Cammack 1976. A molybdenum-containing iron-sulphur protein from *Desulphovibrio gigas*. *Biochem Biophys Res Commun,* 72**,** 782-9.

Mu, P.,M. Zheng,M. Xu,Y. Zheng,X. Tang,Y. Wang,K. Wu,Q. Chen,L. Wang & Y. Deng 2014. N-oxide reduction of quinoxaline-1,4-dioxides catalyzed by porcine aldehyde oxidase SsAOX1. *Drug Metab Dispos,* 42**,** 511-9.

Murashige, K.,D. McDaniel & S. Chaykin 1966. N^1- methylnicotinamide oxidation in hog liver. *Biochimica et Biophysica Acta (BBA)-Enzymology and Biological Oxidation,* 118**,** 556-565.

Nakano, E. & A. H. Whiteley 1965. Differentiation of multiple molecular forms of four dehydrogenases in the teleost, Oryzias latipes, studied by disc electrophoresis. *J Exp Zool,* 159**,** 167-79.

Nirogi, R.,V. Kandikere,R. C. Palacharla,G. Bhyrapuneni,V. B. Kanamarlapudi,R. K. Ponnamaneni & A. K. Manoharan 2013. Identification of a suitable and selective inhibitor towards aldehyde oxidase catalyzed reactions. *Xenobiotica***,** 1-8.

Nishinaka, Y.,H. Masutani,H. Nakamura & J. Yodoi 2001. Regulatory roles of thioredoxin in oxidative stress-induced cellular responses. *Redox Rep,* 6**,** 289-95.

Nishino, T. 1994. The conversion of xanthine dehydrogenase to xanthine oxidase and the role of the enzyme in reperfusion injury. *J Biochem,* 116**,** 1-6.

Nishino, T.,Y. Amaya,S. Kawamoto,Y. Kashima & K. Okamoto 2002. Purification and characterization of multiple forms of rat liver xanthine oxidoreductase expressed in baculovirus-insect cell system. *J Biochem,* 132**,** 597-606.

Nishino, T. & T. Nishino 1989. The nicotinamide adenine dinucleotidebinding site of chicken liver xanthine dehydrogenase: evidence for alteration of the redox potential of the flavin by NAD-binding or modification of the NAD-binding site and isolation of a modified peptide. *J. Biol. Chem. ,* 264**,** 5458-5473.

Nishino, T. & T. Nishino 1997. The conversion from the dehydrogenase type to the oxidase type of rat liver xanthine dehydrogenase by modification of cysteine residues with fluorodinitrobenzene. *J Biol Chem,* 272**,** 29859-64.

Nishino, T. & K. Okamoto 2000. The role of the [2Fe-2s] cluster centers in xanthine oxidoreductase. *J Inorg Biochem,* 82**,** 43-9.

Nishino, T.,K. Okamoto,B. T. Eger,E. F. Pai & T. Nishino 2008. Mammalian xanthine oxidoreductase - mechanism of transition from xanthine dehydrogenase to xanthine oxidase. *FEBS J,* 275**,** 3278-89.

Nishino, T.,L. M. Schopfer & V. Massey 1989. Reactivity of chicken liver xanthine dehydrogenase containing modified flavins. *J Biol Chem,* 264**,** 6075-85.

Obach, R. S. 2004. Potent inhibition of human liver aldehyde oxidase by raloxifene. *Drug Metab Dispos,* 32**,** 89-97.

Obach, R. S.,P. Huynh,M. C. Allen & C. Beedham 2004. Human liver aldehyde oxidase: inhibition by 239 drugs. *J Clin Pharmacol,* 44**,** 7-19.

Ohkubo, M. & S. Fujimura 1978. Loss of activity of an N1-methyl-4-pyridone-5-carboxamide-forming N1-methylnicotinamide oxidase in livers of rats fed 2-acetylaminofluorene. *Cancer Res,* 38**,** 697-702.

Okamoto, K.,B. T. Eger,T. Nishino,S. Kondo,E. F. Pai & T. Nishino 2003. An extremely potent inhibitor of xanthine oxidoreductase. Crystal structure of the enzyme-inhibitor complex and mechanism of inhibition. *J Biol Chem,* 278**,** 1848-55.

Okamoto, K.,B. T. Eger,T. Nishino,E. F. Pai & T. Nishino 2008. Mechanism of inhibition of xanthine oxidoreductase by allopurinol: crystal structure of reduced bovine milk xanthine oxidoreductase bound with oxipurinol. *Nucleosides Nucleotides Nucleic Acids,* 27**,** 888-93.

Okamoto, K.,T. Kusano & T. Nishino 2013. Chemical nature and reaction mechanisms of the molybdenum cofactor of xanthine oxidoreductase. *Curr Pharm Des,* 19**,** 2606-14.

Okamoto, K.,K. Matsumoto,R. Hille,B. T. Eger,E. F. Pai & T. Nishino 2004. The crystal structure of xanthine oxidoreductase during catalysis: implications for reaction mechanism and enzyme inhibition. *Proc Natl Acad Sci U S A,* 101**,** 7931-6.

Osborne, P. J.,M. R. Preston & H.-y. Chen 1997. Azaarenes in sediments, suspended particles and aerosol associated with the River Mersey estuary. *Mar Chem,* 58**,** 73-83.

Pacher, P.,A. Nivorozhkin & C. Szabo 2006. Therapeutic effects of xanthine oxidase inhibitors: renaissance half a century after the discovery of allopurinol. *Pharmacol Rev,* 58**,** 87-114.

Palmer, K. H.,B. Martin,B. Baggett & M. E. Wall 1969. The metabolic fate of orally administered quinidine gluconate in humans. *Biochem Pharmacol,* 18**,** 8145-60.

Pan, S. S.,P. A. Andrews,C. J. Glover & N. R. Bachur 1984. Reductive activation of mitomycin C and mitomycin C metabolites catalyzed by NADPH-cytochrome P-450 reductase and xanthine oxidase. *J Biol Chem,* 259**,** 959-66.

Pandey, S.,S. Parvez,I. Sayeed,R. Haque,B. Bin-Hafeez & S. Raisuddin 2003. Biomarkers of oxidative stress: a comparative study of river Yamuna fish Wallago attu (Bl. & Schn.). *Sci Total Environ,* 309**,** 105-15.

Panoutsopoulos, G. I. & C. Beedham 2004. Enzymatic oxidation of phthalazine with guinea pig liver aldehyde oxidase and liver slices: inhibition by isovanillin. *Acta Biochim Pol,* 51**,** 943-51.

Panoutsopoulos, G. I.,D. Kouretas,E. G. Gounaris & C. Beedham 2005. Enzymatic oxidation of vanillin, isovanillin and protocatechuic aldehyde with freshly prepared Guinea pig liver slices. *Cell Physiol Biochem,* 15**,** 89-98.

Pasalic, D.,N. Marinkovic & L. Feher-Turkovic 2012. Uric acid as one of the important factors in multifactorial disorders - facts and controversies. *Biochemia Medica,* 22**,** 63-75.

Pay, G. F.,R. B. Wallis & D. Zelaschi 1980. A metabolite of sulphinpyrazone that is largely responsible for the effect of the drug on the platelet prostaglandin pathway. *Biochem Soc Trans,* 8**,** 727-8.

Peddinghaus, S.,M. Brinkmann,K. Bluhm,A. Sagner,G. Hinger,T. Braunbeck,A. Eisenträger,A. Tiehm,H. Hollert & S. H. Keiter 2012. Quantitative assessment of the embryotoxic potential of NSO-heterocyclic compounds using zebrafish (*Danio rerio*). *Reproductive Toxicology,* 33**,** 224-232.

Peixoto, F. P.,J. Carrola,A. M. Coimbra,C. Fernandes,P. Teixeira,L. Coelho,I. Conceicao,M. M. Oliveira & A. Fontainhas-Fernandes 2013. Oxidative stress responses and histological hepatic alterations in barbel, barbus bocagei, from vizela river, portugal. *Rev Inter de Contam Amb,* 29**,** 29-38.

Peretz, H.,M. S. Naamati,D. Levartovsky,A. Lagziel,E. Shani,I. Horn,H. Shalev & D. Landau 2007. Identification and characterization of the first mutation (Arg776Cys) in the c-terminal domain of the human molybdenum cofactor sulfurase (HMCS) associated with type II classical xanthinuria. *Mol Genet Metab,* 91**,** 23-9.

Peretz, H.,D. G. Watson,G. Blackburn,T. Zhang,A. Lagziel,M. Shtauber-Naamati,T. Morad,E. Keren-Tardai,V. Greenshpun,S. Usher,H. Shalev,D. Landau & D. Levartovsky 2012. Urine metabolomics reveals novel physiologic functions of

human aldehyde oxidase and provides biomarkers for typing xanthinuria. *Metab,* 8**,** 951-959.

Pirouzpanah, S.,M. R. Rashidi,A. Delazar,S. V. Razavieh & A. Hamidi 2006. Inhibitory effects of Ruta graveolens L. extract on guinea pig liver aldehyde oxidase. *Chem Pharm Bull (Tokyo),* 54**,** 9-13.

Pometto, A. L., 3rd & D. L. Crawford 1983. Whole-cell bioconversion of vanillin to vanillic acid by *Streptomyces viridosporus*. *Appl Environ Microbiol,* 45**,** 1582-5.

Porter, D. J. 1990. Xanthine oxidase-catalyzed reductive debromination of 6-(bromomethyl)-9H-purine with concomitant covalent modification of the FAD prosthetic group. *J Biol Chem,* 265**,** 13540-6.

Prichard, M.,N. G. Ducharme,P. A. Wilkins,H. N. Erb & M. Butt 1991. Xanthine oxidase formation during experimental ischemia of the equine small intestine. *Can J Vet Res,* 55**,** 310-4.

Pryde, D. C.,D. Dalvie,Q. Hu,P. Jones,R. S. Obach & T. D. Tran 2010. Aldehyde oxidase: an enzyme of emerging importance in drug discovery. *J Med Chem,* 53**,** 8441-60.

Rajagopalan, K. & P. Handler 1964a. Hepatic aldehyde oxidase II. differential inhibition of electron transfer to various electron acceptors. *J of Biolo Chem,* 239**,** 2022-2026.

Rajagopalan, K. & P. Handler 1964b. Hepatic aldehyde oxidase III. The substrate-binding site. *Journal of Biological Chemistry,* 239**,** 2027-2035.

Rajagopalan, K. V.,I. Fridovich & P. Handler 1962. Hepatic aldehyde oxidase. I. Purification and properties. *J Biol Chem,* 237**,** 922-8.

Rajagopalan, K. V. & P. Handler 1967. Purification and properties of chicken liver xanthine dehydrogenase. *J Biol Chem,* 242**,** 4097-107.

Rajagopalan, K. V.,P. Handler,G. Palmer & H. Beinert 1968. Studies of aldehyde oxidase by electron paramagnetic resonance spectroscopy. II. Kinetic studies by rapid freezing. *J Biol Chem,* 243**,** 3797-806.

Räsänen, L. A.,U. Karvonen & A. R. Pösö 1993. Localization of xanthine dehydrogenase mRNA in horse skeletal muscle by in situ hybridization with digoxigenin-labelled probe. *Biochem J. ,* 15;292 (Pt 3)**,** 639-41.

Rashidi, M. 1996. *In vitro oxidation of purines by hepatic molybdenum hydroxylases.* PhD Thesis, University of Bradford.

Rashidi, M. R.,C. Beedham,S. Smith & S. Davaran 2007. *In vitro* Study of 6-mercaptopurine Oxidation Catalysed by Aldehyde Oxidase and Xanthine Oxidase. *Drug Metab. Pharmacokinet. ,* 22 299–306.

Rashidi, M. R.,M. Dehghany,G. Dehghan,A. Jouyban & A. Faridi 2013. Aldehyde oxidase activity and stability in water-miscible organic solvents. *Appl Biochem Biotechnol,* 169**,** 901-10.

Rashidi, M. R.,J. A. Smith,S. E. Clarke & C. Beedham 1997. In vitro oxidation of famciclovir and 6-deoxypenciclovir by aldehyde oxidase from human, guinea pig, rabbit, and rat liver. *Drug Metab Dispos,* 25**,** 805-13.

Reinke, L. A.,M. Nakamura,L. Logan,H. D. Christensen & J. M. Carney 1987. *In vivo* and *in vitro* 1-methylxanthine metabolism in the rat. Evidence that the dehydrogenase form of xanthine oxidase predominates in intact perfused liver. *Drug Metab Dispos,* 15**,** 295-9.

Reiter, S.,H. A. Simmonds,N. Zollner,S. L. Braun & M. Knedel 1990. Demonstration of a combined deficiency of xanthine oxidase and aldehyde oxidase in xanthinuric patients not forming oxipurinol. *Clin Chim Acta,* 187**,** 221-34.

Relling, M. V.,J. S. Lin,G. D. Ayers & W. E. Evans 1992. Racial and gender differences in N-acetyltransferase, xanthine oxidase, and CYP1A2 activities. *Clin Pharmacol Ther,* 52**,** 643-58.

Resende, A. D.,E. Rocha & A. Lobo-Da-Cunha 2005. Activity of purine catabolism enzymes during the reproductive cycle of male and female brown trout (*Salmo trutta*). *Trends in Comparative Endocrinol and Neurobiol.* New York: New York Acad Sciences.

Robertson, I. G. & T. J. Bland 1993. Inhibition by SKF-525A of the aldehyde oxidase-mediated metabolism of the experimental antitumour agent acridine carboxamide. *Biochem Pharmacol,* 45**,** 2159-62.

Romao, M. J.,M. Archer,I. Moura,J. J. Moura,J. LeGall,R. Engh,M. Schneider,P. Hof & R. Huber 1995. Crystal structure of the xanthine oxidase-related aldehyde oxido-reductase from *D. gigas. Science,* 270**,** 1170-6.

Sahi, J.,K. K. Khan & C. B. Black 2008. Aldehyde oxidase activity and inhibition in hepatocytes and cytosolic fractions from mouse, rat, monkey and human. *Drug Metab Lett,* 2**,** 176-83.

Sasai, Y. & E. M. De Robertis 1997. Ectodermal patterning in vertebrate embryos. *Dev Biol,* 182**,** 5-20.

Sastry, K. & D. Rao 1982. Chronic effects of mercuric chloride on the activities of some enzymes in certain tissues of the fresh water murrel, *(Channa punctatus). Chemosph,* 11**,** 1203-1209.

Sastry, K. & D. Rao 1984. Effect of mercuric chloride on some biochemical and physiological parameters of the freshwater murrel, Channa punctatus. *Environ Res,* 34**,** 343-350.

Schlenk, D. 1998. Occurrence of flavin-containing monooxygenases in non-mammalian eukaryotic organisms. *Comp Biochem Physiol C Pharmacol Toxicol Endocrinol,* 121**,** 185-95.

Schofield, P. C.,I. G. Robertson & J. W. Paxton 2000. Inter-species variation in the metabolism and inhibition of N-[(2′-dimethylamino) ethyl] acridine-4-carboxamide (DACA) by aldehyde oxidase. *Biochemical pharmacology,* 59**,** 161-165.

Schrader, T.,A. Rienhofer & J. R. Andreesen 1999. Selenium-containing xanthine dehydrogenase from Eubacterium barkeri. *Eur J Biochem,* 264**,** 862-71.

Schultz, I. R.,G. Orner,J. L. Merdink & A. Skillman 2001. Dose-response relationships and pharmacokinetics of vitellogenin in rainbow trout after intravascular administration of 17alpha-ethynylestradiol. *Aquat Toxicol,* 51**,** 305-18.

Schultz, I. R.,A. Skillman,J. M. Nicolas,D. G. Cyr & J. J. Nagler 2003. Short term exposure to 17α ethynylestradiol decreases the fertility of sexually maturing male rainbow trout (*Oncorhynchus mykiss*). *Environ Toxicol Chem,* 22**,** 1272-1280.

Schumann, S.,M. Terao,E. Garattini,M. Saggu,F. Lendzian,P. Hildebrandt & S. Leimkuhler 2009. Site directed mutagenesis of amino acid residues at the active site of mouse aldehyde oxidase AOX1. *PLoS One,* 4**,** e5348.

Schwartz, R. & N. O. Kjeldgaard 1951. The enzymic oxidation of pyridoxal by liver aldehyde oxidase. *Biochem J,* 48**,** 333-7.

Seeley, T. L.,P. B. Mather & R. S. Holmes 1984. Electrophoretic analyses of alcohol dehydrogenase, aldehyde dehydrogenase, aldehyde reductase, aldehyde oxidase and xanthine oxidase from horse tissues. *Comp Biochem Physiol B,* 78**,** 131-9.

Seki, T.,K. Isono,K. Ozaki,Y. Tsukahara,Y. Shibata-Katsuta,M. Ito,T. Irie & M. Katagiri 1998. Priority Paper The metabolic pathway of visual pigment chromophore formation in Drosophila melanogaster. *Europ J Biochem,* 257**,** 522-527.

Shibata, K.,T. Kawada & K. Iwai 1988. Simultaneous micro-determination of nicotinamide and its major metabolites, N1-methyl-2-pyridone-5-carboxamide and N1-methyl-4-pyridone-3-carboxamide, by high-performance liquid chromatography. *J Chromatogr,* 424**,** 23-8.

Shibutani, Y.,T. Ueo,T. Yamamoto,S. Takahashi,Y. Moriwaki & K. Higashino 1999. A case of classical xanthinuria (type 1) with diabetes mellitus and Hashimoto's thyroiditis. *Clin Chim Acta,* 285**,** 183-9.

Shimada, S.,H. K. Mishima,H. Nikaido,S. Kitamura & K. Tatsumi 1989. Purification of aldehyde oxidase from bovine ciliary body. *Curr Eye Res,* 8**,** 721-6.

Singh, R. K.,K. K. Lal,V. Mohindra,P. Punia,R. S. Sah,A. K. Mishra,R. Kumar,B. Mishra & W. Lakra 2010. Assessing genetic differentiation in geographic populations of Labeo calbasu using allozyme markers. *Biochem genet,* 48**,** 760-778.

Slef, W. T. & T. C. Stadtman 2000. Selenium-dependent metabolism of purines: A selenium-dependent purine hydroxylase and xanthine dehydrogenase were purified from *Clostridium purinolyticum* and characterized. *PNAS* 97**,** 7208-7213.

Smith, P. & A. Jamieson 1978. Enzyme polymorphisms in the atlantic mackerel Scomber scombrus. *Comp Biochem & Physiol Part B: Comp Bio chem,* 60**,** 487-489.

Smith, P. K.,R. I. Krohn,G. T. Hermanson,A. K. Mallia,F. H. Gartner,M. D. Provenzano,E. K. Fujimoto,N. M. Goeke,B. J. Olson & D. C. Klenk 1985. Measurement of protein using bicinchoninic acid. *Anal Biochem,* 150**,** 76-85.

Snell, E. E. 1990. Vitamin B6 and decarboxylation of histidine. *Ann N Y Acad Sci,* 585**,** 1-12.

Sorouraddin, M.-H.,E. Fooladi,A. Naseri & M.-R. Rashidi 2008. A novel spectrophotometric method for determination of kinetic constants of aldehyde oxidase using multivariate calibration method. *J Biochem Biophys Methds,* 70**,** 999-1005.

Sorouraddin, M.-H.,M.-Y. Khani,K. Amini,A. Naseri,D. Asgari & M.-R. Rashidi 2011. Simultaneous determination of 6-mercaptopurine and its oxidative metabolites in synthetic solutions and human plasma using spectrophotometric multivariate calibration methods. *BioImpacts : BI,* 1**,** 53-62.

Sorouraddin, M. H.,E. Fooladi,A. Naseri & M. R. Rashidi 2009. Development of a sensitive spectrofluorometric-multivariate calibration method for enzyme kinetic of aldehyde oxidase. *Iran J Pharm Res,* 8**,** 169-177.

Southworth, G.,B. Parkhurst & J. Beauchamp 1979. Accumulation of acridine from water, food, and sediment by the fathead minnow, Pimephales promelas. *Water, Air, and Soil Pollution,* 12**,** 331-341.

Sovadinova, I.,L. Blaha,J. Janosek,K. Hilscherova,J. P. Giesy,P. D. Jones & I. Holoubek 2006. Cytotoxicity and aryl hydrocarbon receptor-mediated activity of n-heterocyclic polycyclic aromatic hydrocarbons: structure-activity relationships. *Environ Toxicol Chem,* 25**,** 1291-7.

Spinneker, A.,R. Sola,V. Lemmen,M. Castillo,K. Pietrzik & M. Gonzalez-Gross 2007. Vitamin B 6 status, deficiency and its consequences-an overview. *Nutrición Hospitalaria,* 22**,** 0212-1611.

Stagg, R. M.,J. Rusin,M. E. McPhail,A. D. McIntosh,C. F. Moffat & J. A. Craft 2000. Effects of polycyclic aromatic hydrocarbons on expression of CYP1A in salmon (*Salmo salar*) following experimental exposure and after the Braer oil spill. *Environ Toxicol Chem,* 19**,** 2797-2805.

Stanulovic, M. & S. Chaykin 1971. Aldehyde oxidase: catalysis of the oxidation of N 1 -methylnicotinamide and pyridoxal. *Arch Biochem Biophys,* 145**,** 27-34.

Stell, J. G.,A. J. Warne & C. Lee-Woolley 1989. Purification of rabbit liver aldehyde oxidase by affinity chromatography on benzamidine sepharose 6B. *J Chromatogr,* 475**,** 363-72.

Stirpe, F. & E. Della Corte 1969. The regulation of rat liver xanthine oxidase. Conversion in vitro of the enzyme activity from dehydrogenase (type D) to oxidase (type O). *J Biol Chem,* 244**,** 3855-63.

Stoddart, A. M. & W. G. Levine 1992. Azoreductase activity by purified rabbit liver aldehyde oxidase. *Biochem Pharmacol,* 43**,** 2227-35.

Streetman, D. S.,J. S. Bertino, Jr. & A. N. Nafziger 2000. Phenotyping of drug-metabolizing enzymes in adults: a review of in-vivo cytochrome P450 phenotyping probes. *Pharmacogen,* 10**,** 187-216.

Stubley, C. & J. Stell 1980. Investigation of the substrate-binding site of aldehyde oxidase. *J Pharm Pharmacol,* 32**,** 51P-51P.

Stubley, C.,J. G. Stell & D. W. Mathieson 1979. The oxidation of azaheterocycles with mammalian liver aldehyde oxidase. *Xenobiotica,* 9**,** 475-84.

Sugihara, K.,Y. Katsuma,S. Kitamura,S. Ohta,M. Fujitani & H. Shintani 2000. Cynomolgus monkey liver aldehyde oxidase: extremely high oxidase activity and an attempt at purification. *Comp Biochem Phys C,* 126**,** 53-60.

Sugihara, K.,Y. Katsuma,C. Tanaka & S. Kitamura 1999. Purification and some properties of hamster liver aldehyde oxidase. *Biol Pharm Bull,* 22**,** 1246-8.

Sugihara, K.,S. Kitamura & K. Tatsumi 1996. S-(-)-nicotine-1'-N-oxide reductase activity of rat liver aldehyde oxidase. *Biochem Mol Biol Int,* 40**,** 535-41.

Sugihara, K.,S. Kitamura,K. Tatsumi,T. Asahara & K. Dohi 1997. Differences in aldehyde oxidase activity in cytosolic preparations of human and monkey liver. *Biochem Mol Biol Int,* 41**,** 1153-60.

Sugihara, K.,S. Kitamura,T. Yamada,S. Ohta,K. Yamashita,M. Yasuda & Y. Fujii-Kuriyama 2001. Aryl Hydrocarbon Receptor (AhR)-Mediated Induction of Xanthine Oxidase/Xanthine Dehydrogenase Activity by 2, 3, 7, 8-Tetrachlorodibenzo-p-dioxin. *Biochem Biophys Res communications,* 281**,** 1093-1099.

Sugihara, K. & K. Tatsumi 1986. Participation of liver aldehyde oxidase in reductive metabolism of hydroxamic acids to amides. *Arch Biochem Biophys,* 247**,** 289-93.

Sugihara, K.,Y. Tayama,K. Shimomiya,D. Yoshimoto,S. Ohta & S. Kitamura 2006. Estimation of aldehyde oxidase activity in vivo from conversion ratio of N1-methylnicotinamide to pyridones, and intraspecies variation of the enzyme activity in rats. *Drug Metab Dispos,* 34**,** 208-12.

Szafarz, M.,M. Lomnicka,M. Sternak,S. Chlopicki & J. Szymura-Oleksiak 2010. Simultaneous determination of nicotinic acid and its four metabolites in rat

plasma using high performance liquid chromatography with tandem mass spectrometric detection (LC/MS/MS). *J Chromatogr B Analyt Technol Biomed Life Sci.,* 878**,** 895-902.

Talwar, D.,T. Quasim,D. C. McMillan,J. Kinsella,C. Williamson & D. S. J. O'Reilly 2003. Optimisation and validation of a sensitive high-performance liquid chromatography assay for routine measurement of pyridoxal 5-phosphate in human plasma and red cells using pre-column semicarbazide derivatisation. *J Chromatogr B,* 792**,** 333-343.

Tatsumi, K. & M. Ishigai 1987. Oxime-metabolizing activity of liver aldehyde oxidase. *Arch Biochem Biophys,* 253**,** 413-8.

Tatsumi, K.,S. Kitamura,M. Kato & K. Hiraoka 1992. Metabolism of sodium nifurstyrenate, a veterinary antimicrobial nitrofuran, in animals and fish. *Drug Metab Dispos,* 20**,** 226-33.

Tatsumi, K.,S. Kitamura & N. Narai 1986. Reductive metabolism of aromatic nitro compounds including carcinogens by rabbit liver preparations. *Cancer Res,* 46**,** 1089-93.

Tatsumi, K.,H. Yamada & S. Kitamura 1983. Evidence for involvement of liver aldehyde oxidase in reduction of nitrosamines to the corresponding hydrazine. *Chem Pharm Bull (Tokyo),* 31**,** 764-7.

Tawa, M.,K. Yamamizu,A. Geddawy,T. Shimosato,T. Imamura,K. Ayajiki & T. Okamura 2011. Impairment by hypoxia or hypoxia/reoxygenation of nitric oxide-mediated relaxation in isolated monkey coronary artery: the role of intracellular superoxide. *J Pharmacol Sci,* 116**,** 188-96.

Tayama, Y.,K. Miyake,K. Sugihara,S. Kitamura,M. Kobayashi,S. Morita,S. Ohta & K. Kihira 2007. Developmental changes of aldehyde oxidase activity in young Japanese children. *Clin Pharmacol Ther,* 81**,** 567-72.

Temple, N. J.,P. Martin & M. Connock 1979. Intestinal peroxisomes of goldfish (*Carassius auratus*) examination for hydrolase, dehydrogenase and carnitine acetyltransferase activities. *Comp Biochem & Physiol Part B: Comp Biochem,* 64**,** 57-63.

Terao, M.,G. Cazzaniga,P. Ghezzi,M. Bianchi,F. Falciani,P. Perani & E. Garattini 1992. Molecular cloning of a cDNA coding for mouse liver xanthine dehydrogenase. Regulation of its transcript by interferons in vivo. *Biochem J,* 283 (Pt 3)**,** 863-70.

Terao, M.,M. Kurosaki,M. M. Barzago,M. Fratelli,R. Bagnati,A. Bastone,C. Giudice,E. Scanziani,A. Mancuso,C. Tiveron & E. Garattini 2009. Role of the molybdoflavoenzyme aldehyde oxidase homolog 2 in the biosynthesis of retinoic acid: generation and characterization of a knockout mouse. *Mol Cell Biol,* 29**,** 357-77.

Terao, M.,M. Kurosaki,M. M. Barzago,E. Varasano,A. Boldetti,A. Bastone,M. Fratelli & E. Garattini 2006. Avian and canine aldehyde oxidases. Novel insights into

the biology and evolution of molybdo-flavoenzymes. *J Biol Chem,* 281**,** 19748-61.

Terao, M.,M. Kurosaki,S. Demontis,S. Zanotta & E. Garattini 1998. Isolation and characterization of the human aldehyde oxidase gene: conservation of intron/exon boundaries with the xanthine oxidoreductase gene indicates a common origin. *Biochem J,* 332 383-93.

Terao, M.,M. Kurosaki,M. Marini,M. A. Vanoni,G. Saltini,V. Bonetto,A. Bastone,C. Federico,S. Saccone,R. Fanelli,M. Salmona & E. Garattini 2001. Purification of the aldehyde oxidase homolog 1 (AOH1) protein and cloning of the AOH1 and aldehyde oxidase homolog 2 (AOH2) genes. Identification of a novel molybdo-flavoprotein gene cluster on mouse chromosome 1. *J Biol Chem,* 276**,** 46347-63.

Thomas, J. A.,B. Poland & R. Honzatko 1995. Protein sulfhydryls and their role in the antioxidant function of protein S-thiolation. *Archives of biochemistry and biophysics,* 319**,** 1-9.

Timbrell, J. 2009. Principles of Biochemical Toxicology, informa healthcare. *New York, US.*

Tom, D. J.,L. E. Lee,J. Lew & N. C. Bols 2001. Induction of 7-ethoxyresorufin-O-deethylase activity by planar chlorinated hydrocarbons and polycyclic aromatic hydrocarbons in cell lines from the rainbow trout pituitary. *Comp Biochem Physiol A Mol Integr Physiol,* 128**,** 185-98.

Tomita, S.,M. Tsujita & Y. Ichikawa 1993. Retinal oxidase is identical to aldehyde oxidase. *FEBS Lett,* 336**,** 272-274.

Truglio, J. J.,K. Theis,S. Leimkuhler,R. Rappa,K. V. Rajagopalan & C. Kisker 2002. Crystal structures of the active and alloxanthine-inhibited forms of xanthine dehydrogenase from *Rhodobacter capsulatus. Structure,* 10**,** 115-25.

Tsujita, M.,S. Tomita,S. Miura & Y. Ichikawa 1994. Characteristic properties of retinal oxidase (retinoic acid synthase) from rabbit hepatocytes. *Biochim Biophys Acta,* 1204**,** 108-16.

Turner, N.,B. Barata,R. C. Bray,J. Deistung,J. Le Gall & J. J. Moura 1987. The molybdenum iron-sulphur protein from *Desulfovibrio gigas* as a form of aldehyde oxidase. *Biochem J,* 243**,** 755-61.

Turner, N.,W. A. Doyle,A. M. Ventom & R. C. Bray 1995. Properties of rabbit liver aldehyde oxidase and the relationship of the enzyme to xanthine oxidase and dehydrogenase. *Eur J Biochem,* 232**,** 646-57.

Ueda, O.,S. Kitamura,Y. Huruse,T. Saito,Y. Kanzaki,Y. Yano,K. Tatsumi & S. Ohta 2001. Metabolism of 2-nitrofluorene, an environmental pollutant, and 2-acetylaminofluorene in fish. *Bull Environ Contam Toxicol,* 66**,** 371-8.

Ueda, O.,S. Kitamura & S. Ohta 2002. Metabolism of 2-nitrofluorene, an environmental pollutant, by liver preparations of *sea bream*, *Pagrus major*. *Xenobiotica,* 32**,** 667-682.

Van der Sluijs, I.,S. M. Gray,M. C. P. Amorim,I. Barber,U. Candolin,A. P. Hendry,R. Krahe,M. E. Maan,A. C. Utne-Palm & H.-J. Wagner 2011. Communication in troubled waters: responses of fish communication systems to changing environments. *Evol Ecol,* 25**,** 623-640.

Van Rompay, K. K. 2012. The use of nonhuman primate models of HIV infection for the evaluation of antiviral strategies. *AIDS Res Hum Retroviruses,* 28**,** 16-35.

Vila, R.,M. Kurosaki,M. M. Barzago,M. Kolek,A. Bastone,L. Colombo,M. Salmona,M. Terao & E. Garattini 2004. Regulation and biochemistry of mouse molybdo-flavoenzymes. The DBA/2 mouse is selectively deficient in the expression of aldehyde oxidase homologues 1 and 2 and represents a unique source for the purification and characterization of aldehyde oxidase. *J Biol Chem,* 279**,** 8668-83.

Vulliet, E. & C. Cren-Olivé 2011. Screening of pharmaceuticals and hormones at the regional scale, in surface and groundwaters intended to human consumption. *Environ Pollut,* 159**,** 2929-2934.

Walton, B. T.,C.-H. Ho,C. Ma,E. O'Neill & G. Kao 1983. Benzoquinolinediones: activity as insect teratogens. *Science,* 222**,** 422-423.

Waud, W. R. & K. V. Rajagopalan 1976. The mechanism of conversion of rat liver xanthine dehydrogenase from an NAD+-dependent form (type D) to an O2-dependent form (type O). *Arch Biochem Biophys,* 172**,** 365-79.

Whitaker, J. R. 1963. Determination of Molecular Weights of Proteins by Gel Filtration of Sephadex. *Anal Chem,* 35**,** 1950-1953.

Wolf, K. & G. Rumsey 1985. The Representative Research Animal: Why Rainbow Trout (Salmo gairdneri Rich.). *J. Appli. Ichthyo,* 1**,** 131-138.

Wollers, S. 2008. Binding of sulfurated molybdenum cofactor to the C-terminal domain of *ABA3* from *Arabidopsis thaliana* provides insight into the mechanism of molybdenum cofactor sulfuration. *J. Biol. Chem.,* 283**,** 9642-9650.

Woolfolk, C. A. & J. S. Downard 1977. Distribution of xanthine oxidase and xanthine dehydrogenase specificity types among bacteria. *J Bacteriol,* 130**,** 1175-91.

Wright, R.,D. A. Clayton,M. G. Riley,J. L. McManaman & J. E. Repine 1999. cDNA cloning, sequencing, and characterization of male and female rat liver aldehyde oxidase (rAOX1). Differences in redox status may distinguish male and female forms of hepatic APX. *J Biol Chem,* 274**,** 3878-86.

Wurzinger, K. H. & R. Hartenstein 1974. Phylogeny and correlations of aldehyde oxidase, xanthine oxidase, xanthine dehydrogenase and peroxidase in animal tissues. *Comp Biochem Physiol B,* 49**,** 171-85.

Xia, M.,R. Dempski & R. Hille 1999. The reductive half-reaction of xanthine oxidase. Reaction with aldehyde substrates and identification of the catalytically labile oxygen. *J Biol Chem,* 274**,** 3323-30.

Xu, J. & R. C. Johnson 1995. aldB, an RpoS-dependent gene in Escherichia coli encoding an aldehyde dehydrogenase that is repressed by Fis and activated by Crp. *J Bacteriol,* 177**,** 3166-75.

Yamamoto, T.,K. Kario,M. Suda,Y. Moriwaki,S. Takahashi & K. Higashino 1991. A case of xanthinuria: a study on the metabolism of pyrazinamide and allopurinol. *Jpn J Med,* 30**,** 430-4.

Yamamoto, T.,Y. Moriwaki,S. Takahashi,T. Hada & K. Higashino 1987. In vitro conversion of pyrazinamide into 5-hydroxypyrazinamide and that of pyrazinoic acid into 5-hydroxypyrazinoic acid by xanthine oxidase from human liver. *Biochem Pharmacol,* 36**,** 3317-8.

Yamamoto, T.,K. Schoonjans & J. Auwerx 2007. Sirtuin functions in health and disease. *Mol Endocrinol,* 21**,** 1745-55.

Yan, L.,D. M. Otterness,T. L. Craddock & R. M. Weinshilboum 1997. Mouse liver nicotinamide N-methyltransferase: cDNA cloning, expression, and nucleotide sequence polymorphisms. *Biochem Pharmacol,* 54**,** 1139-49.

Yasuhara, A.,M. Akiba-Goto,K. Fujishiro,H. Uchida,T. Uwajima & K. Aisaka 2002. Production of aldehyde oxidases by microorganisms and their enzymatic properties. *J Biosci Bioeng,* 94**,** 124-9.

Yee, S. B. & C. A. Pritsos 1997. Comparison of oxygen radical generation from the reductive activation of doxorubicin, streptonigrin, and menadione by xanthine oxidase and xanthine dehydrogenase. *Arch Biochem Biophys,* 347**,** 235-41.

Yielding, K. L. & G. M. Tomkins 1961. An effect of L-leucine and other essential amino acids on the structure and activity of glutamic dehydrogenase. *Proc Natl Acad Sci U S A,* 47**,** 983-9.

Yoshihara, S. & K. Tatsumi 1985. Guinea pig liver aldehyde oxidase as a sulfoxide reductase: its purification and characterization. *Arch Biochem Biophys,* 242**,** 213-24.

Yoshihara, S. & K. Tatsumi 1997. Purification and characterization of hepatic aldehyde oxidase in male and female mice. *Arch Biochem Biophys,* 338**,** 29-34.

Yoshimura, M. & T. Oka 1989. Isolation and structural analysis of the mouse beta-casein gene. *Gene,* 78**,** 267-75.

Yu, C. L.,T. M. Louie,R. Summers,Y. Kale,S. Gopishetty & M. Subramanian 2009. Two distinct pathways for metabolism of theophylline and caffeine are coexpressed in *Pseudomonas putida* CBB5. *J Bacteriol,* 191**,** 4624-32.

Zakrzewska, B. & M. M. Jeźewska 1989. Comparison of xanthine: NAD+ oxidoreductase from liver of toad Bufo viridis and other vertebrates. *Comparative Biochemistry and Physiology Part B: Comparative Biochemistry,* 94**,** 361-365.

Zhao, X. J. & T. Ishizaki 1997. The In vitro hepatic metabolism of quinine in mice, rats and dogs: comparison with human liver microsomes. *J Pharmacol Exp Ther,* 283**,** 1168-76.

Ziegler, I. 2003. The pteridine pathway in zebrafish: regulation and specification during the determination of neural crest cell-fate. *Pigment Cell Res,* 16**,** 172-82.

6.0. Appendices.

6.1. Appendix 1.

Table 1: Fish species order and family.

Common name	Scientific name	Order	Family	Habitat
African Catfish	*Clarias Gariepinus*	Siluriformes	Clariidae	F/P
Blue Fish	*Pomatomus Saltatrix*	Perciformes	Pomatomidae	S/D
Bluegill	*Lepomis Macrochirus*	Perciformes	Centrarchidae	F/D
Brill	*Scophthalmus Rhombus*	Pleuronectiformes	Scophthalmidae	S/D
Black Sole	*Solea Solea*	Pleuronectiformes	Soleidae	S/D
Brown Trout	*Salmo Trutta*	Salmoniformes	Salmonidae	F/P
Carp	*Cyprium Carpio*	Cypriniformes	Cyprinidae	F/P
Cutlips Minnow	*Exoglossum Maxilingua*	Cypriniformes	Cyprinidae	F/P
Common Carp	*Cyprinus Carpio Communis*	Cypriniformes	Cyprinidae	F/D
Channel Catfish	*Icatalurus Punctatus*	Siluriformes	Ictaluridae	F/P
Cod	*Gadus Morhua*	Gadiformes	Gadidae	S/D
Dab	*Limanda Limanda*	Pleuronectiformes	Pleuronectidae	S/D
Electric Catfish	*Malapterurus Electricus*	Siluriformes	Malapteruridae	F/D
Fathead Minnow	*Pimephales Promelas*	Cypriniformes	Cyprinidae	F/P
Florida Pompano	*Trachinotus Carolinus*	Perciformes	Carangidae	S/P
Goldfish	*Carassius Auratus*	Cypriniformes	Cyprinidae	F/P
Great Snakehead	*Ophiocephalus Muralius*	Perciformes	Channidae	F/P
Gurnard	*Chelidonichthys Cuculus*	Scorpaeniformes	Triglidae	S/D
Herring	*Clupea Harengus*	Clupeiformes	Clupeidae	S/P
Haddock	*Melanogrammus Aeglefinus*	Gadiformes	Gadidae	S/D
John Dory	*Zeus Faber*	Zeiformes	Zeidae	S/P
Largemouth Bass	*Micropterus Salmoides*	Perciformes	Centrarchidae	F/P
Lesser Spotted Dogfish	*Scyliorhinus Canicula*	Carcharhiniformes	Scyliorhinidae	S/P
Lemon Sole	*Microstomus Kitt*	Pleuronectiformes	Pleuronectidae	S/D
Margined Madtom	*Noturus Insignis*	Siluriformes	Ictaluridae	F/P
Mozambique Tilapia	*Oreochromis Mossambicus*	Perciformes	Cichlidae	F/P
Mackerel	*Scomber Scombrus*	Perciformes	Scombridoe	S/P
Megrim	*Lepidorhombus Whiffagonis*	Pleuronectiformes	Scophthalmidae	S/D
Northern Hog Sucker	*Hypentelium Nigricans*	Cypriniformes	Catostomidae	F/D
Norfolk Spot	*Leiostomus Xanthurus*	Perciformes	Sciaenidae	S/P
Northern Pike	*Esox Lucius*	Esociformes	Esocidae	F/D
Nile Tilapia Juveniles	*Oreochromis Niloticus*	Perciformes	Cichlidae	F/P
Orange-Fin Labeo	*Labeo Calbasu*	Cypriniformes	Cyprinidae	F/P
Pumpkinseed Sunfish	*Lepomis Gibbosus*	Perciformes	Centrarchidae	F/P
Perch	*Perca Fluviatilis*	Perciformes	Percidae	F/D
Pike	*Esox Lucius*	Esociformes	Esocidae	S/D
Plaice	*Pleuronectes Platessa*	Pleuronectiformes	Pleuronectidae	S/D
Ray	*Dipturus Canutus*	Rajiformes	Rajidae	S/P
Rankin Cod	*Epinephelus Multinotatus*	Perciformes	Serranidae	S/D
Red Emperor	*Lutjanus Sebae*	Perciformes	Lutjanidae	S/D
Smooth Dogfish	*Mustelus Canis*	Carcharhiniformes	Triakidae	S/P
Spangled Emperor	*Lethrinus Nebulosus*	Perciformes	Lethrinidae	S/P
Stoneroller Minnow	*Campostoma Anomalous*	Cypriniformes	Cyprinidae	F/P
Spanish Mackerel	*Scomberonorus Maculatus*	Perciformes	Scombridae	S/D
Sea Mullet	*Menticirrhus Saxatilis*	Perciformes	Sciaenidae	S/D
Summer Flounder	*Paralichthyes Dentatus*	Pleuronectiformes	Paralichthyidae	S/D
White Sucker	*Catostamus Commersoni*	Cypriniformes	Catostomidae	F/D
Walleye	*Stizostedion Vitreum*	Perciformes	Percidae	F/P
Whiting	*Merlangius Merlangus*	Gadiformes	Gadidae	S/P
White Pollack	*Pollachius Virene*	Gadiformes	Gadidae	S/P&D
White Sole	*Solea Solea*	Pleuronectiformes	Soleidae	S/D
White Trout	*Salmo Trutta*	Salmoniformes	Salmonidae	S/D
Yellow Perch	*Perca Flavescens*	Perciformes	Cichlidae	F/P
Zebra Fish	*Danio Rerio*	Cypriniformes	Cyprinids	F/P

Abbreviations: F-freshwater fish, S- saltwater fish, P- pelagic, D-demersal.

6.2. Appendix 2.
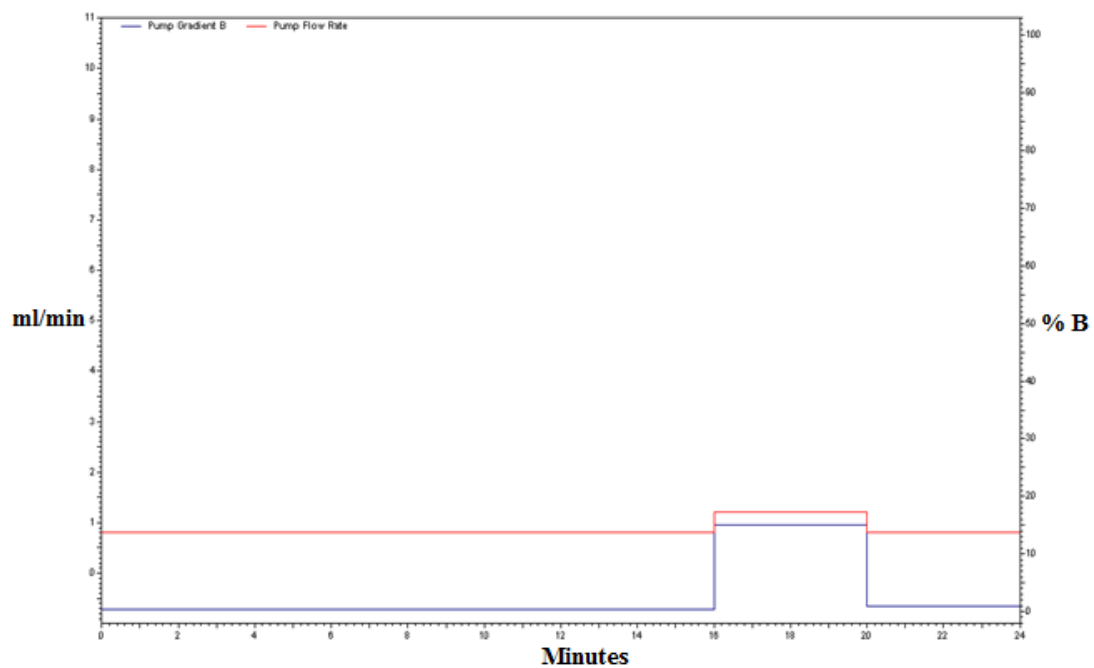
Figure 1: Diagram showing pump flow rate (red line) and pump gradient (blue line) change for allopurinol and oxipurinol.
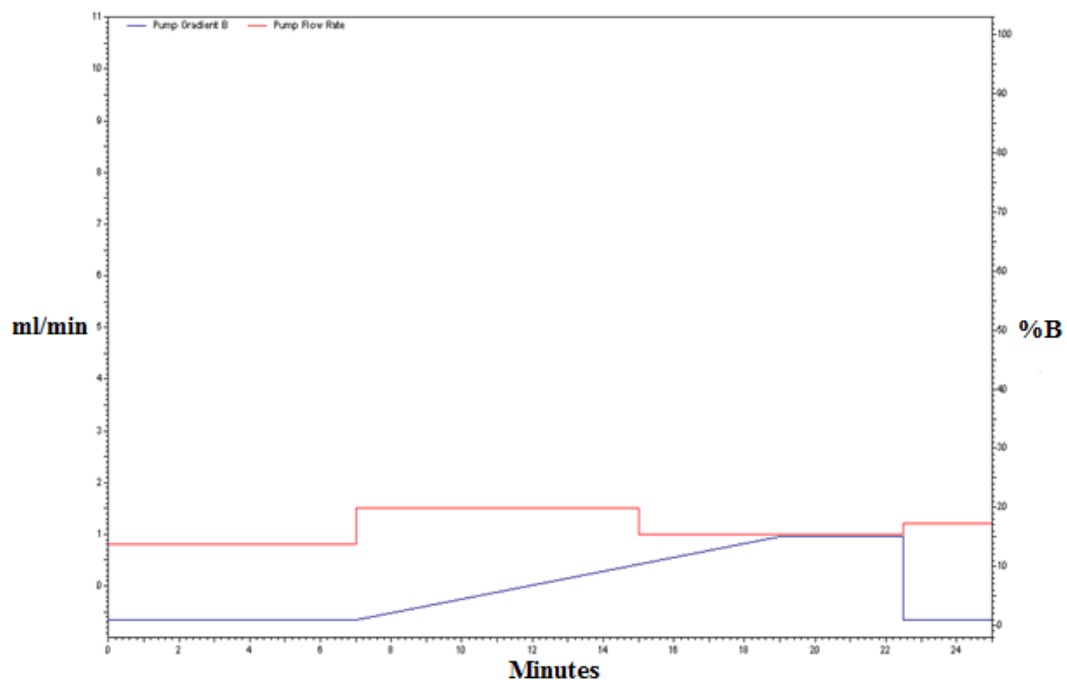
Figure 2: Diagram showing pump flow rate (red line) and pump gradient (blue line) change for purines, phthalazine and pyrazinamide.
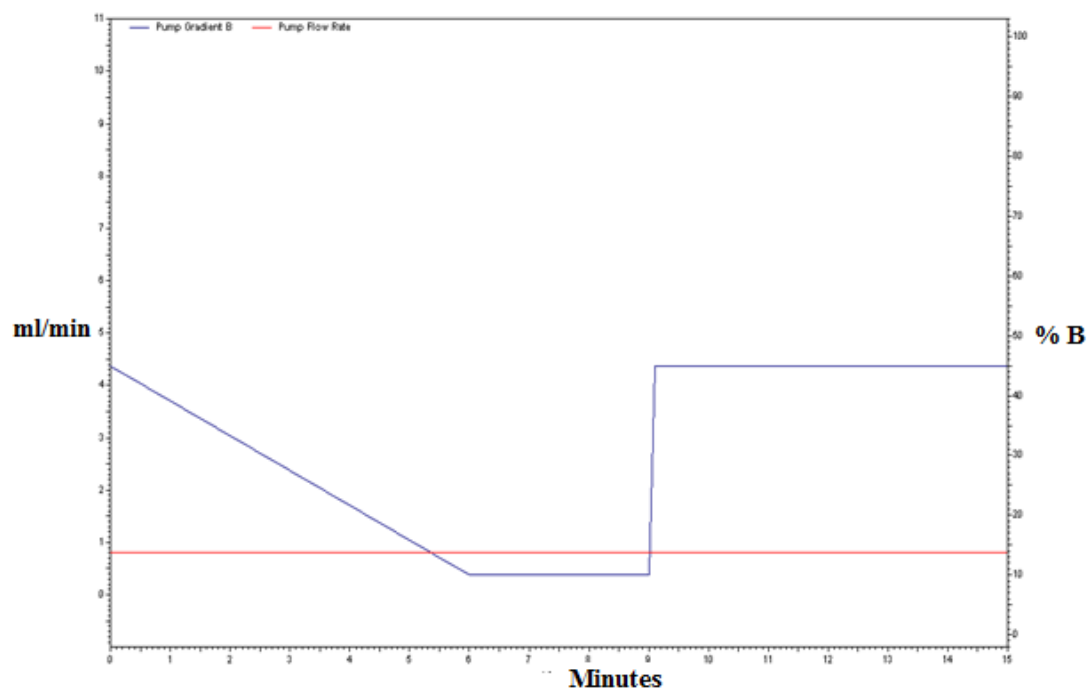
Figure 3:Diagram showing pump flow rate (red line) and pump gradient (blue line) change for N^1-methylnicotinamide.
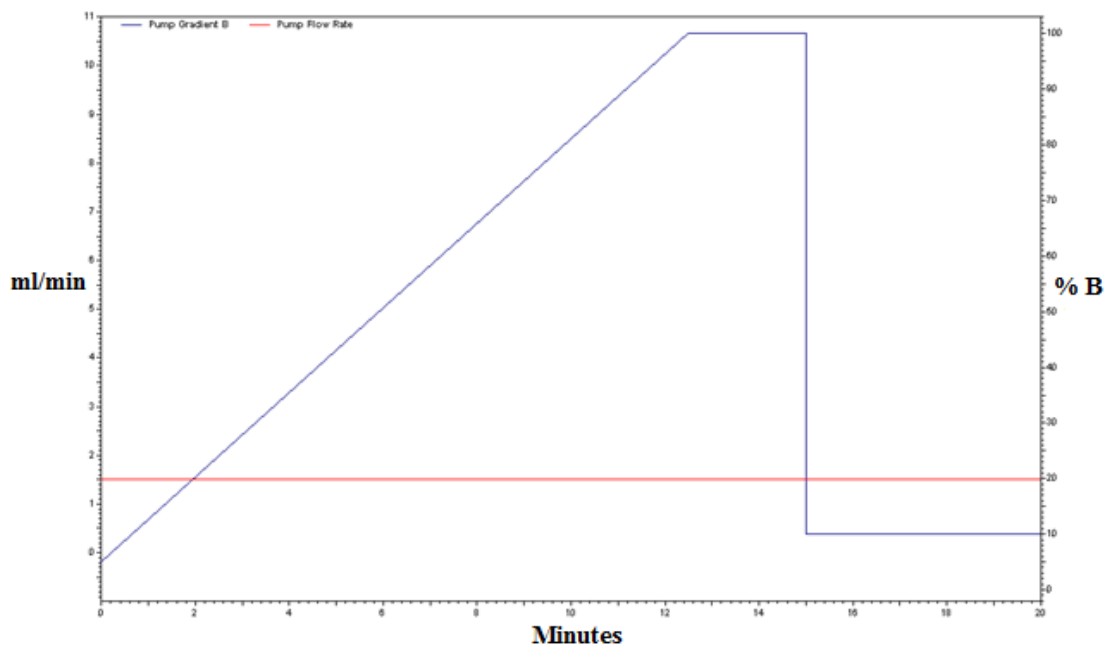

Figure 4:Diagram showing pump flow rate (red line) and pump gradient (blue line) change for phenanthridine and 6(5H)-phenanthridone.

6.3. Appendix 3.

Table 1:% RSD of retention time of three replicates was the same day of calibration standard for intra- day precision.

The % RSD for retention time between injections is in the range of 0.09-3.31.

%RSD for retention time (n=3)					
Analyte	**0.01mM**	**0.02mM**	**0.03mM**	**0.05mM**	**0.1mM**
Allopurinol	0.61	1.23	2.26	0.22	1.28
Cinchonine	1.66	1.68	0.15	2.11	0.74
Hypoxanthine	1.11	1.36	0.39	0.78	0.75
6-Mercaptopurine	2.51	0.68	0.39	1.11	0.17
Methotrexate	0.97	1.01	1.12	1.19	0.27
1-Methylxanthine	1.61	1.25	1.86	1.02	0.61
1-Methyluric acid	0.72	0.98	1.02	1.23	0.88
N^1-methylnicotinamide	1.12	2.13	0.52	0.27	1.66
Oxipurinol	0.87	2.05	1.83	0.59	1.18
Phenanthridine	2.25	3.17	1.13	0.22	0.78
Phenanthridone	2.41	2.14	2.17	1.21	0.26
Phthalazine	0.87	2.21	3.21	1.34	1.19
1-Pthalazone	2.11	1.06	1.27	0.31	0.25
Pyridoxal	1.41	0.18	0.24	0.89	1.86
Pyridoxic acid	2.14	0.77	0.26	1.13	0.66
Pyrazinamide	1.12	1.51	0.57	1.42	1.29
6-Thioxanthine	1.51	2.22	0.35	0.16	2.32
Uric acid	1.22	1.53	0.52	1.37	2.26
Vanillin	1.02	2.23	0.42	0.25	1.16
Vanillic acid	0.77	1.61	0.89	0.35	0.59
Xanthine	1.21	0.98	0.19	0.11	1.79

Table 2:% Accuracy calculated for intra-day analysis of compounds used in HPLC analysis in this study.

Mean ± SD of accuracy (%) (n=3)					
	Nominal concentration				
Analyte	0.01 mM	0.02 mM	0.03 mM	0.05 mM	0.1 mM
Allopurinol	98.2 ± 1.2	99.2 ± 1.1	97.1 ± 0.7	98.5 ± 1.3	98.5 ± 1.7
Cinchonine	97.5 ± 1.5	98.3 ± 0.8	97.8 ± 1.4	105.6 ± 0.2	96.9 ± 1.2
Hypoxanthine	99.6 ± 1.1	99.5 ± 1.7	99.7 ± 2.1	99.5 ± 1.1	99.6 ± 1.9
6-Mercaptopurine	98.2 ± 0.3	97.2 ± 1.6	95.5 ± 1.7	98.8 ± 1.1	99.2 ± 1.7
Methotrexate	99.3 ± 1.3	97.1 ± 1.7	98.9 ± 0.5	96.1 ± 2.4	98.9 ± 1.8
1-Methylxanthine	98.5 ± 2.5	100.3 ± 0.9	99.8 ± 2.3	98.1 ± 0.7	99.9 ± 0.2
1-Methyluric acid	95.1 ± 1.1	97.3 ± 0.4	96.2 ± 0.9	99.9 ± 0.2	96.7 ± 0.7
N^1-methylnicotinamide	95.1 ± 0.7	98.5 ± 0.4	99.9 ± 0.4	100.3 ± 0.7	96.8 ± 1.4
Oxipurinol	99.2 ± 2.1	99.1 ± 1.1	100.4 ± 2.2	96.6 ± 1.9	98.8 ± 2.1
Phenanthridine	100.6 ± 1.9	99.8 ± 1.4	99.2 ± 0.3	99.1 ± 1.3	100.8 ± 1.1
Phenanthridone	99.5 ± 0.7	97.5 ± 0.2	99.5 ± 1.7	99.5 ± 1.1	99.5 ± 0.8
Phthalazine	99.1 ± 1.3	98.7 ± 2.2	95.2 ± 1.7	98.9 ± 1.5	99.8 ± 1.5
1-pthalazone	98.6 ± 1.5	100.4 ± 0.2	98.7 ± 1.8	99.5 ± 2.1	95.6 ± 2.3
Pyridoxal	98.2 ± 0.7	97.9 ± 1.6	95.9 ± 2.3	99.9 ± 0.6	100.2 ± 1.7
Pyridoxic acid	98.4 ± 1.5	95.4 ± 0.7	99.1 ± 2.4	98.2 ± 1.8	99.2 ± 1.3
Pyrazinamide	100.5 ± 0.4	97.3 ± 1.3	99.9 ± 1.1	99.3 ± 1.2	98.3 ± 2.2
6-Thioxanthine	100.2 ± 0.2	98.4 ± 2.3	98.5 ± 1.1	99.8 ± 1.9	98.2 ± 1.3
Uric acid	95.6 ± 1.7	99.7 ± 1.1	99.7 ± 1.2	98.3. ± 1.9	97.2 ± 0.7
Vanillin	97.1 ± 1.2	99.1 ± 1.1	98.8 ± 1.1	95.2 ± 1.7	98.5 ± 0.7
Vanillic acid	97.1 ± 1.7	98.5 ± 1.8	100.5 ± 0.4	97.5 ± 1.3	99.1 ± 0.9
Xanthine	97.4 ± 1.2	99.6 ± 1.3	100.2 ± 0.1	99.8 ± 0.7	99.6 ± 2.1

Analyte	0.01 (mM)	0.02 (mM)	0.03 (mM)	0.05 (mM)	0.1 (mM)	Slope	Intercept	RSQ	LOD (nmol)	LOQ (nmol)
Allopurinol	14726	29588	49432	96833	188236	1926912	-4388	1.00	3	80
Cinchonine	99785	151658	197633	390061	889728	8843599	-21381	0.990	0.2	7
Hypoxanthine	39196	64887	109794	187645	378529	1902	- 3135	0.998	5.4	65
6-Mercaptopurine	39438	79514	139407	288320	591803	6091107	-23441	0.994	4	70
Methotrexate	128570	171092	276739	493204	998593	9945386	-3388	0.997	0.6	0.9
1-Methylxanthine	134653	265966	408825	648214	1250231	6228	15347	0.994	4.3	52
1-Methyluric acid	307169	539389	835522	1431411	2952992	14769	- 22718	0.998	1.7	57
N^1-methylnicotinamide	44454	91846	169578	308302	661872	6764775	-24091	0.996	1	50
Oxipurinol	23394	47904	76786	129660	233588	2714	2357371	1.00	1	50
Phenanthridine	571679	992255	1180187	2130945	4222854	41430984	66235	0.997	2	80
Phenanthridone	132015	260381	397202	689057	1322123	13294923	1474	0.999	2	70
Phthalazine	253827	565518	887197	1506345	2906879	29355401	-7478	0.999	2	70
1-pthalazone	157996	290877	404934	712217	1524442	15199887	-16689	0.998	2	60
Pyridoxal	28160	45701	77618	112825	202247	1944019	7967	0.992	2	70
Pyridoxic acid	31017	50616	87722	138318	230686	2304745	9060	0.987	2	90
Pyrazinamide	70181	148691	217140	331506	640131	6337483	12796	0.998	4	80
6-Thioxanthine	51175	92429	134115	259511	485648	4904335	-1172	0.997	2	70
Uric acid	482658	1095004	1494725	2563976	4955041	24777	30879	0.999	3.5	90
Vanillin	54118	146188	211879	378212	734053	7447551	-6589	0.999	2	60
Vanillic acid	38737	99515	181284	281098	553041	5617796	-4343	0.997	0.1	20
Xanthine	123857	253547	406308	642818	1253249	6273	7542	0.995	4.6	94

Mean area of three injections in the same day of calibration standards (n=3)

Table 3: Regression calculation based on mean area of three replicates in the same day of calibration standards against the actual concentration.
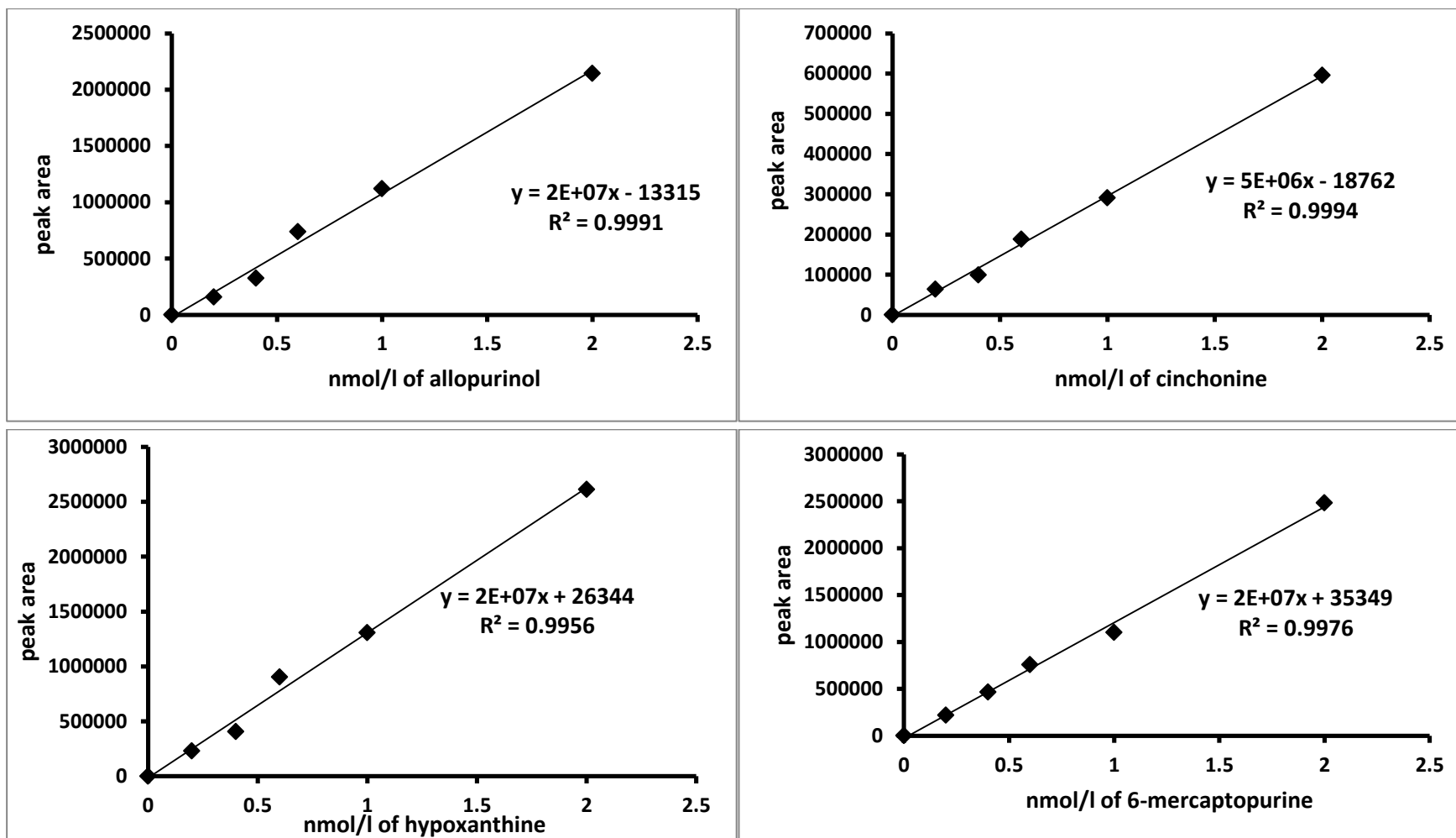
Figure 1: Standard curves for substrates and products used in this study
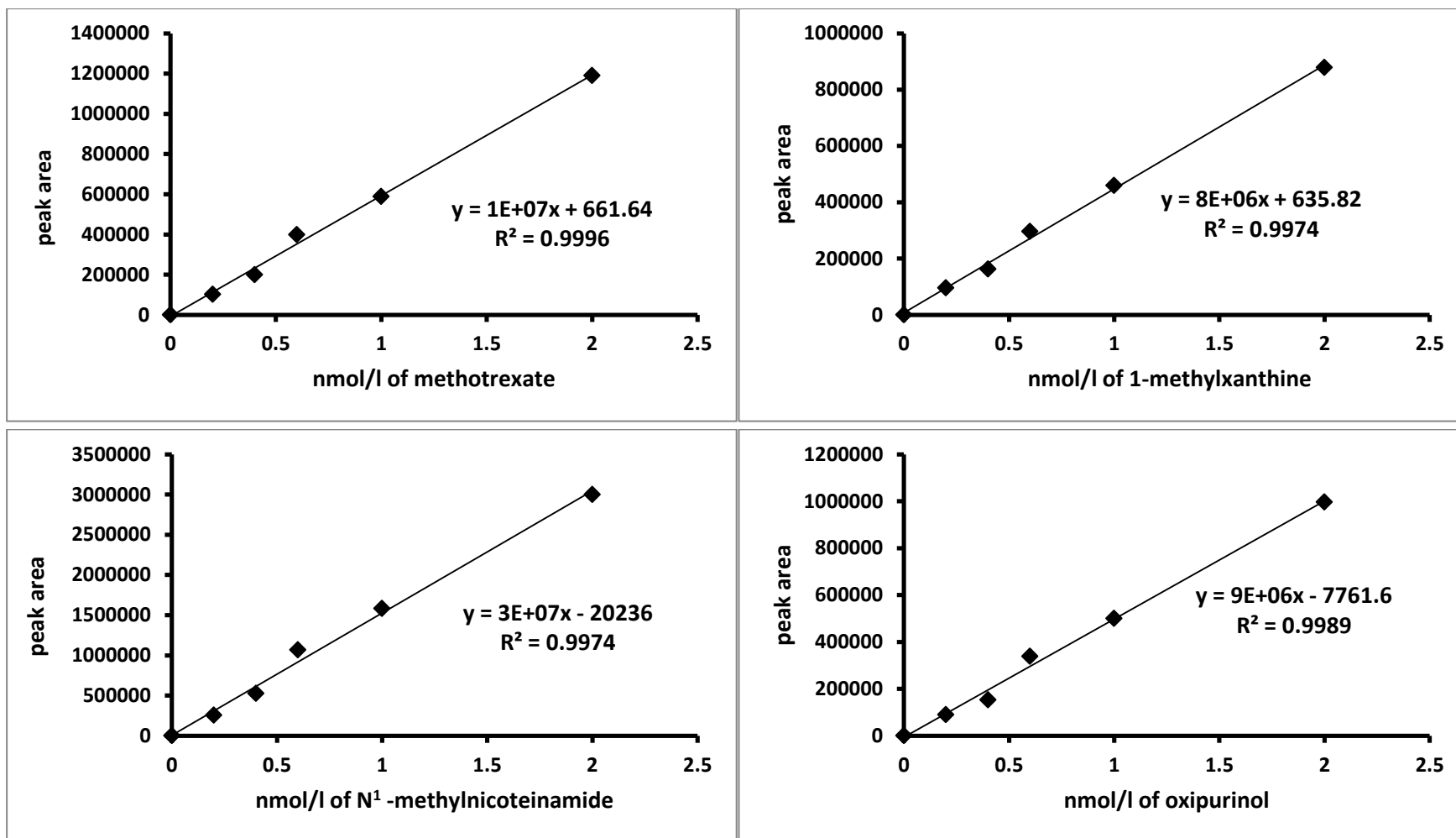
Figure 2: Standard curves for substrates and products used in this study
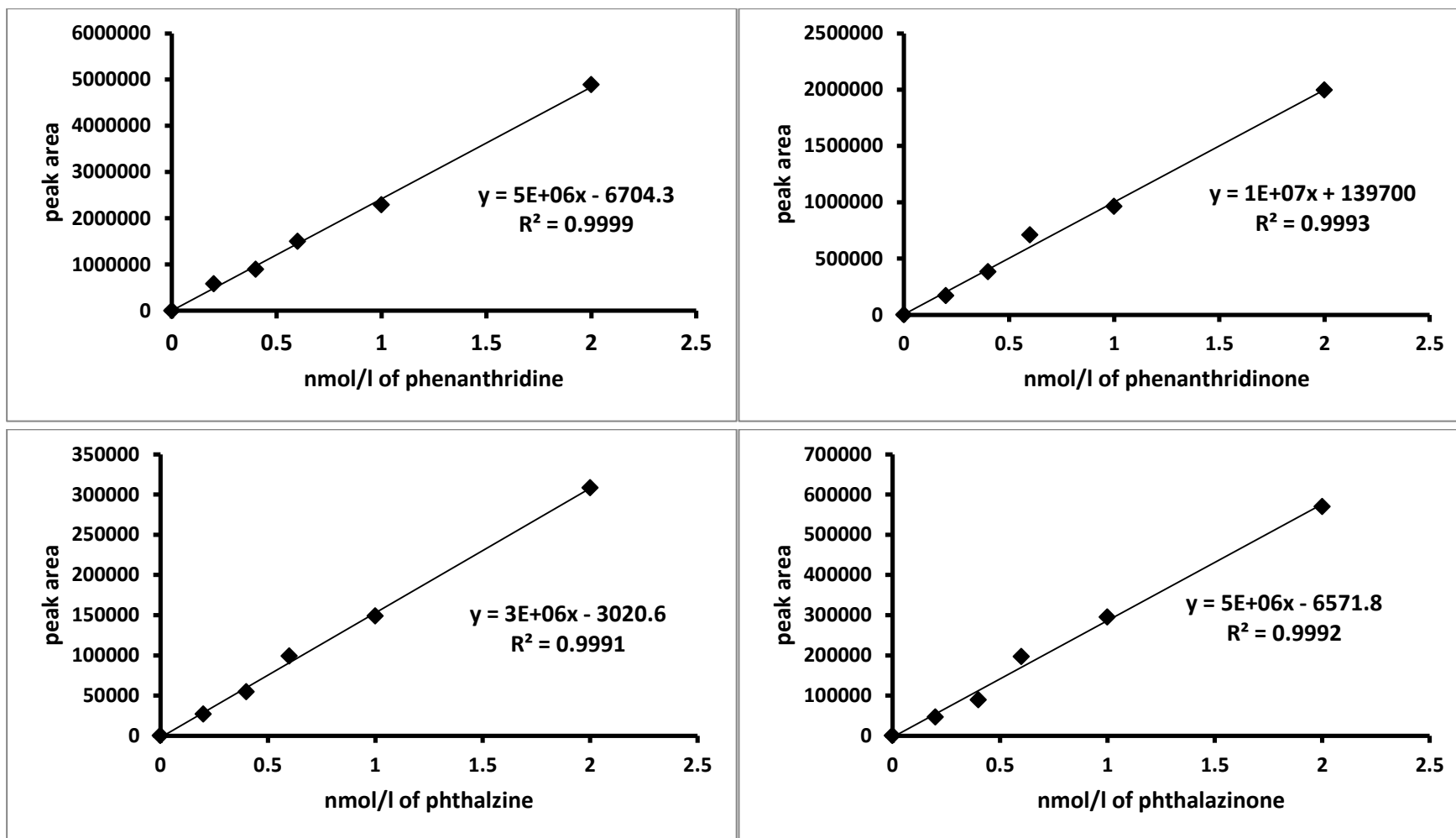
**Figure 3:**Standard curves for substrates and products used in this study
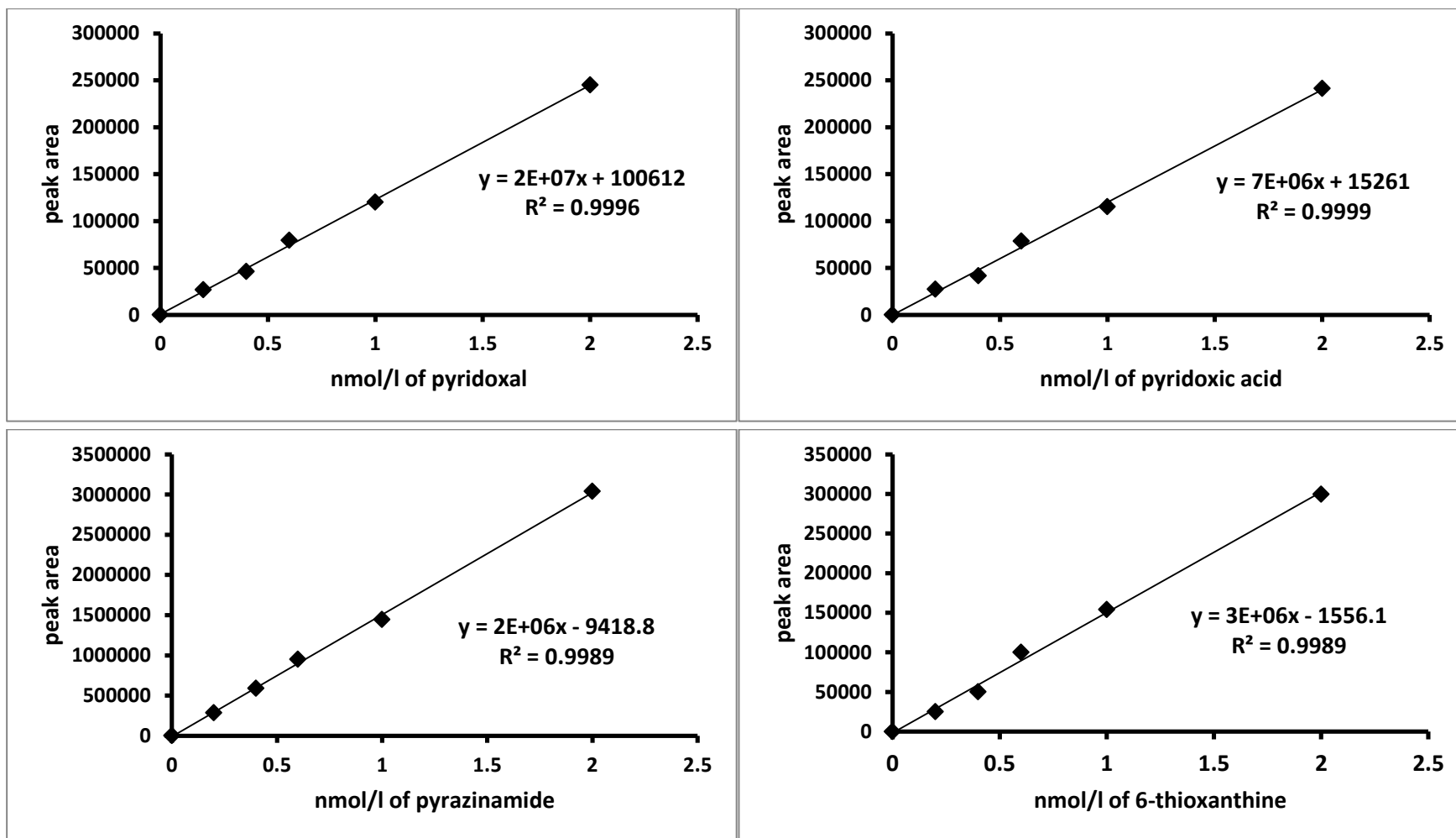
**Figure 4:** Standard curves for substrates and products used in this study
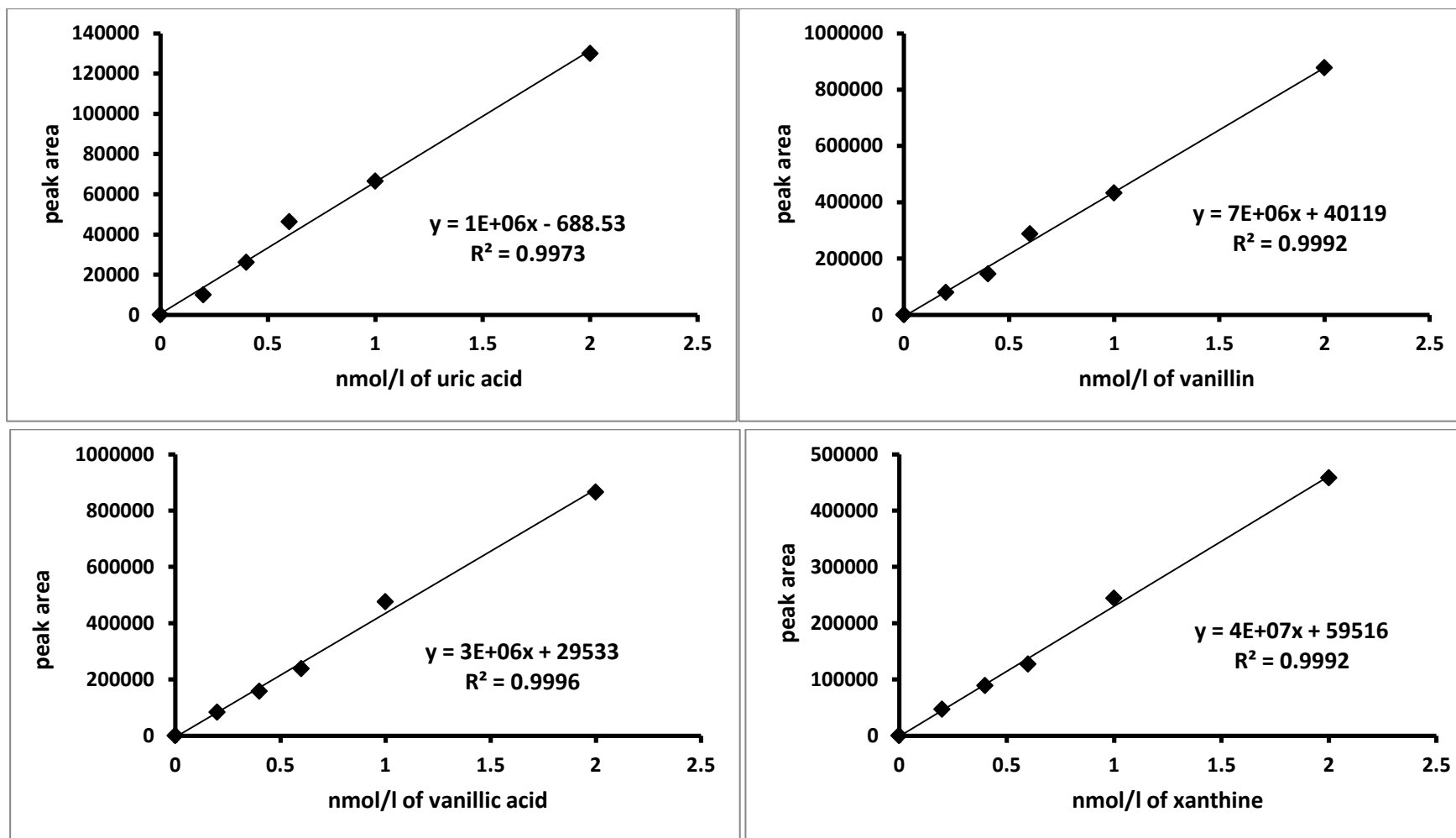
Figure 5: Standard curves for substrates and products used in this study
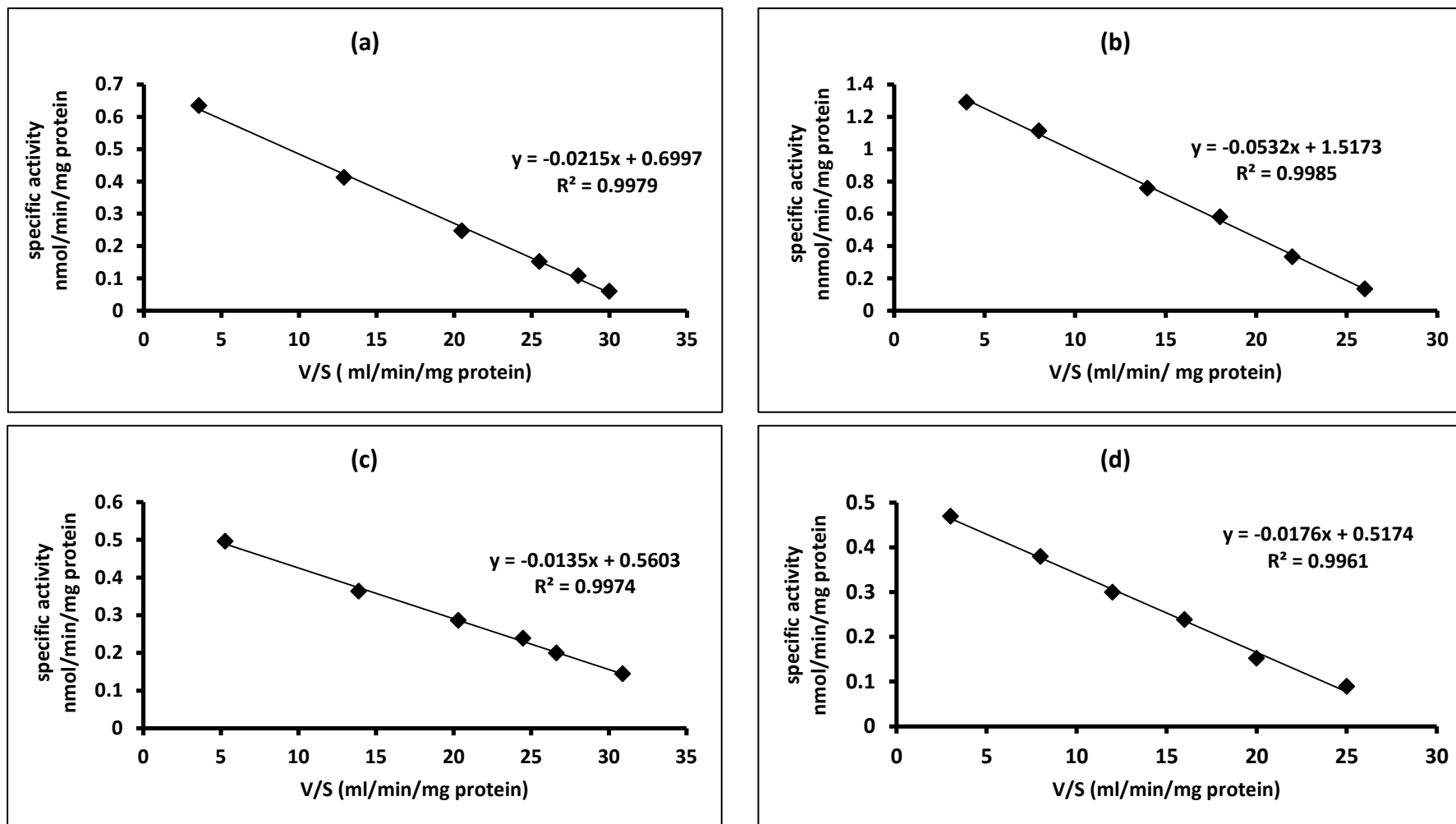
Figure 6: Eadie- Hofstee plot of AOX and XDH activities in trout.(a) AOX-catalyzed oxidation of DMAC. (b) AOX-catalyzed oxidation of vanillin. (c) XDH-catalyzed oxidation of xanthine. (d) XDH-catalyzed oxidation of 1-methylxanthine.The substrates concentrations were 25-100 µM of AOX and XDH substrates. The typical results are from three independent experiments.
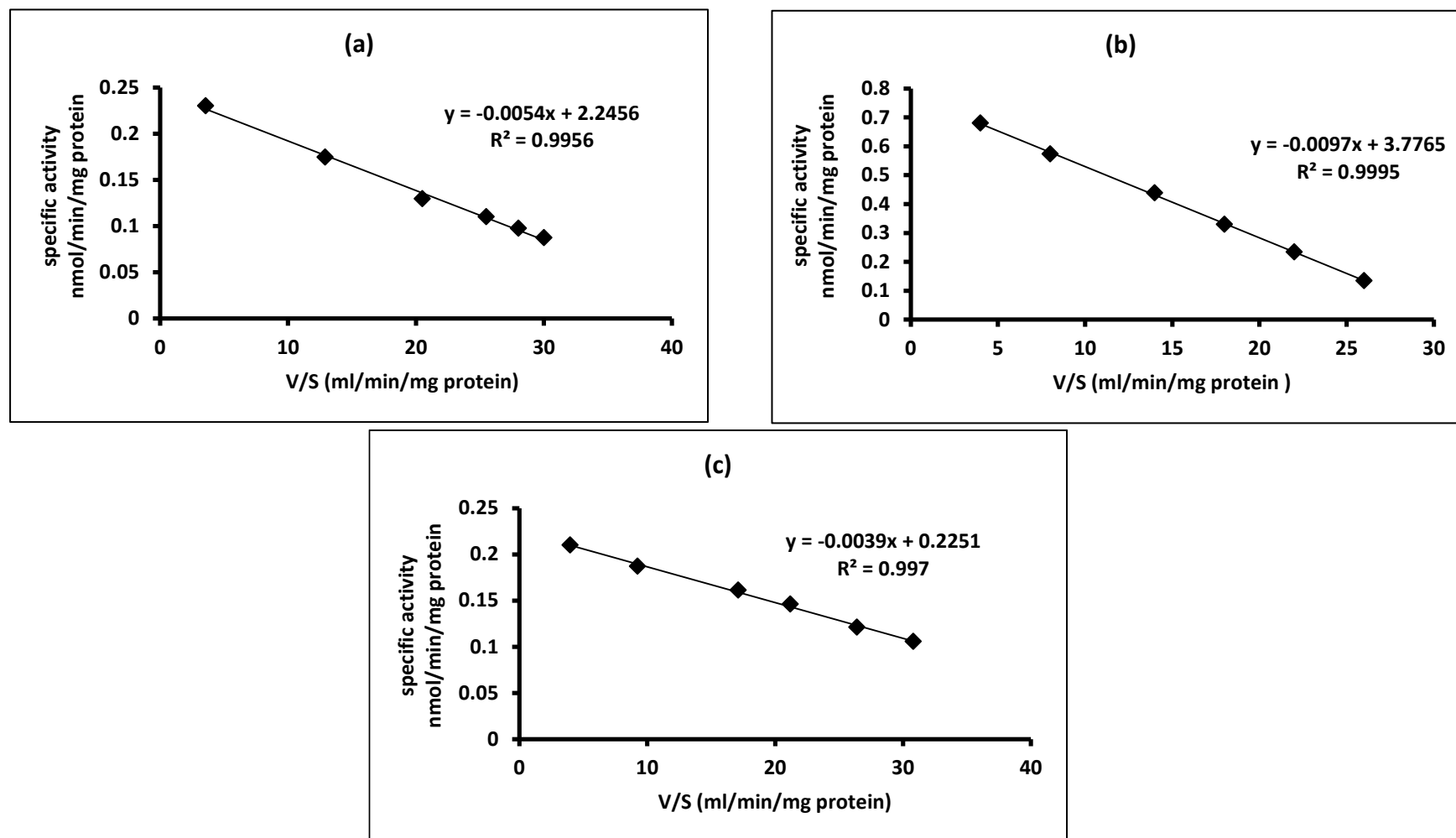
Figure 7: Eadie- Hofstee plot of AOX activities in rat.(a) AOX-catalyzed oxidationof DMAC. (b) AOX-catalyzed oxidation of vanillin. (c) AOX-catalyzed oxidation of phenanthridine. The substrates concentrations were 25-100 μM of AOX substrates. The typical results are from three independent experiments.
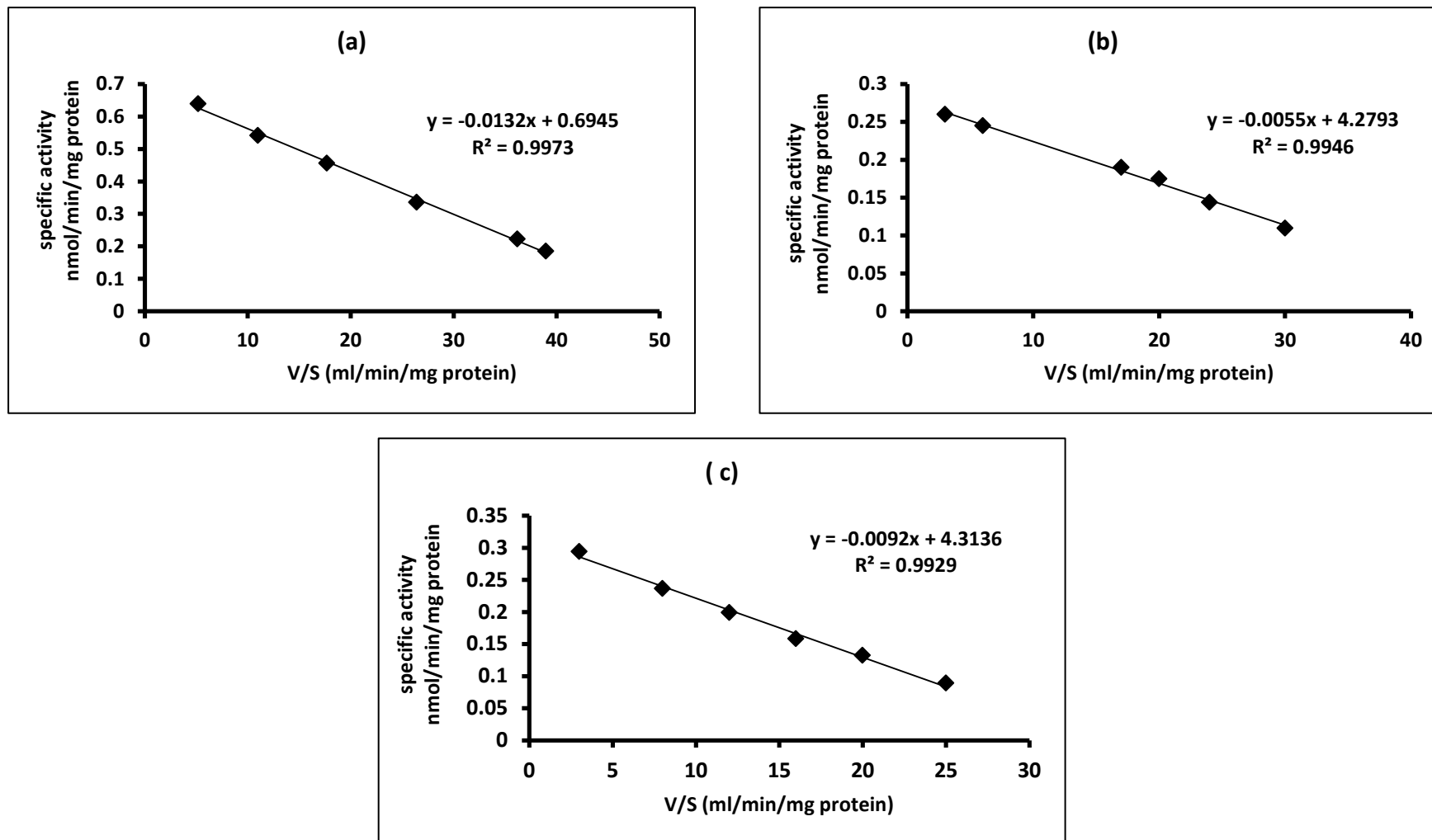
**Figure 8:** Eadie- Hofstee plot of XOR activities in rat. (a) XO-catalyzed oxidation of xanthine. (b) XDH-catalyzed oxidation of xanthine. (c) XDH-catalyzed oxidation of 1-methylxanthine. The substrates concentrations were 25-100 μM of XOR substrates. The typical results are from three independent experiments.
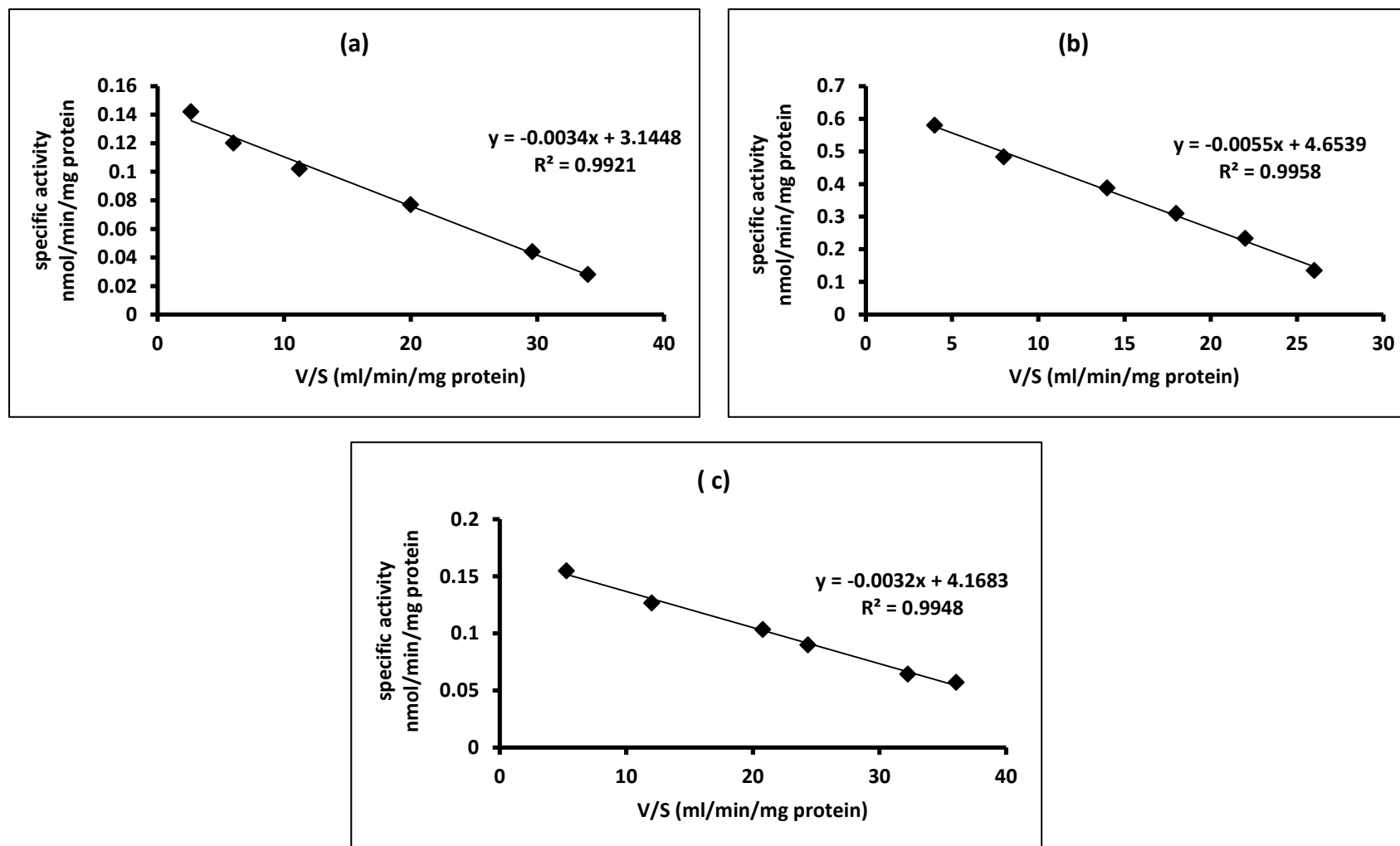
Figure 9: Eadie- Hofstee plot of AOX activities in human. (a) AOX-catalyzed oxidation of DMAC. (b) AOX-catalyzed oxidation of vanillin. (c) AOX-catalyzed oxidation of phenanthridine. The substrates concentrations were 25-100 μM of AOX substrates. The typical results are from three independent experiments.
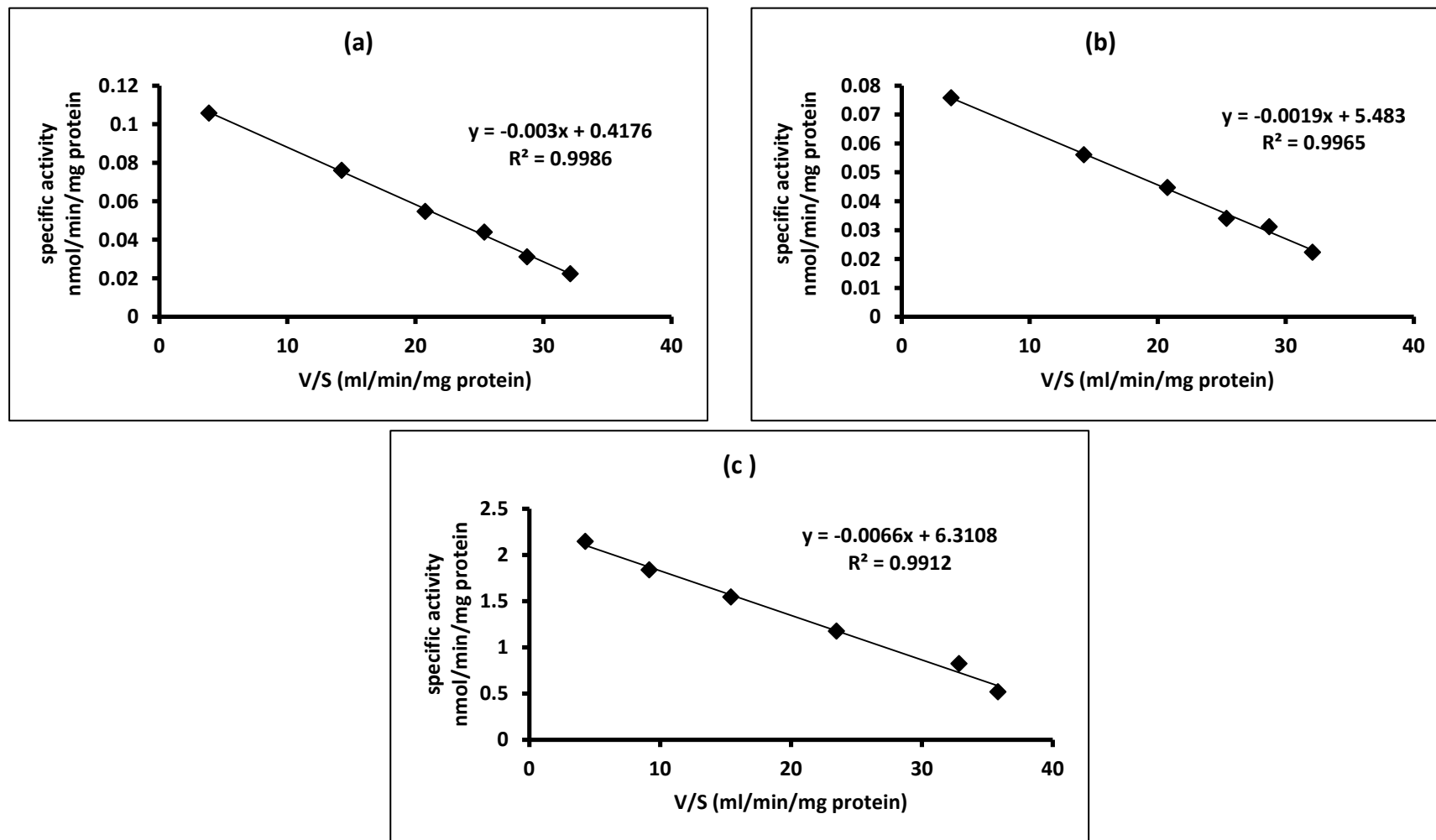
Figure 10: Eadie- Hofstee plot of XOR activities in human. (a) XO-catalyzed oxidation of xanthine. (b) XDH-catalyzed oxidation of xanthine. (c) XDH-catalyzed oxidation of 1-methylxanthine. The substrates concentrations were 25-100 μM of XOR substrates. The typical results are from three independent experiments.
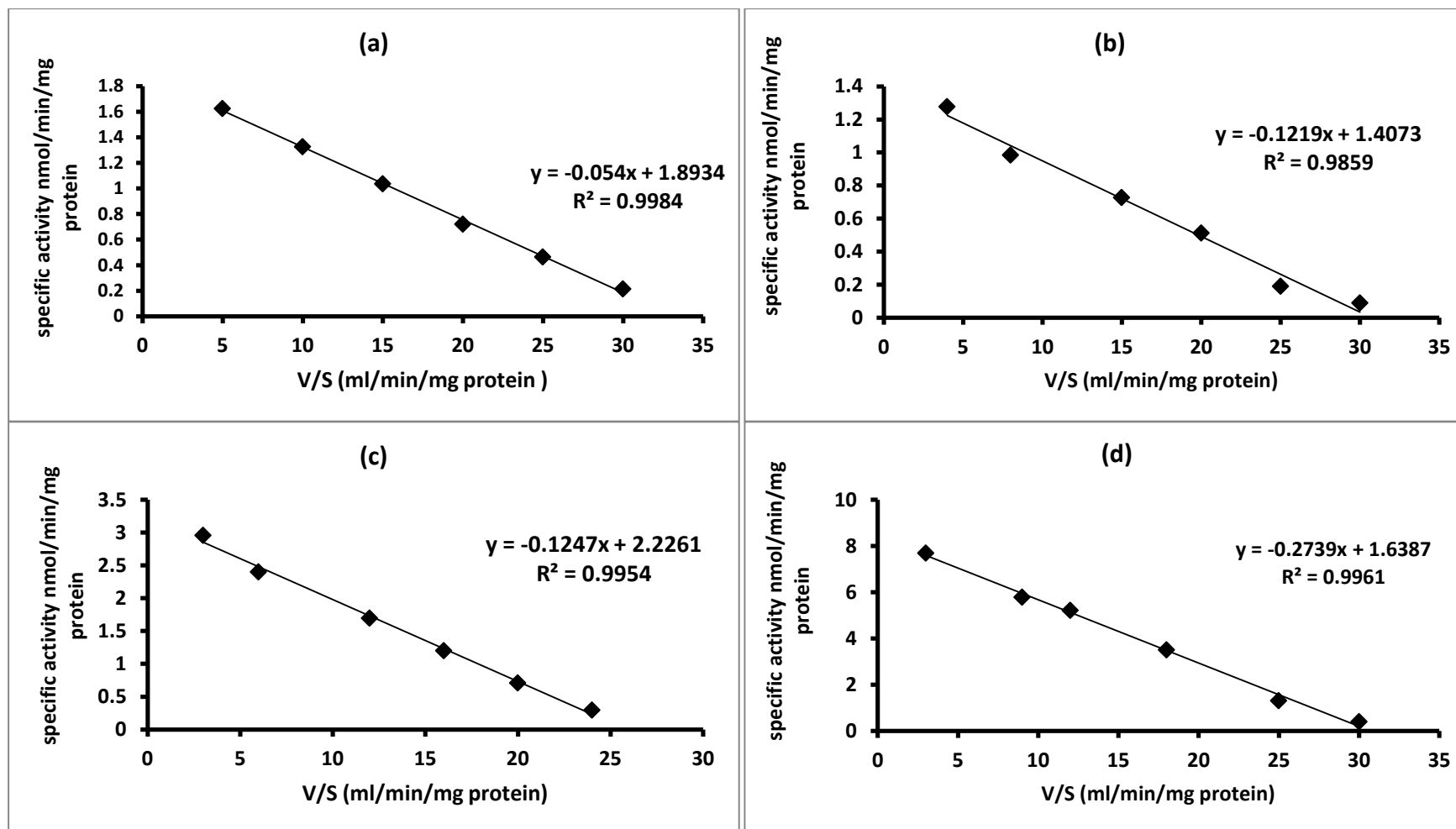
Figure 11: Eadie- Hofstee plot of AOX activities in rainbow trout. (a) AOX-catalyzed oxidation of vanillin. (b) AOX-catalyzed oxidation of pyridoxal. (c) AOX-catalyzed oxidation of all-trans retinal. (d)AOX-catalyzed oxidation of N^1-methylnicotinamide. The substrates concentrations were 25-100 μM of AOX substrates. The typical results are from three independent experiments.
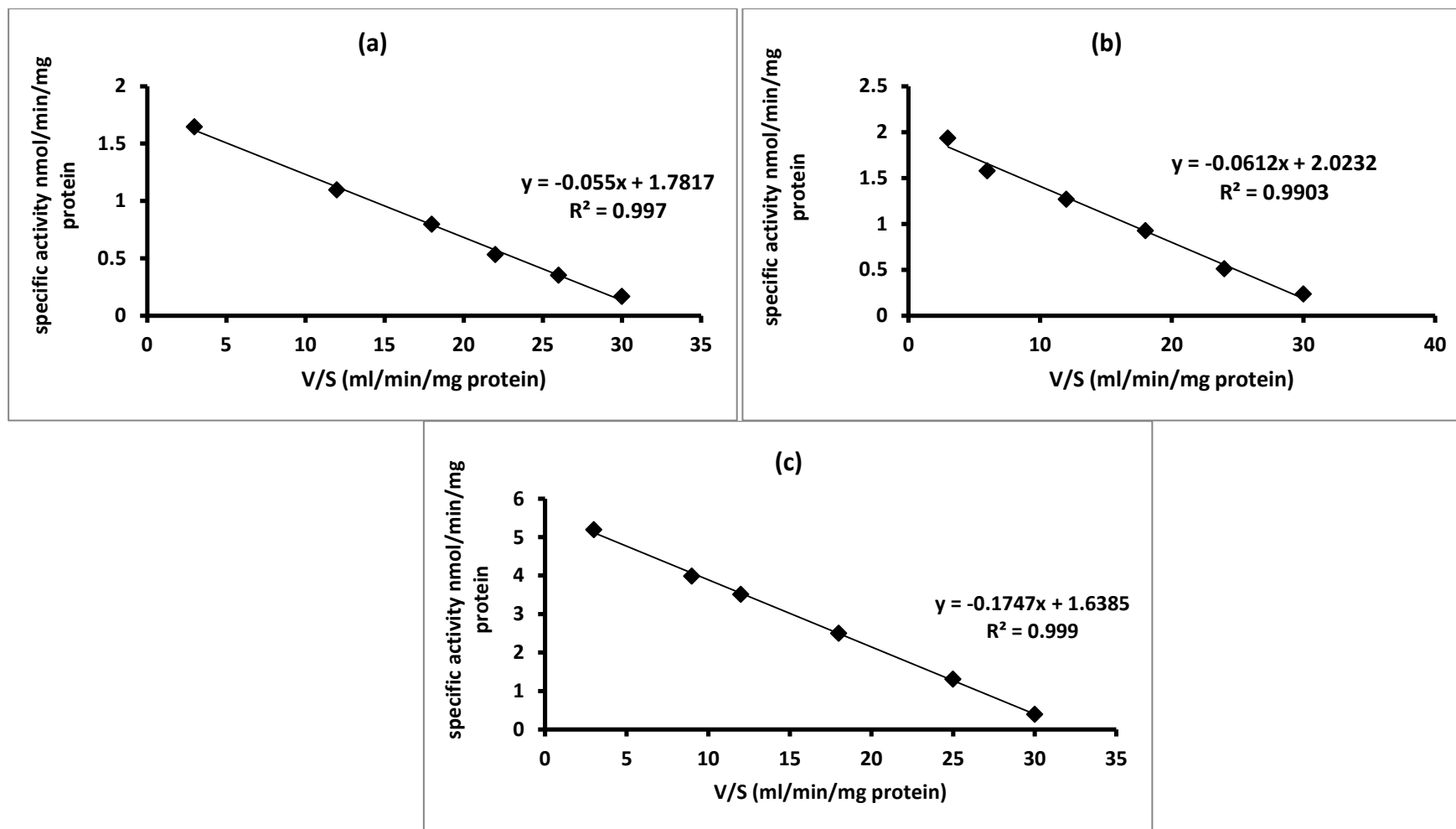
Figure 12: Eadie- Hofstee plot of AOX activities in rainbow trout. (a) AOX-catalyzed oxidation of phenanthridine. (b) AOX-catalyzed oxidation of phthalazine. (c) AOX-catalyzed oxidation of cinchonine. The substrates concentrations were 25-100 μM of AOX substrates. The typical results are from three independent experiments.
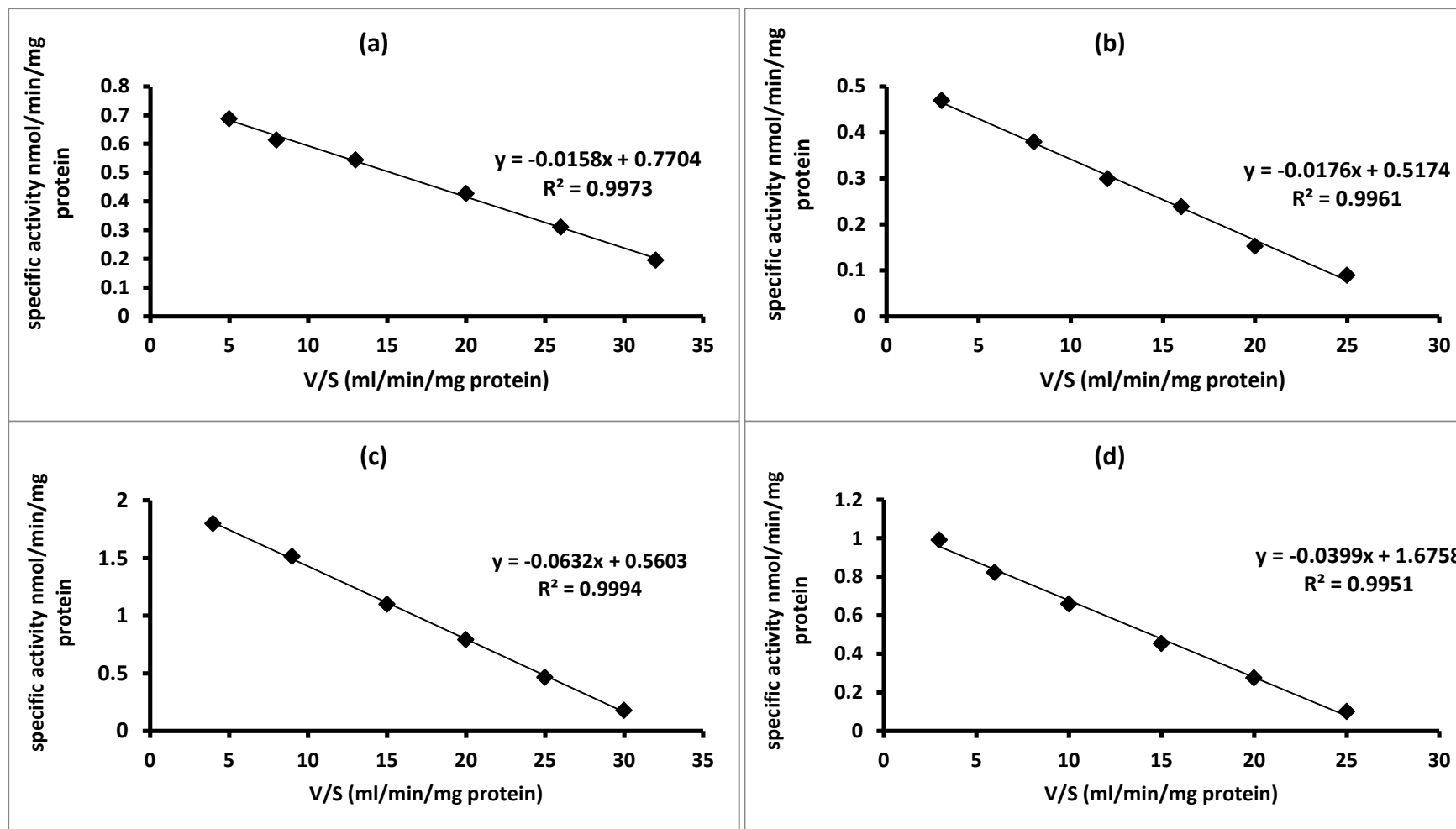
Figure 13: Eadie- Hofstee plot of XOR activities in rainbow trout. (a) XDH-catalyzed oxidation of xanthine. (b) XDH-catalyzed oxidation of 1-methylxanthine. (c) XDH-catalyzed oxidation of allopurinol. (d) XO-catalyzed oxidation of 6-thioxanthine. The substrates concentrations were 25-100 μM of XOR substrates. The typical results are from three independent experiments.
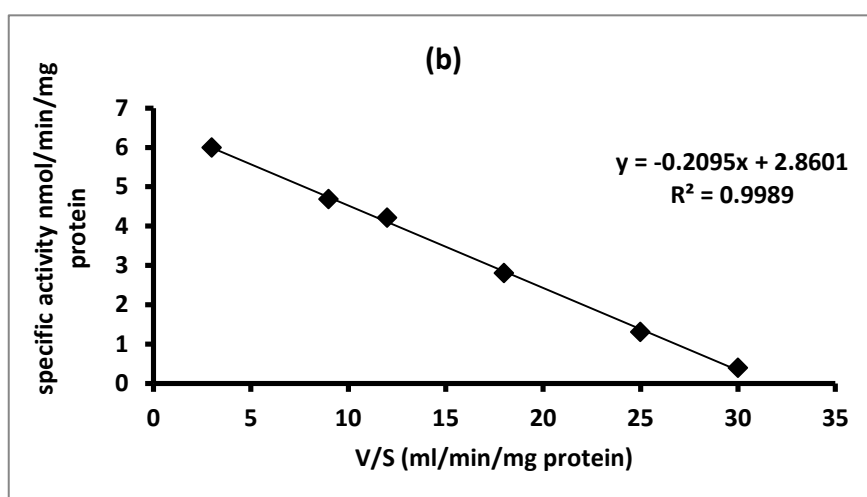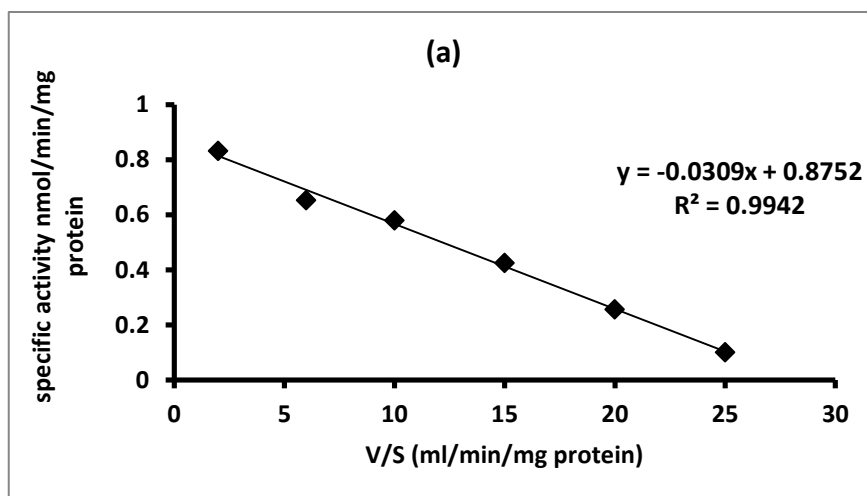
Figure 14: Eadie- Hofstee plot of XOR activities in rainbow trout. (a) XDH-catalyzed oxidation of 6-thioxanthine. (b) XDH-catalyzed oxidation of pyrazinamide. The substrates concentrations were 25-100 μM of XDH substrates. The typical results are from three independent experiments.
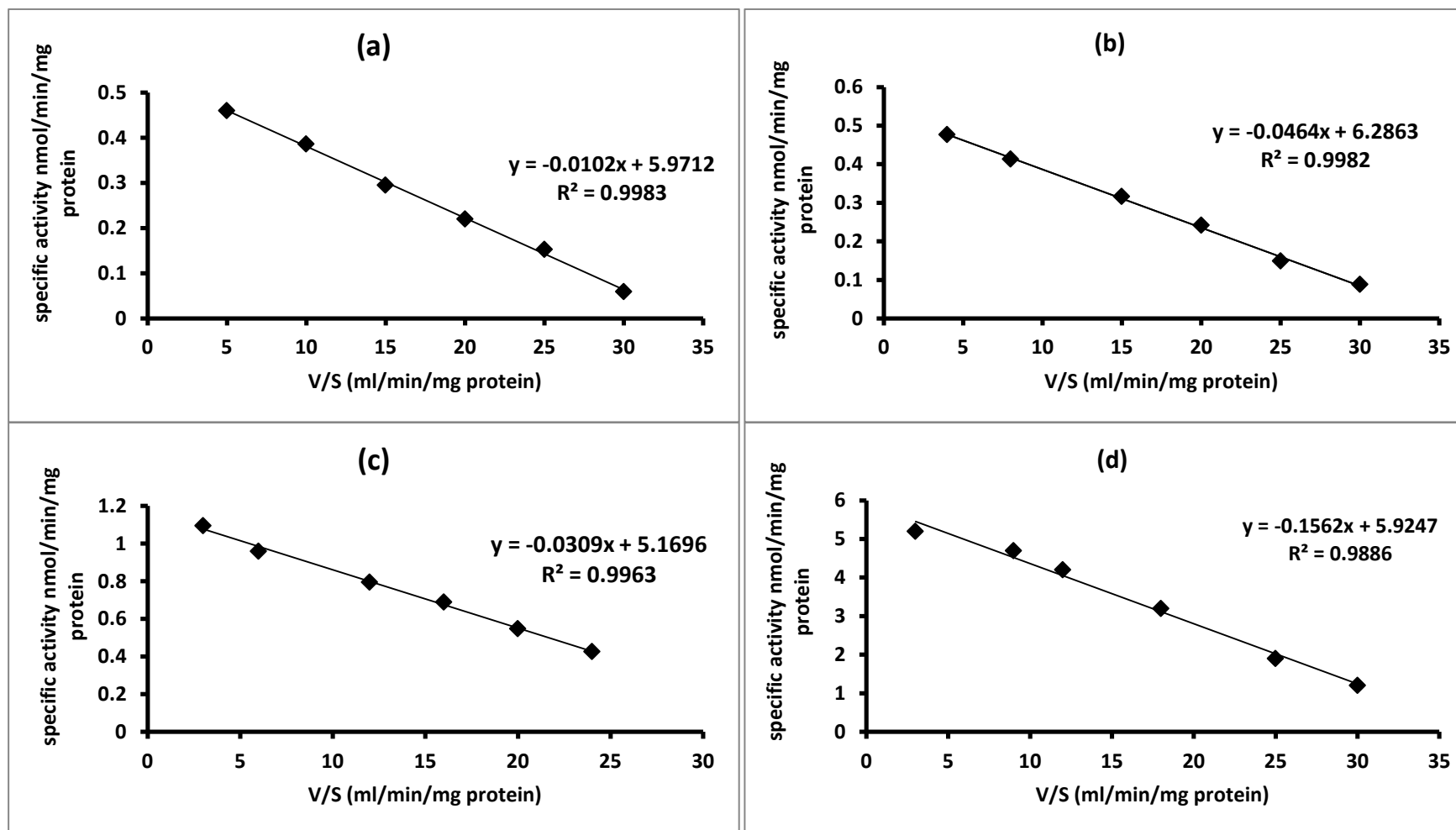
Figure 15: Eadie- Hofstee plot of AOX activities in rat. (a) AOX-catalyzed oxidation of vanillin. (b) AOX-catalyzed oxidation of pyridoxal. (c) AOX-catalyzed oxidation of ATR. (c) AOX-catalyzed oxidation of NMN. The substrates concentrations were 25-100 µM of AOX substrates.

Figure 16: Eadie- Hofstee plot of AOX activities in rat. (a) AOX-catalyzed oxidation of phenanthridine. (b) AOX-catalyzed oxidation of phthalazine. (c) AOX-catalyzed oxidation of cinchonine. (d) AOX-catalyzed oxidation of pyrazinamide. The substrates concentrations were 25-100 μM of AOX substrates.
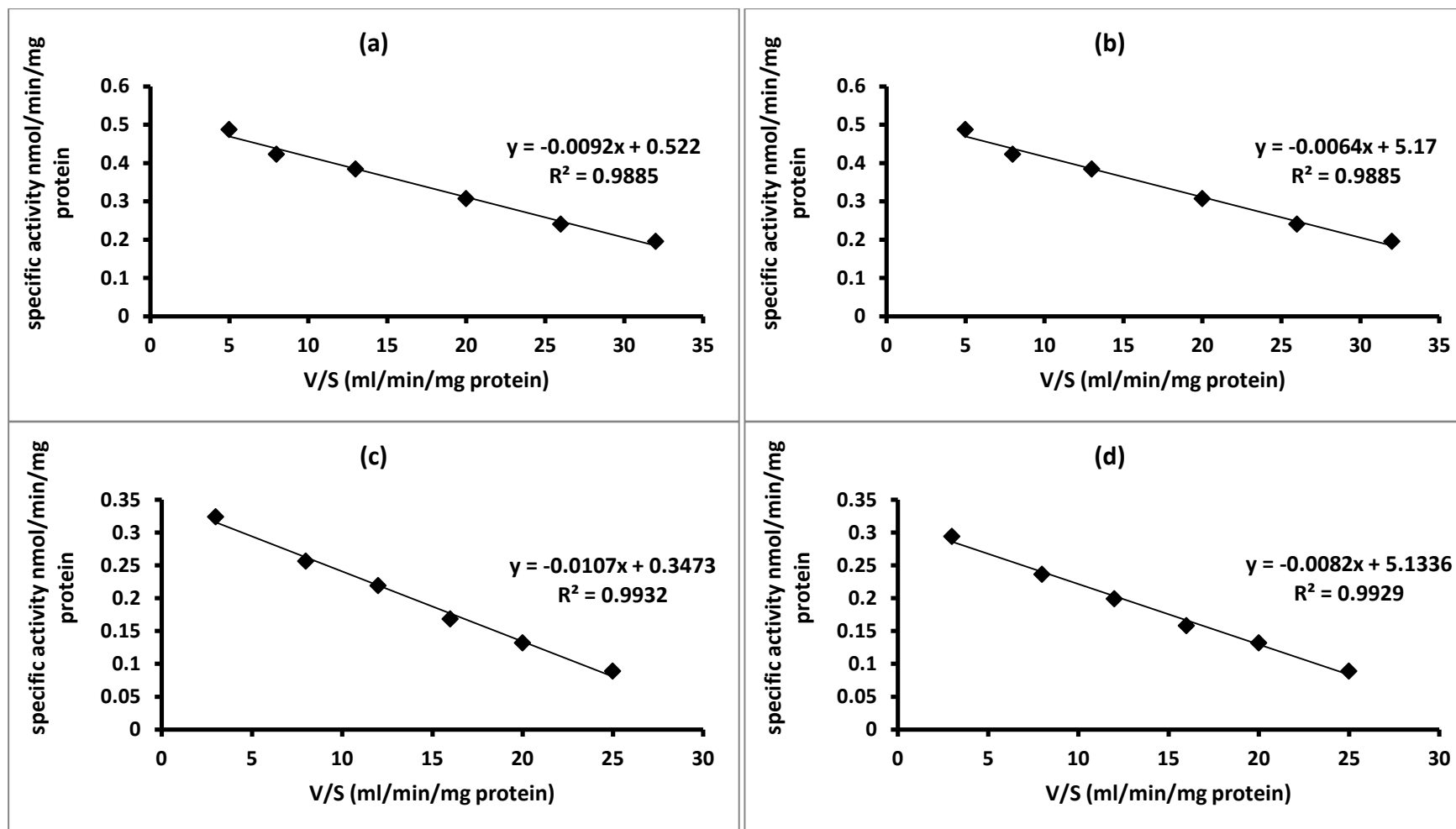
Figure 17: Eadie- Hofstee plot of XOR activities in rat. (a) XO-catalyzed oxidation of xanthine. (b) XDH-catalyzed oxidation of xanthine. (c) XO-catalyzed oxidation of 1-MX. (d) XDH-catalyzed oxidation of 1-MX. The substrates concentrations were 25-100 μM of AOX substrates.
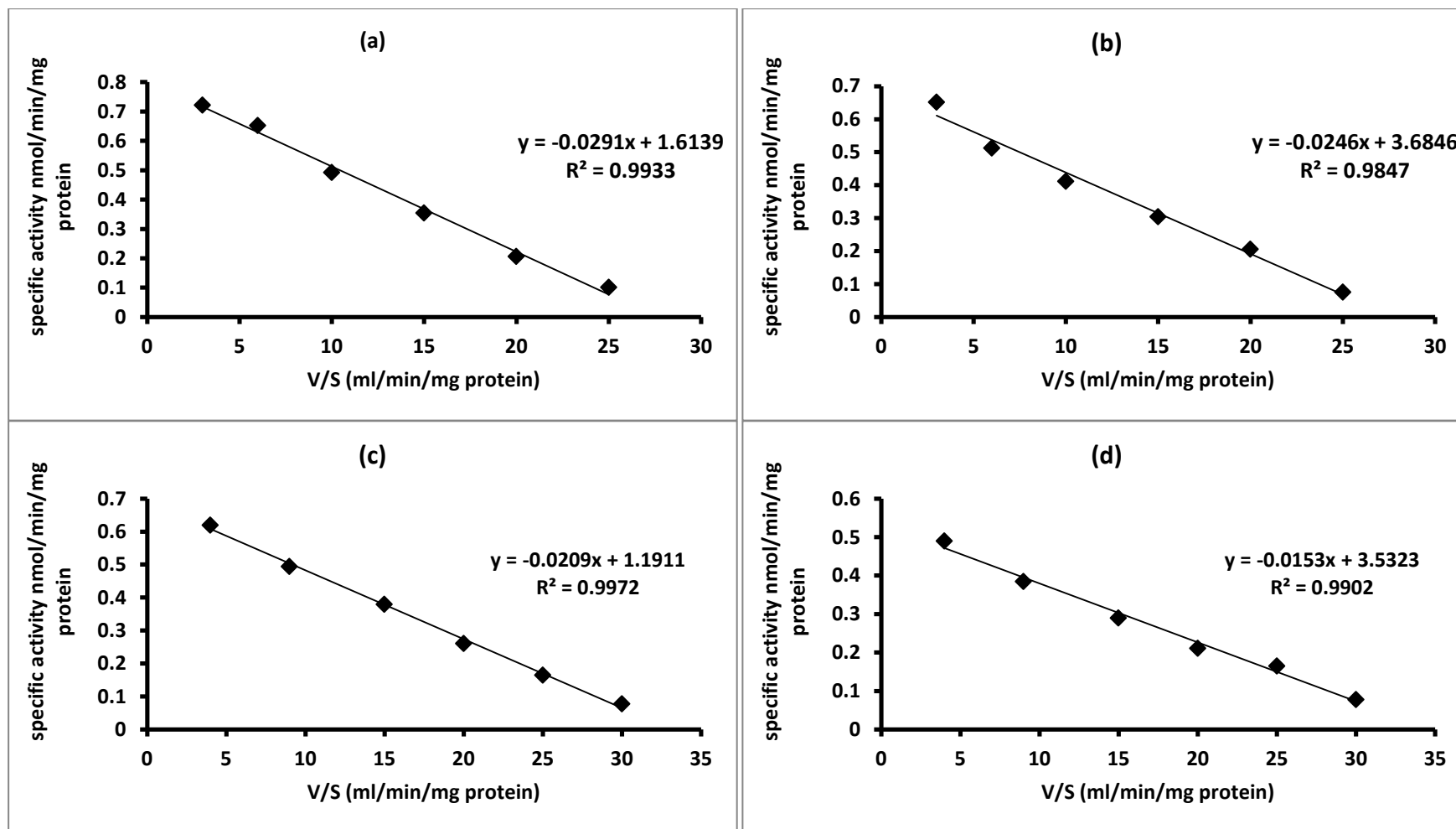
Figure 18: Eadie- Hofstee plot of XOR activities in rat. (a) XO-catalyzed oxidation of 6-MP. (b) XDH-catalyzed oxidation of 6-MP. (c) XO-catalyzed oxidation of allopurinol. (d) XDH-catalyzed oxidation of allopurinol. The substrates concentrations were 25-100 μM of AOX substrates.
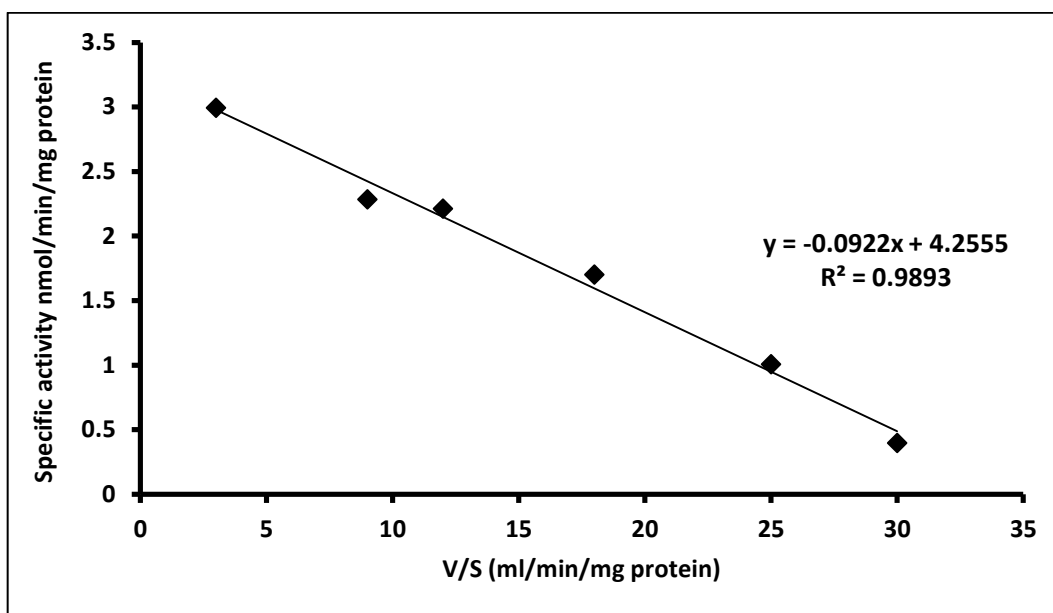
Figure 19: Eadie- Hofstee plot of XDH activities in rat. XDH-catalyzed oxidation of pyrazinamide. The substrates concentrations were 25-100 μM of XDH substrates. The typical results are from three independent experiments.
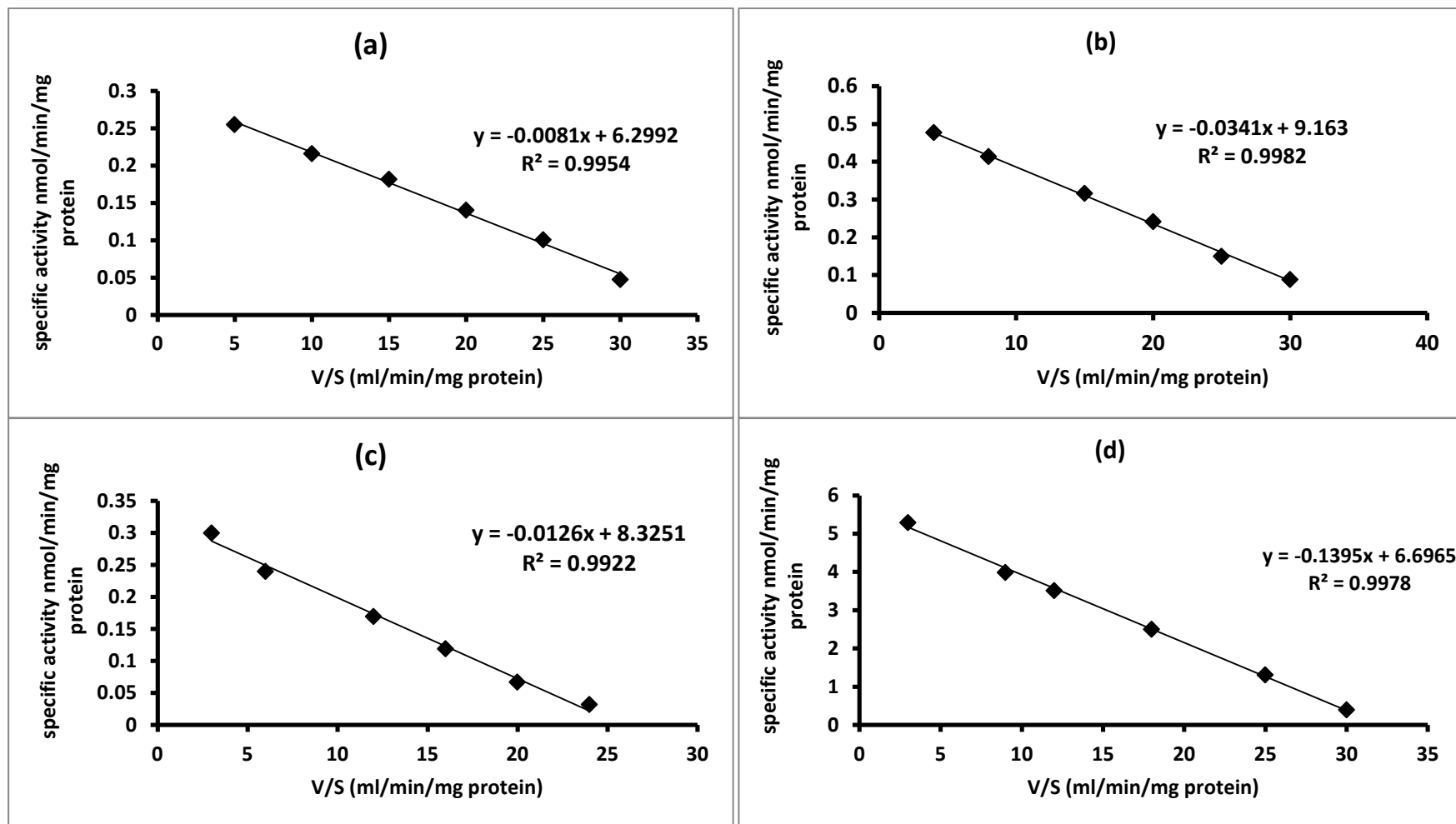
Figure 20: Eadie- Hofstee plot of AOX activities in human. (a) AOX-catalyzed oxidation of vanillin. (b) AOX-catalyzed oxidation of pyridoxal. (c) AOX-catalyzed oxidation of ATR. (d) AOX-catalyzed oxidation of NMN. The substrates concentrations were 25-100 μM of AOX substrates.
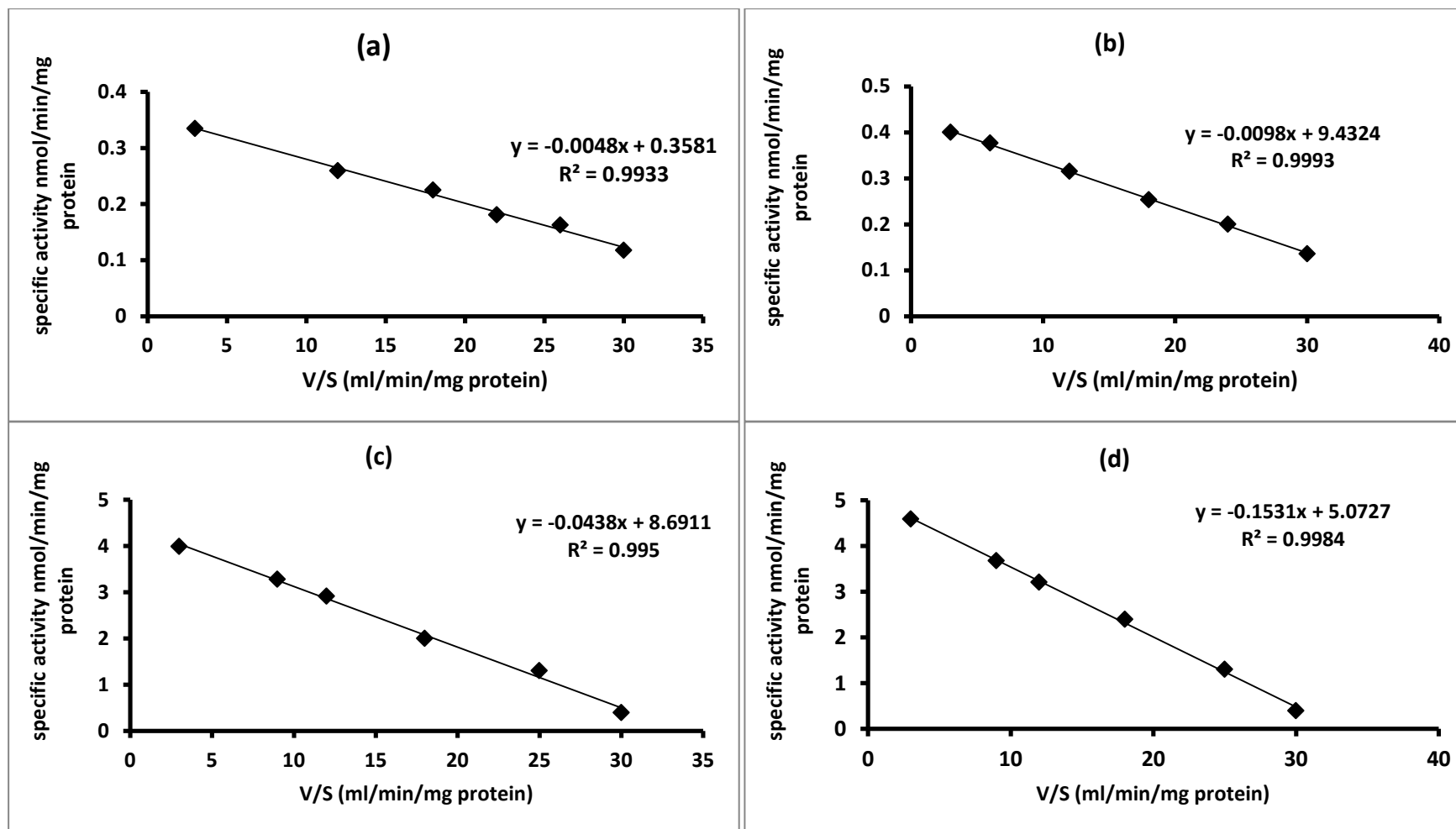
Figure 21: Eadie- Hofstee plot of AOX activities in human. (a) AOX-catalyzed oxidation of phenanthridine. (b) AOX-catalyzed oxidation of phthalazine. (c) AOX-catalyzed oxidation of cinchonine. (d) AOX-catalyzed oxidation of pyrazinamide. The substrates concentrations were 25-100 μM of AOX substrates.
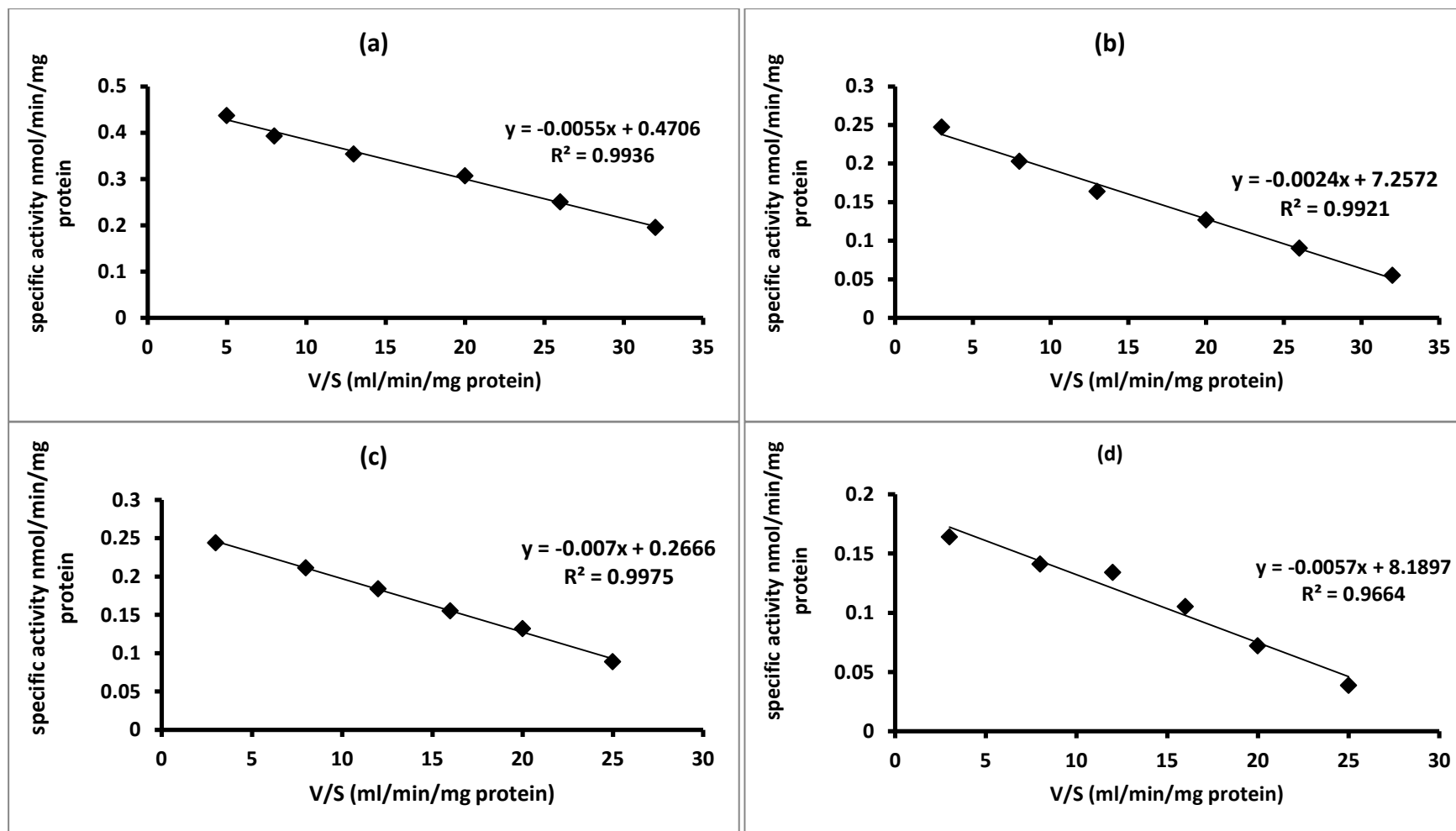
Figure 22: Eadie- Hofstee plot of XOR activities in human. (a) XO-catalyzed oxidation of xanthine. (b) XDH-catalyzed oxidation of xanthine. (c) XO-catalyzed oxidation of 1-MX. (d) XDH-catalyzed oxidation of 1-MX. The substrates concentrations were 25-100 μM of AOX substrates.
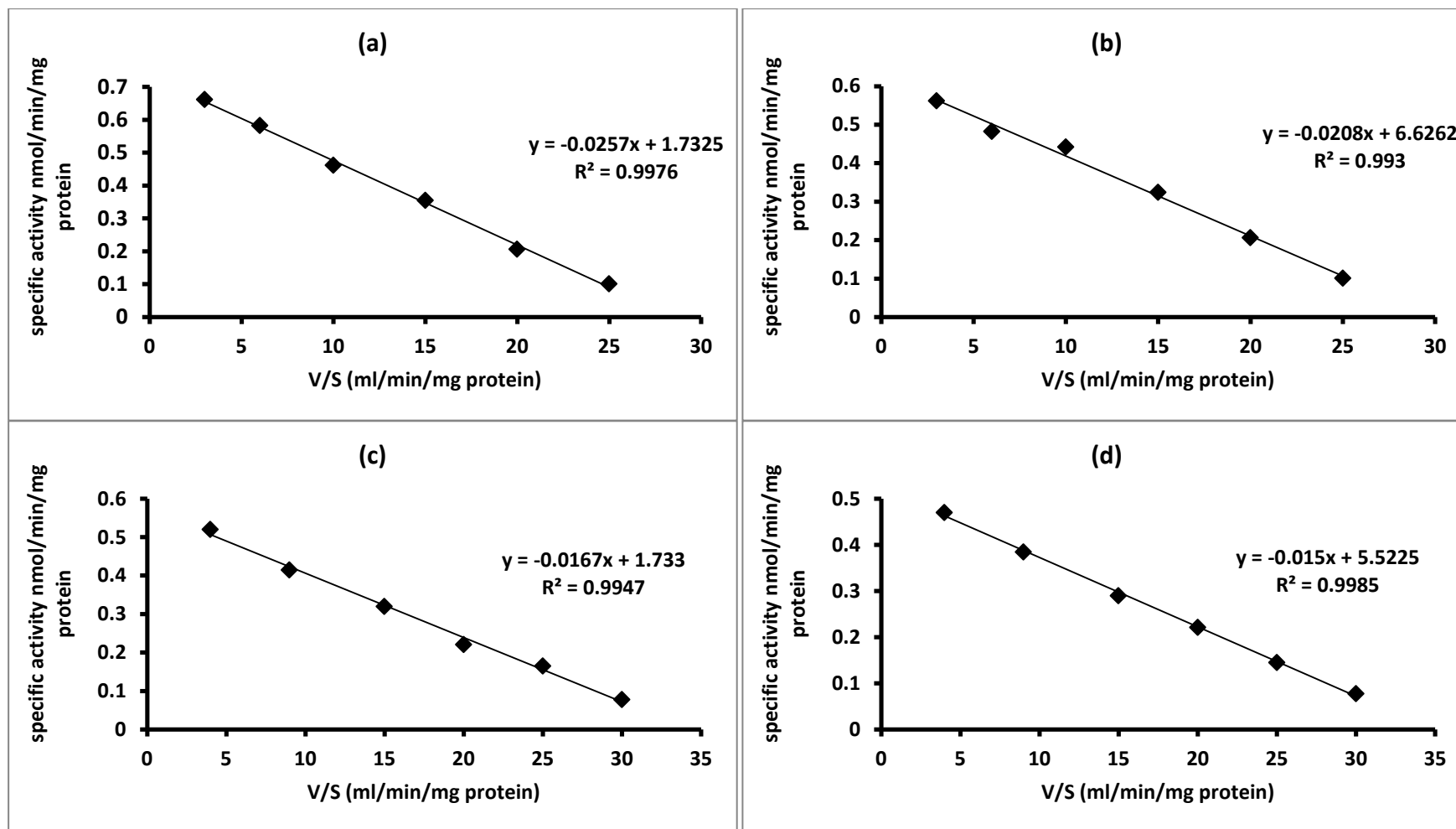
Figure 23: Eadie- Hofstee plot of XOR activities in rat. (a) XO-catalyzed oxidation of 6-MP. (b) XDH-catalyzed oxidation of 6-MP. (c) XO-catalyzed oxidation of allopurinol. (d) XDH-catalyzed oxidation of allopurinol. The substrates concentrations were 25-100 μM of AOX substrates.
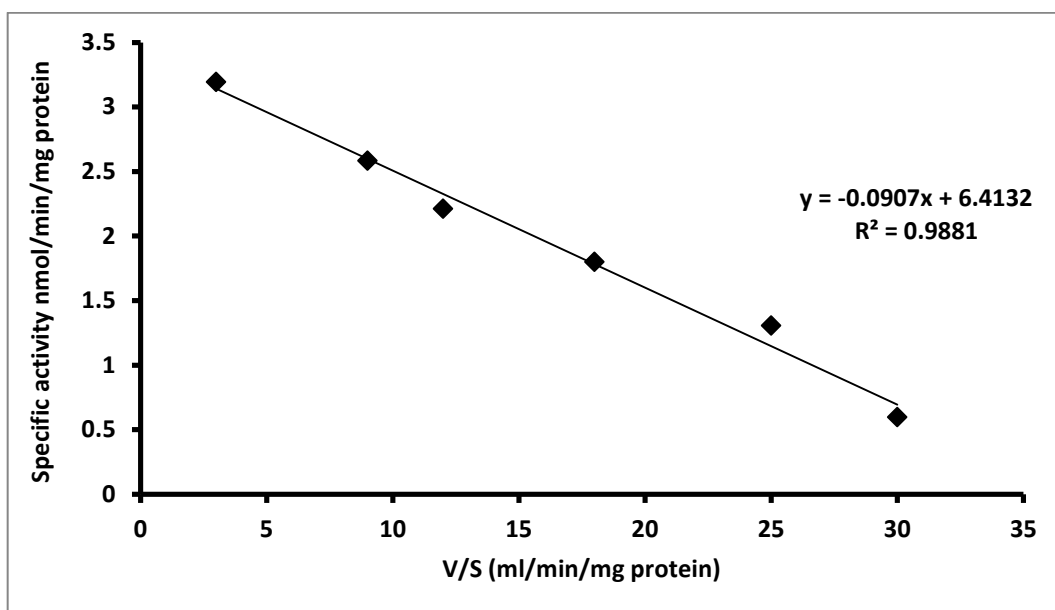
Figure 24: Eadie- Hofstee plot of XOR activities in human. XDH-catalyzed oxidation of pyrazinamide. The substrates concentrations were 25-100 μM of AOX substrates. The typical results are from three independent experiments.
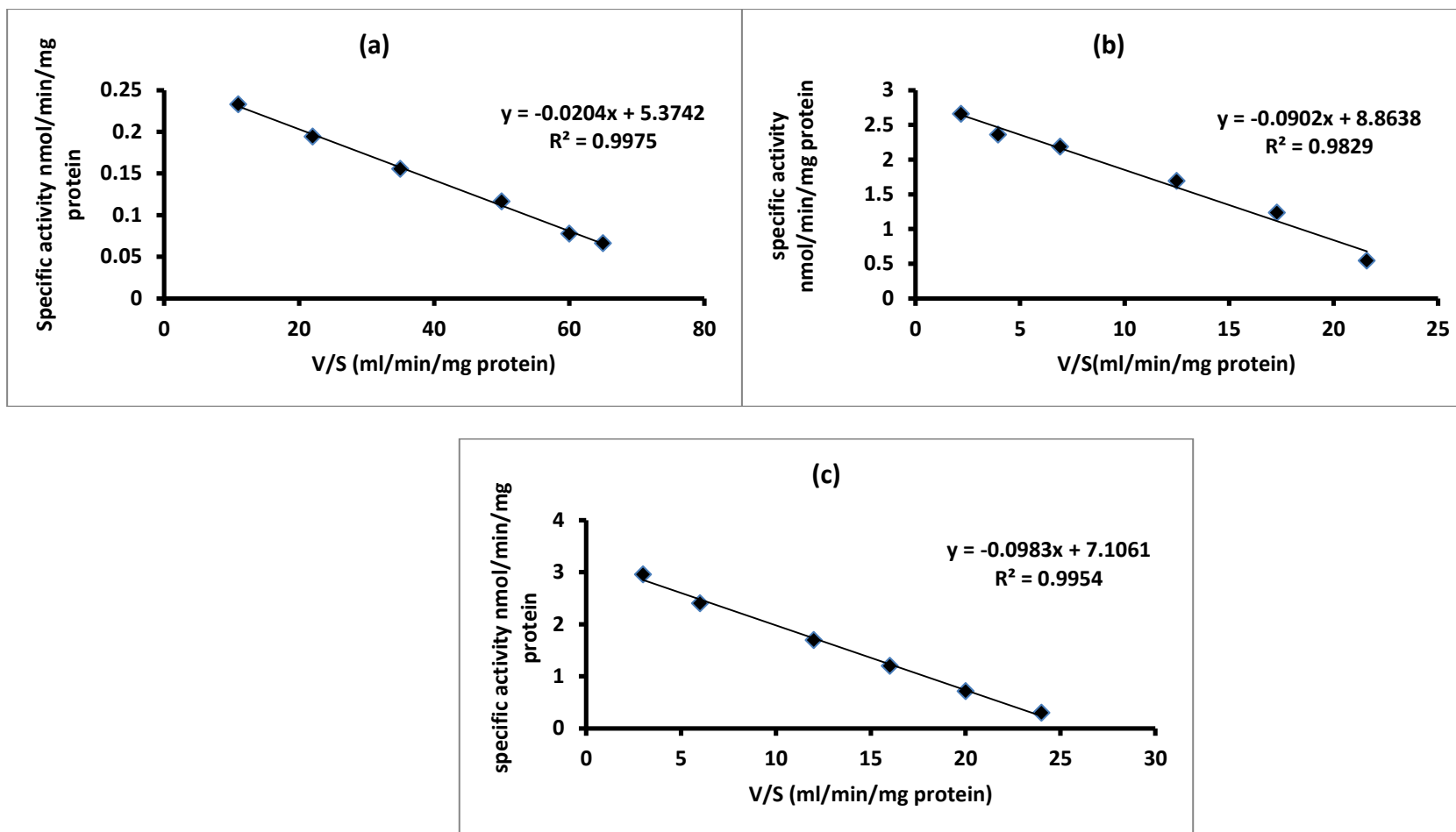
Figure 25: Eadie- Hofstee plot of purified AOX activities in rainbow trout. AOX-catalyzed oxidation of (a) vanillin, (b) pyridoxal and (c) all-trans retinal. The substrates concentrations were 25-100 μM of AOX substrates. The typical results are from three independent experiments.